
Oil Production Greenhouse Gas Emissions Estimator

OPGEE v3.0a

User guide & Technical documentation

Hassan M. El-Houjeiri,^{1,*} Mohammad S. Masnadi,¹ Kourosh Vafi,^{1,*} Patrick Perrier,¹ James Duffy,² Adam R. Brandt^{1,†}

With technical contributions from:

Jingfan Wang¹, Sylvia Sleep,³ Diana Pacheco,⁴ Zainab Dashnadi,³ Andrea Orellana,^{4,*} Jacob Englander,¹ Scott McNally,^{1,*} Heather MacLean,⁴ Joule Bergerson³

¹ Department of Energy Resources Engineering, Stanford University

² California Air Resources Board, Alternative Fuels Section

³ Department of Chemical and Petroleum Engineering, University of Calgary

⁴ Department of Civil and Environmental Engineering, University of Toronto

* Prior affiliation, now employed elsewhere

[†]Corresponding author: abrandt@stanford.edu, +1 (650) 724 8251

October 18th, 2018

Funded by:

California Environmental Protection Agency, Air Resources Board

Contents

1 Acknowledgements	17
I Introduction and user guide	18
2 Introduction	19
2.1 Model motivation	20
2.2 OPGEE model goals	21
2.3 OPGEE model construction	22
3 User guide	27
3.1 Input and output worksheets	28
3.2 Field summary worksheets	29
3.3 Process stage worksheets	30
3.4 Supplementary worksheets	31
3.5 Structure of process stage worksheet	32
3.6 Working with OPGEE	34
3.7 Inputs	44
II Technical documentation	46
4 ‘Active Field’ gathering worksheet	47
4.1 Introduction to the ‘Active Field’ worksheet	48
4.2 GHG calculations on the ‘Active Field’ worksheet	49
4.3 Smart defaults and uncertainty distributions for missing key parameters	51
5 Flow sheet	63
5.1 Flow sheet introduction	64
5.2 Computing properties of flows	64
6 Gathering worksheets	74
6.1 ‘Energy Consumption’ gathering worksheet	75
6.2 ‘GHG Emissions’ gathering worksheet	77
7 Process worksheets	79
7.1 Exploration	80
7.2 Drilling & development	82

7.3	Reservoir	94
7.4	Wellbore/Downhole Pump	98
7.5	Bitumen mining	105
7.6	Separation	117
7.7	Heater-treater (dewatering)	119
7.8	'Crude oil stabilization' worksheet	122
7.9	Heavy oil upgrading	124
7.10	Heavy oil dilution	130
7.11	Crude oil storage	132
7.12	Produced water treatment	135
7.13	Makeup water treatment	140
7.14	Water injection	142
7.15	Steam generation	144
7.16	Flaring	157
7.17	Venting	166
7.18	Gas gathering	168
7.19	Glycol dehydrator	169
7.20	Acid gas removal	179
7.21	Demethanizer	204
7.22	Chiller	215
7.23	Membrane	218
7.24	Ryan-Holmes	221
7.25	Gas flooding compressor	224
7.26	Gas lifting compressor	227
7.27	Gas reinjection compressor	228
7.28	CO ₂ reinjection compressor	229
7.29	Sour gas reinjection compressor	231
7.30	VRU compressor	233
7.31	Pre-membrane compressor	234
7.32	Transmission compressor	235
7.33	LNG liquefaction	236
7.34	LNG Regasification	237
7.35	LNG transport	238
7.36	Storage compressor	239
7.37	Post-storage compressor	240
7.38	HC gas injection wells	241
7.39	CO ₂ injection wells	242
7.40	Sour gas injection wells	243
7.41	Steam injection wells	244
7.42	Gas storage wells	245
7.43	Storage separator	246
7.44	Gas partition A	247
7.45	Gas partition B	248
7.46	Fuel gas consumed	249
7.47	Maintenance	250
7.48	Waste treatment and disposal	251
7.49	Crude oil transport	252
7.50	Petcoke transport	256

7.51 Gas distribution	257
7.52 Fuel gas inputs	258
7.53 Electricity generation and imports	259
7.54 NGL or diluent production or imports	260
7.55 Gas flooding	261
8 Supplemental calculations worksheets	271
8.1 Drivers	271
8.2 Fuel cycle	274
8.3 Embodied emissions	275
8.4 Emissions factors	284
9 Venting and fugitive emissions	288
9.1 Introduction to venting and fugitive emissions	288
9.2 Site-level methods for on-site emissions	289
9.3 Component-level methods for on-site emissions	294
9.4 Statistical analysis of leakage datasets	314
9.5 Off-site emissions	323
9.6 Deprecated OPGEE v2.0 VF modeling methods	324
10 Fundamental data inputs	326
10.1 Global warming potentials	326
10.2 Properties of water and steam	326
10.3 Properties of air and exhaust gas components	327
10.4 Compositions and properties of fuels	327
11 OPGEE limitations	329
11.1 Scope limitations	329
11.2 Technical limitations	329
11.3 Future work	331
A Terminology: Acronyms and abbreviations	332
B Mathematical terms and definitions	334
C Tabulated sources for each production stage	339
D Bulk assessment macro error correction	346
E Changes and updates from previous versions of OPGEE	350
E.1 Changes from OPGEE v2.0a to OPGEE v2.0b	350
E.2 Changes from OPGEE v1.1 Draft E to OPGEE v2.0a	350
E.3 Changes from OPGEE v1.1 Draft D to OPGEE v1.1 Draft E	351
E.4 Changes from OPGEE v1.1 Draft C to OPGEE v1.1 Draft D	351
E.5 Changes from OPGEE v1.1 Draft B to OPGEE v1.1 Draft C	352
E.6 Changes from OPGEE v1.1 Draft A to OPGEE v1.1 Draft B	353
E.7 Changes from OPGEE v1.0 to OPGEE v1.1 Draft A	354
E.8 Changes from OPGEE v1.0 Draft A to OPGEE v1.0	357

List of Figures

2.1	Schematic chart showing included stages within OPGEE.	23
2.2	Proposed workflow for improving emissions estimates using OPGEE.	24
3.1	Example flow table in OPGEE 3.0 Flows are segregated by phase (solid, liquid, gas) or type (electricity). Fundamental properties of each stream, including temperature and pressure, are recorded at the bottom of each flow.	32
3.2	Types of cells. <i>User Free</i> and <i>Default Free</i> cells can be changed, while <i>Locked</i> cells should not be changed due to possibility of compromising model functionality. Flow sheet cells are either calculated in place or looked up from the large flow table.	33
3.3	Data input section of the ' <i>Inputs</i> ' worksheet.	38
3.4	Input data section of ' <i>Reservoir</i> ' worksheet. User inputs are in column M, while defaults are kept as reference in column N.	41
3.5	Graphical results for an example crude oil. These results from ' <i>Active Field</i> ' Tables 1.1 and 1.2, Figures 1.1 and 1.2.	43
3.6	Logical structure of the assessment macro.	45
4.1	Distributions of global oilfield ages. Mean date of discovery (by count not by production-weighted average) is 1978.4.	52
4.2	Distributions of giant oilfield ages. Mean date of discovery (by production-weighted average) is 1960.2.	53
4.3	Distributions of global oilfield depths in bins of 500 ft depth. $N = 4489$ fields, mean = 7238 ft, SD = 3591 ft, median = 6807 ft.	54
4.4	Distributions of oilfield per-well productivity (bbl oil/well-d) for bins of 500 bbl/d, counted by numbers of countries (bar) and by fraction of production (dot) $N = 92$ countries.	54
4.5	Distributions of oilfield per-well productivity (bbl oil/well-d) for all countries with per-well productivities lower than 500 bbl/well-d, counted by numbers of countries (bar) and by fraction of production (dot) $N = 55$ countries.	55
4.6	Ratio of producers to injectors as a function of per-well productivity. Source: Various.	55
4.7	Distributions of major gas species across 135 samples from California associated gas producers.	58
4.8	Distributions of California GORs, binned by crude density.	58

4.9	Exponential WOR model fit with smart default parameters. The best fit to data gives $a_{WOR} = 1.706$ and $b_{WOR} = 0.036$. Regions are colored as follows: Alberta (red), Alaska (green), California (orange), Norway (blue) and UK (beige).	60
4.10	Distribution of SOR values for California and Alberta thermal EOR projects (steamflood, cyclic steam stimulation, steam-assisted gravity drainage).	62
5.1	Standing and Katz [1] Natural Gas Mixture Z-Factor Chart.	71
5.2	Correlation of Upper Portion of Standing and Katz Z-Factor Chart. Source: [2].	72
5.3	Correlation of Lower Portion of Standing and Katz Z-Factor Chart. Source: [2].	72
7.1	Drilling hole diameters for simple, moderate and complex well construction.	84
7.2	All GHGfrack results for drilling fuel consumption in US gallons of diesel (includes both rotary table + mud circulation).	86
7.3	GHGfrack results for drilling fuel consumption segmented by well complexity. Fuel consumption reported in US gallons of diesel (includes both rotary table + mud circulation).	87
7.4	GHGfrack results for drilling fuel consumption. Only simple wells are represented, and the results are segmented by efficiency and wellbore orientation. Fuel consumption reported in US gallons of diesel (includes both rotary table + mud circulation).	88
7.5	Fuel use in hydraulic fracturing as a function of fracturing volume. Each curve represents a different fracturing gradient value, ranging from 0.6 psi/ft to 1.0 psi/ft.	90
7.6	Streams flowing into and out of reservoir-well interface. All streams measured in tonnes per day excepting electricity which is measured in MWh/d.	95
7.7	Streams flowing into and out of the wellbore/downhole pump process. All streams measured in tonnes per day excepting electricity which is measured in MWh/d.	99
7.8	Moody friction factor chart. Source: [3].	102
7.9	An example of a linear pressure traverse curve (GLR= 0).	104
7.10	Streams flowing into and out of the bitumen mining process. All streams measured in tonnes per day excepting electricity which is measured in MWh/d.	106
7.11	Natural gas use in mining operations	110
7.12	Electricity use in mining operations	111
7.13	Non-integrated bitumen mining operation	115
7.14	Upgrader-integrated bitumen mining operation	116
7.15	Streams flowing into and out of the separation process. All streams measured in tonnes per day excepting electricity which is measured in MWh/d.	118

7.16 Streams flowing into and out of the crude oil dewatering process. All streams measured in tonnes per day excepting electricity which is measured in MWh/d.	121
7.17 Streams flowing into and out of the ' <i>Crude oil stabilization</i> ' work- sheet. All streams measured in tonnes per day excepting electricity which is measured in MWh/d.	123
7.18 Streams flowing into and out of the heavy oil upgrading process. All streams measured in tonnes per day excepting electricity which is measured in MWh/d.	125
7.19 Process flow diagram for OPGEE upgrading module	126
7.20 Streams flowing into and out of ' <i>Heavy oil dilution</i> ' worksheet. All streams measured in tonnes per day excepting electricity which is measured in MWh/d.	131
7.21 Streams flowing into and out of crude oil storage module. All streams measured in tonnes per day excepting electricity which is measured in MWh/d.	133
7.22 Streams flowing into and out of produced water treatment process. All streams measured in tonnes per day excepting electricity which is measured in MWh/d.	136
7.23 Streams flowing into and out of makeup water treatment process. All streams measured in tonnes per day excepting electricity which is measured in MWh/d.	141
7.24 Streams flowing into and out of water injection process. All streams measured in tonnes per day excepting electricity which is measured in MWh/d.	143
7.25 Streams flowing into and out of the steam generation process. All streams measured in tonnes per day excepting electricity which is measured in MWh/d.	145
7.26 Once-through steam generator with mass and energy balance terms. Lower case terms are defined per lbmol of input fuel.	147
7.27 Increase of crude contaminant load with increase in crude specific gravity (decrease in API gravity). Data from: Speight (1994) and Swafford (2009).	150
7.28 Gas turbine plus heat recovery steam generator model. Mass flows represented by m and energy flows represented by fuel lower heat- ing value (LHV), electric power out (e) and enthalpy of gases (h).	151
7.29 Predicted turbine exit temperatures for variety of turbines from lit- erature (y -axis) as compared to reported value from the literature (x -axis).	152
7.30 Streams flowing into and out of the flaring process. All streams mea- sured in tonnes per day excepting electricity which is measured in MWh/d.	158
7.31 Flowchart illustrating the logic of the flaring computation worksheet.	159
7.32 Rayleigh distribution fit to 6 wind speed datasets from western United States. Data source: NREL Western Wind Integration Dataset.	163
7.33 Example of OPGEE wind speed distribution for a 30 mph average windspeed input.	164

7.34 Streams flowing into and out of the venting process. All streams measured in tonnes per day excepting electricity which is measured in MWh/d.	167
7.35 Streams flowing into and out of the gas gathering process. All streams measured in tonnes per day excepting electricity which is measured in MWh/d.	168
7.36 Streams flowing into and out of the glycol dehydrator process. All streams measured in tonnes per day excepting electricity which is measured in MWh/d.	170
7.37 Glycol dehydrator process flow diagram from Aspen HYSYS model.	171
7.38 TEG dehydration energy use prediction parity chart. (a) Reboiler thermal inputs [kW]; (b) Pump work [kW]; (c) reflux condenser electrical load [kW]; (d) amine cooler thermal load [kW]. <i>x</i> -axis represents Aspen HYSYS simulation results, <i>y</i> -axis represents OPGEE statistical model predictions. MAD = mean absolute deviation.	173
7.39 Glycol dehydrator simple process flow diagram [4, p. 141].	175
7.40 Streams flowing into and out of the acid gas removal process. All streams measured in tonnes per day excepting electricity which is measured in MWh/d.	180
7.41 Amine process flow diagram from Aspen HYSYS as used in modeling DGA, DEA, DEA-High-Load, and MDEA [5].	182
7.42 Amine process flow diagram from Aspen HYSYS as used in modeling MEA [5].	182
7.43 MEA-based AGR energy use prediction parity chart. (a) Reboiler thermal inputs [kW]; (b) Total pump work (charge+booster) [kW]; (c) reflux condenser thermal load [kW]; (d) amine cooler thermal load [kW]. <i>x</i> -axis represents Aspen HYSYS simulation results, <i>y</i> -axis represents OPGEE statistical model predictions. MAD = mean absolute deviation.	186
7.44 DGA-based AGR energy use prediction parity chart. (a) Reboiler thermal inputs [kW]; (b) Total pump work (charge+booster) [kW]; (c) reflux condenser thermal load [kW]; (d) amine cooler thermal load [kW]. <i>x</i> -axis represents Aspen HYSYS simulation results, <i>y</i> -axis represents OPGEE statistical model predictions. MAD = mean absolute deviation.	187
7.45 DEA-based AGR energy use prediction parity chart. (a) Reboiler thermal inputs [kW]; (b) Total pump work (charge+booster) [kW]; (c) reflux condenser thermal load [kW]; (d) amine cooler thermal load [kW]. <i>x</i> -axis represents Aspen HYSYS simulation results, <i>y</i> -axis represents OPGEE statistical model predictions. MAD = mean absolute deviation.	188
7.46 DEA-high-load-based AGR energy use prediction parity chart. (a) Reboiler thermal inputs [kW]; (b) Total pump work (charge+booster) [kW]; (c) reflux condenser thermal load [kW]; (d) amine cooler thermal load [kW]. <i>x</i> -axis represents Aspen HYSYS simulation results, <i>y</i> -axis represents OPGEE statistical model predictions. MAD = mean absolute deviation.	189

7.47 MDEA-based AGR energy use prediction parity chart. (a) Reboiler thermal inputs [kW]; (b) Total pump work (charge+booster) [kW]; (c) reflux condenser thermal load [kW]; (d) amine cooler thermal load [kW]. <i>x</i> -axis represents Aspen HYSYS simulation results, <i>y</i> -axis represents OPGEE statistical model predictions. MAD = mean absolute deviation.	190
7.48 Amine simple process flow diagram [4, p. 112].	193
7.49 Claus unit modified process flow diagram from Aspen HYSYS as used in developing statistical proxy models.	196
7.50 Desulfurization condensers, heaters, and waste heat exchanger heat duties per kilogram of sulfur produced in different acid gas H ₂ S concentrations.	198
7.51 Tail gas H ₂ O, H ₂ , N ₂ , and CO ₂ mole concentrations in different acid gas H ₂ S concentrations.	198
7.52 Stack gas H ₂ O, H ₂ , N ₂ , and CO ₂ mole concentrations in different acid gas H ₂ S concentrations.	199
7.53 Desulfurization plant downstream mass flow rates vs. different acid gas H ₂ S concentrations (a) Stack effluent mass flow rate (b) Incinerator fuel gas consumption.	200
7.54 Streams flowing into and out of the demethanizer process. All streams measured in tonnes per day excepting electricity which is measured in MWh/d.	205
7.55 Demethanizer modified process flow diagram from Aspen HYSYS as used in developing statistical proxy models.	206
7.56 Demethanizer energy use prediction parity chart (a) Reboiler thermal inputs [kW]; (b) Demethanizer tray 6 duty [kW]; (c) Demethanizer tray 9 duty [kW]; (d) Demethanizer cooler Q-100 duty [kW]. . .	209
7.57 Demethanizer energy use prediction parity chart (a) Reboiler thermal inputs [kW]; (b) Demethanizer tray 6 duty [kW]; (c) Demethanizer tray 9 duty [kW]; (d) Demethanizer cooler Q-100 duty [kW]. . .	209
7.58 Demethanizer NGL stream mole concentration parity chart (a) C ₁ [mol. frac.]; (b) C ₂ [mol. frac.]; (c) C ₃ [mol. frac.]; (d) C ₄ [mol. frac.]. .	210
7.59 Demethanizer Fuel gas stream mole concentration parity chart (a) C ₁ [mol. frac.]; (b) C ₂ [mol. frac.]; (c) C ₃ [mol. frac.]; (d) C ₄ [mol. frac.]. .	210
7.60 Demethanizer Fuel gas stream pressure parity chart.	211
7.61 Streams flowing into and out of the pre-membrane chiller process. All streams measured in tonnes per day excepting electricity which is measured in MWh/d.	216
7.62 Streams flowing into and out of the CO ₂ separation membrane process. All streams measured in tonnes per day excepting electricity which is measured in MWh/d.	219
7.63 Streams flowing into and out of the Ryan-Holmes separation process. All streams measured in tonnes per day excepting electricity which is measured in MWh/d.	222
7.64 Streams flowing into and out of the gas flooding compressor. All streams measured in tonnes per day excepting electricity which is measured in MWh/d.	225

7.65 Streams flowing into and out of the gas lifting compressor. All streams measured in tonnes per day excepting electricity which is measured in MWh/d.	227
7.66 Streams flowing into and out of the gas reinjection compressor. All streams measured in tonnes per day excepting electricity which is measured in MWh/d.	228
7.67 Streams flowing into and out of the CO ₂ reinjection compressor. All streams measured in tonnes per day excepting electricity which is measured in MWh/d.	230
7.68 Streams flowing into and out of the sour gas reinjection compressor. All streams measured in tonnes per day excepting electricity which is measured in MWh/d.	232
7.69 Streams flowing into and out of the VRU compressor. All streams measured in tonnes per day excepting electricity which is measured in MWh/d.	233
7.70 Schematic of associated gas treatment with four main branches. The lower 3 branches model post-breakthrough CO ₂ enhanced oil recovery separation pathways [6].	269
8.1 Casing plan for wells of complex, intermediate, and simple design. Well depths here are illustrative, and all steel consumption intensities are computed per unit length of well (per ft.). See text for sources.	278
8.2 Diagram illustrating cement volume calculations (per unit depth). Cement is presented in grey, while earth is presented in green-brown.	279
8.3 Default OPGEE cementing plan. Default non-conductor, non-surface casing fill-up is twice reported minimum, or 600 ft.	281
9.1 Boundary of venting and fugitive emissions accounting, dividing the process chains into “on-site” and “off-site” emissions.	289
9.2 Schematic of site-level quantification of methane emissions.	290
9.3 Results of fitting linear model to log-transformed leakage fraction as a function of log-transformed production facility throughput.	291
9.4 Results of fitting linear model to log-transformed leakage fraction as a function of log-transformed processing facility throughput.	293
9.5 Schematic of site-level quantification of methane emissions.	294
9.6 Schematic of method for generation of project-level fugitive emissions rates from component-level estimates.	301
9.7 Cumulative contribution of rank-ordered normalize leakage volumes by 10 standard component classes and “other”.	315
9.8 Cumulative contribution of rank-ordered normalize leakage volumes by originating study.	315
9.9 Absolute leakage (kg/d) percentiles (0.1% discretization giving 1000 steps) for equipment generated via 10,000 MC simulations of equipment given equipment component counts above.	317
9.10 Emissions from completions and workovers performed on wells with the use of hydraulic fracturing, as reported to GHGRP datasets. . . .	320
9.11 Emissions from completions and workovers performed on wells without the use of hydraulic fracturing, as reported to GHGRP datasets. .	320

9.12 Cumulative distribution of emissions intensity for wells completed with the use of hydraulic fracturing.	321
9.13 Cumulative distribution of emissions intensity for wells completed without the use of hydraulic fracturing.	321
9.14 Fractional loss rates due to liquids unloading for 3 types of liquids unloading technologies from Allen et al. 2014b [7]. Sample size and mean emissions vary by technology.	324
D.1 The errors fixing/entries adjustment logic.	347
D.2 The errors fixing/entries adjustment logic for non-GOR, gas composition related entries.	348

List of Tables

2.1	Emissions classification, order of magnitude emissions, and significance description.	25
4.1	Mean and median injector to producer ratios.	53
4.2	Data on production, number of production wells, and number of injection wells by offshore field.	56
4.3	GOR values by crude oil API gravity bin.	59
4.4	Indicators of SOR distributions for California and Alberta thermal EOR production. Units are bbl of cold water equivalent (CWE) per bbl of oil.	62
5.1	Properties computed for each stream: Symbol, description, units, and source of relevant equation.	64
5.2	Source of API gravity for oil streams.	66
5.3	Constants in equations for liquid stream properties.	69
7.1	Default inputs for exploration emissions	81
7.2	Hole diameters for different casing sections under three wellbore designs (in.)	83
7.3	Bottomhole depth for different segments (ft.)	83
7.4	Constants for quadratic fit of fracturing fuel consumption equation .	89
7.5	Land use GHG emissions for 30 year analysis period from field drilling and development in OPGEE for conventional oil operations [g CO ₂ eq./MJ of crude oil produced]. Data from Yeh et al [8].	91
7.6	Land use GHG emissions for 150 year analysis period from field drilling and development in OPGEE for conventional oil operations [g CO ₂ eq./MJ of crude oil produced]. Data from Yeh et al [8].	92
7.7	Default inputs for drilling calculations.	93
7.8	Streams flowing into and out of the reservoir-well interface process. I/O denotes input or output stream	95
7.9	Streams flowing into and out of the wellbore/downhole pump process. I/O denotes input or output stream	97
7.10	Streams flowing into and out of the wellbore/downhole pump process. I/O denotes input or output stream	99
7.11	Secondary parameter inputs to the wellbore/downhole pump worksheet	99
7.12	Reynold's number (Re) ranges of different flow patterns. Data from McAllister [9].	102

7.13 Streams flowing into and out of the bitumen mining process. I/O denotes input or output stream	106
7.14 Secondary parameter inputs to the bitumen mining worksheet	106
7.15 Characteristics of operating mining projects	108
7.16 Non-integrated PFT mining energy intensities	111
7.17 Comparison between stand-alone mine energy consumption estimates based on COSIA mine template to integrated NFT mining and upgrading energy consumption reported by AER	113
7.18 Integrated NFT mining energy intensities	114
7.19 Streams flowing into and out of the separation process. I/O denotes input or output stream	118
7.20 Secondary parameter inputs to the separator worksheet	118
7.21 Streams flowing into and out of the crude oil dewatering process. I/O denotes input or output stream	120
7.22 Secondary parameter inputs to the crude oil dewatering worksheet	120
7.23 Streams flowing into and out of the ' <i>Crude oil stabilization</i> ' process. I/O denotes input or output stream	123
7.24 Secondary parameter inputs to the ' <i>Crude oil stabilization</i> ' worksheet	123
7.25 Streams flowing into and out of the heavy oil upgrading process. I/O denotes input or output stream	124
7.26 Inputs to OPGEE upgrading module from the Oil Sands Technology Upgrading Model (OSTUM)	129
7.27 Streams flowing into and out of the ' <i>Heavy oil dilution</i> ' module. I/O denotes input or output stream	131
7.28 Secondary parameter inputs to the ' <i>Heavy oil dilution</i> ' worksheet	131
7.29 Streams flowing into and out of the crude oil storage module. I/O denotes input or output stream	132
7.30 Secondary inputs for crude oil storage.	134
7.31 Streams flowing into and out of the produced water treatment process. I/O denotes input or output stream	135
7.32 Typical concentrations of process water pollutants. Table from Vlasopoulos et al [10].	135
7.33 Categorization of water treatment technologies. Table based on table from Vlasopoulos et al. [10], with minor modifications	137
7.34 Default inputs for surface processing.	139
7.35 Streams flowing into and out of the makeup water treatment process. I/O denotes input or output stream	140
7.36 Streams flowing into and out of the water injection process. I/O denotes input or output stream	142
7.37 Streams flowing into and out of the steam generation process. I/O denotes input or output stream	144
7.38 Hydrogen constant a_H as a function of API gravity.	149
7.39 Gas turbine model results for hypothetical turbines A-D. These results serve as input data to OPGEE GT model.	152
7.40 Default inputs for steam injection calculations.	155
7.41 Streams flowing into and out of the flaring process. I/O denotes input or output stream	157
7.42 Sources of flaring data and construction notes	157

7.43 Data requirements for utilizing field-specific flaring calculation.	158
7.44 Stoichiometric relationships for complete combustion.	162
7.45 Default inputs for venting, flaring, and fugitive emissions.	165
7.46 Streams flowing into and out of the venting process. I/O denotes input or output stream	166
7.47 Streams flowing into and out of the gas gathering process. I/O denotes input or output stream	168
7.48 Streams flowing into and out of the glycol dehydrator process. I/O denotes input or output stream	169
7.49 Settings for non-varying operating parameters in Aspen HYSYS TEG dehydration unit simulations. Source "def." is OPGEE assumed default from prior model versions.	171
7.50 Ranges of independent variables explored in TEG dehydration Aspen HYSYS modeling.	172
7.51 Default inputs for surface processing.	177
7.52 Streams flowing into and out of the acid gas removal process. I/O denotes input or output stream	180
7.53 Settings for non-varying operating parameters in Aspen HYSYS AGR unit simulations. Source "def." is OPGEE assumed default from prior model versions.	183
7.54 Ranges of independent variables explored in generating predictive equations for AGR energy use. DEA-HL = DEA-high-load	184
7.55 Settings for fixed operating parameters in Aspen HYSYS desulfurization plant simulations.	197
7.56 Default inputs for surface processing.	202
7.57 Streams flowing into and out of the demethanizer process. I/O denotes input or output stream	204
7.58 Settings for fixed operating parameters in Aspen HYSYS demethanizer plant simulations.	207
7.59 Ranges of independent variables explored in generating predictive proxy models using Aspen HYSYS for demethanizer plant.	207
7.60 Default inputs for surface processing.	213
7.61 Streams flowing into and out of the pre-membrane chiller process. I/O denotes input or output stream	215
7.62 Default inputs for surface processing.	217
7.63 Streams flowing into and out of the CO ₂ separation membrane process. I/O denotes input or output stream	218
7.64 Default inputs for surface processing.	220
7.65 Streams flowing into and out of the Ryan-Holmes separation process. I/O denotes input or output stream	221
7.66 Default inputs for Ryan-Holmes process.	223
7.67 Streams flowing into and out of the gas flooding compressor. I/O denotes input or output stream	224
7.68 Streams flowing into and out of the gas lifting compressor. I/O denotes input or output stream	227
7.69 Streams flowing into and out of the gas reinjection compressor. I/O denotes input or output stream	228

7.70 Streams flowing into and out of the CO ₂ reinjection compressor. I/O denotes input or output stream	229
7.71 Streams flowing into and out of the sour gas reinjection compressor. I/O denotes input or output stream	231
7.72 Streams flowing into and out of the VRU compressor. I/O denotes input or output stream	233
7.73 Default inputs for Transport.	255
7.74 Minimum Miscibility Pressure and API Gravity Default Correlation. Source: [11].	262
7.75 Temperature Adjustment to Minimum Miscibility Pressure Default Correlation Source: [11].	262
7.76 Default inputs for production and extraction.	265
7.77 Description of OPGEE's Associated Gas Processing Schemes	268
8.1 Types and size ranges of the drivers embedded in OPGEE.	271
8.2 Default inputs for drivers calculations.	273
8.3 Cement blends modeled in OPGEE. ^a	280
8.4 Combustion technologies and fuels included in OPGEE.	285
8.5 ARB data used in the calculation of venting emissions factors (unit specified below). Source: [12].	286
8.6 ARB data used in the calculation of fugitives emissions factors (unit specified below). Source: [12].	286
8.7 ARB data for gas dehydrators, for systems with and without vapor recovery systems (VRS). Source: [13].	287
8.8 An example of EPA emissions factors for oil and gas production components (g/unit-yr). Source: [14].	287
9.1 Studies considered for inclusion.	302
9.2 Data types found in studies determined to contain original data of types activity factors (AF), leakage fraction (LF), leakage quantity (LQ), or default-zero (DZ). AF data include equipment quantification (EQ), component quantification (CQ), or activity quantification (AQ).	304
9.3 Component counts for standard equipment-component pairs, resulting from computations performed on OPGEE supplemental VF worksheet.	310
9.4 Sources of data on fraction leaking components.	312
9.5 Resulting fraction leaking (FL) data for the standardized component categories defined above.	312
9.6 Properties of emissions distributions for component-level emissions.	314
9.7 Properties of emissions distributions by originating study.	314
9.8 Properties of each category of gas well completion or well workover, sorted by application of hydraulic fracturing (HF) and application of emissions reduction method (flaring or reduced emissions completions (REC)).	322
9.9 Properties of reported liquids unloading fractional loss rates from Allen et al. 2014b [7].	323

9.10 Loss rates for off-site emissions, all expressed in fraction of gas flow into the process stage of note.	325
A.1 Acronyms and abbreviations.	332
B.1 Mathematical symbols and subscripts.	335
C.1 Emissions sources from exploratory operations. For inclusion: 0 = not included, 1 = included.	340
C.2 Emissions sources from drilling operations.	341
C.3 Emissions sources from production and extraction operations.	342
C.4 Emissions sources from surface processing operations.	343
C.5 Emissions sources from maintenance operations.	343
C.6 Emissions sources from waste treatment and disposal operations. . .	344
C.7 Emissions sources from transport.	345

1 Acknowledgements

The construction and improvement of OPGEE has benefitted from significant technical and financial support.

Because OPGEE is an open-source project, we would like to acknowledge technical support, feedback, error corrections, and other useful suggestions from the following individuals: Jessica Abella (ICF International), Joule Bergerson (University of Calgary), Kevin Cleary (California Air Resources Board), John Courtis (California Air Resources Board), Trevor Demayo (Chevron), Cheryl Dereniwski (IHS), Jacob Englander (Stanford University), Jackie Forrest (IHS), Sebastian Galarza (International Council on Clean Transportation), Deborah Gordon (Carnegie Endowment for Global Peace), Gary Howorth (Energy Redefined), Johnathan Lillien (Chevron), Ella Lowry (Stanford University), Christopher Malins (International Council on Clean Transportation), Jeremy Martin (Union of Concerned Scientists), Simon Mui (Natural Resources Defense Council), Don O'Connor (S&T² Consultants), Jeff Rosenfeld (ICF International), Greg Schively (Booz Allen Hamilton), Timothy Skone (National Energy Technology Laboratory), Yuchi Sun (Stanford University), Luke Tonachel (Natural Resources Defense Council), Stefan Unnasch (Life Cycle Associates, LLC), Ann-Catarin Vaage (Statoil), Michael Wang (Argonne National Laboratory), Wojciech Winkler (European Commission, DG Climate).

Of course, all remaining errors and omissions remain the responsibility of the model authors.

We would like to acknowledge funding support for the development of OPGEE from the California Environmental Protection Agency, Air Resources Board (primary funder through research grants 10-418 and 13-408). We would like to acknowledge additional funding support for OPGEE development and application from: Carnegie Endowment for Global Peace; European Commission, Directorate General Climate; International Council on Clean Transportation; and Stanford University School of Earth Sciences.

Part I

Introduction and user guide

2 Introduction

The Oil Production Greenhouse gas Emissions Estimator (OPGEE) is an engineering-based life cycle assessment (LCA) tool that estimates greenhouse gas (GHG) emissions from the production, processing, and transport of crude petroleum. The system boundary of OPGEE extends from initial exploration to the refinery gate (see Figure 2.1).

This technical documentation introduces OPGEE and explains the calculations and data sources in the model. First, the overall goals and motivation for OPGEE are described. Then, the general structure of OPGEE is introduced with a brief explanation of the worksheets contained in the model. Next, each production stage is explained in detail, outlining the methods and assumptions used to generate estimates of energy use and emissions for that stage. Then supplemental calculation worksheets are outlined. Next, the gathering worksheets which collect and aggregate intermediate results are described. Lastly, we describe the worksheets that contain fundamental data inputs.

Box 1.1. Goals of OPGEE

1. Build a rigorous, engineering-based model of GHG emissions from oil production operations.
2. Use detailed data, where available, to provide maximum accuracy and flexibility.
3. Use public data wherever possible.
4. Document sources for all equations, parameters, and input assumptions.
5. Provide a model that is free to access, use, and modify by any interested party.
6. Build a model that easily integrates with existing fuel cycle models and could readily be extended to include additional functionality (e.g. refining)

2.1 Model motivation

Current research suggests that GHG emissions from petroleum production can be quite variable [15–22]. Facilities will have low GHG emissions per unit of energy produced if they do not rely on energy intensive production methods and apply effective controls to fugitive emissions sources. In contrast, some crude oil sources can have higher GHG emissions if they rely on energy-intensive production methods.

The variability in crude oil production emissions is partly due to the use of energy-intensive secondary and tertiary recovery technologies [20, 23, 24]. Another major factor is significant variation in the control of venting, flaring and fugitive (VFF) emissions [25–27]. Other emissions arise from increased pumping and separation work associated with increased fluid handling in depleted oil fields (i.e., fields with a high water-oil ratio).

The existing set of general fuel cycle emissions models, exemplified by GREET and GHGenius [24, 28], cover a wide range of transport fuels, from biofuels to electric vehicles. These broad models have the advantage of being publicly available and transparent. Unfortunately, they lack process-level detail for any particular fuel cycle and only represent pathway averages. For example, conventional crude oil production in GREET is modeled using a common default production pathway, fuel mix, and energy efficiency. While these LCA tools have been useful to date, future regulatory approaches will require a more specific method of assessing the differences between crude oil sources.

2.2 OPGEE model goals

The goals of OPGEE development are listed in Box 1.1.

First, OPGEE is built using engineering fundamentals of petroleum production and processing. This allows more flexible and accurate emissions estimations from a variety of emissions sources.

OPGEE is constructed using *Microsoft Excel* to ensure transparency and maximum accessibility by stakeholders, including industry, governments, and members of the public. OPGEE will be available for download from Stanford University servers, and servers of future institutions in which Adam Brandt is employed. This will ensure its future availability. Regular updates of the model are expected in intervals of 1-2 years.

Another goal of OPGEE is the generation of comprehensive documentation. Model functions and input data are documented within the *Excel* worksheet to allow effective use and modification of the tool by users. Additionally, this document serves to explain model calculations and assumptions and provides information on model data sources.

2.3 OPGEE model construction

2.3.1 Model functional unit

The functional unit of OPGEE is 1 MJ of crude petroleum delivered to the refinery entrance (a well-to-refinery, or WTR process boundary). This functional unit is held constant across different production and processing pathways included in OPGEE. This functional unit allows integration with other fuel cycle models that calculate refinery emissions per unit of crude oil processed, and to enable integration with refinery emissions models such as PRELIM [29]. The heating value basis can be chosen as lower or higher heating value (LHV or HHV), depending on the desired basis for the emissions intensity. The model defaults to LHV basis for best integration with GREET.

2.3.2 Model scope and focus

OPGEE includes emissions from all production operations required to produce and transport crude hydrocarbons to the refinery gate (see Figure 2.1 for model system boundaries). Included production technologies are: primary production (e.g. water injection), secondary production (e.g. water flooding), and major tertiary recovery technologies (also called enhanced oil recovery or EOR, e.g. CO₂ EOR). Bitumen mining and upgrading processes are also included.

2.3.3 Spreadsheet structure

OPGEE is modular in structure, with interlinked worksheets representing each production stage. Within each major production stage, a number of activities and processes occur (e.g., fluid production or fluid injection). Calculations take place sequentially and are numbered in a hierarchical fashion (see Box 2.1 for explanation of pointers to the model in this document).

2.3.4 Modeling detail and default specifications

OPGEE models oil production emissions in more detail than previous LCA models. For example, the energy consumed in lifting produced fluids (oil, water, and associated gas) to the surface is computed using the fundamental physics of fluid lifting, accounting for friction and pump efficiencies.

Increased modeling detail results in an increase in the number of model parameters. All required inputs to OPGEE are assigned default values that can be kept as is or changed to match the characteristics of a given oil field or marketable crude oil blend. If only a limited amount of information is available for a given facility, most input values will remain equal to defaults. In contrast, if detailed field-level data are available, a more accurate emissions estimate can be generated.

For some processes and sub-processes, correlations or relationships are developed for defaults, which we call "smart defaults". For example, the amount of water produced with oil (water-oil-ratio, or WOR) affects the energy consumed in lifting, handling, and separating fluids. If the WOR is known, it can be inputted directly. However, in some regions, water production is not reported, so OPGEE

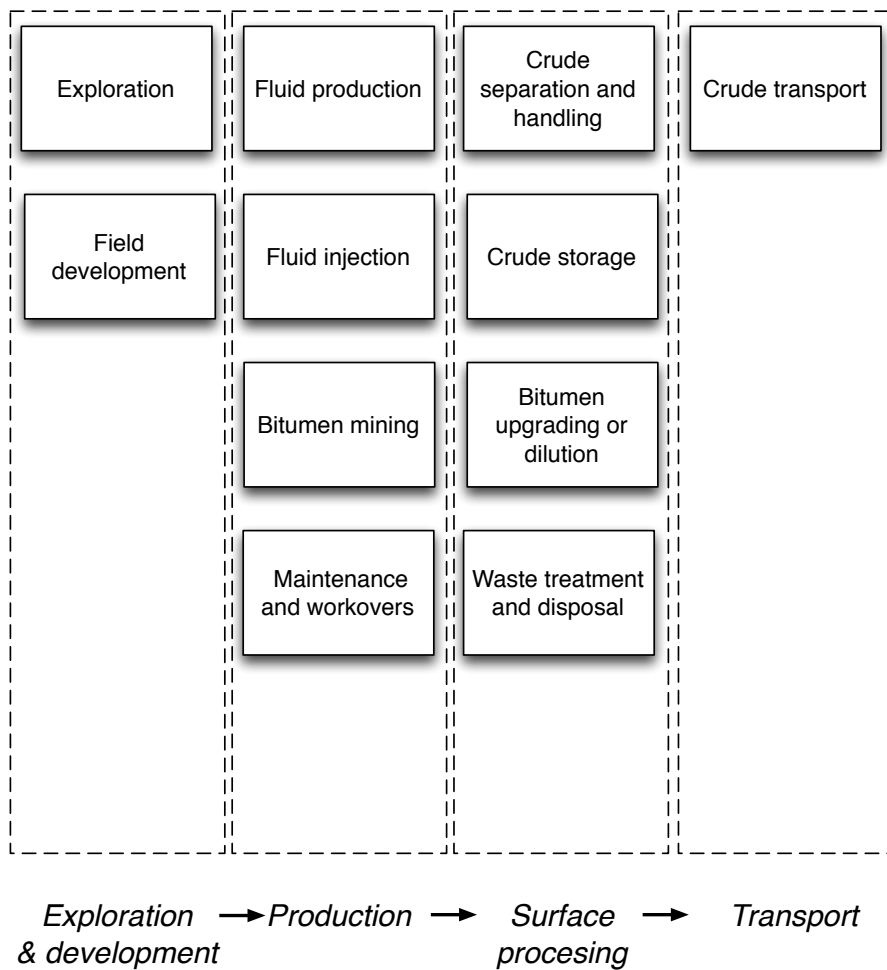


Figure 2.1: Schematic chart showing included stages within OPGEE.

includes a statistical relationship for water production as a function of reservoir age (see Section 4.3.0.7 for a description of the analysis underlying this smart default).

A workflow for updating and improving the data basis and accuracy of an emissions estimate using OPGEE is shown in Figure 2.2. This workflow represents one possible way that OPGEE could be used.

2.3.5 Emissions sources classification

Each process stage or sub-process in OPGEE can result in a variety of emissions sources. For example, the '*Drilling & Development*' process stage includes the terrestrial drilling sub-process. Terrestrial drilling could include the following emissions sources:

- Combustion emissions from drilling rig prime mover;
- Flaring emissions from drilling rig;
- Vents and other upset emissions from drilling rig;

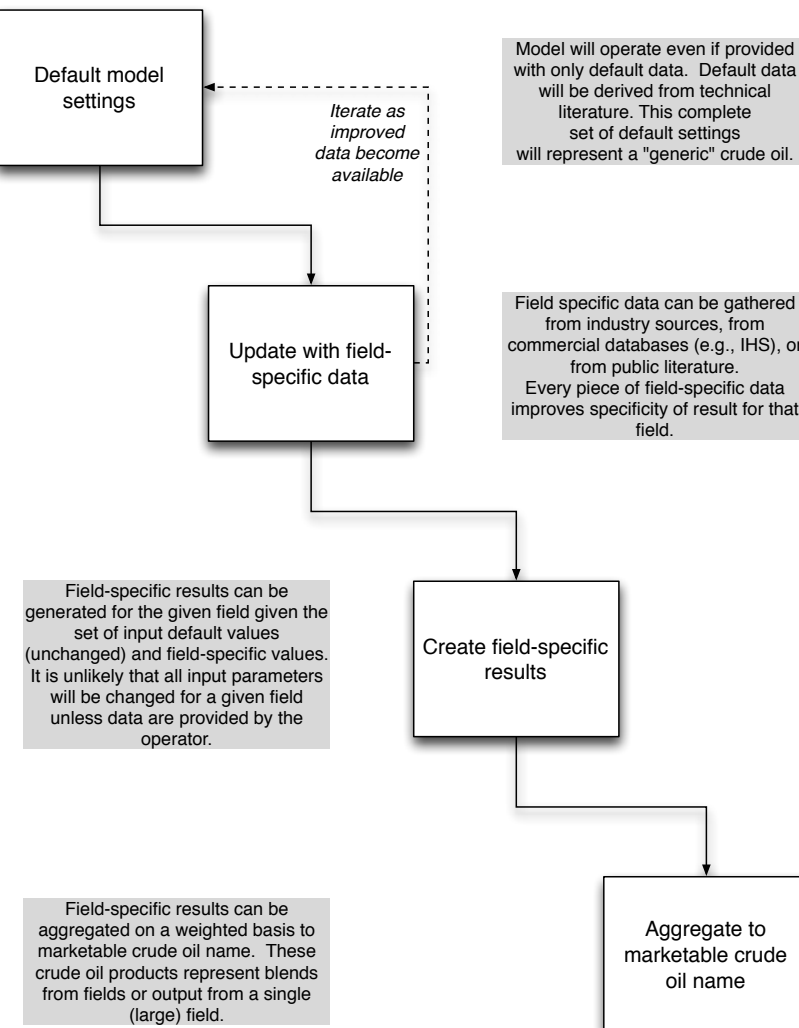


Figure 2.2: Proposed workflow for improving emissions estimates using OPGEE.

- Combustion emissions from work performed in land clearing and site preparation;
- Biogenic emissions from ecosystem disturbance during development;
- Embodied emissions in cement and casing;
- Embodied emissions in other consumable materials (e.g., fracturing sand)

Note that these emissions sources are of significantly different magnitude and have different causation and potential methods of mitigation. In total, over 100 emissions sources are classified in OPGEE v3.0a across all process stages (e.g., all included processes and sub-processes). See Appendix C for a complete tabulation and classification of emissions sources. Model coverage is also shown in the 'Model Coverage' tab of OPGEE v3.0a.

Table 2.1: Emissions classification, order of magnitude emissions, and significance description.

Class	Est. mag. [gCO ₂ /MJ]	Description
*	0.01	Minor emissions sources not worthy of further study or estimation. This is the most common classification. One-star emissions are accounted for by adding a value for miscellaneous minor emissions.
**	0.1	Minor emissions sources that are often neglected but may be included for physical completeness.
***	1	Sources that can have material impacts on the final GHG estimate, and therefore are explicitly modeled in OPGEE.
****	10	Sources that are large in magnitude (though uncommon). Examples include steam production for thermal oil recovery and associated gas flaring. These sources are significant enough to require their own dedicated OPGEE modules.

2.3.6 Emissions source significance cutoffs

It would be infeasible (and counter-productive) to attempt to estimate the magnitude of every emissions source listed in Appendix C. Fortunately, a small number of emissions sources will result in most of the emissions from petroleum production operations.

For this reason, emissions sources included in the OPGEE system boundary are classified by estimated emissions magnitude. These emissions magnitudes are meant to represent *possible* emissions magnitudes from a source, not the actual emissions that would result from that source for any particular field. An order-of-magnitude estimation approach is used, with each source assigned a rating in “stars” from one-star (*) to four-star (****) corresponding to 0.01 to 10 g CO₂ eq. per MJ of crude oil delivered to the refinery gate. These classifications are explained in Table 2.1.

Emissions estimated to be one-star emissions (*) are not modeled in OPGEE due to insignificant magnitude. Since these small sources are known to have non-zero emissions, they are included in the overall emissions estimate by including a “small sources” term. Two-star (**) sources are included simply or are included in the small sources term. Often, two-star sources are minor in magnitude, but are modeled due to the need to model the physics and chemistry of crude oil production and processing.¹ Three-star (***) sources are explicitly modeled in OPGEE. Four-star sources (****) are modeled in detail with stand-alone modules to allow variation and uncertainty analysis.

‘Results 2.8’

2.3.7 Data sources

Because of the need for transparent data basis, OPGEE uses data from a variety of technical reference works. For example, emissions factors are derived from standard engineering references from the American Petroleum Institute (API) and Environmental Protection Agency (EPA) [30?]. A large number of technical references, journal articles, and fundamental data sources have been consulted during the construction of OPGEE, including:

- Exploration and drilling [30–37]

¹No strict criteria exist to determine the inclusion or exclusion of two-star sources. Modeler judgement is applied to determine the need for modeling these sources.

- Production and surface separations [4, 14, 30, 38? –65]
- Secondary and tertiary recovery [66–71]
- Water treatment and waste disposal [37, 60, 63, 72–75]
- Venting, flaring, and fugitive emissions [14, 38–40, 40–46, 76–80]
- Petroleum transport and storage [9, 43, 46, 56, 79, 81–84]

3 User guide

OPGEE is divided into four types of worksheets: (1) input sheets, (2) process stage worksheets, (3) supplementary worksheets, and (4) output gathering worksheets.

3.1 Input and output worksheets

'Inputs' worksheet Data are entered on the input worksheet in OPGEE v3.0a. This worksheet is labeled '*Inputs*' and is colored green. The user can input a simplified set of ≈ 50 data inputs on the '*Inputs*' worksheet. Data for hundreds of fields can be entered on the '*Inputs*' sheet. The data entered by the user are stored on the '*Inputs*' sheet without modification, so the '*Inputs*' sheet can be used to compile and store data for a variety of operations.

OPGEE v3.0a is run from the '*Inputs*' sheet. The user enters the starting field of analysis and the ending field of analysis and presses the "Run Assessment" button. See more detail about using the model below.

'Results' worksheet Results generated by OPGEE are stored in the '*Results*' worksheet. '*Results*' compiles information for the analyzed crude oils, and represents the holding sheet for all changed parameters that are adjusted by OPGEE algorithms. The '*Results*' sheet should be the place where the user obtains final results for runs of a particular field.

Note that the '*Results*' worksheet is the repository of all results for fields that are analyzed as part of a multi-field assessment.

3.2 Field summary worksheets

Field summary worksheets present information about the field most recently analyzed. Flows for the field under analysis are presented and organized in the '*Flow Sheet*' worksheet. Process stage calculations are compiled into summed energy consumption (including energy co-production credits) and summed GHG emissions (including any offsets from co-produced energy). Output worksheets have brown-colored tabs.

'Active Field' worksheet The '*Active Field*' worksheet presents summary inputs and results in tabular and graphical form for the most recently processed field. After a run involving multiple fields, '*Active Field*' retains the data from last field assessed and does not save results for prior fields. '*Active Field*' allows for detailed tracking and analysis of the results for an individual field. The '*Active Field*' worksheet is described in Section 4.

The '*Active Field*' worksheet serves as a holding place for information on the field currently under analysis during a particular OPGEE run, and logic on the sheet applies many of the "smart defaults" defined below. For this reason, the '*Active Field*' worksheet should not be modified by the user (at least without great care).

'Flow Sheet' worksheet The '*Flow Sheet*' worksheet tracks all flows into and out of each process unit. All flows for a set of tracked liquid, gas, and solid products are tracked from primary extraction from geologic deposits until final disposition. The '*Flow Sheet*' is the key sheet for navigating to process level calculations.

'Energy Consumption' worksheet The '*Energy Consumption*' worksheet gathers data on energy consumption for sub-processes from all process worksheets. Each main process worksheet is included in the gathering table. All energy consumed is summed by type across all stages. This gross consumption is used to compute net consumption and energy imports and exports. The '*Energy Consumption*' worksheet is described in Section 6.1

'GHG Emissions' worksheet The '*GHG Emissions*' worksheet takes the energy quantities consumed in each stage and converts them to emissions using emissions factors. It also gathers any emissions associated with land use change and VFF emissions. Emissions are computed as gCO₂eq./d. The '*GHG Emissions*' worksheet is described in Section 6.2.

3.3 Process stage worksheets

Process stage worksheets form the core of OPGEE, and are where most model calculations occur. These worksheets have red-colored tabs.

Process stage worksheets are most easily accessed through the '*Flow Sheet*' tab, where each process unit or process stage is represented by a box with a "go to" button. Press the "go to" button for each process unit to jump to that process unit to examine calculations.

3.4 Supplementary worksheets

Supplementary worksheets support calculations throughout OPGEE, including: calculating intermediate outputs in the process stage worksheets, compiling output in the gathering worksheets, and calculating results in the '*Active Field*' worksheet. Supplementary worksheets have blue-colored tabs.

'Electricity' worksheet This worksheet determines the offsite electricity mix and calculates the energy consumption in onsite electricity generation (other than electricity co-generated with steam). The '*Electricity*' worksheet is described in Section ??.

'Drivers' worksheet This worksheet provides a database of energy consumption for different types and sizes of prime movers (gas and diesel engines, gas turbines and electric motors). The '*Drivers*' worksheet is described in Section 8.1.

'Fuel Cycle' worksheet This worksheet retrieves and calculates the fuel cycle energy consumption and GHG emissions for the calculation of credits/debits from fuel exports/imports. The '*Fuel Cycle*' worksheet is described in Section 8.2.

'Emission Factors' worksheet This worksheet retrieves and builds emissions factors for the calculation of combustion and non-combustion GHG emissions from energy use and losses. The '*Emissions Factors*' worksheet is described in Section 8.4.

'Venting & Fugitives' worksheet This worksheet calculates in detail the GHG emissions associated with Venting and fugitives. The '*Venting & Fugitives*' worksheet is described in Section ??.

'Fuel Specs' worksheet This worksheet provides fuel specifications required for OPGEE calculations. The '*Fuel Specs*' worksheet is described in Section 10.

'Inputs' worksheet This worksheet provides other needed data inputs such as conversion factors and steam enthalpies. The '*Input Data*' worksheet is described in Section 10.

<u>Flows into process</u>					
1	Stream number:		1	100	25
2	Stream description:	reservoir	reservoir	reservoir	
3	Phase	Component	Unit	Mass	Mass
4	Solid	Petroleum coke	tonne/d	—	—
5	Liquid	Unstabilized crude oil	tonne/d	208.9	—
6	Liquid	Raw bitumen	tonne/d	—	—
7	Liquid	Stabilized crude oil	tonne/d	—	—
8	Liquid	Upgraded crude oil	tonne/d	—	—
9	Liquid	Diluted crude oil	tonne/d	—	—
10	Liquid	NGL/ Diluent	tonne/d	—	—
11	Liquid	Water	tonne/d	29.3	1027.5
12	Liquid	Total liquids	tonne/d	238.2	1027.5
13	Gas	N ₂	tonne/d	—	0.9
14	Gas	O ₂	tonne/d	—	—
15	Gas	CO ₂	tonne/d	—	4.4
16	Gas	H ₂ O	tonne/d	—	—
17	Gas	CH ₄	tonne/d	—	22.3
18	Gas	C ₂ H ₆	tonne/d	—	2.0
19	Gas	C ₃ H ₈	tonne/d	—	1.5
20	Gas	C ₄ H ₁₀	tonne/d	—	1.0
21	Gas	CO	tonne/d	—	—
22	Gas	H ₂	tonne/d	—	—
23	Gas	H ₂ S	tonne/d	—	0.6
24	Gas	SO ₂	tonne/d	—	—
25	Gas	Total gas	tonne/d	—	32.5
26	Electricity	Total Elec.	MWh/d	—	—
27	Phase	Property	Unit	Value	Value
28	all	Temp	F	150.0	150.0
29	all	Pressure	psia	1556.6	1556.6

Figure 3.1: Example flow table in OPGEE 3.0 Flows are segregated by phase (solid, liquid, gas) or type (electricity). Fundamental properties of each stream, including temperature and pressure, are recorded at the bottom of each flow.

3.5 Structure of process stage worksheet

Most process stage worksheets are divided into four main sections: (1) Flows, (2) Inputs, (3) Calculations, (4) Outputs.

3.5.1 Flows

The flows section of each process stage worksheet tracks flows into the process and flows out of the process. Flows are denominated in tonnes per day (with the exception of electricity, denominated in MWh per day).

Flow cells are bold if directly computed in that sheet, and standard weight font if drawn directly from the flow table (for example, as an input to the process unit).

3.5.2 Inputs

The input data section is where the user enters the input parameters (e.g., API gravity, production volume). Inputs are divided into three types:

1. Key parameters

User free	Free to change
Default free	Holds default value
User dependent	Dependent or calculated, do not change
Default dependent	Dependent or calculated, do not change
Flow computed	Computed on the sheet
Flow from flow table	Pulled from another sheet

Figure 3.2: Types of cells. *User Free* and *Default Free* cells can be changed, while *Locked* cells should not be changed due to possibility of compromising model functionality. Flow sheet cells are either calculated in place or looked up from the large flow table.

2. Secondary parameters

3. Parameters defined on other sheets

Key parameters are drawn directly from the '*Active Field*' sheet. Secondary parameters are parameters that are used in the calculations in a process stage sheet, but are not fundamental enough to warrant inclusion on the '*Active Field*' sheet. Parameters defined on other sheets include anything previously defined, computed, or entered as a secondary parameters on another worksheet.

The input section of each worksheet has two data columns: *User* and *Default*, in columns M and N, respectively. The cells within the *User* column are the active cells, used to generate results in the calculations section. The cells within the *Default* column are used for reference, bookkeeping of default values, and generating defaults using correlations based on field data.

3.5.3 Calculations

Below the input data section is the calculations section of a worksheet, where intermediate model outputs are calculated. These intermediate outputs are summarized and compiled by the gathering worksheets to provide the overall energy and emissions measures compiled in the '*Outputs*' worksheet.

3.5.4 Outputs

The outputs section holds the summary results in terms of energy use and emissions that are later collected in the summary sheets.

3.5.5 Types of model cells

Four main types of cells exist in the calculation columns M and N: *User Free*, *User Locked*, *Default Free*, *Default Locked* (See Figure 3.2). As might be expected, locked cells should not be changed.¹ This is typically because locked cells contain formulas that draw on other cells and therefore should not be changed. "User Free" cells are cells that allow entry of user data.

¹Note: 'locked' cells are not locked via Excel password-protected locking mechanism, so they can be changed if desired by the user. However, this should be done with care, as the model can easily be rendered inoperable.

Box 2.1: Using OPGEE documentation and model together

OPGEE model documentation aligns with the model itself. Pointers to the model are contained in the right-hand margin of the model documentation in red, italic text. For example, the bubblepoint solution gas oil ratio is computed in row 65 of the '*Reservoir*' worksheet, and would be referred to in the right-hand margin as *Reservoir Row 65*

3.6 Working with OPGEE

This section explains how to work with OPGEE. Box 2.1 shows how to best use this documentation in concert with the OPGEE model itself.

3.6.1 Primary interaction

The easiest way to use OPGEE (which this document calls "primary" interaction) is to input key parameters for a field or set of fields to the '*Inputs*' sheet. These key parameters have the following characteristics:

- They have a significant effect on the GHG emissions from an oil and gas operation;
- They vary significantly across different operations and therefore could cause variability between different fields or projects;
- They are likely to be measured or are well-understood by operators.

The list of key inputs is a relatively small list of important factors. Other factors excluded from this list are left to process worksheets.

3.6.1.1 Controls on the '*Inputs*' worksheet

The '*Inputs*' worksheet is where key field parameters are entered for each field to be analyzed (see Figure 3.3). These key parameters are explained below.

'Inputs 1.1 - 1.8'

Production methods Controls to turn on or off production methods including down-hole pump, water reinjection, gas reinjection, water flooding, gas lifting, gas flooding, steam flooding, oil sands mine (integrated with upgrader), and oil sands mine (non-integrated with upgrader).

'Inputs 1.1'

- Downhole pump: This option is used to allow production when the naturally occurring energy of the reservoir does not suffice to produce fluids at a desired wellhead pressure.
- Water reinjection: This option is used when injecting a fraction of the produced water. This option does not apply if the amount of water injected is more than the amount of water produced after treatment.
- Gas reinjection: This option is used when injecting a percentage of the amount of gas produced. This option does not apply if the amount of gas injected is more than the amount of gas remaining after processing and VFF losses. The remaining gas is shown in the '*Gas Balance*' worksheet.

- Water flooding: This option is used when injecting an amount of water which is more than the amount of water produced. The amount of water injected is determined by the injection ratio (given in bbl water/bbl oil) and the fraction of water produced to reinjection/flooding must be set to 1.0. **The option of water reinjection must be turned OFF when the option of water flooding is turned ON.**
- Gas lifting: This option is used when gas is not injected into the reservoir, but injected into production string to reduce the pressure at the reservoir interface and induce production from the reservoir.
- Gas flooding: This option is used when injecting an amount of natural gas which is more than the amount of gas remaining after processing. The amount of gas injected is determined by the injection ratio (given in scf/bbl oil) and the fraction of remaining natural gas to reinjection must be set to 1.0. Alternately, this option can also be used when modeling EOR by flooding of nitrogen and carbon dioxide. **The option of gas reinjection must be turned OFF when the option of gas flooding is turned ON AND natural gas is selected as the flood gas.**
- Steam flooding: This EOR option is used when steam is injected to extract heavy crude oil. When this option is turned ON, steam-to-oil ratio (SOR) is needed to be entered or OPGEE will use its SOR default. The option of offshore field should be turned OFF when the option of steam flooding is turned ON.
- Oil sands mine (integrated or non-integrated with upgrader): The mining projects are mostly related to the Canadian oil sands. see section 7.5 for more details.

Field properties Field properties, including field location, field name, field age, field depth, oil production volume, number of producing wells, number of water injecting wells, production tubing diameter, productivity index, average reservoir pressure, average reservoir temperature, and whether the field is onshore (0) or offshore (1).

'Inputs 1.2'

Fluid properties A variety of fluid properties, including API gravity of crude oil and composition of produced associated gas (N_2 , CO_2 , C_1 , C_2 , C_3 , C_4+ , and H_2S molar concentrations).

'Inputs 1.3'

Production practices A variety of production practices or operating ratios. These include gas-to-oil ratio (GOR), water-to-oil ratio (WOR), water-injection ratio, gas lifting injection ratio, gas flooding injection ratio, the choice of flood gas (natural gas, N_2 , and CO_2), carbon dioxide enhanced oil recovery (CO_2 -EOR) related parameters (the percentage of the total injected CO_2 that is newly acquired, the source of CO_2 , and the percentage of the CO_2 sequestration credit assigned to the oilfield), steam-to-oil ratio (SOR), fraction of required electricity generated on site, fraction of remaining gas reinjected, fraction of water produced reinjected, fraction of steam generation via co-generation and volume fraction of diluent. WOR, GOR, and SOR are common parameters and self explanatory. Other less common parameters are explained below.

'Inputs 1.4'

- Water injection ratio: The ratio of the amount of water injected in water flooding to the amount of oil produced. This is required only when the option of water flooding is turned ON.
- Gas lifting injection ratio: The ratio of the amount of gas injected for lifting to the amount of liquid (water + oil) produced. The amount of gas injected for gas lifting **does not** include gas injected into the reservoir. This is required only when the option of gas lifting is turned ON.
- Gas flooding injection ratio: The ratio of the amount of gas injected in gas flooding to the amount of oil produced. This is required only when the option of gas flooding is turned ON.
- Flood Gas: The choice flood gas (natural gas, N₂, CO₂). This is required only when the option of gas flooding is turned ON.
- Percentage of total CO₂ injected that is newly acquired: The total amount of CO₂ injected consists of the sum of recycled CO₂ (that was previously injected, produced, and separated) and newly acquired CO₂ that is being injected for the first time. This is required only if the option of gas flooding is turned ON and CO₂ is the selected flood gas.
- Source of CO₂: CO₂ can be acquired either from natural subsurface reservoirs or captured from anthropogenic sources such as power plants. This is required only if the option of gas flooding is turned ON and CO₂ is the selected flood gas.
- Percentage of sequestration credit assigned to the oilfield: Greenhouse gas emissions-related legislation may allow the oilfield to claim a sequestration credit for CO₂ sequestered during CO₂-EOR operations. If such a credit applies, then this parameter controls the proportion assigned to the oilfield. This is required only if the option of gas flooding is turned ON and CO₂ is the selected flood gas.
- Fraction of required electricity generated onsite: This parameter determines the fraction of the electricity required that is generated onsite not including electricity co-generation with steam generation. The fraction entered can be greater than 1.0, designating electricity export to the grid.
- Fraction of remaining gas reinjected: This parameter determines the fraction of gas remaining that is reinjected into the reservoir. In the case of methane gas flooding this fraction must be equal to 1.0 (the amount of gas injected is more than the amount of gas remaining).
- Fraction of water produced reinjected: This parameter determines the fraction of water produced after treatment that is reinjected into the reservoir. In the case of water flooding this fraction must be equal to 1.0 (the amount of water injected is more than the amount of water produced).
- Fraction of steam generation via co-generation: OPGEE allows the modeling of steam generation for thermal EOR with or without electricity co-

generation. This parameter determines the share of steam generation via co-generation of electricity.

Processing practices Variables which represent the use of heater/treaters and stabilizer columns during oil phase separation, upgrader type, the choice of associated gas processing (AGR, dehydrator, demethanizer, and CO₂ EOR-related processing options), the ratio of gas flared to oil produced, and the ratio of gas vented to oil produced. Some parameters are explained below.

'Inputs 1.5'

- Heater/treater: Binary variables (0 or 1) are used to determine the use of a heater/treater in the oil-water separation process. 1 is used to turn ON the heater/treater and 0 is used to turn OFF the heater/treater. More detailed choices for heater/treaters are made in the '*Surface Processing*' worksheet.
- Stabilizer column: Binary variables (0 or 1) are used to determine the use of a stabilizer column in the oil-gas separation process. 1 is used to turn ON the stabilizer column and 0 is used to turn OFF the stabilizer column. The stabilizer column is defined in section 7.8.
- Associated gas processing path: A set of 7 gas processing configurations are allowed to be chosen by setting value in this cell from 1 to 8. These options range from no gas processing (1) to extensive gas processing and CO₂ separation via cryogenic separation (8). Significant detail is provided on these gas processing paths below.
- Ratio of flaring to oil production: This is the ratio of gas flared to oil produced.
- Ratio of venting to oil production: This is the ratio of gas vented (not including operational venting or default leaks) to oil produced. **This ratio only includes venting used for gas disposal, as an alternative to flaring. It does not address normal operational vents and leaks.** Other default leaks are accounted in the '*Venting & Fugitives*' worksheet.
- Volume fraction of diluent: In some cases heavy crude is diluted after production using light hydrocarbons. This parameter determines the fraction of diluent or natural gas liquid (NGL) in diluted crude. The default case is the minimum NGL blend as determined by user inputs. The process model produces NGL in the demethanizer (if applicable), a fraction of which is blended as specified in the '*Surface Processing*' worksheet.

Land use impacts Parameters that determine the GHG emissions from land use change, '*Inputs 1.6*' including ecosystem carbon richness and relative disturbance intensity.

'Inputs 1.6'

- Ecosystem carbon richness: Ecosystem carbon richness controls the amount of carbon emissions per unit of disturbed land, and varies from semi-arid grasslands (low potential carbon emissions) to forested (high potential carbon emissions).
- Field development intensity: The intensity of development can be chosen to be low, medium, or high. High intensity development resembles California

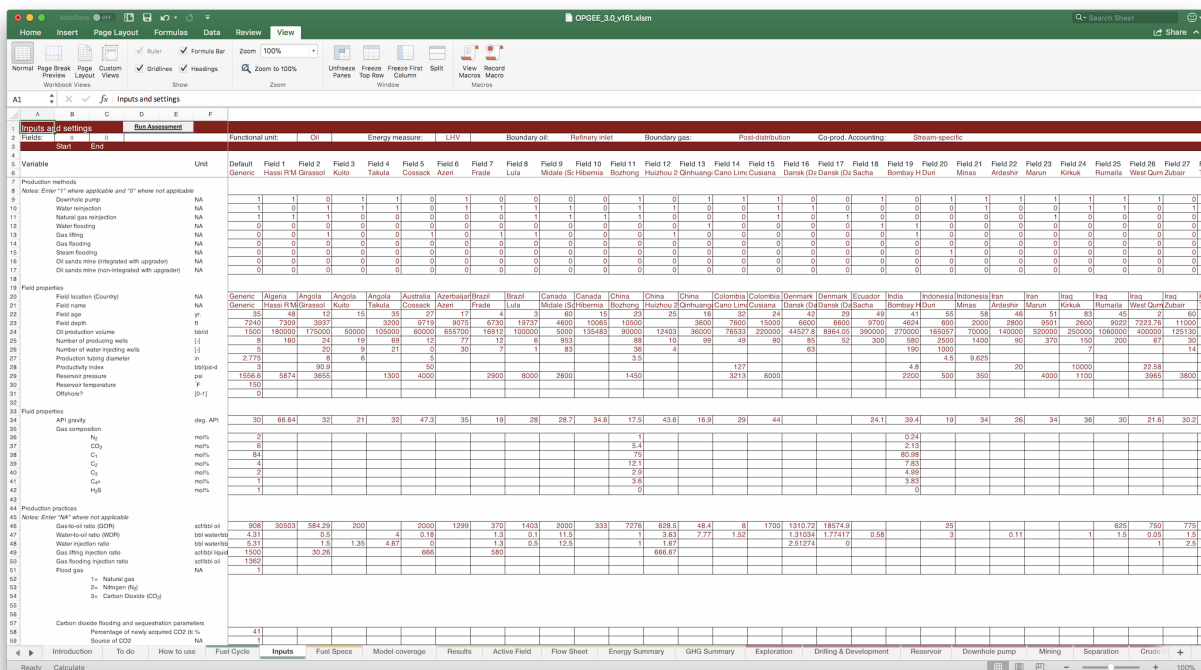


Figure 3.3: Data input section of the '*Inputs*' worksheet.

thermal EOR operations, well production and injection wells are drilled on tight spacing. Low intensity development resembles conventional natural gas development or directional drilling from centralized drill pads, where the land disturbed per well is small.

Crude oil transport Parameters which determine transport modes and distances. This includes the fraction of crude oil transported by each mode of transport and the transport distance (one way) of each mode. The total fraction of all modes may exceed 1.0 because more than one transportation leg may be involved for transporting the crude oil from field to refinery.

'Inputs 1.7'

Small emissions sources An added term to account for all emissions sources that are not explicitly included in OPGEE through calculations. Tables C.1 through C.7, as well as the ‘*Model Organization*’ worksheet in OPGEE, describe which sources are explicitly included in the model. All sources that are not explicitly included are deemed to small to model, and are included in the small emissions sources term.

'Inputs 1.8'

Parameters for multiple fields can be entered at a single time. After entry into '*Inputs*', values for key parameters are propagated to other worksheets as needed for calculations. Therefore, if a key parameter (such as API gravity) is to be changed, it **must** be changed on the front '*Inputs*' worksheet so that it is changed identically in all calculations.

OPGEE provides defaults for all required input parameters; these can be replaced with user inputs where data are available. In some cases, OPGEE calculates ‘smart default’ values dynamically based on user inputs for other parameters. For instance, the default flaring volume is determined from NOAA data based on the

specified field location [27]. These smart defaults can also be overruled by user inputs.

3.6.2 Secondary interaction

If more detailed data are available for a given oil production operation, and more specific estimates are desired, secondary interaction can be pursued by changing parameters on process-stage specific worksheets and supplementary worksheets.

It should not be necessary to change these secondary input parameters in basic use of OPGEE. The secondary parameters include parameters with less effect on the resulting emissions, that are not highly variable across operations, or that are less likely to be known by model users. Examples include compressor suction pressure and temperature, type of prime mover, or pump efficiency. Note that some of these parameters (e.g., pump efficiency) have significant effects on model results, but are not believed to be highly variable across fields.

All secondary input parameters are free for the user to change in the input data sections of the process stage worksheets. Parameters that are classified as *User Locked* (see Figure 3.2 above) should not be changed because they are either calculated from other primary inputs or derived from the '*Inputs*' worksheet.

Figure 3.4 shows the input data section of the '*Production & Extraction*' worksheet. Moving left to right across the screen, features of interest include:

Parameters and sub-parameters In columns A through K, the names and descriptions of parameters and calculation results are numbered in a hierarchical fashion. Each parameter or calculation result has a unique number to allow ease of reference to the model. For example, the water specific gravity (2.1.2) is calculated using the concentration of dissolved solids (1.2.1.1).

User and default columns Columns M and N include the user and default inputs for the production calculations. Column M is always used in the final calculations. Column N is included for reference, and includes default values. Before any user input is changed, all user values are equal to default values.

Free and locked cells As shown in Figure 3.2 above, *User Free* and *Default Free* cells are included with light tones, while *User Locked* and *Default Locked* cells are included with dark tones. For example, in Figure 3.4 the highlighted cell M37 represents the mol% of methane (C_1) in the associated gas. Because this quantity is a key input parameter and is defined on the '*Inputs*' worksheet, it is marked here as *User Locked*. Therefore, if the user wishes to change the gas composition, this should be done on the '*Inputs*' worksheet where gas composition is classified as *User Free*.

Units In column O, units are listed for all input parameters, variables, and calculation results (where applicable).

User and default reference Columns Q and S are spaces to record the data sources of input parameters. Where applicable, the source of the default value is listed in the *Default reference* column. If a user changes a parameter to a non-default value, they can place any desired information about the source (such as author, page, dataset, vintage, data quality, expected uncertainty, etc.) in the *User reference* column.

Notes To the right of the default reference column is the notes column (not shown, column Y). The *Notes* column contains explanatory notes or other information that may be useful to the user.

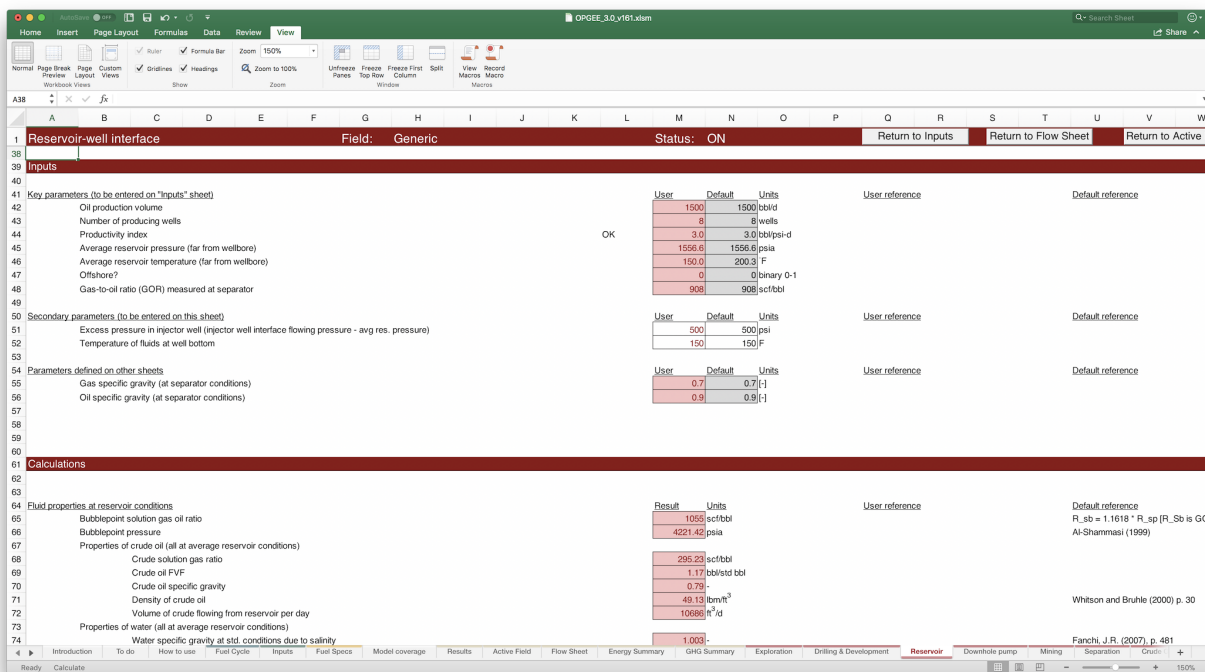


Figure 3.4: Input data section of 'Reservoir' worksheet. User inputs are in column M, while defaults are kept as reference in column N.

3.6.3 Checking for errors

It is possible to mistakenly enter data that are invalid, contradictory, or otherwise result in errors.

A summary indicator for model errors appears in the 'Results' worksheet as the "Overall Check." An overall check error is the result of an error in any of the fields that included in the model run, which appears as an error in the "Field by Field Check." To investigate an error in a specific field, the "End field" should be set equal to the field number of the field in question and the "Run Assessment" button should be clicked again. This will populate the 'Active Field' worksheet with the calculations regarding the error-causing field. Here, the error can be traced to a particular worksheet and cell by examining the 'Specific error checks.' Specific error checks can be debugged by moving to the worksheet and cell in question and tracing any logical or inputs errors that have flagged that error check. Common sources of errors include logical errors in pathway selection (e.g., more than one mutually exclusive technology selected) and input errors (e.g., gas composition sums to more than 100 mol%).

'Results 2.14'

'Results 2.13'

*'Active Field
4.1.1 - 7.1.29'*

Hints for using OPGEE without errors are given in Box 2.2.

Box 2.2: Hints for using OPGEE without errors

1. Do not change formulas in *User locked* or *Default locked* cells, as these can result in mis-calculation;
2. Always check error reports in '*Results*' section 2.14 and, if necessary, section 2.13, for errors before considering results final;
3. Use care to collect physically realistic and consistent data where default values will be overwritten (e.g., if depth of field is greatly increased, operating pressure will often increase as well);
4. To ensure reproducibility of results, document any sources for user inputs in the 'User Reference' column;
5. Save individual field assessments as separate worksheets to prevent incorrect propagation of changed cells.

Model error check:

OK

Table 1.1: Summary GHG emissions

GHG emissions [gCO ₂ eq/MJ]	
Active field	Girassol
Exploration	0.00
Drilling	0.04
Production	0.08
Processing	0.62
Maintenance	0.00
Waste	0.00
VFF	5.37
Misc.	0.50
Transport	0.93
Offsite emissions	-0.29
CO ₂ Sequestration	0.00
Net lifecycle emissio	7.24

Notes: Copy highlighted column and paste 'as numbers' to generate a record

Figure 1.1: Summary GHG emissions

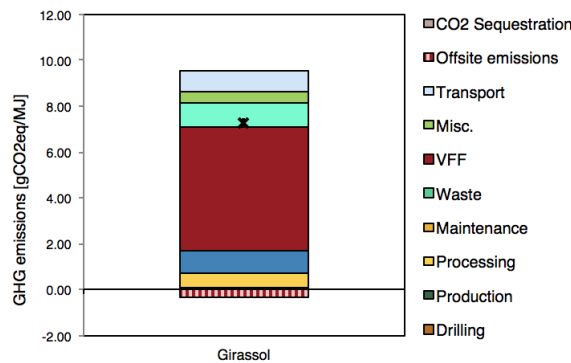


Table 1.2: Summary energy consumption

Energy consumption [MJ/MJ]	
	Girassol
Exploration	0.00
Drilling	0.00
Production	0.00
Processing	0.01
Maintenance	0.00
Waste	0.00
Transport	0.01
Total	0.024

Notes: Copy highlighted column and paste 'as numbers' to generate a record

Figure 1.2: Summary energy consumption

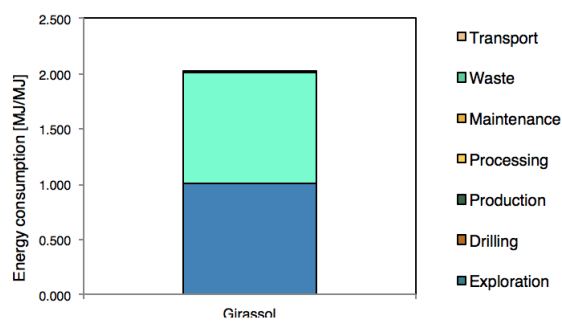


Figure 3.5: Graphical results for an example crude oil. These results from 'Active Field' Tables 1.1 and 1.2, Figures 1.1 and 1.2.

3.6.4 Results

After the user enters data to the '*Inputs*' sheet and clicks the Run Assessment button, OPGEE computes the resulting GHG emissions. The results are for the last field (End field) analyzed are stored in the '*Active Field*' sheet, while the results from all fields are stored in the '*Results*' in tabular form in gCO₂ equivalent GHG emissions per MJ LHV crude oil delivered to the refinery gate.² Emissions are broken down by stage (generally) or by type, with fugitive emissions for all process stages summed together for convenient interpretation as 'VFF' emissions. Total energy consumed per unit of energy delivered to the refinery gate is also presented in tabular and graphical form. These tabular and graphical results are illustrated in Figures 3.5.

'Active Field
Table 1.1'
'Results 2.1 - 2.14'
'Active Field Fig. 1.1'
'Active Field Table 1.2,
Figure 1.2'

²The heating value basis of the denominator crude oil can be changed so that emissions are calculated per MJ HHV of refinery input. This can be changed on the '*Fuel Specs*' worksheet. See discussion below in Section 10.4.

3.7 Inputs

3.7.1 Further details regarding the Inputs sheet

OPGEE has a built-in capability to analyze a number of fields or oil production projects and bookkeep the results for comparison and further analysis.

The capability to analyze multiple fields simultaneously is provided by a Microsoft VBA macro. In addition to running a number of fields in sequence, the macro programmatically resolves significant errors that arise from input data inconsistencies. It also automates iterative calculations such as the reconfiguration of gas composition in the case of gas lift or setting gas export to zero by incrementally increasing gas reinjection.

At the top of the '*Inputs*' worksheet the user enters the fields to be assessed by entering the starting field and the ending field. In the input data section the user enters available data for each assessed field. When limited datasets are available, the assessment macro will complete the datasets by filling required inputs with defaults and smart defaults where applicable. The results are generated for all fields in one computational run. The macro is started by pressing the "Run Assessment" command button.

'Inputs 1.1-1.8'

3.7.2 Assessment macro description

Figure 3.6 shows the outer structure of the assessment macro. For every field under study, the macro first copies user entries into the ('*Active Field*') worksheet. It then checks for empty user entries. For every empty user input, the macro copies the default value from the ('*Active Field*') worksheet. In the case of "0" entry for the number of producing wells, a warning appears and prompts the user to enter a valid number of producing wells. When the data set of the field under study is complete, the macro copies the complete set of data into the ('*Active Field*') worksheet, initiates the error correction and entry adjustments procedure, and returns the completed and corrected/adjusted set of data into the ('*Results*') worksheet. Finally the macro copies the full data set back into the ('*Active Field*') worksheet and returns the results into the ('*Results*') worksheet. The same process is repeated for each field under study.

The assessment macro is capable of fixing errors, performing iterative calculations and adjusting input parameters where necessary. It is not practical to perform these computational tasks manually when assessing a large number of projects (100+). The macro ensures consistent treatment across all fields. Errors that are addressed in the macro include:

- Discrepancies between country-average default flaring rate and entered GOR (e.g., flaring module predicts more flaring than field has gas available);
- Discrepancies between default fugitive emissions of gaseous components and gas available from production;
- Requirement to iteratively solve for the gas composition in the wellbore in the case of gas lift;
- Error with productivity index resulting in negative bottomhole pressures;

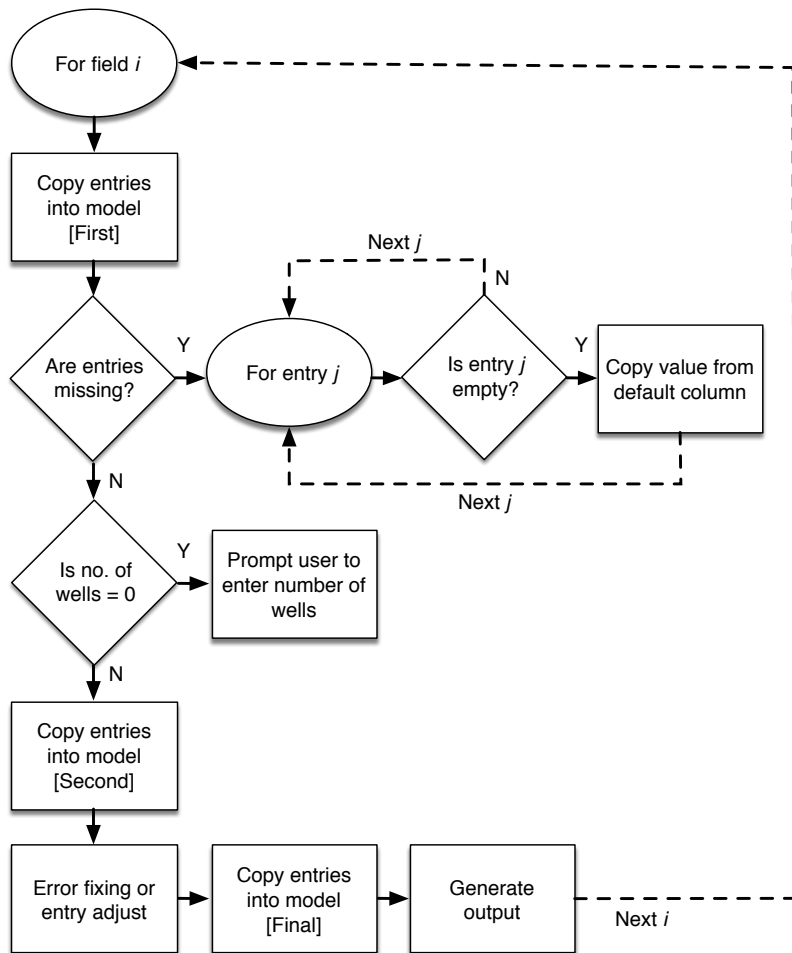


Figure 3.6: Logical structure of the assessment macro.

- Error resulting from very large frictional lifting penalties due to too-small default wellbore diameter;
- Requirement to iteratively solve for gas reinjected to result in 0 gas export.

Appendix D details the functioning of these error correction features.

Part II

Technical documentation

4 ‘*Active Field*’ gathering worksheet

4.1 Introduction to the '*Active Field*' worksheet

4.2 GHG calculations on the '*Active Field*' worksheet

In this worksheet the total energy consumption and GHG emissions for the most recently processed field are calculated and displayed in graphical form. Both the total energy consumption and total GHG emissions are calculated by process stage (e.g., Production & Extraction). First the total energy consumption is calculated as:

$$E_{tot} = \frac{E_{tot,dir} + E_{tot,ind} + EL_{VFF}}{E_{tot,out}} \quad [\text{MJ/MJ}_{out}] \quad (4.1)$$

where E_{tot} = total energy consumption of the process [MJ/MJ_{out}]; $E_{tot,dir}$ = total direct energy consumption (calculated in the '*Energy Consumption*' worksheet as net energy consumption) [MMBtu/d]; $E_{tot,ind}$ = total indirect energy consumption (calculated in the '*Energy Consumption*' worksheet) [MMBtu/d]; EL_{VFF} = total energy loss from VFF emissions [MMBtu/d]; and $E_{tot,out}$ = total process energy output [MMBtu/d]. The total process energy output is calculated as:

$$E_{tot,out} = Q_o \text{HV}_o + E_{ngl,blend} - E_{co,net} \quad [\text{MMBtu/d}] \quad (4.2)$$

where $E_{tot,out}$ = total process energy output [MMBtu/d]; Q_o = volume of oil production [bbl/d]; HV_o = heating value of crude oil [MMBtu/bbl];

$E_{ngl,blend}$ = amount of produced NGL that is added to crude oil [MMBtu/d]; and $E_{co,net}$ = net crude oil consumption, if applicable [MMBtu/d]. The heating value HV for the denominator crude oil can be selected as LHV or HHV.

If the allocation of co-products is done by energy value and not displacement then eq. (4.2) becomes:

$$E_{tot,out} = Q_o \text{HV}_o + E_{ngl,blend} - E_{co,net} + |\sum_k E_{k,exp}| \quad \text{and } E_{k,exp} < 0 \quad (4.3)$$

where $|\sum_k E_{k,exp}|$ = absolute sum of all energy exports [MMBtu/d].

Total energy consumption is allocated by process stage using the fraction of direct energy consumed in a stage (not including the energy consumption of electricity generation). The allocation of energy consumption to different process stages has no effect on the total energy consumption.

For each process stage, GHG emissions are broken down into three categories: (i) combustion/land use, (ii) VFF, and (iii) credit/debt. For combustion/land use emissions, the direct GHG emissions and land use GHG emissions associated with the process stage are summed in the '*GHG emissions*' worksheet. The direct GHG emissions from electricity generation, if any, are divided between the production & extraction and surface processing stages based on the shares of total direct energy consumption between these stages.

VFF emissions associated with a process stage are summed from the '*GHG emissions*' worksheet. Indirect GHG emissions calculated in the '*GHG emissions*' worksheet represent the total net credit/debt, which is allocated by process stage using the same allocation method used for allocating the total energy consumption.

This sheet also includes CO₂ sequestration credited accruing to the oilfield, which are described in Section 7.55.0.1.

Finally, the total energy consumption and GHG emissions from the process stages of crude oil extraction and surface processing of associated fluids are integrated with the total energy consumption and GHG emissions of crude oil trans-

'Active Field'

3.1.1. - 3.7.1,

Table 1'

'Active Field'

5.1.1. - 5.9.1'

Fuel Specs 1.1'

'GHG'

Emissions Table

1'

'GHG'

Emissions Table

1'

'GHG'

Emissions Table

2'

port to the refinery to calculate the life cycle energy consumption and GHG emissions on a well-to-refinery basis. The life cycle GHG emissions, for example, are calculated as:

$$EM_{LC} = EM_{PP,tot} \epsilon_{CT} + EM_{CT,tot} \left[\frac{\text{gCO}_2\text{eq}}{\text{MJ}_{ref}} \right] \quad (4.4)$$

where EM_{LC} = life cycle GHG emissions [gCO₂eq/MJ_F]; $EM_{PP,tot}$ = total GHG emissions from the process stages of crude oil production and processing [gCO₂eq/MJ_{out}]; ϵ_{CT} = crude oil transport loss factor (calculated based on the amount of crude oil lost in transportation) [-]; and $EM_{CT,tot}$ = total GHG emissions from transport [gCO₂eq/MJ_{ref}]. 1 MJ_{out} is one MJ of energy output from crude oil production and processing; and 1 MJ_{ref} is one MJ at refinery gate.

The life cycle energy consumption and GHG emissions are shown in tabular and graphical formats with full GHG emissions breakdown. The total GHG emissions has a separate category for VFF emissions. The energy content of fuels lost to VFF emissions is not tracked as a separate category of energy consumption.

*'Active Field
Tables 1.1 - 1.2
Figures 1.1 - 1.2
'*

4.3 Smart defaults and uncertainty distributions for missing key parameters

4.3.0.1 Default field age

Field age data were collected for global oil fields. A total of 6,502 global oil fields were collected from the Oil & Gas Journal 2010 *Worldwide Oil Field Production Survey* [85]. A total of 4837 of these fields had reported discovery dates. No data are available on date of first production, although this will most commonly occurs less than 5 years after discovery.

The histogram of field discovery dates is shown in Figure 4.1. Because the dataset has poor coverage of field-specific production data, a production-weighted average age figure was not thought to provide an accurate representation of the true production-weighted age distribution, so this was not calculated. The mean date of discovery in the dataset was 1972.1. If a conservative 3 year development timeline is assumed, an average of 35 years has elapsed between 1975 and 2010.

*'Active Field
2.2.3'*

However, many of these fields are likely small fields that do not supply large quantities of oil to the global export markets. It is known that giant oilfields are somewhat older on average than the general field population [86–89]. A database of 116 giant oilfields was collected (defined as all producing over 100 kbb/d in the year 2000) [87, Appendix A]. In total, these 116 fields produced \approx 32,000 kbb/d, or some 43% of global oil production in 2000.

These giant fields have a count distribution and production-weighted average age distribution that are somewhat older than the complete set of global fields. Figure 4.2 shows these distributions. The production-weighted average discovery year of the sample was 1960.2, for an average age of 40 years since discovery at the time of production data collection (weighted by year 2000 production data). Data on giant oilfield production in 2010 are not available. Due to the general global slowdown in the discovery of giant fields since the 1970s, it is likely that the age distribution of giant oilfields has not shifted in step with advancing years. Therefore, the production-weighted average age for large fields is likely now greater than 40 years.

4.3.0.2 Default field depth

Field depth data were collected for a large number of global oil fields [85]. A total of 6,502 global oil fields were collected from the Oil & Gas Journal 2010 *Worldwide Oil Field Production Survey*. Of these fields, 4,489 fields had depth data presented. For fields where a range of depths was presented, the deeper depth is used.

The distribution of depths by number of fields per depth range is presented in Figure 4.3. Because of sporadic reporting of production data in the same dataset, a production-weighted depth figure was not thought to provide an accurate representation. The mean depth for these 4,489 fields is 7,238, or \approx 7,240 ft. The standard deviation is 3,591 ft. The depth distribution has a longer right (deep) tail than left (shallow) tail, so the mean is somewhat larger than the median (median = 6,807 ft).

*'Active Field
2.2.4'*

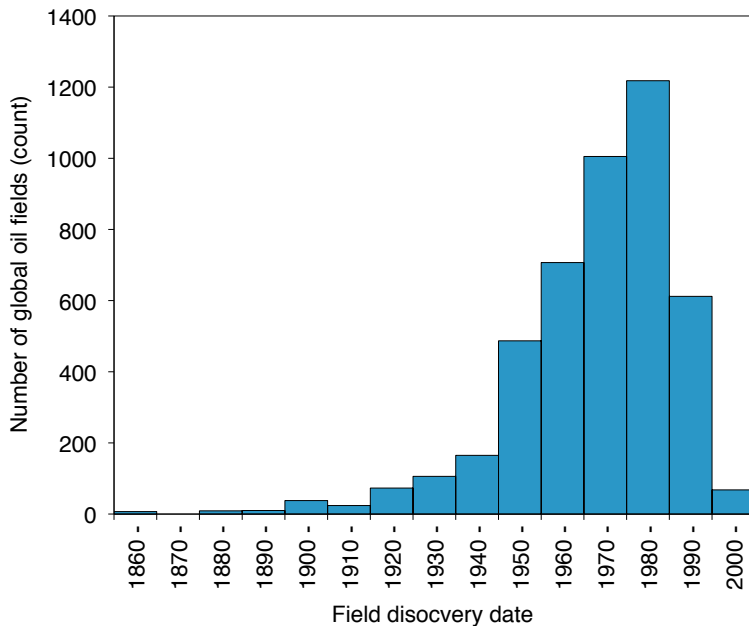


Figure 4.1: Distributions of global oilfield ages. Mean date of discovery (by count not by production-weighted average) is 1978.4.

4.3.0.3 Default production per well

Country-level oil production data and numbers of producing wells were collected for a large number of oil producing countries. Data from a total of 107 oil producing countries were collected from the *Oil & Gas Journal 2010 Worldwide Oil Field Production Survey* [90]. Production data and operating well counts for 2008 were collected from 92 of these 107 countries.

The distribution of per-well productivities for all countries is shown in Figure 4.4. A majority of oil producing countries produced less than 500 bbl/well-d. Weighting these well productivities by country-level share of global production, we see a very similar distribution.

Because of the large number of countries producing less than 500 bbl/well-d, we plot the distribution for countries under 500 bbl/well-d (see Figure 4.5). For the 55 countries with per-well productivity less than 500 bbl/well-d, the most common productivity by number of countries was the 0-25 bbl/well-d. However, when weighted by total production, the most common productivity bin is 75-100 bbl/well-d.

In 2008, the world produced 72822 kbbl/d from 883691 wells, for an average per-well productivity of 82 bbl/well. However, the very low productivity of the US oil industry (representing ≈ 512000 wells) pulls down this average significantly. Non-US producers averaged a per-well productivity of 183 bbl/well-d, which is used as default well productivity in OPGEE.

'Active Field
2.2.6'

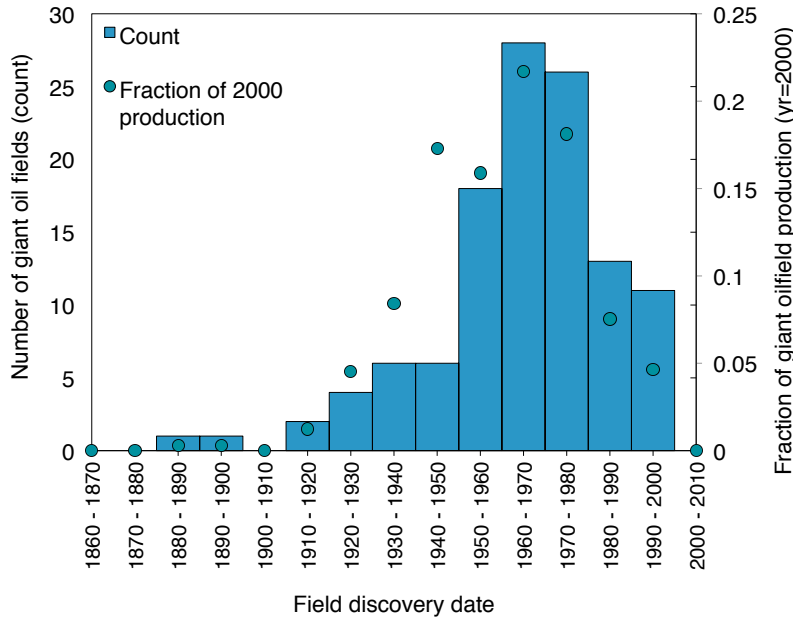


Figure 4.2: Distributions of giant oilfield ages. Mean date of discovery (by production-weighted average) is 1960.2.

Table 4.1: Mean and median injector to producer ratios.

Prod. well productivity	Mean	Median
0-10 bbl/d	0.193	0.143
10 - 100 bbl/d	0.326	0.254
100 - 1000 bbl/d	0.578	0.532
> 1000 bbl/d	0.716	0.831

4.3.0.4 Default number of injector wells

The default number of injector wells is a smart default based on the number of producing wells. To model this relationship, data from California, Alaska, and a variety of offshore fields was collected [91, 92]. Data from offshore fields is provided in Table 4.2 below. Per-well productivity across these fields ranges from less than 10 bbl/d to over 10,000 bbl/d.

A strong relationship is seen between the productivity of producing wells and the number of injection wells required. Highly productive wells require a significantly larger number of injectors. Figure 4.6 shows the relationship between the per-well productivity of a field and the ratio of injectors to producers.

From these data, a relationship was generated for the mean and median ratio for each logarithmic bin of production well productivity (see Table 4.1). Median values for each bin are used to define the smart default for the number of injector wells.

'Active Field
2.2.7'

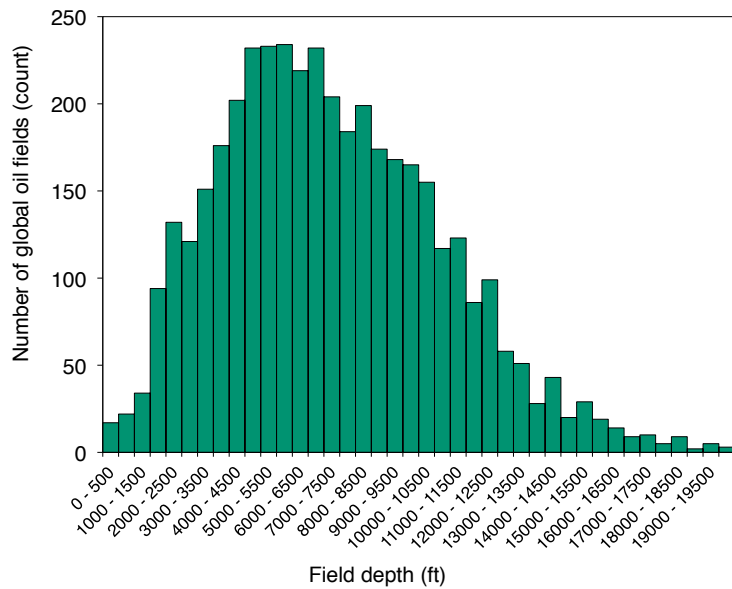


Figure 4.3: Distributions of global oilfield depths in bins of 500 ft depth. $N = 4489$ fields, mean = 7238 ft, SD = 3591 ft, median = 6807 ft.

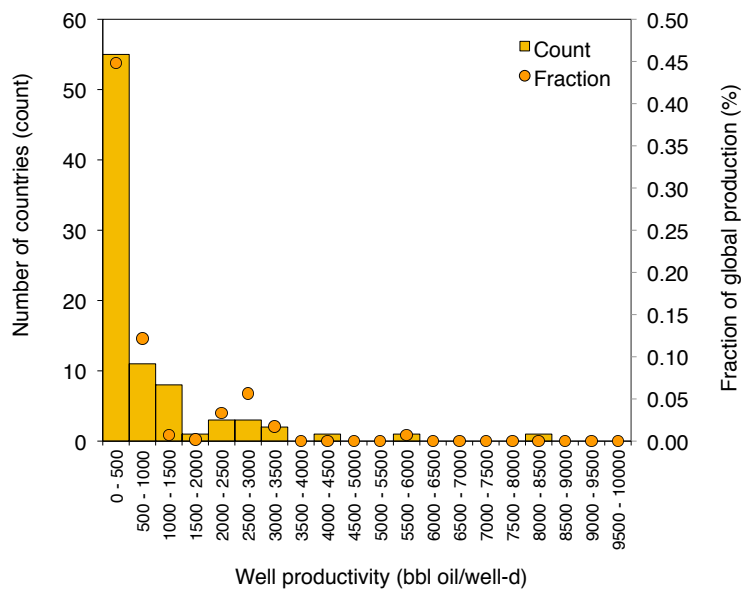


Figure 4.4: Distributions of oilfield per-well productivity (bbl oil/well-d) for bins of 500 bbl/d, counted by numbers of countries (bar) and by fraction of production (dot) $N = 92$ countries.

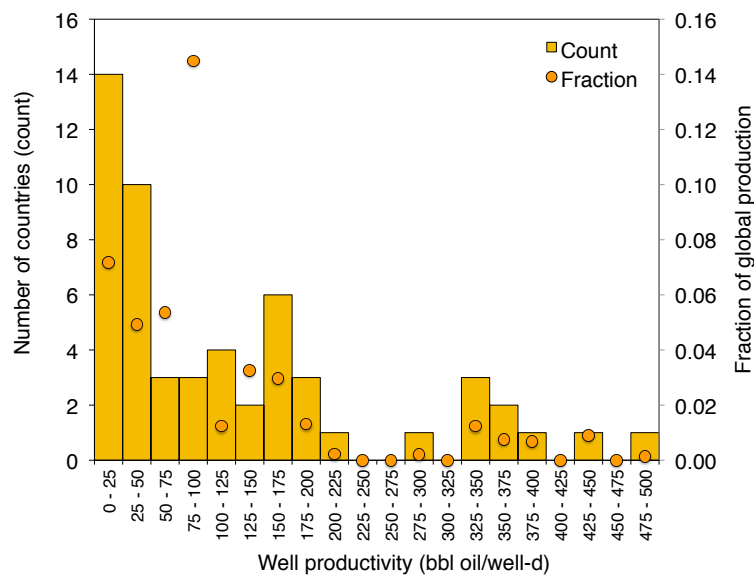


Figure 4.5: Distributions of oilfield per-well productivity (bbl oil/well-d) for all countries with per-well productivities lower than 500 bbl/well-d, counted by numbers of countries (bar) and by fraction of production (dot) $N = 55$ countries.

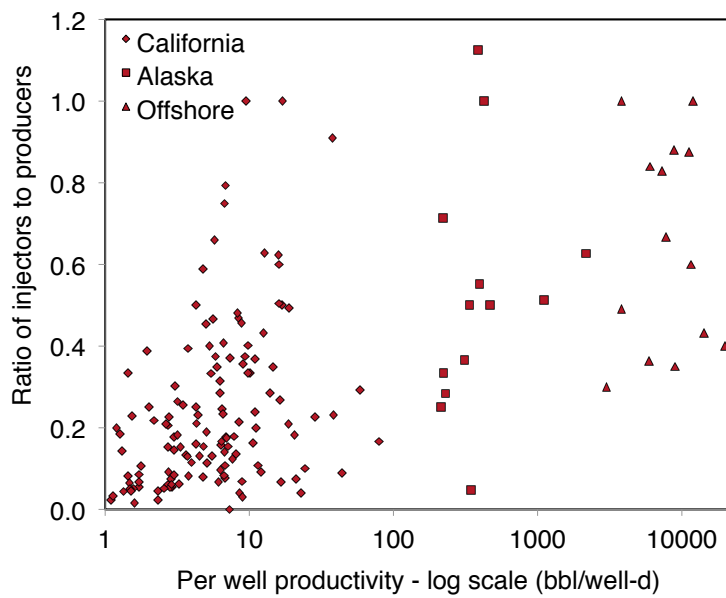


Figure 4.6: Ratio of producers to injectors as a function of per-well productivity. Source: Various.

Table 4.2: Data on production, number of production wells, and number of injection wells by offshore field.

Field	Prod. wells	Inj. wells	Prod. (bbl/d)	References
Dalia Gimboa	37 3	31 4	240000 14000	http://www.offshore-technology.com/projects/dalia/ http://www.statotoil.com/en/OurOperations/TradingProducts/CrudeOil/Crudeoilassays/Page/Gimboa.aspx http://www.offshore-technology.com/projects/girassol/ http://www.offshore-technology.com/projects/greater-plutonio/ http://www.exxonmobil.com/crudeoil/about_crudes_hungo.aspx http://www.fluor.com/projects/Pages/ProjectInfoPage.aspx?prjid=93 http://www.exxonmobil.com/crudeoil/about_crudes_kissanje.aspx http://www.ogj.com/articles/print/volume-103/issue-38/special-report/kizomba-b-attains-production-capacity-early.html
Hungo	20 30	20 26	240000 130000	http://www.fluor.com/projects/Pages/ProjectInfoPage.aspx?prjid=93
Kissanje	25	21	150000	http://www.fluor.com/projects/Pages/ProjectInfoPage.aspx?prjid=93
Mondo	17	17	65000	http://www.fluor.com/projects/Pages/ProjectInfoPage.aspx?prjid=93
Pazflor	25	22	220000	http://www.fluor.com/projects/Pages/ProjectInfoPage.aspx?prjid=93
Azeri	58	25	823000	http://www.fluor.com/projects/Pages/ProjectInfoPage.aspx?prjid=93
Albacora Leste	16	14	180000	http://www.fluor.com/projects/Pages/ProjectInfoPage.aspx?prjid=93
Bijupira	9	6	70000	http://www.fluor.com/projects/Pages/ProjectInfoPage.aspx?prjid=93
Frade	11	4	65000	http://www.fluor.com/projects/Pages/ProjectInfoPage.aspx?prjid=93
Jubarte	20	7	180000	http://www.fluor.com/projects/Pages/ProjectInfoPage.aspx?prjid=93
Lula	5	2	100000	http://www.fluor.com/projects/Pages/ProjectInfoPage.aspx?prjid=93
Marlim	102	50	390000	http://www.fluor.com/projects/Pages/ProjectInfoPage.aspx?prjid=93
Marlim Sul	41	34	300000	http://www.fluor.com/projects/Pages/ProjectInfoPage.aspx?prjid=93
Polvo	10	3	30000	http://www.fluor.com/projects/Pages/ProjectInfoPage.aspx?prjid=93
Roncador	40	24	460000	http://www.fluor.com/projects/Pages/ProjectInfoPage.aspx?prjid=93
Sapinhoa	10	10	120000	http://www.fluor.com/projects/Pages/ProjectInfoPage.aspx?prjid=93

4.3.0.5 Default gas composition

The default gas composition for associated gas from oil production is derived from reported gas composition data from 135 California oil fields [12]. Species concentration distributions for major gas species is shown in Figure 4.7. In order to remove outliers, all compositions with methane concentration less than 50% were removed from the dataset (17 data points removed out of 135). The resulting mean compositions were rounded and used in OPGEE for default gas composition.

'Active Field
2.3.2'

4.3.0.6 Smart default for GOR

The gas-oil ratio (GOR) varies over the life of the field. The amount of gas able to be evolved from crude oil depends on its API gravity, the gas gravity, and the temperature and pressure of the crude oil [93, p. 297]. As the reservoir pressure drops, increasing amounts of gas evolve from the liquid hydrocarbons (beginning at the bubble point pressure if the oil is initially undersaturated) [93]. This tends to result in increasing producing GOR over time. Also, lighter crude oils tend to have a higher GOR.

Because of this complexity, a static single value for GOR is not desirable. However, all data required to use empirical correlations for GOR is not likely to be available for all crude oils modeled. Therefore we use California producing GORs to generate average GORs for three crude oil bins.

'Active Field
2.4.1'

Crude oils are binned by API gravity into heavy ($< 20^{\circ}$ API), medium ($\geq 20, < 30^{\circ}$ API), and light crude ($\geq 30^{\circ}$ API). Each California oil field is assigned an average API gravity using the following procedure:

1. API gravity by pool is collected from DOGGR datasets [94–96] and digitized.
2. If a range of API gravities is given for a single pool, the high and low specific gravities are averaged to obtain a single specific gravity value per pool, which is then converted back to API gravity.
3. The above steps give a set of single API values by pool. Each field has between 1 and 17 pools that have data in DOGGR field properties datasets.
4. Each field is assigned an average API gravity using the following method:
 - a) if a single pool API value is given for the field, that is used;
 - b) if multiple pool API gravities are given, and production data are available by pool, the pools are weighted by production level in 2009 DOGGR annual data (again by first converting to specific gravity then converting back to API gravity).
5. The above procedure results in a single API gravity for each field in California.

The associated gas GOR for 179 California oil fields was compiled for 2009 [97, 98]. These data are binned as above based on their weighted average API gravity value. Outliers with GOR in excess of 10,000 scf/bbl were removed. The distributions, mean, and median values for each crude bin were generated (see Figure 4.8 for plot of distributions and Table 4.3 for listing of mean and median GORs by bin).

The mean GORs are used to assign a smart default for each bin.

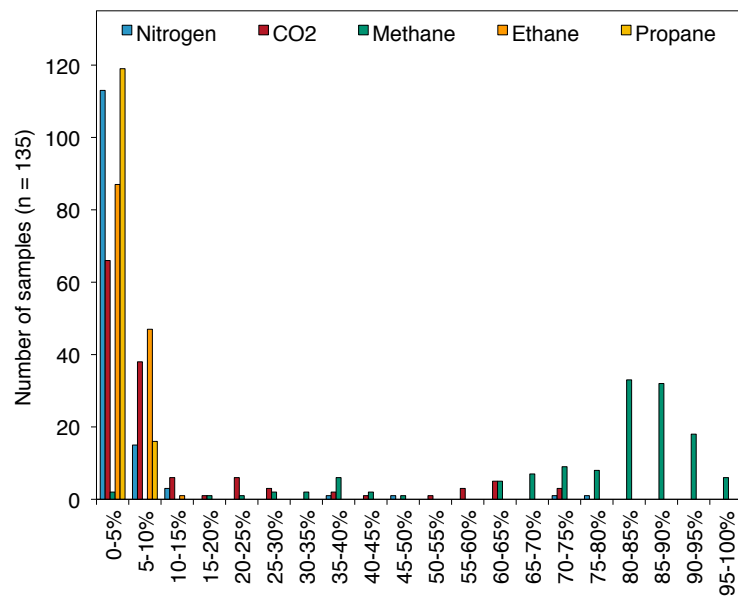


Figure 4.7: Distributions of major gas species across 135 samples from California associated gas producers.

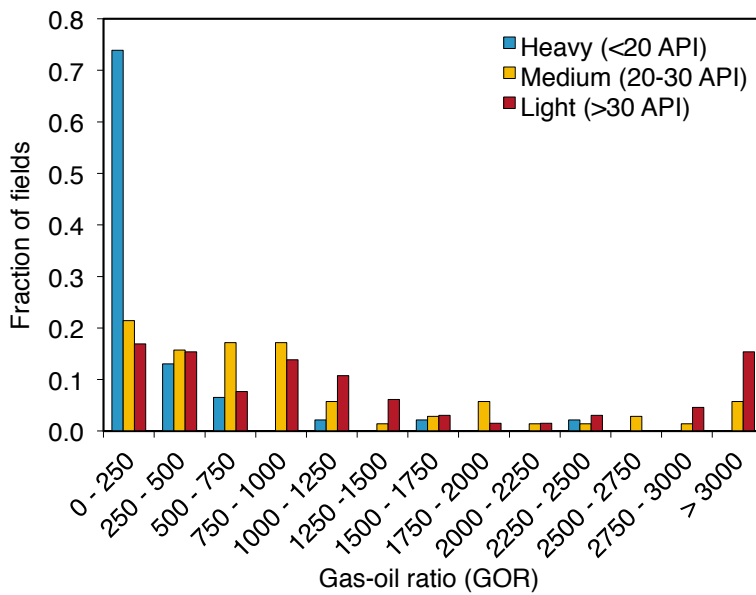


Figure 4.8: Distributions of California GORs, binned by crude density.

Table 4.3: GOR values by crude oil API gravity bin.

Crude bin	Num. fields [#]	Gravity range [°API]	Avg. gravity [°API]	Mean GOR [scf/bbl]	Median GOR [scf/bbl]
Heavy	45	< 20	15.3	227	8
Medium	69	≥ 20, ≤ 30	24.3	908	621
Light	65	> 30	35.0	1297	877

4.3.0.7 Default water oil ratio (WOR)

A smart default for the water oil ratio as a function of field age was generated using data from large fields in various world regions.

Data on oil and water production were extracted from reports issued by California Division of Oil, Gas and Geothermal Resources (DOGGR), Alberta Energy Resources Conservation Board (ERCB), Alaska Oil and Gas Conservation Commission (AOGCC), United Kingdom Department of Energy and Climate Change (DECC), and the Norwegian Petroleum Directorate (NPD). For the Norwegian fields, water production data were not available prior to the year 2000. For Alberta fields, data were not available prior to 1962. Only data for the first 60 years of production were included. Only California fields contained data beyond 55 years, and therefore we excluded these years to avoid possibly atypical depleted field behavior in California from significantly affecting the least squares fit.

'Active Field
2.4.2'

Because the majority of crude oil that is marketed globally originates from larger oil fields, fields that have produced less than 100 million m³ (630 million bbl) of crude oil were excluded. Also excluded from the analysis were fields that produce heavy crude using steam injection.

Additionally, a small number of fields were excluded because of apparent data anomalies or unusual events that may have affected oil or water production. Both the Redwater field in Alberta and the Ninian field in UK North Sea were excluded for data anomalies. These fields have highly unusual water production data that can only be plausibly attributed to data entry error. Also, the Elk Hills field in California was excluded because it was part of the National Petroleum Reserve for many years and the Piper field in the UK was excluded because oil production was halted for several years. In total, data from 24 giant oil fields (10 onshore and 14 offshore) were included in the analysis. The largest and the only super-giant field to be included is Prudhoe Bay.

The default WOR is represented by an exponential function:

$$WOR(t) = a_{WOR} \exp[b_{WOR}(t - t_0)] - a_{WOR} \quad \left[\frac{\text{bbl water}}{\text{bbl oil}} \right] \quad (4.5)$$

where a_{WOR} = fitting constant for the initial WOR in time = t_0 [bbl water/bbl oil]; b_{WOR} = exponential growth rate [1/y]; t_0 = initial year of production (or year of discovery if year of first production unavailable) [y]; and t = year being modeled (independent variable) [y]. Note that the pre-exponential a_{WOR} is subtracted to force WOR to start at 0 when $t = t_0$. This model was fit to the collected data using a nonlinear least-squares fit from multiple starting points to ensure robustness. The results of fitting this model to the smart default fit values, compared to oil fields from a variety of world regions, is shown in figure 4.9. The resulting fit gives $a_{WOR} = 1.706$ and $b_{WOR} = 0.036$.

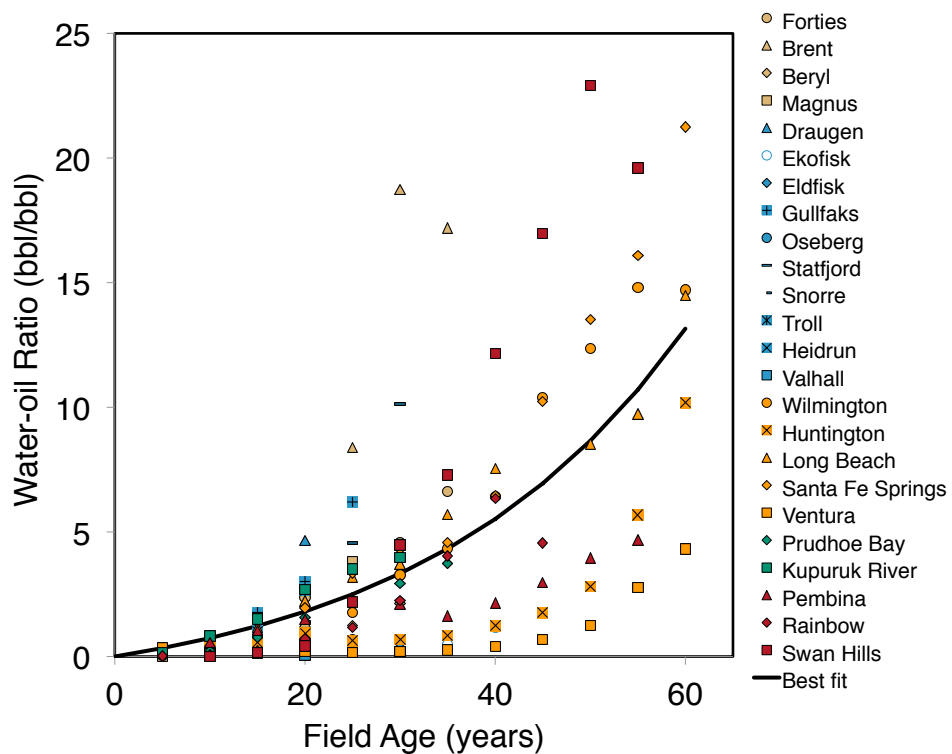


Figure 4.9: Exponential WOR model fit with smart default parameters. The best fit to data gives $a_{WOR} = 1.706$ and $b_{WOR} = 0.036$. Regions are colored as follows: Alberta (red), Alaska (green), California (orange), Norway (blue) and UK (beige).

4.3.0.8 Default waterflooding volume

The volume of water injected in a waterflooding project is meant to maintain reservoir pressure. As a default value, OPGEE assumes that the surface volume is replaced, such that the total oil produced plus the water produced is reinjected, or the injection per bbl = 1 + WOR.

*'Active Field
2.4.3'*

4.3.0.9 Default flood gas injection ratio

This is the ratio of the volume of flood gas injected [scf] to the volume of oil produced [bbl]. The volume of the oil is measured after bulk processing has removed the associated gas. The default flood gas injection ratio value depends on the choice of flood gas. If natural gas is selected as the flood gas, then the default ratio is calculated as follows:

$$R_{fl} = 1.5 \cdot GOR \quad \left[\frac{\text{scf gas}}{\text{bbl oil}} \right] \quad (4.6)$$

where R_{fl} = flood gas injection ratio [scf/bbl] and GOR is the gas-oil-ratio [scf/bbl].

*'Active Field
2.4.5'*

If N₂ is selected as the flood gas, then R_{fl} is 1,200 scf/bbl. This is based on the immiscible nitrogen flood operation at the Cantarell field in Mexico to maintain reservoir pressure. As described in the Gas flooding section, the field operating equipment is designed to inject 1,200 MMscf/d [99]. In 2008, the injection rate was approximately 1,200 MMscf/d and the field was producing approximately 1.2 million bbl/d, leading to a default ratio of 1,200 scf/bbl [?].

If CO₂ is selected as the flood gas, then default R_{fl} is 10,000 scf/bbl. As with all injection ratios, R_{fl} changes over the life cycle of the flood project. It can also vary based on the specific reservoir engineering strategies selected by the operator. An example comes from DiPietro and Murrel (2013), who presented data from Kinder Morgan indicating that the injection ratio during the overall lifespan of an anonymous representative project was 6,000 scf/bbl.

Another example is provided by Pyo et al. [?], who reviewed the performance of a CO₂ flood at the Joffre Viking Pool in Alberta, Canada that had been active for approximately 30 years. The overall flood gas injection ratio during the life of the project was 10,800 scf/bbl; the ratios for the individual injector-producer well patterns within the field varied from 3,500 to 24,900 scf/bbl.

The OPGEE default flood gas injection ratios are presented only as representative values that provide an order-of-magnitude estimate. Actual field data should be obtained when possible.

4.3.0.10 Proportion of injected CO₂ that is newly acquired

The OPGEE default for the proportion of CO₂ that is newly acquired (not previously injected) is 41%. This figure is from the Malone et al. [100] discussion of an offshore CO₂ flood project at Weeks Island, Louisiana over an 9-year period (based on dates in the original reference by Johnston [?]). As with the flood gas injection ratio, actual data should be used if possible.

4.3.0.11 Default for steam-oil-ratio (SOR)

Because the SOR is a key parameter driving GHG emissions from thermal oil production operations, we examine default values for SOR in more detail.

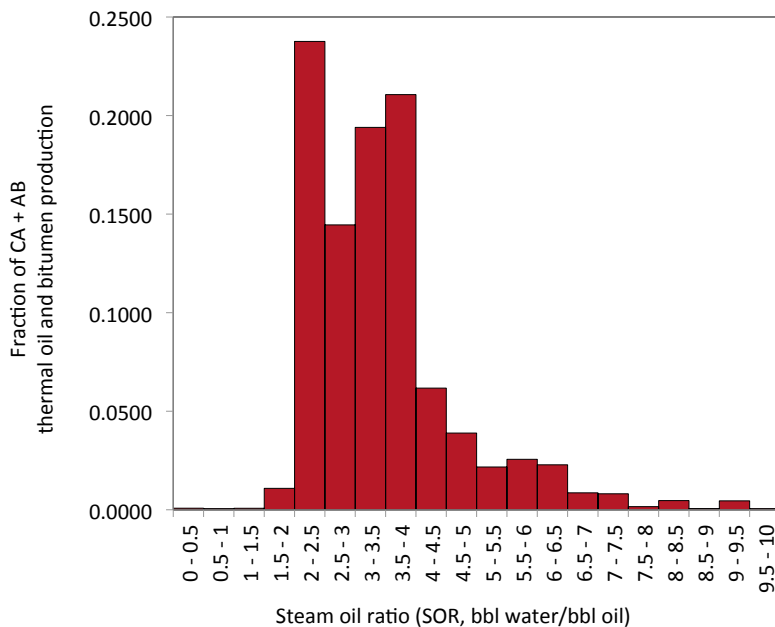


Figure 4.10: Distribution of SOR values for California and Alberta thermal EOR projects (steamflood, cyclic steam stimulation, steam-assisted gravity drainage).

Table 4.4: Indicators of SOR distributions for California and Alberta thermal EOR production. Units are bbl of cold water equivalent (CWE) per bbl of oil.

	Mean - SOR_f	Mean - SOR_i
California - 2009	3.32	4.29
California - 2010	3.41	Unk.
Alberta - 2009	3.58	NA
Alberta - 2010	3.32	NA

SOR data are collected for California and Alberta thermal oil recovery operations for 2010 and 2011 [91, 98, 101–103].

For California operations, incremental SOR is calculated for 2009 using volumes of steam injected and reported incremental production due to steam injection. ‘Total’ SOR is also calculated for 2009 using total production by field and total steam injection. For 2010, only monthly data are available, so incremental production data are not available. Therefore, only total SOR is reported.

For Alberta operations, data on bitumen produced and steam injected were collected for 24 thermal recovery projects (SAGD and CSS). No data were available on incremental rather than total production, and it is not clear what incremental production figures would represent bitumen operations where non-enhanced production would be very small.

Production volumes are binned by SOR for both regions and reported in Figure 4.10. Averages for SOR are presented in Table 4.4. The default SOR in OPGEE v3.0a is a conservative 3.0 bbl CWE per bbl oil.

5 Flow sheet

Table 5.1: Properties computed for each stream: Symbol, description, units, and source of relevant equation.

Symbol	Description	Units	Source	Notes
--------	-------------	-------	--------	-------

5.1 Flow sheet introduction

The flow sheet is the main organizing sheet for OPGEE. It includes graphical representation of the process flows and numerical results for all streams in all phases. The streams are numbered 1-300 (with gaps for forward compatibility). At the top of the table, each stream contains a mass flow of a given set of possible substances. In the lower section of the flow table, a variety of other characteristics of each stream are computed. These properties are computed for all streams using equivalent formulas.

To refer to a given stream property, the “Index” function in Excel is used. The syntax of the Index function is as follows:

```
Index([Table], [Row], [Column])
```

where [Table] is the name of the table being accessed, and [Row] and [Column] are the row and column of the entry desired.

In order to call a quantity from the Flow table, the proper syntax would then be:

```
Index(FlowTable, PROP_NAME, STREAM_NUM)
```

where PROP_NAME is the name of the property desired and STREAM_NUM is the number of the stream of interest.

The property names are defined as follows in Table 5.1. After Table 5.1 the method of computing each property is given below.

5.2 Computing properties of flows

5.2.1 Mass flows

Mass flows per day are denominated or M_X where X is a place holder for a given stream component [tonne/d]. The following streams are recognized in OPGEE:

- **PC** – Petroleum coke streams
- **O** – Oil streams
- **LPG** – Liquified petroleum gas streams
- **W** – Water stream
- **N2** – Nitrogen stream
- **O2** – Oxygen stream
- **CO2** – Carbon dioxide stream

- `H2O` – Water vapor stream
- `C1` – Methane stream
- `C2` – Ethane stream
- `C3` – Propane stream
- `C4` – Butane stream
- `CO` – Carbon monoxide stream
- `H2` – Hydrogen stream
- `H2S` – Hydrogen sulfide stream
- `SO2` – Sulfur dioxide stream

The only solid component tracked in the '*Flow sheet*' is petroleum coke `PC`. Petroleum coke is a solid form of primarily carbon, generated at crude oil upgrading and refining facilities.

Three liquid components are tracked in the '*Flow sheet*'. Oil streams `O` are defined as hydrocarbon streams that are liquid at standard temperature and pressure. For simplicity, bitumen is considered a liquid oil stream. Oil streams vary from API gravity of 6 °API (heavy bitumen) to 70 °API (light condensate or diluent). Liquified petroleum gas (LPG) streams `LPG` is a stream that is gaseous at ambient temperature and pressure but will liquify at low pressures and therefore is commonly transported in dense form (commonly mixtures of mostly propane and butane). Water `W` can be brackish or fresh water.

Twelve gas components are tracked in the '*Flow sheet*'. These include constituents of air (`N2`, `O2`, `CO2`, and `H2O`). Note that water vapor is represented by `H2O` while liquid phase water is tracked as `W`. Next are the four light hydrocarbons, `C1` - `C4`. Some sources distinguish a species in gas called "pentanes plus". Given that these are liquid at standard temperature and pressure, these would be considered a very light oil stream. Similarly, lease condensate and natural gas plant liquids are also tracked as oil `O`. Lastly, minor constituents are tracked: `CO`, `H2`, `H2S`, and `SO2`.

5.2.2 Electricity flows

Electricity is tracked by its energy flow rate per day [MWh/d] `E_EL`. No distinction is made between high voltage or low voltage electricity, nor do we distinguish between DC and AC power.

5.2.3 Properties of phases

Certain properties are tracked for the composite of all phases in the stream. These include temperature [°F] `T`, absolute temperature [°R], `T_ABS`, pressure [psia] `P`.

Each stream is also classified as containing oil `OIL_01`, containing liquid phase water `WAT_01`, and containing gases `GAS_01`. These are 0-1 binary variables used in logical flows for computing properties of different streams.

Table 5.2: Source of API gravity for oil streams.

Stream num.	Stream name	Source of API gravity term	Default	Notes
1	Crude oil in reservoir	API_grav	30° API	
2	Bitumen in mine	API_Bitumen	30° API	
3	Crude oil at well bottom	API_grav	30° API	
4	Crude oil at wellhead	API_grav	30° API	
5	Bitumen from mine to upgrader	API_Bitumen	30° API	
6	Bitumen from mine to dilution	API_Bitumen	30° API	
7	Crude oil after separator	API_grav	30° API	
8	Crude oil to stabilizer	API_grav	30° API	
9	Crude oil to storage	API_grav	30° API	
10	Stabilized crude to storage	API_grav	30° API	
11	Upgraded crude to storage	API_grav	30° API	
12	Diluted bitumen to storage	API_grav	30° API	
13	Crude oil to transport	API_grav	30° API	
14	Transported crude oil at refinery	API_grav	30° API	
15	Petcoke export from upgrader	-	-	
16	NGL/diluent to dilution	API_diluent	30° API	
17	LPG to blend with crude oil	API_diluent	30° API	
18	LPG to direct sales	API_diluent	30° API	
19	Crude oil to upgrader	API_grav	30° API	
20	Crude oil in dilution	API_grav	30° API	

5.2.4 Properties of oil

A number of properties of oil are tracked. These properties are a function of oil chemistry (heating value) as well as the temperature and pressure of the stream (solution gas oil ratio).

API gravity of oil The API gravity of the oil is tracked as variable `API_0`. For conventional oil streams, this is defined as equal to the defined parameter `API_grav` (streams given in Table 5.2). For bitumen streams it is equal to defined parameter `Bitumen_API`. For diluent streams it is equal to `Diluent_API`. For LPG the API gravity is not computed as this parameter is not typically used to represent these products.

Specific gravity of oil The specific gravity of the oil is tracked as variable `GAMMA_0`. It is computed from the API gravity as follows:

$$\gamma_o = \frac{141.5}{131.5 + API} \quad [\frac{\text{g}}{\text{g}}]. \quad (5.1)$$

$$GAMMA_0 = \frac{141.5}{131.5 + API_0} \quad [\frac{\text{g}}{\text{g}}]. \quad (5.2)$$

This equation holds for conventional oil, bitumen, and diluent. For LPG streams the density is assumed equal to 550 kg/m^3 , or midway between the density of propane (504 kg/m^3 at 60°F) and butane (600 kg/m^3 at 60°F).

Solution gas oil ratio of oil The solution gas oil ratio R_s [GOR_OS] is the amount of gas in solution in a crude oil as a function of a number of properties. If there is more gas present than this amount, the gas will start to evolve from the oil into a separate gas phase (i.e., the gas will start to bubble out of the oil). As recommended in Fanchi [55], we re-arrange the bubblepoint pressure relationship to solve for the amount of gas in solution at a given pressure. We use the bubblepoint pressure relationship of Al-Shammasi (1999), as reproduced in [55, vol 1, Table 6.6]:

$$R_s = \frac{p^{\left(\frac{1}{a_2}\right)} \gamma_o^{\left(-\frac{a_1}{a_2}\right)} e^{\left(\frac{a_3}{a_2} \gamma_o \gamma_g\right)}}{\gamma_g T_{abs}} \quad [\frac{\text{scf}}{\text{bbl}}] \quad (5.3)$$

If the resulting gas oil ratio is larger than the bubblepoint pressure gas oil ratio (R_b), then the equation defaults to the bubblepoint gas oil ratio. The equation for bubblepoint gas oil ratio is given below in Eq. ??.

Oil formation volume factor The oil formation volume factor B_o [OVF] is the ratio of the number of barrels that a barrel of oil will occupy in the reservoir over the number of stock tank (standard) barrels that the oil will occupy. The oil formation volume factor is a function of the solution gas oil ratio, the temperature, and the pressure of the fluid, with the gas in solution being the largest determinant. The oil FVF at the bubblepoint pressure is generated via bubblepoint oil FVF correlations [FVF_SAT]. We use the bubblepoint oil formation volume factor correlation from Al-Shammasi [55, Table A-3, p. 317][?]:

$$B_{ob} = a_1 + a_2 R_s (T_r - 60) + a_3 \left(\frac{R_s}{\gamma_o} \right) + a_4 \left(\frac{T_r - 60}{\gamma_o} \right) + a_5 R_s \left(\frac{\gamma_g}{\gamma_o} \right) \quad [\frac{\text{bbl}}{\text{STB}}] \quad (5.4)$$

this correlation is useful for saturated oil, or oil with its associated gas at the maximum amount (i.e., as pressure drops gas is evolved).

For undersaturated oil, oil holds less gas in solution than it could at that temperature and pressure. In this case the pressure is above the bubblepoint pressure and the oil formation volume factor varies using a different functional form. The undersaturated oil FVF [FVF_UNSAT] is:

$$B_o = B_{ob} e^{[c_o(p_b - p)]} \quad [\frac{\text{bbl}}{\text{STB}}] \quad (5.5)$$

where c_o is the isothermal compressibility of oil, p_b the bubblepoint pressure of oil, and p the pressure of the stream.

We use the correlation of Al-Mahoun [?] for the isothermal compressibility term [55, Table A-5, p. 320]. First, term X is computed [ISO_X]:

$$X = a_1 R_s + a_2 R_s^2 + a_3 \gamma_g + a_4 (T_{abs})^2 \quad [-] \quad (5.6)$$

where R_s is the solution gas oil ratio [scf/bbl], γ_g is the gas specific gravity [-] and T_{abs} is the absolute temperature [$^{\circ}\text{R}$]. From this term the isothermal compressibility c_o [ISO_CO] can be computed as:

$$c_o = \frac{X \ln \left(\frac{p}{p_b} \right)}{p_b - p} \quad \left[\frac{1}{\text{psi}} \right] \quad (5.7)$$

Finally, we can use these two terms to compute the oil FVF [FVF_UNSAT]. If $p < p_b$, B_{ob} is used, while if $p \geq p_b$ then B_o is used.

Density of oil Using the above terms, the density of crude `RHO_O_LB` can then be computed in using the following relation [55, p. 277]:

$$\rho_o = \frac{a_1 \gamma_o + a_2 \gamma_g R_s}{B_o} \quad [\frac{\text{lbm}}{\text{ft}^3}] \quad (5.8)$$

where γ_g is the specific gravity of gas (defined below in Eq. ??) and a_1 and a_2 are the densities of water and air at standard conditions. This value is also converted to SI units [kg/m^3] `RHO_O`. For LPG the density is assumed to be 550 kg/m^3 .

Volumetric flow rate of oil The volumetric flow rate of oil is then given by the mass flow rate m_o and the density of crude oil:

$$Q_o = \frac{m_o}{\rho_o} \quad [\frac{\text{m}^3}{\text{d}}] \quad (5.9)$$

Energy density of oil The energy density (heating value per unit mass) of oil is computed using a polynomial correlation for LHV of crude as a function of crude API gravity from the API Technical Databook, eq. 14A1.3-3:

$$LHV_o = a_1 + a_2 API - a_3 API^2 - a_4 API^3 \quad [\frac{\text{btu LHV}}{\text{lbm}}] \quad (5.10)$$

This is then converted to SI units [MJ/kg]. A similar polynomial function can be used to compute the HHV of oil as a function of API gravity:

$$HHV_o = a_1 + a_2 API - a_3 API^2 - a_4 API^3 \quad [\frac{\text{btu HHV}}{\text{lbm}}] \quad (5.11)$$

For LPG streams the energy density is assumed equal to 50 MJ/kg .

Energetic flow rate of oil The energetic flow rate of oil can then be computed using the above terms:

$$F_{LHV,o} = Q_o LHV_o \quad (5.12)$$

5.2.5 Properties of gas

Properties of the gas phase components of each stream are computed below the oil properties.

Total moles of gas The total number of moles of gas in a stream `TOTMOLGAS` is given by:

$$n_{tot} = \sum_i^n \left(\frac{m_i}{MW_i} \right) \quad [\frac{\text{mol}}{\text{d}}] \quad (5.13)$$

where i is the species index for gas species noted above, m_i is the mass of gas flow for species i [g] and MW_i is the molecular weight of gas species i [g/mol].

Molar fraction species The mole fraction x_i for each species i – `MOL_FRAC_N2` ... `MOL_FRAC_SO2` – is given by:

$$x_i = \frac{m_i}{MW_i n_{tot}} \frac{1}{n_{tot}} \quad [\text{mol fraction}] \quad (5.14)$$

where n_{tot} is the total molar flow [mol/d], m_i is the mass flow of each gas species i [g/d], and MW_i is the molecular weight of species i [g/mol].

Table 5.3: Constants in equations for liquid stream properties.

Eq. num.	Description	Term	Value	Units	Source
5.3	Solution gas oil ratio	a_1	5.527215	-	[?]
5.3	Solution gas oil ratio	a_2	0.783716	-	[?]
5.3	Solution gas oil ratio	a_3	1.841408	-	[?]
5.4	Bubblepoint oil FVF	a_1	1	-	[?]
5.4	Bubblepoint oil FVF	a_2	5.25E-07	-	[?]
5.4	Bubblepoint oil FVF	a_3	1.81E-04	-	[?]
5.4	Bubblepoint oil FVF	a_4	4.49E-04	-	[?]
5.4	Bubblepoint oil FVF	a_5	2.06E-04	-	[?]
5.6	Isothermal compressibility	a_1	-1.37E-05	[bbl/scf]	[?]
5.6	Isothermal compressibility	a_2	-1.93E-08	[bbl ² /scf ²]	[?]
5.6	Isothermal compressibility	a_3	2.41E-02	[\cdot]	[?]
5.6	Isothermal compressibility	a_4	-9.26E-03	[1/ $^{\circ}$ R ²]	[?]
5.8	Density of oil	a_1	62.428	[lbm/ft ³]	[55]
5.8	Density of oil	a_2	0.0136	[lbm-bbl/ft ³ -scf]	[55]
5.10	Lower heating value of oil	a_1	16796	[btu LHV/lbm]	[?]
5.10	Lower heating value of oil	a_2	54.4	[btu LHV/lbm- $^{\circ}$ API]	[?]
5.10	Lower heating value of oil	a_3	0.217	[btu LHV/lbm- $^{\circ}$ API ²]	[?]
5.10	Lower heating value of oil	a_4	0.0019	[btu LHV/lbm- $^{\circ}$ API ³]	[?]
5.11	Higher heating value of oil	a_1	17672	[btu LHV/lbm]	[?]
5.11	Higher heating value of oil	a_2	66.6	[btu LHV/lbm- $^{\circ}$ API]	[?]
5.11	Higher heating value of oil	a_3	0.316	[btu LHV/lbm- $^{\circ}$ API ²]	[?]
5.11	Higher heating value of oil	a_4	0.0014	[btu LHV/lbm- $^{\circ}$ API ³]	[?]

Gas specific gravity Gas specific gravity γ_g is the density of gas compared to the density of air, measured at standard conditions `GAMMA_G`. Gas specific gravity is computed as:

$$\gamma_g = \frac{\sum_i x_i M W_i}{M W_{air}} \quad [-] \quad (5.15)$$

Total flow rate in standard cubic feet Gas flow rate in units of millions of standard cubic feet `TOTMMSCF` is given by n_{tot} multiplied by the moles per standard cubic foot `mol_per_scf`.

Ratio of specific heats Ratio of the constant-pressure specific heat capacity C_p [J/g-K] and the constant volume specific heat capacity C_v [J/g-K] is needed in compressor equations. For a mixture of gases we compute C_p/C_v as follows `CpCvRatio`:

$$\gamma = \frac{\sum_i m_i C_{p,i}}{\sum_i m_i C_{v,i}} \quad [-] \quad (5.16)$$

where C_p and C_v are the mass-specific (not mole-specific) heat capacities.

Pseudocritical temperature The pseudocritical temperature and pressure of a gas mixture are easily determinable approximations of the true critical parameters [93, p. 111]. OPGEE uses a mixing rule to calculate the pseudocritical parameters based on the critical temperatures and pressures of the components of the gas mixture, weighted according to the specific composition of the mixture [104]. The uncorrected pseudocritical temperature is computed in a macro as `PseudoCriticalTemperature()`:

$$a = \sum_i x_i \left(\frac{T_{c,i}}{p_{c,i}} \right) \quad (5.17)$$

$$b = \sum_i x_i \left(\frac{T_{c,i}}{p_{c,i}} \right)^{0.5} \quad (5.18)$$

$$J = \frac{1}{3}a + \frac{2}{3}b^2 \quad (5.19)$$

$$K = \sum_i x_i \left(\frac{T_{c,i}}{p_{c,i}^{0.5}} \right) \quad (5.20)$$

$$T_{pc} = \frac{K^2}{J} \quad (5.21)$$

$$p_{pc} = \frac{K^2}{J^2} \quad (5.22)$$

where x_i are the mole fractions of gases in the mixture, $T_{c,i}$ is the critical temperature of species i , $p_{c,i}$ is the critical pressure of species i . T_{pc} is the uncorrected pseudocritical temperature of the gas mixture [$^{\circ}\text{R}$] and p_{pc} is the uncorrected pseudocritical pressure of the gas mixture [psia].

The presence of carbon dioxide (CO_2) or hydrogen sulfide (H_2S) in a hydrocarbon gas mixture impart acidic (sour) qualities that alter the pseudocritical parameters and must be accounted for. OPGEE accounts for the presence of hydrogen sulfide (up to 74% of the gas composition) or carbon dioxide (up to 54% of the gas composition) using a correction factor to adjust the pseudocritical temperature and pressure [105], adapted from Fanchi et al. [55, p. 229].

The corrected pseudocritical temperature is given by first computing the deviation parameter ϵ :

$$\epsilon = 120 \left[(x_{\text{CO}_2} + x_{\text{H}_2\text{S}})^{0.9} - (x_{\text{CO}_2} + x_{\text{H}_2\text{S}})^{1.6} \right] + 15 \left[x_{\text{H}_2\text{S}}^{0.5} - x_{\text{H}_2\text{S}}^4 \right]. \quad [{}^{\circ}\text{R}] \quad (5.23)$$

Using ϵ the corrected pseudocritical temperature is given by:

$$T'_{pc} = T_{pc} - \epsilon \quad [{}^{\circ}\text{R}] \quad (5.24)$$

and the corrected pseudocritical pressure is given by:

$$p_c = \frac{p_{cu} T'_{pc}}{T_{pc} - x_{\text{H}_2\text{S}}(1 - x_{\text{H}_2\text{S}})(T_{pc} - T'_{pc})} \quad [\text{psia}] \quad (5.25)$$

Pseudoreduced temperature and pressure The pseudoreduced parameters of a gas mixture are calculated using methods from McCain [93, p. 111]. The pseudoreduced temperature T_{pr} is given by:

$$T_{pr} = \frac{T}{T'_{pc}} \quad (5.26)$$

where T'_{pc} is the corrected pseudocritical temperature from above. The pseudoreduced pressure p_{pr} is given by:

$$p_{pr} = \frac{p}{p'_{pc}} \quad (5.27)$$

where p'_{pc} is the corrected pseudocritical pressure.

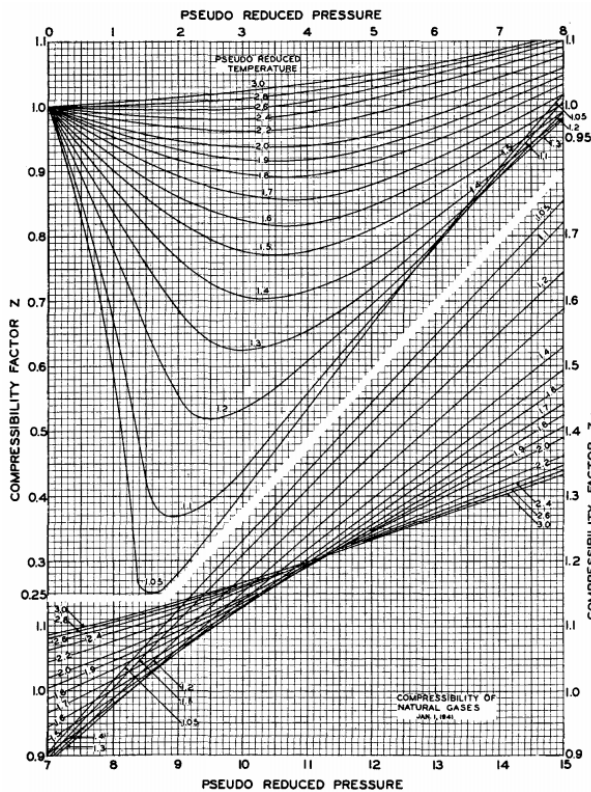


Figure 5.1: Standing and Katz [1] Natural Gas Mixture Z-Factor Chart.

Gas compressibility factor (Z-factor) Compression-related calculations account for the compressibility factor (Z-factor) of the gas being compressed **Z_FACTOR**. The Z-factor of a gas measures the degree to which its properties differ from ideal gas behavior and is dependent on pressure and temperature conditions.

For compression of nitrogen (N_2) [106], carbon dioxide (CO_2) [107], air [108], or oxygen (O_2) [109], OPGEE refers to z-factor data generated using the National Institute of Standards and Technology's REFPROP thermodynamic software package, which uses equations of state to generate compressibility factors [110].

The experimentally-determined Standing and Katz hydrocarbon Z-factor correlation chart (Figure 5.1 [1]) presents compressibility factors for a hydrocarbon gas mixture based on its pseudoreduced temperature and psudoreduced pressure [1]. When hydrocarbon gas mixtures are compressed, OPGEE uses a correlation generated from the Standing and Katz chart to calculate an approximate Z-factor for each stage of compression [2]. The correlations for the upper and lower portions of the chart are presented in Figure 5.2 and Figure 5.3, respectively. These correlations are implemented in a VBA user-defined formula `zfactor(T_R, P_R)`.

'Input data Table 2.7'

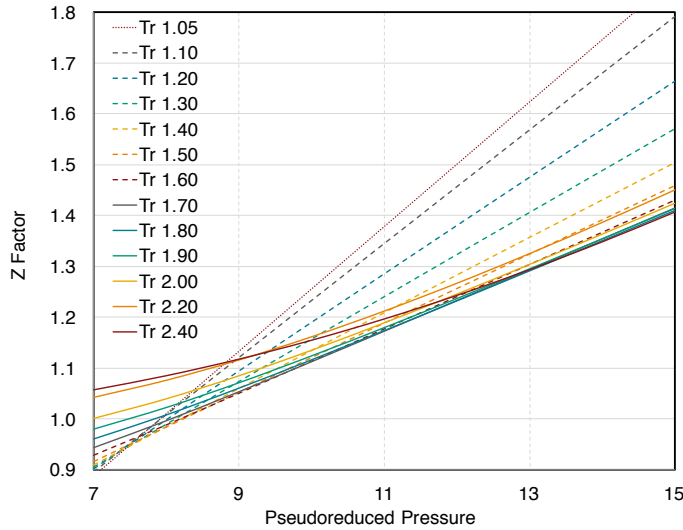


Figure 5.2: Correlation of Upper Portion of Standing and Katz Z-Factor Chart. Source: [2].

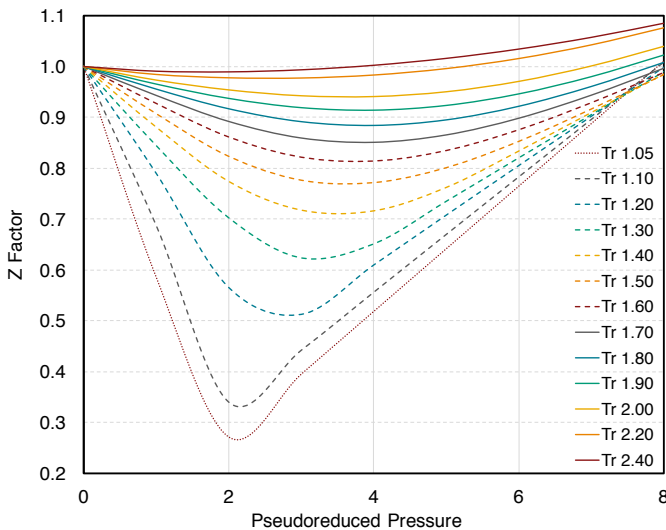


Figure 5.3: Correlation of Lower Portion of Standing and Katz Z-Factor Chart. Source: [2].

Gas formation volume factor The gas formation volume factor **GVF** is the ratio of the volume of gas at the temperature and pressure of the stream in question to the volume of the same amount (moles) of gas at standard conditions.

Given the Z-factor computed above **Z_FACTOR**, the gas volume ratio can be computed as:

$$FVF_g = \frac{Z p_0 T}{p T_0} \quad \left[\frac{\text{m}^3}{\text{std m}^3} \right] \quad (5.28)$$

where T is the absolute temperature of the stream [$^{\circ}\text{R}$], T_0 is the ambient absolute temperature **Amb_temp** [$^{\circ}\text{R}$], p is the pressure of the stream [psia] and p_0 is

ambient pressure [psia] `Amb_press`.

Gas density Gas density `RHO_G` is given by the MW of gas relative to air, the density of air at standard conditions, and the gas formation volume factor:

$$\rho_g = \frac{\rho_{air} \gamma_g}{FVF_g} \quad \left[\frac{\text{tonne}}{\text{m}^3} \right] \quad (5.29)$$

Gas molecular weight The molecular weight of the gas in a particular stream `MW_G` is given by the mole-fraction-weighted molecular weight of species in the stream:

$$MW_g = \sum_i x_i MW_i \quad (5.30)$$

where x_i is the mole fraction of species i – `MOL_FRAC_N2` ... `MOL_FRAC_SO2` – and MW_i is the molecular weight of species i [g/mol].

Gas volumetric flow rate The volumetric flow rate of gas per day `Q_G` [m^3/d] is given by:

$$Q_g = \frac{m_{tot,g}}{\rho_g} \quad \left[\frac{\text{m}^3}{\text{d}} \right] \quad (5.31)$$

Gas energy density The energy density of the gas `LHV_G` `LHV_G_1b` is given by the mass-fraction weighted energy densities of the species: [ADD EQUATION]

Total gas energetic flow rate The total gas energetic flow rate for a given stream is given by:

$$Q_{LHV,g} = m_{tot,g} LHV_g \quad (5.32)$$

5.2.6 Properties of water

Specific gravity of water The specific gravity of produced water `GAMMA_W` at standard conditions is calculated using [55, p. 481]:

$$\gamma_w = 1 + C_{sd} 0.695 \times 10^{-6} \quad [-] \quad (5.33)$$

where C_{sd} = concentration of dissolved solids (also known as TDS) [mg/L]. The constant 0.695×10^{-6} has units of [L/mg].

'Production
& Extraction
2.1.2'

Water formation volume factor The water formation volume factor `WVF` is assumed to be 1.0 for all streams. Because water is nearly incompressible, equations for B_w nearly always produce values near 1 (i.e., 1.03), so reduce model complexity and possible requirements for iterative calculations by fixing B_w to 1.0.

Water density Water density `RHO_W` is given by the specific gravity of water and the water formation volume factor:

$$\rho_w = \frac{\gamma_w \rho_{w,0}}{B_w} \quad \left[\frac{\text{tonne}}{\text{m}^3} \right]. \quad (5.34)$$

where $\rho_{w,0}$ is the density of pure water [1000 kg/m^3]. Because we assume $B_w = 1$ for simplicity, $\rho_w = \gamma_w \rho_{w,0}$.

Water flow rate Water flow rate is computed from mass flow rate of water m_w for a given stream and the density of water ρ_w for that stream:

$$Q_w = \frac{m_w}{\rho_w} \quad \left[\frac{\text{m}^3}{\text{d}} \right] \quad (5.35)$$

[CHANGE FLOWS IN EXCEL TO BE Q RATHER THAN F].

6 Gathering worksheets

This section explains three worksheets in OPGEE which are used to collect output from intermediate calculations in process stage and supplemental worksheets. This collected output is used to calculate the overall WTR energy consumption and GHG emissions of the study crude. These gathering worksheets are the '*Energy Consumption*', '*GHG Emissions*', and '*Active Field*' worksheets.

6.1 ‘Energy Consumption’ gathering worksheet

In the ‘Energy Consumption’ gathering worksheet, energy use is summed in order of process stages, from Exploration to Waste disposal. For consistency, all energy inputs are summed on a daily basis, either as thermal energy (MMBtu/d) or as electrical energy (kWh/d). All energy types are classified using a fuel code. The primary energy types included are: 1A) Natural gas; 1B) Natural gas liquids; 2) Diesel fuel; 3) Electricity; 4) Crude oil.

First, the amount and type of fuel consumed by each process stage (e.g., Exploration, Drilling & Development, etc) is collected using nested if then statements. Second, the fuel consumption is summed by fuel type (e.g., natural gas, diesel) to calculate the gross energy consumption.

The gross energy consumption can include double counted energy. For example, the electricity consumed to drive a pump may be generated onsite and the energy consumed to generate that electricity would also be counted as natural gas or diesel, resulting in double counting.

The net energy consumption is calculated by fuel type. The net energy consumption is equal to the gross energy consumption for all fuels except for electricity. The net energy consumption of electricity is calculated as:

$$E_{el,net} = E_{el,gr} - E_{el,gen} \quad [\text{MMBtu}] \quad (6.1)$$

where $E_{el,net}$ = net electricity consumption [MMBtu/d]; $E_{el,gr}$ = gross electricity consumption [MMBtu/d]; and $E_{el,gen}$ = total electricity generated onsite [MMBtu/d]. The total electricity generated onsite includes electricity generated using an onsite generator or simple turbine and electricity co-generated in the steam generation system, if applicable. In other words, the net electricity consumption is equal to the electricity imported from the grid, if any.

Once the net energy consumption is calculated by fuel type the energy exports/imports are calculated by fuel type. Energy exports/imports are used to calculate indirect (offsite) energy consumption and GHG emissions by fuel type. Indirect energy consumption and GHG emissions are associated with the production and transport (production only in case of exports) of the fuel consumed directly. The exports/imports of natural gas are calculated as:

$$E_{ng,exp} = E_{ng,gr} - E_{ng,fuel} + E_{ng,mu} - E_{ng,rec} \quad \left[\frac{\text{MMBtu}}{\text{d}} \right] \quad (6.2)$$

where $E_{ng,exp}$ = natural gas export/import [MMBtu/d]; $E_{ng,gr}$ = gross natural gas consumption [MMBtu/d]; $E_{ng,fuel}$ = natural gas produced as fuel after gas lifting/re-injection [MMBtu/d]; $E_{ng,mu}$ = make up natural gas for gas flooding [MMBtu/d], if applicable; and $E_{ng,rec}$ = natural gas recovered from venting and fugitives. The produced gas remaining to be used as a process fuel is equal to 0 MMBtu/d in the case of gas flooding where 100% of produced gas is re-injected. Negative $E_{ng,exp}$ represents gas exports. Positive $E_{ng,exp}$ represents gas imports.

The exports/imports of natural gas liquid (NGL) is calculated as:

$$E_{ngl,exp} = E_{ngl,gr} - E_{ngl,fuel} \quad \left[\frac{\text{MMBtu}}{\text{d}} \right] \quad (6.3)$$

where $E_{ngl,exp}$ = NGL export/import [MMBtu/d]; $E_{ngl,gr}$ = gross NGL consumption [MMBtu/d]; and $E_{ngl,fuel}$ = amount of NGL produced as fuel [MMBtu/d].

‘Energy Consumption Table 1’
‘Energy Consumption Table 2’

‘Energy Consumption Table 1’

‘Energy Consumption Table 3’

The import of diesel is equal to gross diesel consumption. The export of diesel does not apply because diesel is not produced in upstream operations. The export/import of electricity is equal to electricity net consumption as calculated in eq. (6.1). Positive net electricity consumption is equal to electricity imported from the grid and negative net electricity consumption is equal to electricity exported to the grid. Crude oil export/import does not apply because crude oil is the main product. Any crude oil used as a process fuel on site is subtracted from the amount produced and shipped (see Section 4).

Finally, the indirect energy consumption by fuel type is calculated. The indirect energy consumption is calculated as:

'Energy Consumption Table 4'

$$\begin{aligned}
 E_{k,ind} &= E_{k,exp} E_{k,FC} && \text{for } E_{k,exp} > 0 \\
 E_{k,ind} &= E_{k,exp} E_{k,DS} && \text{for } E_{k,exp} < 0 \text{ and displacement} \\
 E_{k,ind} &= 0 && \text{for } E_{k,exp} < 0 \text{ and allocation by energy value}
 \end{aligned} \tag{6.4}$$

where k refers to the fuel type; $E_{k,ind}$ = indirect energy consumption [MMBtu/d]; $E_{k,exp}$ = fuel export/import [MMBtu/d]; $E_{k,FC}$ = fuel cycle energy consumption [MMBtu/MMBtu]; and $E_{k,DS}$ = energy consumption of displaced system in case of fuel export [MMBtu/MMBtu]. For details on the energy consumption of fuel cycles and displaced systems, see Section 8.2.

6.2 ‘GHG Emissions’ gathering worksheet

The GHG emissions gathering worksheet compiles and computes emissions of all emissions types across all process stages. The first step is the calculation of direct GHG emissions from the different components of the model. Direct GHG emissions are calculated as:

$$EM_{s,k} = E_{s,k,gr} EF_{s,k} \left[\frac{\text{gCO}_2\text{eq}}{\text{d}} \right] \quad (6.5)$$

where s = emissions source (e.g., downhole pump driver); k = fuel type; $EM_{s,k}$ = direct GHG emissions from the consumption of fuel k in source s [gCO₂eq/d]; and $E_{s,k,gr}$ = gross energy consumption of fuel k in source s [MMBtu/d]; and $EF_{s,k}$ = emissions factor of source s using fuel k [g CO₂ eq./MMBtu]. This equation does not apply to electricity, where direct GHG emissions are equal to 0 gCO₂eq./d.

Next, the GHG emissions from land use, flaring, and venting/fugitives are calculated by process stage. This includes gathering emissions calculated in each process stage and supplemental worksheets.

The next step is the calculation of indirect GHG emissions by fuel import type. The indirect GHG emissions are calculated as:

$$\begin{aligned} EM_{k,ind} &= E_{k,exp} EM_{k,FC} && \text{for } E_{k,exp} > 0 \\ EM_{k,ind} &= E_{k,exp} EM_{k,DS} && \text{for } E_{k,exp} < 0 \text{ and displacement} \\ EM_{k,ind} &= 0 && \text{for } E_{k,exp} < 0 \text{ and allocation by energy value} \end{aligned} \quad (6.6)$$

where k refers to the fuel type; $EM_{k,ind}$ = indirect GHG emissions from fuel consumption [gCO₂eq/d]; $E_{k,exp}$ = fuel export/import [MMBtu/d]; $EM_{k,FC}$ = fuel cycle GHG emissions [gCO₂eq/MMBtu]; and $EM_{k,DS}$ = GHG emissions from displaced system in case of fuel export [gCO₂eq/MMBtu]. For details on the GHG emissions of fuel cycles and displaced systems, see section 8.2.

Finally, the GHG emissions gathering worksheet considers the impact of CO₂ sequestration. Sequestration-related calculations are applicable only if gas flooding is selected as a production practice and CO₂ is selected as the flood gas. Table 3 is an overview of system-level calculations related to CO₂ sequestration.

The CO₂ sequestration credited to the oilfield is included in the overall calculations in the ‘Results’ worksheet. It is calculated by first considering the source of the CO₂. If the CO₂ was acquired from a naturally occurring subterranean source then no sequestration credit accrues because this CO₂ was already sequestered. A sequestration credit is applicable only if the CO₂ originated from an anthropogenic source — it must have been captured during industrial process such as coal combustion.

Furthermore, depending on the specific regulations and laws governing CO₂ sequestration, the credit may accrue either to the CO₂ capturing facility or to the oilfield operator injecting it into a reservoir. OPGEE also deducts CO₂ that is released due to long-term reservoir leakage and an oilfield operator’s decision to conduct terminal phase blow-down operations. OPGEE’s consideration of long-term leakage and operator blow-down is described in Section 7.55.0.1.

If the carbon dioxide used for EOR is anthropogenic, then the overall CO₂ sequestration credit accruing to the oilfield is calculated as:

$$CR_{CO_2} = P_{oilfield} \cdot (Seq_{CO_2} - Blow_{CO_2} - Leakage_{CO_2}) \left[\frac{\text{gCO}_2}{\text{d}} \right] \quad (6.7)$$

‘GHG Emissions Table 1’

‘GHG Emissions Table 1’

‘GHG Emissions Table 2’

‘GHG Emissions Table 3’

‘Active Field 2.4.7.2’

‘Production & Extraction 1.2.9.2, 1.2.9.3’

where CR_{CO_2} = CO₂ sequestration credit assigned to the oilfield [gCO₂/d]; $P_{oilfield}$ = proportion of the overall sequestration credit assigned to the oilfield [-]; S_{eqCO_2} = CO₂ sequestration rate [gCO₂/d]; B_{lowCO_2} = CO₂ lost from the reservoir from terminal blow-down operations [gCO₂/d]; and $L_{eakageCO_2}$ = the amount of CO₂ leaving the reservoir from long-term leakage [gCO₂/d].

7 Process worksheets

This section explains the main assumptions and calculations for each process worksheet. Items discussed include user assumptions and choices, process calculation assumptions, calculations of input parameters, and calculations of intermediate outputs.

7.1 Exploration

Emissions from petroleum exploration occur during clearing of land for seismic surveys, operation of seismic survey equipment, drilling of exploratory wells, and from fugitive emissions during drilling operations. Offsite emissions occur due to other materials and services consumed during drilling (e.g., computing energy consumed during seismic data processing). A complete list of emissions sources, along with their categorization and estimated magnitude, is shown in Table C.1.

Required inputs for exploration emissions include the following terms gathered from the '*Active Field*' worksheet:

- Field depth [ft]
- Is field offshore [0-1]
- Field production rate [bbl/d]

*'Exploration
1.1'*

Required inputs to be entered for secondary interaction on the '*Exploration Emissions*' worksheet include:

- Distance of travel for survey
- Weight of land survey vehicle
- Weight of ocean survey vehicle
- Dry holes drilled per field found
- Exploratory or scientific wells drilled after field discovery (non-producing)

*'Exploration
1.2.1 - 1.2.5'*

The default values for these inputs are noted in Table 7.1.

7.1.1 Calculations for petroleum exploration

The survey vehicle energy consumption (e.g., seismic survey ship or seismic survey trucks) are calculated as:

$$E_{EXP} = \sum_j y_j m_j D_j U E_j \quad (j \in S, T) \quad (7.1)$$

$$[\text{mmBtu}] = [-] [\text{ton}] [\text{mi}] \left[\frac{\text{Btu}}{\text{ton-mi}} \right]$$

where y_j is a binary variable representing whether exploration mode S (ship-based exploration) or T (truck-based exploration) is performed [-]; m_j is the weight of exploration vehicle j [ton], D_j is the distance traveled by exploration vehicle j [mi], and UE_j is the energy-specific effectiveness of transport type j [Btu/ton-mi], as computed on the '*Transport*' worksheet.

'Transport 2.2'

Energy consumed in drilling exploratory wells is computed using drilling energy intensity computed on the '*Drilling & Development*' sheet.

Energy consumed in exploration is computed as a fraction of the total lifetime energy production assumed produced from the field. This quantity is derived in the '*Drilling & Development*' sheet, as described below.

7.1.2 Defaults for petroleum exploration

Table 7.1 shows the default settings for petroleum exploration.

Table 7.1: Default inputs for exploration emissions

Param.	Description	Eq. no.	Default	Literature range	Unit	Sources	Notes
D_j	Distance exploration mode j travels (same for S and T)	-	10,000	-	[mi]		a
m_S	Weight of exploration ship	-	100	-	[ton]		b
m_T	Weight of exploration truck	-	25	-	[ton]		c
UE_S	Effectiveness of exploration ship	-	27	-	[Btu/ton-mi]	[111]	
UE_T	Effectiveness of exploration truck	-	969	-	[Btu/ton-mi]	[111]	

^a Simple assumption for distance of travel to remote exploration site. Distance traveled during actual survey is assumed by default to be small compared to distance to field location.

^b Simple assumption for weight of exploration ship

^c Simple assumption for weight of exploration truck

7.2 Drilling & development

7.2.1 Introduction to drilling & development

Drilling and development operations result in a variety of emissions. Well drilling and installation of production equipment results in on-site energy use (e.g., for rigs and other construction equipment) as well as indirect offsite energy use (e.g., embodied energy consumed to manufacture well casing). Drilling and development also results in land use impacts, which can release biogenic carbon from disturbed ecosystems and soils [8]. In addition, fugitive emissions can occur during the drilling process. A list of emissions sources, along with their categorization and estimated magnitude, is shown in Table C.2.

7.2.2 Calculations for drilling & development

Three aspects of field drilling and development are modeled in OPGEE v3.0a: drilling energy consumption, hydraulic fracturing energy consumption, and land use impacts. Other emissions from drilling and development are not explicitly modeled and therefore would be accounted for in the small sources term. The parameters and variables used in the drilling and development model equations are listed in Table 7.7.

'Active Field
3.8'

7.2.2.1 Emissions from drilling

Drilling oil wells consumes fuel. This fuel is consumed on site in prime movers (generally diesel engines) for a variety of purposes: to power mud pumps; apply torque to drill string; pull drill string; raise, lower and retrieve subsurface monitoring equipment; and pump cement.

Relationships for these functions are derived from the open-source drilling energy intensity model *GHGfrack* [112–114]. The GHGfrack model is developed with extensive documentation and validation efforts [112, 113].

In order to develop correlations for use in OPGEE v3.0a, we ran a number of cases in GHGfrack. First, three well complexity settings are designed in GHGfrack (see Figure 7.1). These well complexity designs are also used in the '*Embodied Emissions*' worksheet, as described below. The *Simple* well design has one string of surface casing and one string of production casing. The *Moderate* well design has one string of surface casing, one string of intermediate casing, and one string of production casing. The *Complex* well design has one string of surface casing, two strings of intermediate casing, and one string of production casing. These wellbore designs are derived from examples in industry texts [35]. For each casing design an appropriate set of true vertical depth (TVD) values is chosen based on well complexity. *Simple* wells are assumed to range between 0 ft and 12,000 ft deep, *Moderate* wells are between 4,000 and 16,000 feet deep, while *Complex* wells are between 12,000 and 20,000 feet deep. Each TVD is incremented in segments of 1000 ft.

'Drilling & Development 1.2'

Each well casing design plan is designed for four wellbore diameters, called *Small*, *Medium*, *Large* and *Extra-large*. The diameters (hole diameter not casing diameter) for each of these cases is listed for each well complexity in Table 7.2. These hole diameters are chosen from API casing-hole size charts [35, Figure 11.22]. The resulting depth ranges for each casing string section are given in Table 7.3.

Table 7.2: Hole diameters for different casing sections under three wellbore designs (in.)

String	Simple			Moderate			Complex		
	Small	Med	Large	Extra-large	Small	Med	Large	Extra-large	Extra-large
Conductor	-	-	-	-	-	-	-	-	-
Surface	12.250	12.250	14.750	14.750	12.250	14.750	14.750	17.500	17.500
Intermediate 1	5.875	6.125	6.500	7.875	8.750	10.625	12.250	14.750	14.750
Intermediate 2	5.875	6.125	6.500	7.875	5.875	6.125	7.875	12.250	12.250
Production	5.875	6.125	6.500	7.875	5.875	6.125	7.875	9.500	9.500

Table 7.3: Bottomhole depth for different segments (ft.)

String	Simple	Moderate	Complex
Conductor	50	50	50
Surface	250 - 2,000	1,000 - 2,000 2,000 - 4,000	2,000 6,000
Intermediate 1	-	-	9,000-12,000
Intermediate 2	-	4000 - 16,000	12,000-20,000
Production	1,000 - 12,000		

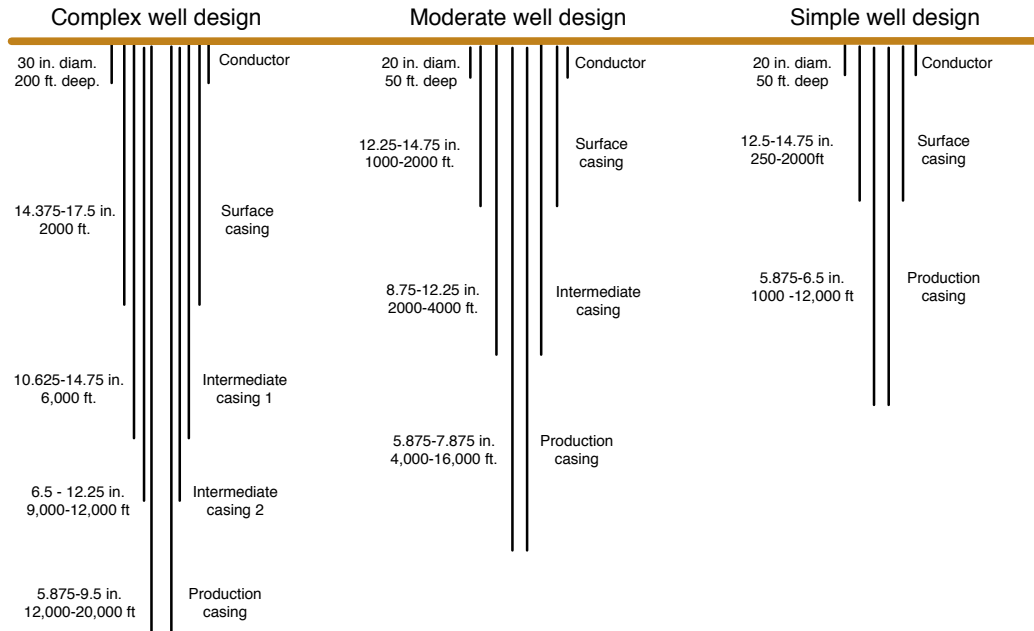


Figure 7.1: Drilling hole diameters for simple, moderate and complex well construction.

In addition, the energy efficiencies of rotary table/drill string torque provision and mud pump work are varied. The moderate efficiency settings for these terms are 45% and 65% respectively [113]. The low and high efficiency settings are 40% and 50% for the rotary table and 60% and 70% for the mud pumps, respectively.

The resulting energy consumption for rotary table and mud circulation uses are therefore modeled as:

$$E_D = E_D^{rt} + E_D^{mp} \quad (7.2)$$

Where E_D^{rt} is the energy consumed in rotary table work provision and E_D^{mp} is the energy consumed in mud circulation pumps.

The energy consumption for rotary table work E_D^{rt} is computed using the torque and torque factors as noted in GHGfrack documentation [113]:

$$E_D^{rt} = BHP^{rt} \times t, \quad (7.3)$$

or,

$$E_D^{rt} = \frac{2\pi TN}{33,000\eta} \times t, \quad (7.4)$$

where BHP^{rt} , is the brake horsepower required by the rotary table [hp], and t is the amount of time that the rotary table is operating [h]. BHP is computed using the torque T [ft-lb_f], rotational speed N [rpm], and overall electro-mechanical efficiency of the rotary table drive system η [-]. The value 33,000 is a unit conversion factor. These values are set equal to GHGfrack defaults in all results presented below. If the user wishes to change torque or other rotary table inputs, please use the GHGfrack model directly.

The energy consumption for mud circulation is computed using the overall pressure drop in the mud circulation system [113]:

$$E_D^{mp} = BHP^{mp} \times t, \quad (7.5)$$

or,

$$E_D^{mp} = \frac{\Delta P_{mp} Q}{1714\eta} \times t, \quad (7.6)$$

where ΔP_{mp} is the pressure drop that must be overcome by the mud pump [psi], Q is the mud flowrate [gal. per min.], t is the time of mud pump operation [h] and 1714 is a conversion factor.

This pressure drop ΔP_{mp} is made up of a series of terms, including:

$$\Delta P_{mp} = \Delta P_{fric} + \Delta P_{dynamic} + \Delta P_{dm} - \Delta P_{hydrostatic} + \Delta P_{other} \quad (7.7)$$

where subscripts refer to different pressure drop terms. The *fric* pressure drop is due to friction in drill string and annulus, modeled using a set of laminar and turbulent pipe and annulus flow models using different assumptions regarding non-Newtonian nature of drilling fluids (see *GHGfrack* documentation [112, 113]). The *dm* term corresponds to energy imparted on the mud motor and converted to rotational motion of the bit. In developing results for OPGEE, all *GHGfrack* mud circulation settings are left at *GHGfrack* defaults. If the user wishes to mud circulation inputs, please use the *GHGfrack* model directly.

Given overall energy term E_D , we can compute fuel use in drilling as follows:

$$F_D = \frac{E_D \eta_{gs}}{LHV_{di}} \quad (7.8)$$

where F_{DD} is the fuel use in drilling and development [gal], η_{gs} is the efficiency of the drilling prime mover (diesel engine) [-], and LHV_{di} is the lower heating value of diesel fuel [mmBtu/gal].

A number of other *GHGfrack* settings are required. For simplicity, in each model run, the drill pipe outer diameter (OD) [in] is set equal to 2.5 in. smaller than the smallest casing string inner diameter (ID). In all cases, the drill pipe ID is set equal 0.5 in. smaller than the drill pipe OD. The drill collar OD is set equal to 1.5 in. smaller than the smallest casing string ID. The drill collar ID is set equal 0.5 in. smaller than the drill collar OD. Also, in each well design, the last segment is set to an inclination angle of either 0° (vertical) or 90° (horizontal). We do not apply a slanted transition zone (i.e., a 45° zone).

Given all of the above variables, a total of 816 *GHGfrack* model runs are computed using an automated macro. The resulting depths and fuel consumption quantities for all runs are illustrated in Figure 7.2.

As can be seen, there is a wide range of energy consumption values for each depth. To further understand drivers of emissions, we then segment these results into results from simple, moderate, and complex wells (Figure 7.3).

We can further segment these results by separating vertical and horizontal wells and by noting the effect of rotary table and mud pump efficiency. This process is illustrated in Figure 7.4 for the case of simple wells only.

Using these segmented results, we construct a drilling intensity factor per-foot of drilled well for vertical wells. Because the results in Figure 7.4 are largely linear within a given efficiency setting and well geometry, we can use a linear model segmented by well category. Fuel intensity factors FI [gal diesel fuel/ft.] are constructed separate for each “line” in Figure 7.4 as follows: vertical wells are segmented by well-complexity, well diameter, and assumed efficiency setting. A linear

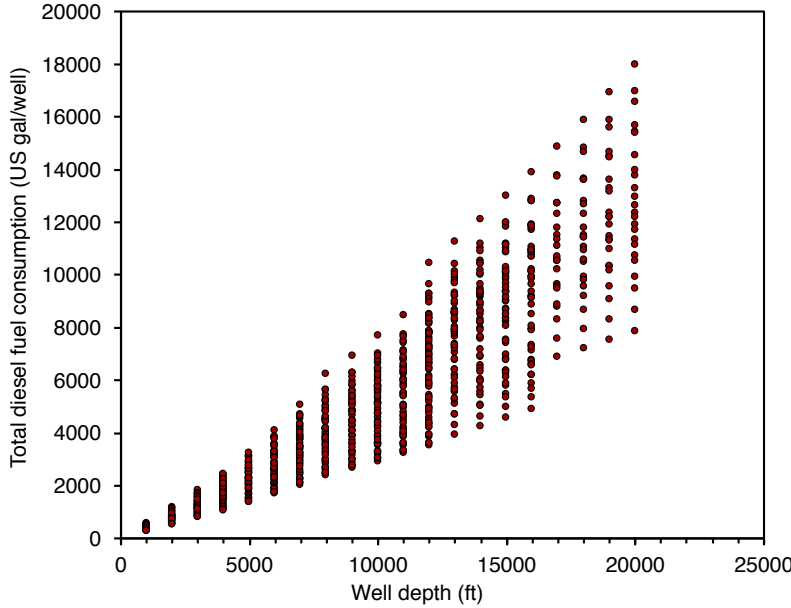


Figure 7.2: All GHGfrack results for drilling fuel consumption in US gallons of diesel (includes both rotary table + mud circulation).

slope is computed to estimate the fuel intensity factor FI by summing the total fuel use across all wells in a given well complexity-well size category and summing the total distance drilled across all wells in that category:

$$FI_D^{v,cat} = \frac{\sum_{i \in cat} F_D^i}{\sum_{i \in cat} D_v^i} \quad (7.9)$$

where i is the index for wells, $i \in cat$ represents the subset of all wells i that are included in a given well-complexity, well diameter, and efficiency setting category. D_v^i is the vertical distance drilled (TVD) for each vertical well in the particular category. These tabulated fuel intensity factors FI are included in OPGEE and selected using logic for each field depending on field well construction practices.

To compute the excess fuel required to drill horizontal wells, we compare each horizontal well to the vertical well of the same total drilling distance and compute the additional fuel use associated with making each well have a horizontal segment. This additional fuel use can then be divided for each well by the length of the horizontal segment. This gives a horizontal well fuel intensity factor FI :

$$FI_D^{h,cat} = \frac{\sum_{i \in cat} (F_D^{i,h} - F_D^{i,v})}{\sum_{i \in cat} D_h^i} \quad (7.10)$$

Where $F_D^{i,h}$ is the fuel consumed in the horizontal version of well i and $F_D^{i,v}$ is the fuel consumed in the vertical version of the same well i [gal diesel]. The horizontal distance D_h for a given well is the distance of the terminal well segment (horizontal). This computation results in an incremental fuel consumption per ft. of horizontal well drilled [gal/ft. horizontal].

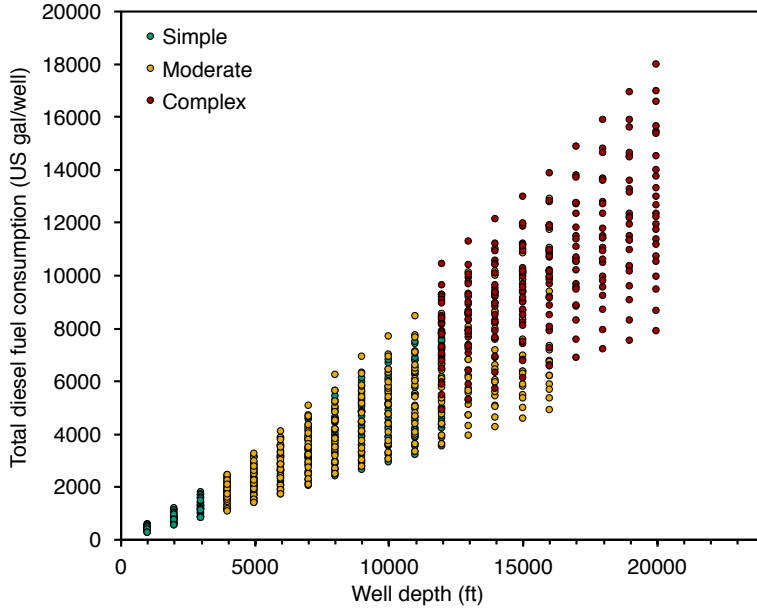


Figure 7.3: GHGfrack results for drilling fuel consumption segmented by well complexity. Fuel consumption reported in US gallons of diesel (includes both rotary table + mud circulation).

Using these two factors, we can compute the total fuel required to drill a horizontal or vertical well i using a single expression:

$$F_D^i = D_v^i \left(FI_D^{v,i} \right) + f_h D_h^i \left(FI_D^{v,i} + FI_D^{h,i} \right) \quad (7.11)$$

where f_h is the fraction of wells [0-1] with horizontal segment of length D_h [ft].

Drilling energy consumption must be amortized over the producing life of a well. Also, drilling and development energy must account for drilling of water injection wells. The lifetime productivity of wells varies by orders of magnitude, depending on the quality of the oil reservoir and its size. We include three cases for the productivity of wells from prior studies of embodied energy in oilfield operations [?]. Three options are allowed, corresponding to “low”, “medium”, and “high” per-well cumulative productivity. These settings correspond approximately to average production in the US, global average, and OPEC average productivity. Numerical values are 150 kbbi/well, 800 kbbi/well and 7,000 kbbi/well, respectively [? , Supporting Information Table S1].

The energy intensity of drilling per unit of energy produced is therefore calculated as follows:

$$ei_{DR} = \frac{F_D N_W LHV_{di}}{Q_{o,tot} LHV_o} \quad [\text{mmBtu}/\text{mmBtu}] \quad (7.12)$$

'Drilling & Development 2.3'

where ei_{DR} = energy intensity of drilling [$\text{mmBtu}/1000 \text{ ft}$]; h_W = average well depth [1000 ft]; $Q_{o,tot}$ = total lifetime productivity per well drilled [bbl oil/well]; and LHV_o = lower heating value of the crude produced [mmBtu LHV/bbl].

The energy intensity of drilling tends to be small when amortized over total well productivity, with values on order 10^{-6} to 10^{-2} mmBtu/mmBtu.

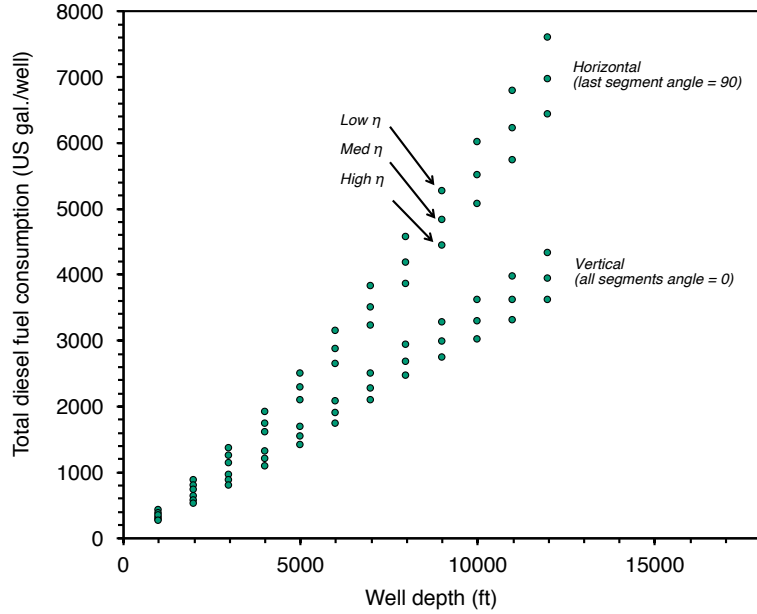


Figure 7.4: GHGfrack results for drilling fuel consumption. Only simple wells are represented, and the results are segmented by efficiency and wellbore orientation. Fuel consumption reported in US gallons of diesel (includes both rotary table + mud circulation).

7.2.2.2 Emissions from hydraulic fracturing

The practice of hydraulic fracturing can consume large amounts of energy. This is because modern high-volume multi-stage hydraulic fracturing requires injecting large amounts of fluid at high pressures. *GHGfrack* models the injection of hydraulic fracturing fluids by accounting for the pressure required for fracturing:

$$\Delta P_{hf} = \Delta P_{fracture} + \Delta P_{fric} - \Delta P_{hydrostatic}, \quad (7.13)$$

where $\Delta P_{fracture}$ is the fracturing pressure required to overcome the fracturing gradient [psi], ΔP_{fric} is the frictional pressure drop during injection [psi], and $\Delta P_{hydrostatic}$ is the contribution from the hydrostatic head of water in the wellbore [psi].

As in the case of mud pump injection energy, the energy requirements of hydraulic fracturing are calculated from the pressure drop as follows:

$$E_D^{hf} = \frac{\Delta P_{hf} Q_{hf}}{1714\eta} \times t, \quad (7.14)$$

and the fuel consumption due to hydraulic fracturing is computed similarly to the fuel consumption due to drilling:

$$F_D^{hf} = \frac{E_D^{hf} \eta_{gs}}{LHV_{di}}. \quad (7.15)$$

We compute the fuel consumption due to hydraulic fracturing using *GHGfrack* for numerous cases and use the results to create simple correlations for use in OPGEE. We use a number of default *GHGfrack* assumptions during the runs, including:

Table 7.4: Constants for quadratic fit of fracturing fuel consumption equation

Fracturing gradient [psi/ft]	<i>a</i>	<i>b</i>	<i>c</i>
0.60	588.55	-488.77	1184.50
0.65	599.49	-246.27	1349.20
0.70	511.30	575.63	964.32
0.75	499.47	924.06	1012.50
0.80	566.77	1090.40	1101.60
0.85	570.18	1378.20	1162.60
0.90	523.67	1882.70	1233.90
0.95	664.49	1512.60	1922.70
1.00	477.57	3025.40	752.02

- Injection string ID = 5 in.
- Horizontal lateral length = 5000 ft.
- Fracturing fluid density = 9.0 lbm/gal.
- Viscosity = 1 cp
- Pipe roughness = 0.00008 in
- Length of fracturing stage = 300 ft
- Number of computational segments = 10
- Pump efficiency = 65%
- Injection time = 48 hr

In order to generate the relationships used in OPGEE, we vary two key inputs to the *GHGfrack* hydraulic fracturing module: (1) amount of fracturing fluid injected, and (2) fracturing gradient. In these runs, the fracturing gradient is varied from 0.6 psi/ft to 1.0 psi/ft in increments of 0.05 psi/ft. Also, in these runs the amount of fluid injected is varied from 1 to 5×10^6 gallons in increments of 1×10^6 gallons. Therefore, a total of 45 *GHGfrack* fracturing simulations are performed.

The results from these *GHGfrack* simulations are shown in Figure 7.5. We fit quadratic functions to each set of results from the same fracturing gradient value. In each case, the r^2 value is ≥ 0.999 . The resulting quadratic function coefficients are used in OPGEE to predict hydraulic fracturing energy use in a particular field based on the volume of fracturing fluid injected. The equation used is:

$$F_D^{hf} = aV_{hf}^2 + bV_{hf} + c \text{ [gal diesel]} \quad (7.16)$$

where *a*, *b* and *c* are fitting constants unique to each fracturing gradient. The results for the fitting constants *a*, *b* and *c* are shown in Table 7.4.

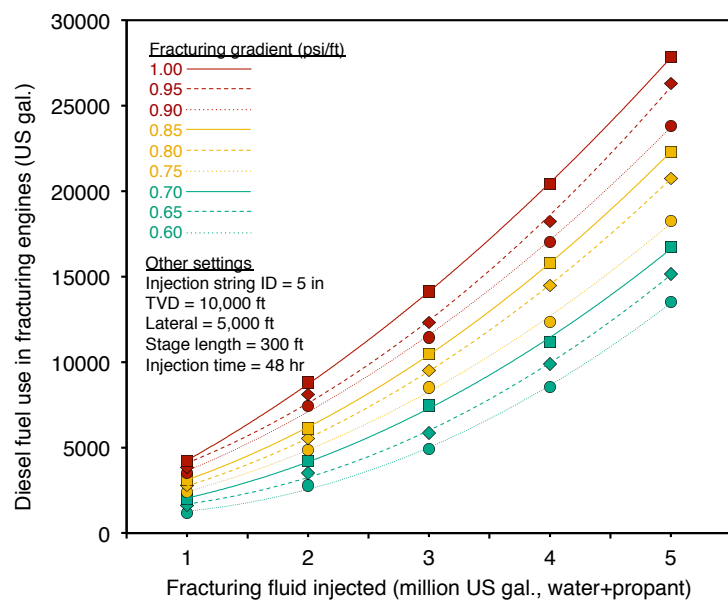


Figure 7.5: Fuel use in hydraulic fracturing as a function of fracturing volume. Each curve represents a different fracturing gradient value, ranging from 0.6 psi/ft to 1.0 psi/ft.

Table 7.5: Land use GHG emissions for 30 year analysis period from field drilling and development in OPGEE for conventional oil operations [g CO₂ eq./MJ of crude oil produced]. Data from Yeh et al [8].

	Low carbon stock (semi-arid grasslands)			Moderate carbon stock (mixed)			High carbon stock (forested)		
	Low int.	Med. int.	High int.	Low int.	Med. int.	High int.	Low int.	Med. int.	High int.
Soil carbon	0.03	0.13	0.35	0.22	0.57	1.93	0.40	1.01	3.51
Biomass	0.00	0.00	0.00	0.34	0.68	1.47	0.68	1.36	2.94
Foregone seq.	0.00	0.00	0.00	0.01	0.01	0.01	0.01	0.01	0.02

7.2.2.3 Emissions from land use impacts

Land use impacts during drilling and field development are included in OPGEE for three categories: soil carbon that is oxidized upon disturbance of land, biomass carbon that is oxidized due to biomass disturbance, and emissions from foregone sequestration, due to the fact that biomass carbon sequestration is slowed on cleared land. For each of these impacts, emissions estimates from Yeh et al. [8] are included. Yeh et al. measured impacts over a 150 year period, which is not in alignment with other analyses that use 30 year land use impact calculations. For this reason, calculations from Yeh et al. were modified to reduce the timeframe for analysis to 30 years, reducing the amount of regrowth possible [115].

The user has the option to choose a 30 year or 150 year analysis timeframe. The default analysis timeframe is set to 30 years.

In order to estimate land use GHG emissions, three settings are required. First, the crude production method must be chosen. The options for crude production method include conventional production via wellbore (primary, secondary, and tertiary recovery of conventional and heavy hydrocarbons, including in situ recovery of bitumen) and mining-based production of bitumen.

Next, the carbon richness of the ecosystem is specified. Options include low, moderate, and high carbon richness. Low carbon richness estimates are derived from California production in the semi-arid to arid central valley of California [8]. The high carbon richness estimates are derived from forested regions in Alberta (e.g., rocky mountain foothills) [8]. Moderate carbon richness is considered a mixed ecosystem with carbon richness between these ecosystems.

Lastly, the intensity of field development must be specified. High intensity field development corresponds to high fractional disturbance, such as in a field drilled on tight spacing. Low intensity field development corresponds to a sparsely developed field with little fractional disturbance. Moderate field development occurs between these two extremes. Work by Yeh et al. [8] can be consulted for satellite images of low and high field development intensity.

Emissions associated with each choice are shown in Table 7.6 in units of gCO₂eq GHGs per MJ of crude oil produced.

'Drilling & Development'
1.3.2.3'

'Emissions Factors Tables'
1.6.1.7'

'Drilling & Development'
1.2.13'
'Drilling & Development'
1.1.3,1.1.4'

'Drilling & Development'
1.1.10'

'Drilling & Development'
1.1.11'

'Emissions Factors Tables'
1.6.1.7'

7.2.3 Defaults for drilling & development

Default values for drilling & development calculations are shown in Tables 7.7 and 7.6.

Table 7.6: Land use GHG emissions for 150 year analysis period from field drilling and development in OPGEE for conventional oil operations [g CO₂ eq./MJ of crude oil produced]. Data from Yeh et al [8].

	Low carbon stock (semi-arid grasslands)			Moderate carbon stock (mixed)			High carbon stock (forested)		
	Low int.	Med. int.	High int.	Low int.	Med. int.	High int.	Low int.	Med. int.	High int.
Soil carbon	0.03	0.13	0.35	0.10	0.35	1.50	0.16	0.57	2.65
Biomass	0.00	0.00	0.00	0.01	0.09	0.33	0.02	0.17	0.65
Foregone seq.	0.00	0.00	0.00	0.02	0.03	0.05	0.03	0.05	0.09

Table 7.7: Default inputs for drilling calculations.

Param.	Description	Eq. no.	Default	Literature range	Unit	Sources	Notes
D_v	Vertical depth of wells		7240	100-20,000	[ft]		a
D_h	Length of horizontal segment of well		5000	1000-10,000	[ft]		a
f_h	Fraction of wells with horizontal segment	-	0	0 - 1	[fraction horizontal]		
F^{lh}_D	Horizontal drilling incremental fuel intensity	-	0.380	0.218 - 0.459	[gal/ft. horizontal]	[113]	b
F^v_D	Vertical drilling fuel intensity	-	0.404	0.226 - 0.724	[gal/ft.]	[113]	b
N_W	Number of total wells, prod. and inj.	-	13	-	[Wells]	-	c
$Q_o,_{tot}$	Cumulative production per well over life of well	-	800	150 - 7,000	[kbbi/well]	[?]	d
LHV_{di}	Lower heating value of diesel fuel	-	128.5	128.5	[mBtu/gal]	[111]	e
LHV_o	Lower heating value of crude oil	-	5.51	5.15 - 6.18	[mmBtu/bbl]	[116]	e

^a Low and high drilling efficiency constants found from fitting data. Default set to low intensity.

^b Exponential increase with drilling depth. Low intensity drilling actually has slightly higher growth rate.

^c Default well depth chosen to be depth of field h . Range of field depths is large in practice.

^d Cumulative production per well from Brandt [?].

^e Lower heating value of crude depends on density and composition, we use relationship from Schmidt [116].

7.3 Reservoir

Pressure in the reservoir drives fluids toward the (lower pressure) wellbore bottom. The amount of flow depends on the pressure differential and the properties of the rock. At the wellbore bottom the fluids have some bottomhole flowing pressure that serves as the baseline pressure in artificial lifting calculations (see below). In addition to artificial lifting, water can be injected into the reservoir to support reservoir pressure and increase oil recovery [69, p. 1].

The streams flowing into and out of the reservoir-well interface process are shown in Figure 7.6 and are listed in Table 7.8. The secondary inputs to the reservoir sheet are listed in Table ??.

Table 7.8: Streams flowing into and out of the reservoir-well interface process. I/O denotes input or output stream

Flow name	Stream	I/O	Source/Destination	Units	Notes
Oil from reservoir	1	I	Reservoir	[t/d]	
Water from reservoir	100	I	Reservoir	[t/d]	
Gas from reservoir	25	I	Reservoir	[t/d]	
Oil at well bottom	3	O	Well/downhole pump	[t/d]	
Water at well bottom	101	O	Well/downhole pump	[t/d]	
Gas at well bottom	26	O	Well/downhole pump	[t/d]	

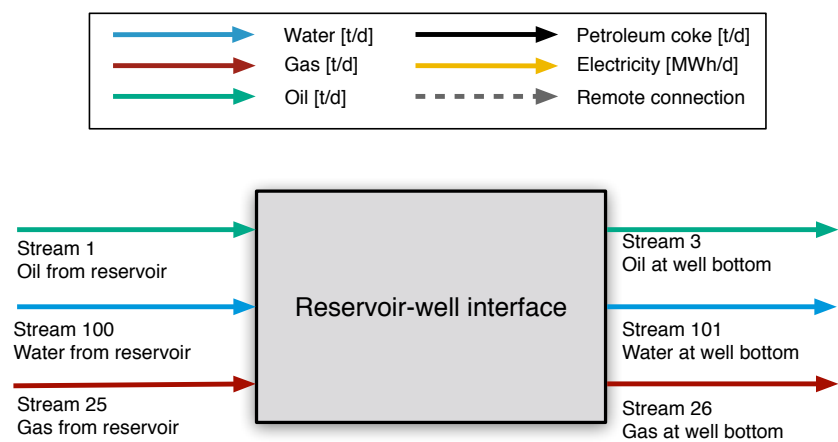


Figure 7.6: Streams flowing into and out of reservoir-well interface. All streams measured in tonnes per day excepting electricity which is measured in MWh/d.

An important part of the reservoir flow problem is to understand the nature of flow and in what phases the hydrocarbon material will be flowing to the wellbore.

The bubblepoint pressure is the pressure at which the solution gas will start to evolve from the oil into a separate gas phase (i.e., the gas will start to bubble out of the oil). We use the bubblepoint pressure relationship of Al-Shammasi (1999), as reproduced in [55, vol 1, Table 6.6]:

$$P_b = \gamma_o^{a_1} \times [R_b \gamma_g (T_r + 459.67)]^{a_2} \times e^{(-a_3 \gamma_o \gamma_g)} \quad [\text{psi}] \quad (7.17)$$

where P_b is the bubblepoint pressure of the oil, γ_o is the oil specific gravity (water = 1), γ_g is the gas specific gravity (air = 1), T_r is the reservoir temperature [$^{\circ}\text{F}$], and a_1 , a_2 , and a_3 are fitting constants. R_b is the bubblepoint solution gas oil ratio [scf/bbl], discussed below. At a given pressure, this equation can be rearranged to find the amount of gas in solution, so it is used to compute the solution GOR for various conditions as well [55, p. 273]

The average reservoir temperature T_r is either given as a data input or filled with an OPGEE smart default given the reservoir depth. The default relationship is:

$$T_r = 70 + 1.8 \frac{h}{100} \quad [{}^{\circ}\text{F}] \quad (7.18)$$

where 70 $^{\circ}\text{F}$ is the default yearly average surface temperature, h is the reservoir depth [ft], and 1.8 is the geothermal gradient in $^{\circ}\text{F}$ per 100 ft.

The amount of gas in solution at the bubblepoint is important for modeling flow. Valko and McCain (2003) give a means to estimate the bubble point gas-oil ratio from the separator gas oil ratio [117]. Since OPGEE takes separator gas oil ratio GOR as an input, we use this correlation [117, eq. 3-3]:

$$R_b = 1.1618 \times \text{GOR} \quad \left[\frac{\text{scf}}{\text{bbl}} \right] \quad (7.19)$$

where GOR is the separator GOR, which is most commonly reported in the literature, and as drawn from the 'Active Field' working sheet.

The equation given above for bubblepoint pressure 7.17 can be rearranged to solve for the solution gas oil ratio. Given an actual reservoir pressure below the bubblepoint, the amount of gas in solution at reservoir conditions can be solved for [55, Vol. 1, sec 6.5].

The water formation volume factor, B_w , or the ratio of bbl of water in the reservoir to bbl of water at stock tank conditions [bbl/STB] is given by a correlation from McCain, reproduced in Fanchi 2007 [55, p. 483]:

$$B_w = (1 + \Delta V_{wp})(1 + \Delta V_{wT}) \quad \left[\frac{\text{bbl}}{\text{STB}} \right] \quad (7.20)$$

where the first term is the change in volume due to pressure and the second is the change in volume due to temperature. These are computed as follows:

$$\Delta V_{wp} = a_1 + a_2 T_r + a_3 T_r^2 \quad (7.21)$$

$$\Delta V_{wT} = a_4 p_r T_r + a_5 p_r^2 T_r + a_6 p_r + a_7 p_r^2 \quad (7.22)$$

These correlations must be applied to the density of water at standard conditions, which varies with the salinity of the water.

'Reservoir
M68'

'Active Field
K69'

'Reservoir
M67'

'Reservoir
M70'

'Reservoir
M79'

'Reservoir
M78'

Table 7.9: Streams flowing into and out of the wellbore/downhole pump process. I/O denotes input or output stream

Parameter name	Eq. term	Default value	Range	Units	Source	Notes
Excess pressure in injection well		500		[psi]		Assumption
Temperature of fluids at well bottom		150		[°F]		Assumption
Reservoir permeability		100		[mD]		Assumption
Reservoir pay thickness		500		[ft]		Assumption
Bubblepoint pressure constant 1	a_1	5.527215	-	[·]		[?]
Bubblepoint pressure constant 2	a_2	0.783716	-	[·]		[?]
Bubblepoint pressure constant 3	a_3	1.841408	-	[·]		[?]
Oil FVF constant 1	a_1	1	-	[·]		[?]
Oil FVF constant 2	a_2	5.253E-07	-	[·]		[?]
Oil FVF constant 3	a_3	0.000181	-	[·]		[?]
Oil FVF constant 4	a_4	0.000449	-	[·]		[?]
Oil FVF constant 5	a_5	0.000206	-	[·]		[?]
Water FVF constant 1	a_1	-0.010001	-	[·]		[?]
Water FVF constant 2	a_2	0.0001334	-	[·]		[?]
Water FVF constant 3	a_3	5.507e-7	-	[·]		[?]
Water FVF constant 4	a_4	-1.95e-9	-	[·]		[?]
Water FVF constant 5	a_5	-1.73e-13	-	[·]		[?]
Water FVF constant 6	a_6	-3.59e-7	-	[·]		[?]
Water FVF constant 7	a_7	-2.25e-10	-	[·]		[?]
Bubblepoint gas-oil-ratio	GOR_b	1055	-	[scf/bbl]		[117]
Reservoir temperature	T_r	200	-	[°F]		
Specific gravity of gas	γ_g	0.69	0.6-0.8	[g/g]		a
Specific gravity of oil	γ_o	0.88	0.75-1.05	[g/g]	[?]	b

a - Computed from gas properties using MW of gases and gas composition. At OPGEE defaults, gas sg = 0.69.

b - Specific gravity of oil is a function of reported oil API gravity. Lookup from [116] in 'Fuel Specs' sheet.

The productivity index, PI, is defined as [118, p. 23]:

$$PI = \frac{Q_{l,W}}{(p_r - p_{wf})} \quad \left[\frac{\text{bbl}}{\text{psi-d}} \right] \quad (7.23)$$

where PI = well productivity index [bbl liquid/psi-d]; $Q_{l,W}$ = liquid production per well [bbl liquid/d]; p_r = average reservoir pressure [psi]; and p_{wf} = wellbore pressure [psi]. The increase in production requires an increase in pressure drawdown at a constant productivity index. In OPGEE a default productivity index of 3.0 [bbl liquid/psi-d] is assumed to calculate the pressure drawdown. The user has to control the inputs to satisfy the condition of $p_{wf} \geq 0$. The pressure for lifting can either be applied by a downhole pump or by gas lift; in OPGEE these methods may be used individually or simultaneously.

[JEFF: ADD DESCRIPTION OF GAS PHASE PRESSURE DROP]

7.4 Wellbore/Downhole Pump

As production from a field proceeds the reservoir pressure will decrease. To maintain economic viability, artificial lift equipment is used to enhance production rates. Most commonly, energy is added to the reservoir fluids through the use of a down-hole pump [118, p. 2]. Another method is gas lifting, which entails injecting gas into the production string to decrease the density of the column of oil and water in the production tubing.

The streams flowing into and out of the wellbore/downhole pump process are shown in Figure 7.7 and are listed in Table 7.8.

Table 7.10: Streams flowing into and out of the wellbore/downhole pump process. I/O denotes input or output stream

Flow name	Stream	I/O	Source/Destination	Units	Notes
Oil at well bottom	3	I	Reservoir/well interface	[t/d]	
Water at well bottom	101	I	Reservoir/well interface	[t/d]	
Gas at well bottom	26	I	Reservoir/well interface	[t/d]	
Fuel gas - Downhole pump	150	I	Fuel gas system	[t/d]	
Electricity - Downhole pump	175	I	Electricity generation and imports	[MWh/d]	
Lifting gas to wellbore	42	I	Lifting gas compressor	[t/d]	
Oil at wellhead	4	O	Separation	[t/d]	
Water at wellhead	102	O	Separation	[t/d]	
Gas at wellhead	27	O	Separation	[t/d]	
Wellhead leaks to air	250	O	Environment - Atmosphere	[t/d]	

Table 7.11: Secondary parameter inputs to the wellbore/downhole pump worksheet

Parameter name	Default value	Units	Source	Notes
Concentration of dissolved solids	5000	[mg/l]	[?]	-
Wellhead pressure	1000	[psi]	[4]	-
Wellhead temperature	150	[°F]	Assumption	-
Friction factor	0.02	[-]	[?]	-

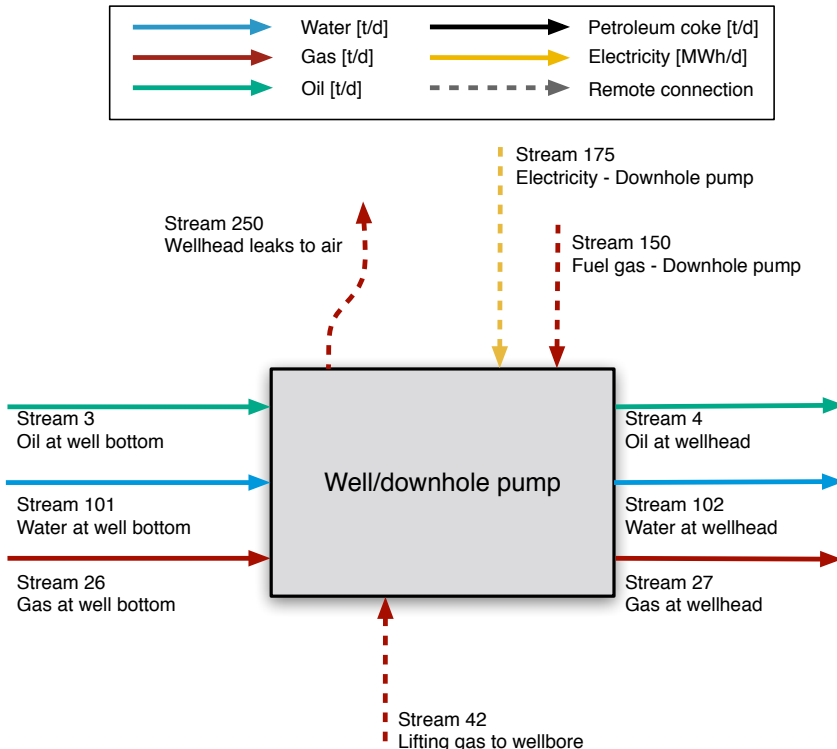


Figure 7.7: Streams flowing into and out of the wellbore/downhole pump process. All streams measured in tonnes per day excepting electricity which is measured in MWh/d.

Most common artificial lifting and improved oil recovery techniques are included in OPGEE. These include: downhole pump, gas lift, water flooding, gas flooding, and steam injection. In the '*Inputs*' worksheet the user is prompted to choose a combination of techniques applicable to the modeled operation.

A complete list of emissions sources from production, along with their estimated magnitude, is shown in Table C.3. A list of all of the equation parameters, including their default values and sources, is included in Table 7.76.

Energy for lifting is required to overcome the pressure traverse, i.e., the pressure drop between the subsurface reservoir and the surface wellhead. The pressure traverse arises due to two factors: (i) flow against gravity, and (ii) frictional losses. The pressure required for lifting is calculated by adding the wellhead pressure to the pressure traverse and subtracting the wellbore pressure. The artificial lifting methods that can be chosen in OPGEE are: (i) downhole pump, and (ii) gas lift. The pressure required for lifting is equal to the discharge pressure of the downhole pump. The power required to generate the required discharge pressure depends on the discharge flow rate and pump efficiency. Finally the energy required to drive the pump is calculated based on the power requirement (expressed as brake horsepower).

The calculation of the energy required in water injection- and gas injection-based EOR uses the user inputs for injection volume and discharge pressure. Smart defaults are in place to help assign the discharge pressure taking into account the well depth and frictional losses.

The energy required for steam flooding requires rigorous modeling of steam generation. An additional complexity is caused by the modeling of electricity co-generation at steam projects. These calculations are explained in Section ??, which covers steam generation emissions.

In the case of gas lift, if the user enters the volume of gas injected and the discharge pressure, OPGEE will compute the compression energy. However, OPGEE is not sensitive to changes in the gas lift, i.e. the dynamics between the volume of gas lift and the lifting head are not considered. The calculation of these dynamics is beyond the scope of a linear GHG estimator. This requires a two phase flow model, which is not included in OPGEE v3.0a.

Default values for production and extraction calculations are shown in Table 7.76.

7.4.0.1 Oil specific gravity

The specific gravity of crude oil is usually reported as API gravity, measured at 60 °F. The API gravity is related to the specific gravity γ_o by:

$$^{\circ}\text{API} = \frac{141.5}{\gamma_o} - 131.5 \quad [-] \quad (7.24)$$

*'Production
& Extraction
2.1.1'*

where API gravity and γ_o are dimensionless measures. The specific gravity is the ratio of the oil density to the density of water [9, p. 478].

7.4.0.2 Gas specific gravity

The specific gravity of associated gas is calculated as [118, p. 10]:

*'Production
& Extraction
2.1.4'*

$$\gamma_g = \frac{\rho_{gsc}}{\rho_{asc}} \quad [-] \quad (7.25)$$

where ρ_{gsc} = gas density at standard conditions [lbm/ft³]; and ρ_{asc} = air density at standard conditions [lbm/ft³]. Standard temperature is 60 °F; standard pressure is 14.7 psia [4, p. 35]. The gas density at standard conditions is calculated using:

$$\rho_{gsc} = \frac{p_b \text{MW}_g}{R T_b} \quad \left[\frac{\text{lbm}}{\text{ft}^3} \right] \quad (7.26)$$

where MW_g = molecular weight of the associated gas mixture [lbm/lbmol]; p_b = base pressure [psia]; and T_b = base temperature [°R]; R = gas constant [ft³-psia/lbmol-°R]. The molecular weight is calculated from the molecular weights and molar fractions of the gas constituents.

7.4.0.3 Well pressure traverse

The pressure traverse is the total pressure required to lift the crude oil mixture against gravity and overcome friction and kinetic losses. This is equal to the pressure drop along the well tubing from the wellbore to the wellhead. This pressure drop has two main components: (i) the elevation component, which is the pressure drop due to gravity; and (ii) the friction component, which is the pressure drop due to liquid contact with the inner walls of the well tubing.

The first step in the estimation of the pressure traverse is the calculation of the total head as:

$$h_{tot} = h_{el} + h_f \quad [\text{ft}] \quad (7.27)$$

where h_{tot} = total head [ft]; h_{el} = well depth [ft]; and h_f = friction head [ft]. The friction head is calculated using the Darcy formula [9, p. 447]:

$$h_f = \frac{f h_{el} v_{l,W}^2}{2 D_p g_c} \quad [\text{ft}] \quad (7.28)$$

where f = Moody friction factor [-]; h_{el} = well depth [ft]; $v_{l,W}$ = pipeline flow velocity [ft/s]; D_p = pipeline diameter [ft]; and g_c = gravitational constant, 32.2 [lbm-ft/lbf-s²]. A major determinant of friction losses is the pipeline diameter or production tubing diameter (D_p). API production tubing diameters range from 1.05 to 4.5 inches ID; the API system is a petroleum industry standardized measuring system [54, p. 106].

A Moody friction factor chart is shown in Figure 7.8 [3]. f varies with the Reynold's Number (Re) and/or pipeline roughness, depending on whether the flow regime is laminar or turbulent [9, p. 481]. Table 7.12 shows the Re ranges of different flow patterns.

The Moody friction factor is estimated using simplifications for the default case as follows: Water and oil are assigned viscosities of 1 and 10 cP, respectively. The viscosity of the oil-water mixture is assigned the volume-weighted viscosity of the two fluids.¹

*'Production
& Extraction
1.2.2,2.2.1'*

¹This simplification does not account for the complexity of oil-water mixture viscosity, but is used as a first-order approximation. Heavy oil can have very high viscosities as well.

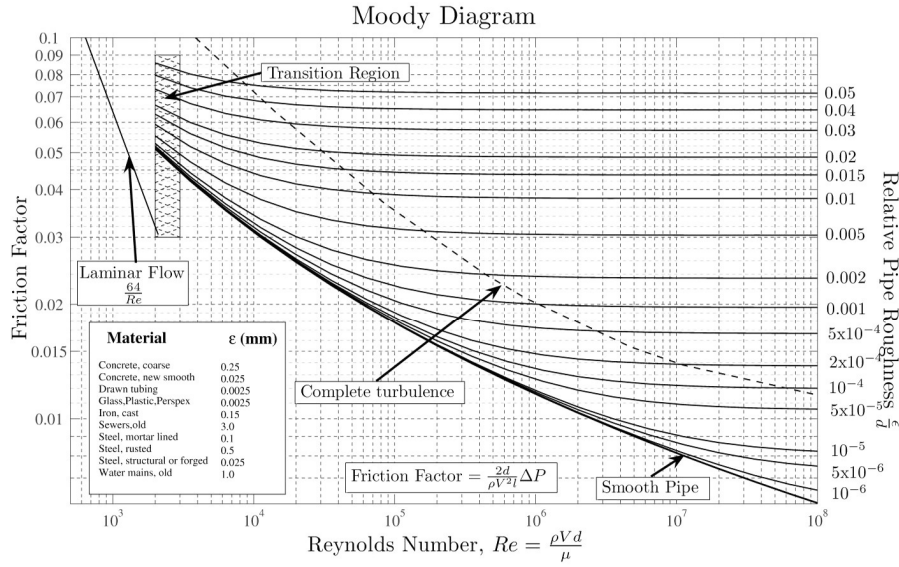


Figure 7.8: Moody friction factor chart. Source: [3].

Table 7.12: Reynold's number (Re) ranges of different flow patterns. Data from McAllister [9].

Flow pattern	NRe [-]
Laminar flow	$Re < 2000$
Transition flow	$2000 \leq Re \leq 4000$
Turbulent flow	$Re > 4000$

The Reynolds number, Re , is calculated as follows [119, p. 46]:

$$Re = \frac{1.48 Q_l \rho_l}{D_p \mu_l} \quad (7.29)$$

where Q_l is the total liquid production rate [bbl/d]; ρ_l is the liquid density (oil-water mixture) [lbm/ft³]; D_p is the wellbore production diameter [in], and μ_l is the fluid viscosity [cP]. Roughness of commercial steel of 0.0018 in is assumed [120], for a relative roughness r of 0.0006. The approximate friction factor is calculated as follows [120, p. 625]:

$$f = \left(\frac{-1}{1.8 \log \left(\left[\frac{6.9}{Nre} \right] + \left[\frac{r}{3.7} \right]^{1.11} \right)} \right)^2 \quad (7.30)$$

This equation gives a friction factor f of 0.02 for default conditions. The friction factor is a user input on the 'Production & Extraction' worksheet and can be adjusted by the user.

The pipeline flow velocity is calculated as:

$$v_{l,W} = \frac{Q_{l,W}}{A_p} \quad [\text{ft/s}] \quad (7.31)$$

where $Q_{l,W}$ = wellbore flow rate or liquid production per well [ft^3/s]; and A_P = the cross sectional area of the pipe [ft^2]. The wellbore flow rate is calculated as:

$$Q_{l,W} = \frac{Q_l}{N_W} \quad [\text{ft}^3/\text{s}] \quad (7.32)$$

where Q_l = total rate of liquid production [ft^3/s]; and N_W = number of producing wells. The total rate of liquid production is calculated as:

$$Q_l = Q_o(1 + \text{WOR}) \quad [\text{ft}^3/\text{s}] \quad (7.33)$$

where Q_o = total rate of oil production [bbl/d]; WOR= water-to-oil ratio [bbl/bbl]. The total rate of liquid production is converted from [bbl/d] to [ft^3/s].

The pressure traverse is estimated using the total head as [9, Table 1, p. 455]:

$$p_{trav,tot} = 0.43h_{tot}\gamma_l \quad [\text{psi}] \quad (7.34)$$

where $p_{trav,tot}$ = total pressure traverse [psi]; 0.43 = fresh water gradient at 60 °F [psi/ft] [69, p. 25]; h_{tot} = total head [ft]; and γ_l = the specific gravity of the crude oil mixture [-], calculated as:

$$\gamma_l = \gamma_o\lambda_o + \gamma_w\lambda_w \quad [-] \quad (7.35)$$

where γ_o = the specific gravity of oil [-]; γ_w = the specific gravity of water [-]; λ_o = fraction of oil [fraction]; and λ_w = fraction of water [fraction]. The fraction of oil is calculated as:

$$\lambda_o = \frac{Q_o}{Q_o(1 + \text{WOR})} \quad [-] \quad (7.36)$$

The elevation component of the pressure traverse is estimated using a linear one phase flow model where the gas-to-liquid ratio is equal to zero (GLR= 0) and the temperature and pressure effects are ignored. Figure 7.9 shows an example of a linear pressure-traverse curve for a particular production rate and fluid properties. The slope of the curve is the relative density of the flowing oil-water mixture. For GLR>0 the relationship becomes non-linear and the pressure traverse becomes less sensitive to changes in the well depth with increasing GLR [54, p. 27]. However, the generation of a non-linear relationship requires the application of the multi-phase flow correlations which requires an iterative, trial-and-error solution to account for the changes in flow parameters as a function of pressure. Due to the complexity of this approach, we do not implement multi-phase flow in OPGEE v3.0a.

7.4.0.4 Pressure for lifting

The second step after estimating pressure traverse is the calculation of the pressure for lifting which is the pressure required by artificial means (e.g., pump) to lift the oil-water mixture to the surface at the desired wellhead pressure. The pressure for lifting is calculated as:

$$p_{lift} = (p_{trav,tot} + p_{wh}) - p_{wf} \quad [\text{psi}] \quad (7.37)$$

where p_{lift} = pressure for lifting [psi]; $p_{trav,tot}$ = total pressure traverse [psi]; p_{wh} = wellhead pressure [psi]; and p_{wf} = bottomhole pressure [psi]. The wellbore pressure is calculated from the average reservoir pressure by subtracting the pressure drawdown. The pressure drawdown is the difference between the reservoir pressure and the bottomhole pressure [118, p. 22].

*'Production
& Extraction
2.2.2'*

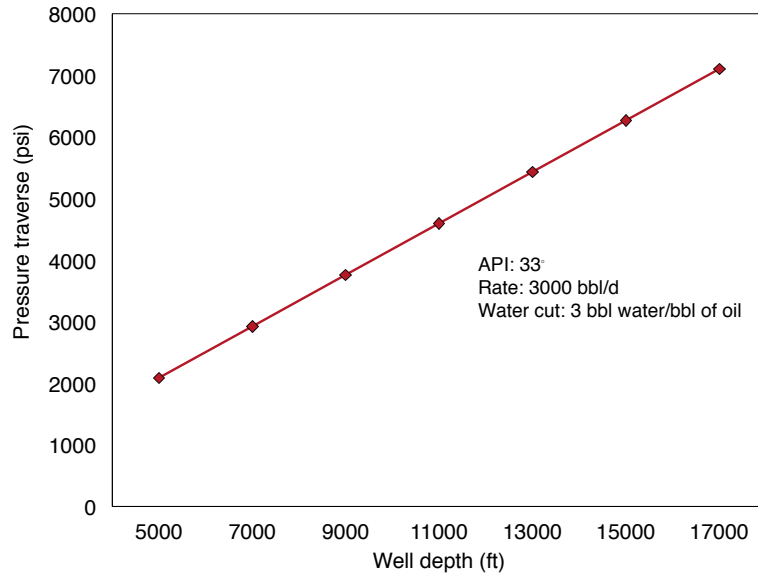


Figure 7.9: An example of a linear pressure traverse curve (GLR= 0).

7.4.0.5 Pump brake horsepower

The brake horsepower (BHP) is calculated using the pump discharge flow rate and the pumping pressure as [69, p. 27]:

*'Production
& Extraction
2.2.3'*

$$\text{BHP}_P = \frac{1.701 \times 10^{-5} Q_d \Delta p}{\eta_P} \quad [\text{hp}]$$

This is equivalently expressed as:

$$\text{BHP}_P [\text{hp}] = \frac{\frac{1[\text{hp}]}{1714[\text{gpm-psi}]} \frac{42[\text{gal}]}{24[\frac{\text{hr}}{\text{d}}] 60[\frac{\text{min}}{\text{hr}}]} Q_d \left[\frac{\text{bbl}}{\text{d}} \right] \Delta p [\text{psi}]}{\eta_P} \quad (7.38)$$

where BHP_P = brake horsepower [hp]; Q_d = pump discharge rate [bbl/d]; Δp = pumping pressure [psi]; and η_P = pump efficiency [%]. The term 1714 is a dimensionless factor that converts between [hp] and [gpm-psi]. The pumping pressure is the difference between pump discharge and suction pressures. The default suction pressure is 0 psi. In the case of a downhole pump the pumping pressure is equal to the pressure for lifting as calculated in eq. (7.37).

7.5 Bitumen mining

Bitumen mining takes in raw bitumen ore (containing sand, bitumen, and water) and produces cleaned and separated bitumen ready for upgrading or dilution.

The streams flowing into and out of the bitumen mining process are shown in Figure 7.10 and are listed in Table 7.13.

Table 7.13: Streams flowing into and out of the bitumen mining process. I/O denotes input or output stream

Flow name	Stream	I/O	Source/Destination	Units	Notes
Bitumen at mine	2	I	Bitumen mine	[t/d]	
Fuel gas - Mining	167	I	Fuel gas system	[t/d]	
Electricity - Mining	193	I	Electricity generation and imports	[MWh/d]	
Bitumen from mine to upgrader	5	O	Separation	[t/d]	
Bitumen from mine to dilution	6	O	Separation	[t/d]	
Mine offgas to flare	84	O	Environment - Atmosphere	[t/d]	
Mine face fugitives and tailings pond emissions	281	O	Environment - Atmosphere	[t/d]	

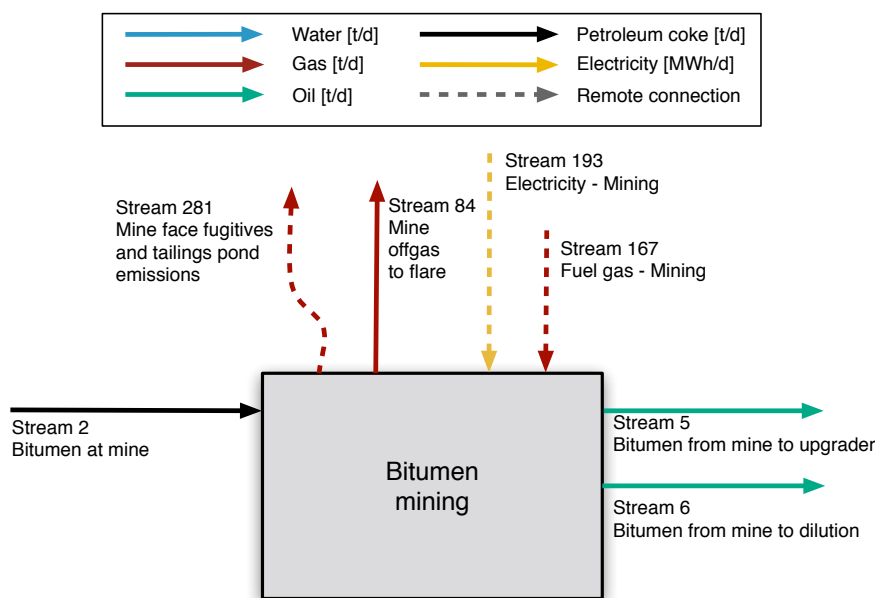


Figure 7.10: Streams flowing into and out of the bitumen mining process. All streams measured in tonnes per day excepting electricity which is measured in MWh/d.

Table 7.14: Secondary parameter inputs to the bitumen mining worksheet

Parameter name	Default value	Units	Source	Notes
Mined bitumen temperature	80	[°F]	Assumption	-
Mined bitumen pressure	14.7	[psi]	Assumption	-
Mined bitumen API gravity	8	[°API]	Assumption	-
Fraction of gas consumed in equip	[0-1]	[-]	Assumption	-

There are seven mining projects currently operating in the Canadian oil sands as of late 2015. The characteristics of each mining operation are summarized in Table ???. One of the main differences between oil sands mines is the bitumen froth treatment technology used. Once oil sands material is mined it is transported to a separation facility where hot water is added to produce an oil sands slurry. The slurry is brought to an extraction facility where gravity drainage is used to remove larger solids and produce a bitumen froth, a mixture of bitumen, fine solids, and water. This bitumen froth undergoes froth treatment, in which a light hydrocarbon (either naphthenes or paraffins) acts as a solvent and separates bitumen from other material contained in the bitumen froth. Older projects (those constructed prior to 2002) all employ naphthenic froth treatment (NFT), while projects constructed from 2002 onwards (with the exception of the CNRL Horizon project which employs NFT) employ paraffinic froth treatment (PFT).

The bitumen produced at NFT facilities is of lower quality, containing a higher percentage of asphaltenes and more residual water and solids. Bitumen produced at NFT mines must therefore go through upgrading to synthetic crude oil (SCO) and cannot be diluted and sent directly to refineries, as is the case for bitumen produced at PFT facilities. Generally NFT mines include an upgrader located at the mine site. Because natural gas and electricity consumed for the mine and the upgrader are delivered to the site altogether, the facilities share a common cogeneration system and a significant amount of waste heat from the upgrader is used in the bitumen separation process.

Disentangling use by mining operations alone is challenging given the complex nature of operations. Importantly, the Alberta Energy Regulator (AER) reports natural gas and electricity consumption for integrated mining and upgrading facilities together without specifying the quantities of natural gas and electricity consumed for mining alone. The exception to this is the Syncrude Aurora (NFT) project, as bitumen produced at that site is transported to the Syncrude Mildred Lake (NFT) project for upgrading at the Mildred Lake upgrading facility. Also, the Suncor upgrader located at the mine site also upgrades bitumen produced at Suncor's Firebag in situ project. Bitumen produced by the stand-alone Shell Muskeg River and Jackpine (PFT) mines is upgraded at the stand-alone Shell Scotford upgrader, however as the upgrader is located off-site the energy consumption for the mines is reported separately from the upgrading process. The Imperial Kearn project is the only mining project that produces diluted bitumen (known as dilbit) that is sent directly to refineries without undergoing any intermediate upgrading. Of all the mining projects, the Suncor upgrader produces some diesel fuel that is combusted as a fuel on-site.

Public Data Available Data are available from a number of public sources. First, the AER publishes monthly Statistical Reports on oil sands operations. Most useful are ST39: *Alberta Mineable Oil Sands Plant Statistics*, which was published from 1970-2002 and 2008-2014 [121]; as well as ST43: *Alberta Oil Mineable Oil Sands Plant Statistics - Annual*, which was published in years 2003-2007 [122]. These statistical reports tabulate monthly energy consumption, flared/wasted fuels, and electricity, bitumen, and SCO production for each oil sands project. Some projects operated by the same company receive fuel at one mine and then deliver fuel to the other mine and so report the total fuel consumption under the mine that receives the fuel

Table 7.15: Characteristics of operating mining projects

Mine	Year	Cap. (bbl/d)	Sep.	Int. upgr.?	Notes
Suncor	1967	490,000	NFT	Yes	Upgrader also processes bitumen produced from Suncor Firebag in situ project.
Syncrude Mildred Lake	1978	150,000	NFT	Yes	Upgrader also processes bitumen produced at Syncrude Aurora mine.
Syncrude Aurora	2001	200,000	NFT	No	Waste heat from Syncrude Mildred Lake upgrader used in Syncrude Aurora mine.
CNRL Horizon	2008	250,000	NFT	Yes	
Shell Muskeg River	2002	155,000	PFT	No	Bitumen transported to stand-alone Shell Scotford upgrader.
Shell Jackpine	2010	100,000	PFT	No	Bitumen transported to stand-alone Shell Scotford upgrader.
Imperial Kearn	2013	220,000	PFT	No	Only mine that produces diluted bitumen.

(e.g., Syncrude's Mildred Lake and Aurora projects) rather than reporting the fuel consumption for each project separately [123].

Definitions provided by AER for energy consumption reported in the AER's ST39 and ST43 reports include definitions of some potentially ambiguous data [123]:

- SCO Fuel Use: The total volume of SCO combusted as fuel at the facility.
- SCO Plant Use: The total volume of SCO used at the facility for uses other than fuel.
- Bitumen Flared/Wasted: The total volume of unrecovered crude bitumen from spills, upgrading slops, tanks dewatering etc.

Note that diesel fuel consumption for each project is collected by the AER but not reported in any of the AER's reports [123]. One project, Suncor, does report that the upgrader produces diesel fuel that is used as fuel on site for mining operations. This use is reported under the AER as SCO fuel consumption [121].

Another important data source are engineering "templates" generated by the Canada's Oil Sands Innovation Alliance (COSIA). COSIA has published two mine templates that contain material and energy flow diagrams for the two froth treatment technologies (naphthenic froth treatment and paraffinic froth treatment) employed in the oil sands [124, 125]. For each froth treatment technology, energy and material flows are presented for two possible oil sands ore qualities: low grade ore at 9 wt.% bitumen, and high grade ore at 12 wt.%. The COSIA Mine Templates provide approximate energy consumption values for a representative mining project based on existing oil sands operations but not representative of any currently operating oil sands project.

A last source of data is the Alberta Environmental Monitoring, Evaluation, and Reporting Agency (AEMERA), which has published estimates of fugitive GHG emissions from mine face, tailings ponds, and 'other' (e.g., emissions from pipe fitting and equipment leaks, releases from pressure relief valves, tanks, and sewage lagoons) for each oil sands company operating a mining project from January 1st, 2011 to December 31st, 2014 [126]. The fugitive GHG emissions generated by AEMERA are developed from figures reported by companies to the Government of

Alberta under the Specified Gas Emitters Regulation (AB, 2007). The estimated fugitive CH₄ emissions from oil sands mine face and tailings ponds reported by AEMERA are close to the numbers reported elsewhere [127, 128].

In order to capture the range of mining projects, OPGEE models two template mining operations:

- an upgrader-integrated mine using naphthenic froth treatment (NFT) separation technology;
- A stand-alone mine using paraffinic froth treatment (PFT) separation technology.

As can be seen in Table ?? above, the integrated mine and upgrader using NPT separation is more indicative of older large-scale mining projects developed in the 1970s and 1980s, such as the Suncor and Syncrude operations. Additionally, the more recently developed CNRL Horizon project is an integrated NFT mine. The non-integrated mine with PFT separation is more representative of modern developments such as Albian Sands (Shell), Aurora (Syncrude), Jackpine (Shell), and Kearl (Imperial).

Public natural gas and electricity consumption literature data available, AER facility-reported data and COSIA Mine Template ranges, is presented in Figures 7.11 and 7.12, respectively, below. Production-weighted average energy consumption is reported for both 2014 and over the project life based on the AER data reported for each facility. The shaded regions represent the natural gas consumption for NFT and PFT mines presented in the COSIA Mine Template for low grade and high grade ore. Note that no corresponding graph can be created for diesel consumption due to lack of consistent reporting of diesel use in AER datasets.

There is some challenge in interpreting reported public data. First, note that natural gas consumption reported by AER for Suncor, Syncrude Mildred Lake, and CNRL Horizon mines includes natural gas consumed in on-site upgraders. Similarly, electricity consumption reported by AER for Suncor, Syncrude Mildred Lake, and CNRL Horizon mines include electricity consumed in on-site upgraders. Lastly, the Shell Muskeg River mine receives the majority of natural gas that is consumed at Shell Jackpine mine, meaning that per-mine consumption at each Shell mine is between the two reported values (high for Muskeg River and very low for Jackpine). The separation of stand-alone vs. integrated upgrading mines, is discussed more fully below.

Modeling of non-integrated PFT mining operations The non-integrated mining operation is illustrated in Figure 7.13. The energy imports to the stand-alone mining operation include diesel imports, electricity imports, and natural gas imports. Some mining operations co-generate power on site and may also export power. The mine takes in raw bitumen ore and exports diluted bitumen for shipment to upgraders or direct shipment to refineries.

The default values for energy use in non-integrated PFT mining operations are computed as follows:

- Natural gas consumption is modeled using the AER 2014 production-weighted average for three stand-alone PFT projects (Shell Muskeg River, Shell Jackpine, and Imperial Kearl).

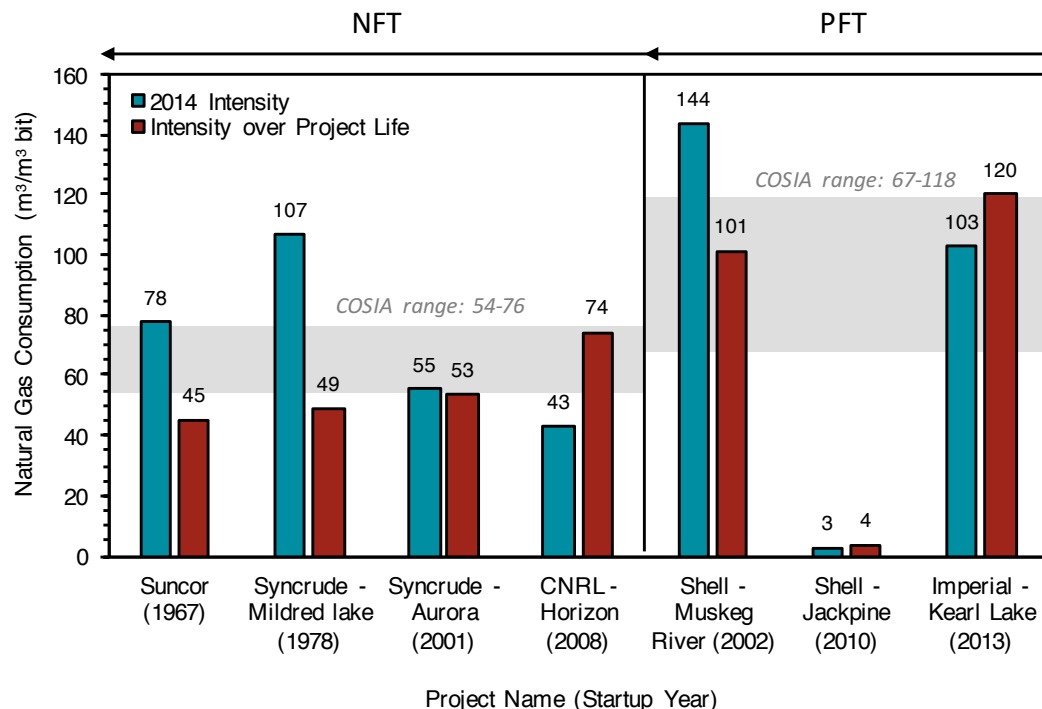


Figure 7.11: Natural gas use in mining operations

- Electricity consumption is modeled using the AER 2014 production-weighted average for three stand-alone PFT projects (Shell Muskeg River, Shell Jackpine, and Imperial Kearl).
- Diesel consumption is estimated as the average of COSIA reported high and low ranges of diesel consumption, as reported for low-grade (9 wt.% and high-grade (12 wt.%) ores respectively. The range from the COSIA templates is used as the range of diesel consumption rate.
- Diluent blending rates are modeled using AER 2014 production-weighted averages from the stand-alone PFT projects (Shell Muskeg River, Shell Jackpine, and Imperial Kearl). Volumetric blending rates over all months averaged 25.4% diluent in dilbit. The range over 2014 was from 24.3% to 26.5%. Although Kearl dilutes bitumen with SCO (creating “syn-bit”) the dilution fraction was nearly identical to those of Muskeg River and Jackpine.

Table 7.16 gives results as used in OPGEE, results for the AER production-weighted average, COSIA template average, and COSIA template range.

Proposed modeling of integrated NFT mining operations The integrated mining operation is illustrated in Figure 7.14. The net flows across the process boundary are roughly equivalent to the stand-alone mining operation, with some exceptions. First, large volumes of diluent are not used to reduce the viscosity of bitumen, as upgrading the bitumen to SCO renders it ready for pipeline transport. Also, two new co-products can be exported from the system: process gas and coke. Therefore, emissions credits should be given for these fuels if they are exported. Lastly,

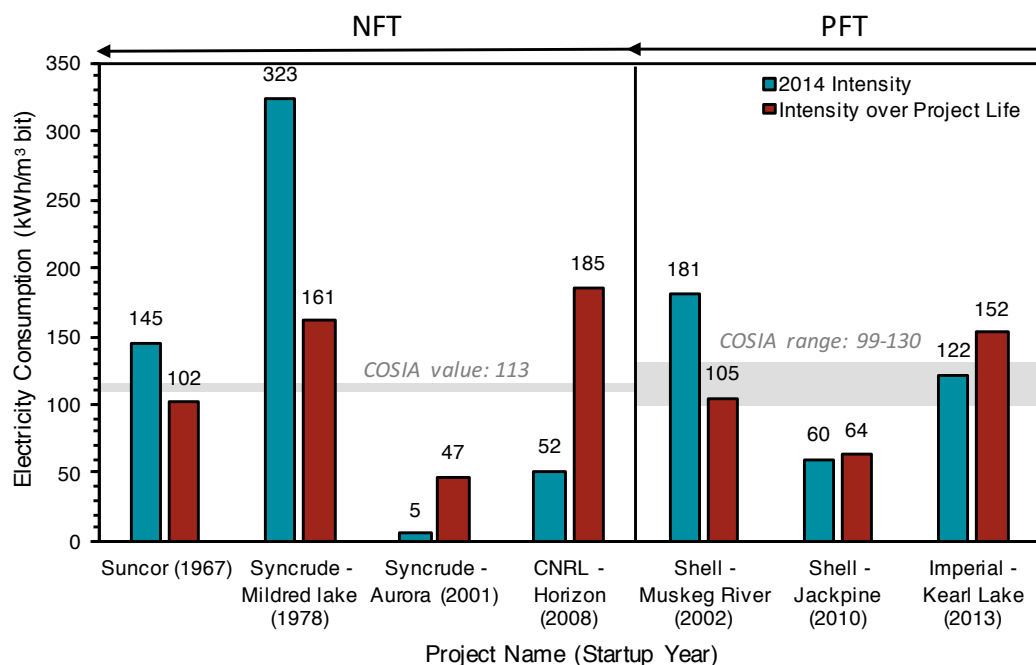


Figure 7.12: Electricity use in mining operations

new internal flows between upgrader and mine include heat recovered from upgrader operations that is used in mine ore separations, as well as upgrader product streams (distillate fuels) that are consumed in mining trucks. New internal consumption at the upgrader can include coke and process gas.

Due to sharing of waste heat at integrated mining and upgrading projects, some efficiency is gained through process integration. Suncor and Jacobs (2012) estimate that 30 percent of total natural gas required at a project can be reduced by using low-grade waste heat from an integrated upgrader for the bitumen extraction process.

Updated OPGEE default values for stand-alone NFT mines are taken directly

Table 7.16: Non-integrated PFT mining energy intensities

Fuel	OPGEE value	AER avg.	PW	COSIA avg.	COSIA range	Notes
Natural gas	85	85		93	67 – 118	
Electricity cons.	125	125		114	99 – 130	
Electricity gen.	77	77		114	96 – 132	
Frac. elect. gen. onsite	0.6	0.6		1.0	1.0 – 1.0	
Diesel	12.5	-		12.5	9 – 16	a

Continued on next page...

Continued from previous page

Fuel	AER prod-weighted avg.	COSIA avg.	COSIA range	Notes
Diluent	25.4%	25.4%	-	-

^a COSIA Mine Template ranges presented for low (9%) and high (12%) grade ore.

from the COSIA NFT Mine Template [125]. The efficiency factor from Suncor and Jacobs [129] is multiplied by the COSIA stand-alone mining natural gas consumption to approximate the natural gas consumed solely by the mine at an integrated mining and upgrading facility. These values are compared to the energy consumption for integrated mining and upgrading projects in Table 7.17. The remaining energy for integrated projects not attributed to mining is approximately that consumed in the upgrading process. For example, if we compare Suncor and Syncrude natural gas consumption (total) less that estimated used in upgrading, we get values approximately equal to the COSIA stand-alone NFT mine less a 30% integration benefit ($40\text{-}45 \text{ m}^3 \text{ per } m^3$).

Table 7.17: Comparison between stand-alone mine energy consumption estimates based on COSIA mine template to integrated NFT mining and upgrading energy consumption reported by AER

Fuel	OPGEE value ^a	COSIA SA NFT ^b	AER reported ^c	Suncor	Syn crude	Suncor	Syn crude	Upgrading est: ^d
Natural gas cons.	45	65 (54 – 76)	78	77	30	30	37	
Electricity cons.	113	113	145	166	30	30	63	

^a Natural gas consumption for mining portion of an integrated mining and upgrading project calculated by subtracting the percentage of natural gas Suncor and Jacobs [129] estimate will be saved through sharing of waste heat.

^b Includes mining energy consumption estimates provided in COSIA Mine Templates for a representative stand-alone NFT mine.

^c 2014 operating data reported in AER Statistical Report ST39. Suncor and Syn crude projects have on-site upgraders so AER data is reported for both mining and upgrading.

^d Estimate of energy consumed from upgrading calculated by subtracting the estimated energy consumed for mining in integrated projects from the mining and upgrading energy consumption reported to the AER. The values presented in the table for upgrading are per m³ of SCO produced by the on-site upgrader (17,200,000 m³ and 15,200,000 m³ for Suncor and Syn crude upgraders, respectively), whereas the energy consumption values for mined bitumen presented in the table are per m³ of bitumen produced.

^e The range presented in the table for natural gas consumption from the COSIA Mine Template for NFT projects is based on the low and high estimates for natural gas consumption for high grade and low grade oil sands ore, respectively. The same values for electricity consumption are reported for low and high grade ore in the NFT COSIA Mine Template (113 kWh/m³ bitumen).

Table 7.18: Integrated NFT mining energy intensities

Fuel	OPGEE value	AER avg.	PW	COSIA avg.	COSIA range	Notes
Natural gas	45	-		65	54 – 76	^a
Electricity cons.	113	-		113	113 – 113	
Electricity gen.	114	-		114	96 – 132	
Frac. elect. gen. onsite	1	-		1.0	0.8 – 1.2	
Diesel	11	-		11	9 – 13	^b

^a Note from Table 7.17 above that the COSIA stand-alone NFT mine consumption must be reduced by the heat integration benefit. That is, OPGEE value of 45 m³ per m³ bitumen should be compared to 65×(1.0 – 0.3)) [125]

^b COSIA Mine Template ranges presented for low (9%) and high (12%) grade ore.

In order to enable self-consistent treatment of integrated mining and upgrading, the following conventions are applied:

- Integrated mining and upgrading operations use the same upgrading models described below in Section 7.9.
- Any benefits associated with upgrading integration result in less net consumption of mining consumables that flow across conventional mine boundary (i.e., diesel, electricity, natural gas).
- Emissions associated with on-site use of fuels by upgrader are calculated on the upgrading sheet.

These conventions allow for computation of the benefits of integrated mining and upgrading operations, while also maintaining computations of emissions impacts of operations.

The default values for energy use in upgrader-integrated NFT mining operations are therefore computed as follows:

- Natural gas consumption is modeled using COSIA stand-alone NFT mine less a 30% integration benefit. This is approximately equal to the reported values of Suncor and Syncrude less estimated upgrading consumption.
- Electricity consumption is modeled using COSIA electricity use at a stand-alone NFT mine. No integration benefit applicable.
- Diesel consumption is estimated as the average of COSIA reported high and low ranges of diesel consumption, as reported for low-grade (9 wt.% and high-grade (12 wt.%) ores respectively.

For both integrated and non-integrated mining operations, the emissions and energy use are tracked simply. For example, diesel fuel use in non-integrated mining operations is computed as:

$$Q_{di}^{MN} = Q_{db}^{MN} I_{di}^{MN} \quad (7.39)$$

where Q_{di}^{MN} is diesel consumed in non-integrated mining operations [gal/d], Q_{db}^{MN} is diluted bitumen output from the non-integrated mining operation [bbl/d], and I_{di}^{MN} is the diesel fuel intensity of non-integrated mining operations [gal/bbl]. This

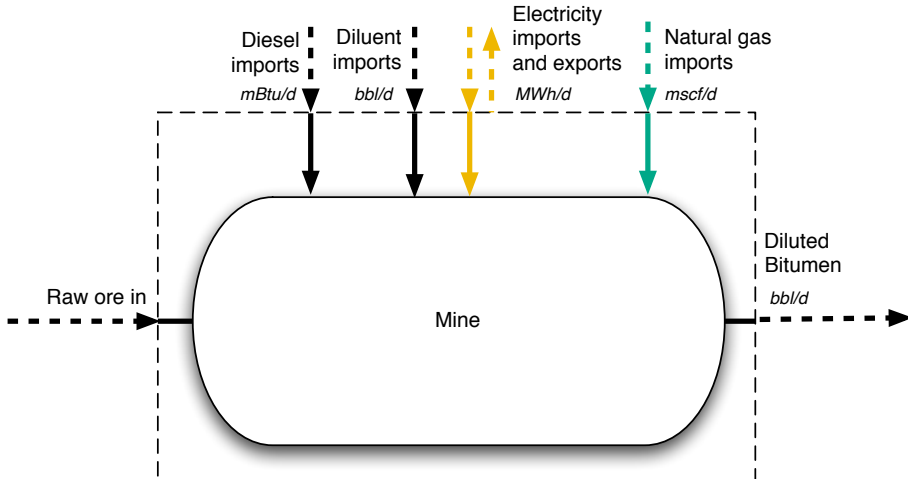


Figure 7.13: Non-integrated bitumen mining operation

quantity of diesel fuel consumed can then be converted into an energy consumption rate:

$$E_{di}^{MN} = Q_{di}^{MN} LHV_{di} \quad (7.40)$$

where LHV_{di} is the lower heating value of diesel fuel [mBtu LHV/gallon]. This quantity can then be gathered on the '*Energy Consumption*' gathering sheet and used to compute emissions on the '*GHG Emissions*' gathering sheet.

Similar quantities are computed for all main inputs to non-integrated mining operations by using intensities of electricity use (I_{el}^{MN}) and natural gas (I_{ng}^{MN}). For the case of integrated mining and upgrading operations, the relevant intensities for diesel, electricity, and natural gas are similarly named (I_{di}^{MI} , I_{el}^{MI} , and I_{ng}^{MI} respectively). Recall via convention above that consumption of coke or refinery process gas is computed as part of upgrading operations in Section 7.9.

After these mine-type-specific calculations are performed, the overall consumption due to mining is then computed using binary variables from the '*Active Field*' sheet. For the case of diesel energy consumption:

$$E_{di} = y^{MN} E_{di}^{MN} + y^{MI} E_{di}^{MI} \quad (7.41)$$

where y^{MN} and y^{MI} represent binary variables for mining-non-integrated and mining-integrated, respectively.

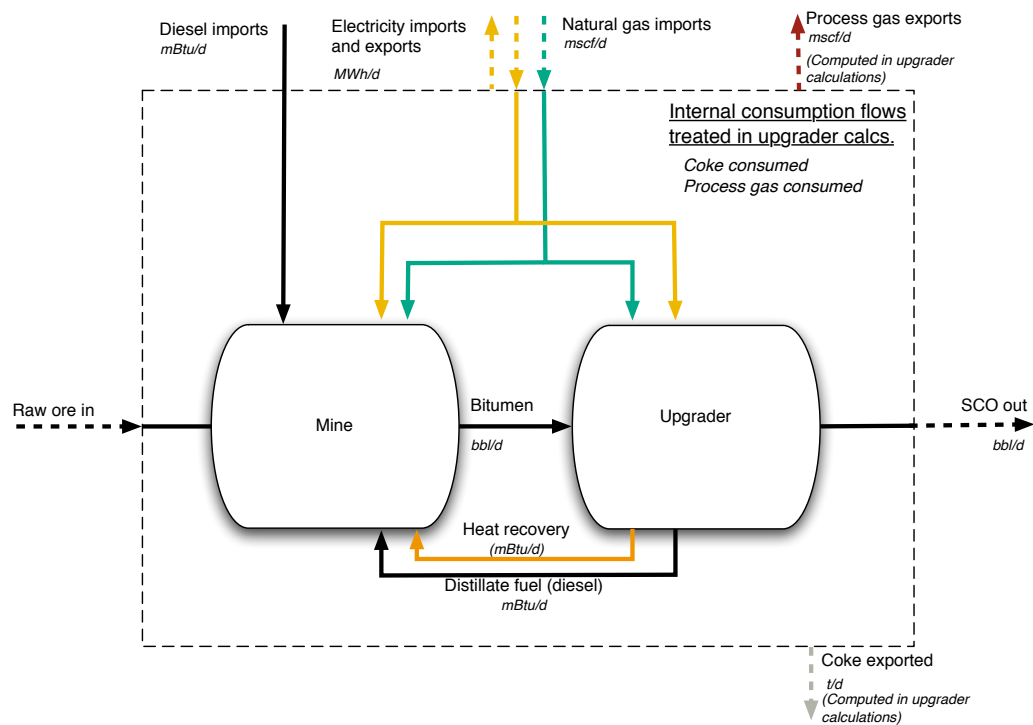


Figure 7.14: Upgrader-integrated bitumen mining operation

7.6 Separation

The streams flowing into and out of the separation process are shown in Figure 7.15 and are listed in Table 7.19.

[TBD: ADD WHOLE SECTION ON SEPARATION, INCLUDING THE COMPRESSION FOR STAGE 2 AND STAGE 3]

Table 7.19: Streams flowing into and out of the separation process. I/O denotes input or output stream

Flow name	Stream	I/O	Source/Destination	Units	Notes
Oil at wellhead	4	I	Wellbore/downhole pump	[t/d]	
Water at wellhead	102	I	Wellbore/downhole pump	[t/d]	
Gas at wellhead	27	I	Wellbore/downhole pump	[t/d]	
Oil after separator	7	O	Crude oil dewatering	[t/d]	
Water after separator	103	O	Produced water treatment	[t/d]	
Gas after separator	28	O	Flaring	[t/d]	
Separator leaks to air	251	O	Environment - Atmosphere	[t/d]	

Table 7.20: Secondary parameter inputs to the separator worksheet

Parameter name	Default value	Units	Source	Notes
Amount of water in inlet gas	52	[lb/mmscf]	[4, p. 160]	-
Entrained water as a fraction of oil emulsion	14	[wt%]	[4]	-
Number of separator stages	3	[stages]	Assumption	-
Final separator pressure	150	[psi]	Assumption	-
Final separator temperature	90	[°F]	Assumption	-
Separator compressor - Ratio of specific heats	1.28	[-]	[?]	-
Separator compressor - Compressor eff.	0.75	[%]	Assumption	-
Separator compressor - Prime mover	2	[option]	Assumption	1=e ⁻ , 2=NG
Wells per separator	10	[wells]	Assumption	-

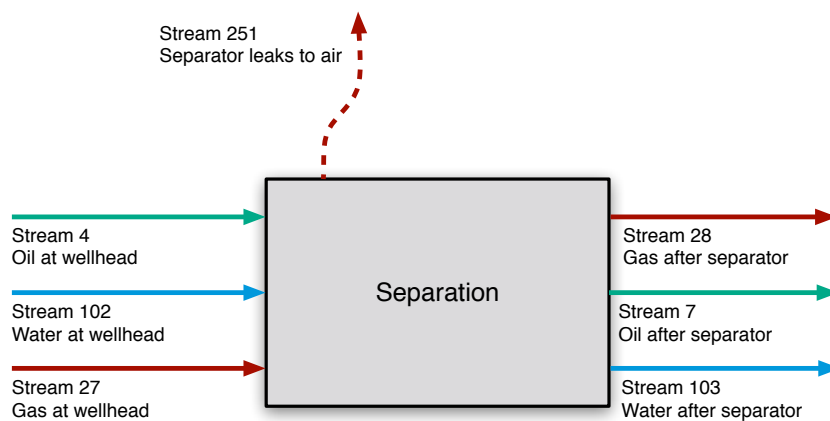
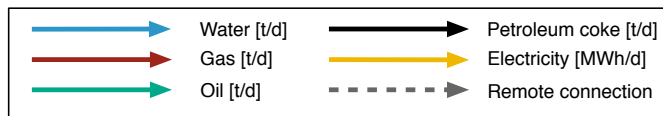


Figure 7.15: Streams flowing into and out of the separation process. All streams measured in tonnes per day excepting electricity which is measured in MWh/d.

7.7 Heater-treater (dewatering)

Removing free water from crude oil can be accomplished by passive chemical and gravitational methods that do not use heat. Because no fuel is used in passive gravitational separation techniques, they do not cause significant GHG emissions. However, based on the properties of the oil, gravity separation techniques may not be sufficient to produce crude oil with the desired water content required for transport and sales. Additional separation may be provided by a crude oil heater-treater, which may be turned ON or OFF in OPGEE, [Active Field J109](#) to remove entrained water remaining after passive separation.

The streams flowing into and out of the '*Heater-Treater*' sheet are shown in Figure 7.16 and are listed in Table 7.24.

To model heat capacity differences between water and oil [60, p. 303], OPGEE assumes that oil entering a heater-treater contains only entrained water. The free water proportion that was not separated prior to the application of heat is assumed to be negligible (1-2%) [130, Section 5.4.2].

The mass flow of incoming oil and water are given by the constituents of \vec{r} which leaves the separator: $m_{\vec{r},o}$ and $m_{\vec{r},w}$. The enthalpy change required is calculated using:

$$\boxed{\text{M58}} \quad \Delta H_{HT} = \Delta T_{HT} (m_{\vec{r},o} C_{p_o} + m_{\vec{r},w} C_{p_w}) (1 + \epsilon_{HT}) \left(\frac{1}{10^6} \right) \quad [\frac{\text{MMBtu}}{\text{d}}] \quad (7.42)$$

where ΔH_{CD} = heat duty [MMBtu/d]; C_{p_o} = specific heat of oil [Btu/lb-°F]; C_{p_w} = specific heat of water [Btu/lb-°F]; ΔT_{HT} = difference between treating and feed temperatures, $T_{HT} - T_{\vec{r}}$ [°F]; and ϵ_{CD} = heat loss [fraction]. The specific heat capacity of oil is a function of the temperature of the oil and its API gravity. From the Campbell equation, presented in Manning and Thompson [4]:

$$\boxed{\text{M57}} \quad C_{p_o} = a_1 T_{o,ave} API + a_2 API + a_3 T_{o,ave} + a_4 \quad [\frac{\text{Btu}}{\text{lb-}^{\circ}\text{F}}] \quad (7.43)$$

where the values of constants $a_1 \dots a_4$ are given in Table 7.24. $T_{o,ave}$ is the average temperature of oil, taken as the straight average of the feed oil temperature $T_{\vec{r}}$ and the treating temperature T_{HT} :

$$\boxed{\text{M56}} \quad T_{o,ave} = \frac{T_{\vec{r}} + T_{HT}}{2} \quad [\frac{\text{Btu}}{\text{lb-}^{\circ}\text{F}}] \quad (7.44)$$

Default values are: [M42](#) 165 °F for treating temperature T_{HT} ; 1 Btu/lb-°F for specific heats of water; and 0.02 for heat loss [60, p. 136 and 303]. Lastly, the enthalpy change of the fluids is multiplied by an efficiency factor:

$$\boxed{\text{M59}} \quad E_{HT} = \Delta H_{HT} \times \eta_{HT} \quad [\frac{\text{MMBtu}}{\text{d}}] \quad (7.45)$$

Table 7.21: Streams flowing into and out of the crude oil dewatering process. I/O denotes input or output stream

Flow name	Stream	I/O	Source/Destination	Units	Notes
Oil after separator	7	I	Separation	[t/d]	
Fuel gas - Dewatering	160	I	Fuel gas system	[t/d]	
Electricity - Dewatering	184	I	Electricity generation and imports	[MWh/d]	
Crude to stabilizer	8	O	Stabilizer	[t/d]	
Crude to storage	9	O	Crude oil storage	[t/d]	
Crude to upgrading	19	O	Heavy oil upgrading	[t/d]	
Crude to dilution	20	O	Heavy oil dilution	[t/d]	
Water from dewatering	115	O	Produced water treatment	[t/d]	

Table 7.22: Secondary parameter inputs to the crude oil dewatering worksheet.

Parameter name	Cell	Eqn. term	Default value	Units	Source	Notes
Treating temperature	M42	T_{HT}	165	[°F]	[4]	-
Heat loss	M43	ϵ_{HT}	2	[%]	[4]	-
Type of heater	M44	-	1	[option]	Assumption	1=NG, 2=e ⁻
Heater fuel use factor	M45	η_{HT}	1.3	[J/J]	[131]	-
Campbell eq. - a1	M47	a_1	1.390e-6	-	[4]	-
Campbell eq. - a2	M48	a_2	1.847e-3	-	[4]	-
Campbell eq. - a3	M49	a_3	6.320e-4	-	[4]	-
Campbell eq. - a4	M50	a_4	3.520e-1	-	[4]	-
Specific heat capacity water	M51	C_{pw}	1	[Btu/lb-°F]	[4]	-

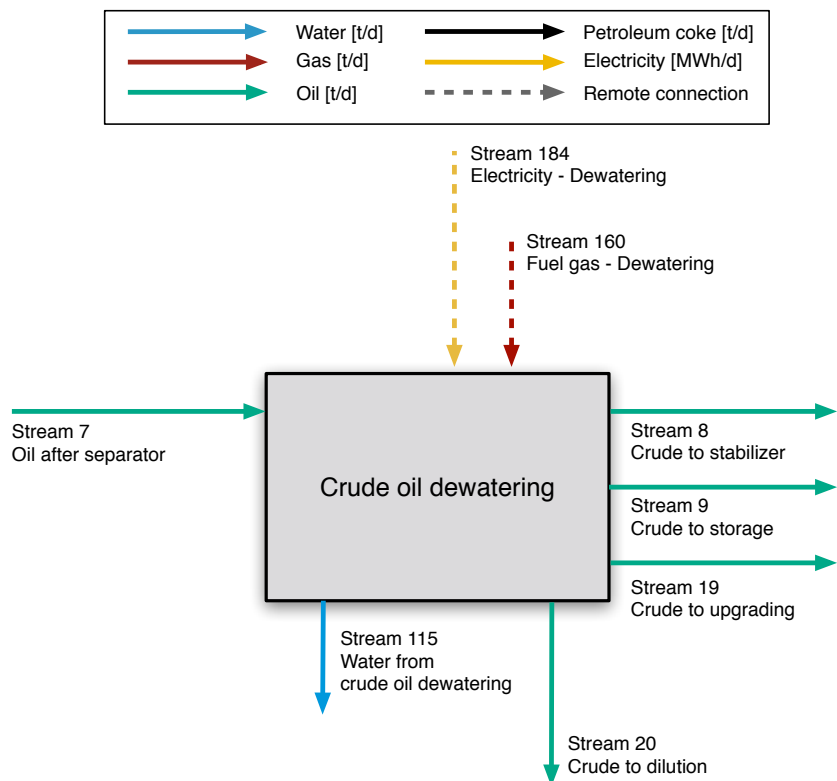


Figure 7.16: Streams flowing into and out of the crude oil dewatering process. All streams measured in tonnes per day excepting electricity which is measured in MWh/d.

7.8 ‘Crude oil stabilization’ worksheet

Following the removal of water content, stabilization is the next phase of the bulk separation process, and is most commonly applied to gas-rich light crude. This involves the removal of dissolved natural gas [60, p. 159].

The streams flowing into and out of the crude oil stabilization process are shown in Figure 7.17 and are listed in Table 7.23.

The default type of stabilizer in OPGEE is a high-pressure stabilizer (100 psi) which requires a higher reboiler temperature compared to a low-pressure stabilizer. The use of a stabilizer column is an important assumption because a heat source is required to provide the required temperature. OPGEE assumes a direct-fired heater.

The stabilizer column heat duty is calculated as:

$$\boxed{\text{M70}} \quad \Delta H_S = \Delta T_S m_{\overline{8},o} C_{p_o} \left(1 + \epsilon_S \right) \left(\frac{1}{10^6} \right) \quad [\frac{\text{MMBtu}}{\text{d}}] \quad (7.46)$$

where ΔH_S = heat duty [MMBtu/d]; ΔT_S = difference between reboiler and feed temperatures ($T_S - T_{\overline{8},o}$) [$^{\circ}\text{F}$]; $m_{\overline{8},o}$ is the mass of oil flowing into the stabilizer as stream $\overline{8}$ [lb/d]; C_{p_o} = specific heat capacity of oil [Btu/lb- $^{\circ}\text{F}$]; and ϵ_S = heat loss [fraction]. The default stabilizer temperature is 344 $^{\circ}\text{F}$ for the reboiler.

The specific heat capacity of oil is calculated using the Campbell equation [4], shown above in Eq. 7.43 [\[M62\]](#).

Fractional heat loss is 0.02 [\[M44\]](#) [60, p. 136, 161, 163] and boiler energy consumption to enthalpy ratio is 1.25 [\[M46\]](#) for natural gas and 0.37 kWh/Btu for electricity.

[\[M47\]](#)

The amount of gas evolved in the stabilizer is calculated as the difference between the solution gas oil ratio at the inlet pressure and temperature [\[M64\]](#) and at the outlet pressure and temperature [\[M65\]](#) using the equation of Al-Shammasi, described above in Eq. 7.17.

Table 7.23: Streams flowing into and out of the '*Crude oil stabilization*' process. I/O denotes input or output stream

Flow name	Stream	I/O	Source/Destination	Units	Notes
Crude to stabilizer	8	I	Crude oil dewatering	[t/d]	
Fuel gas - Stabilizer	161	I	Fuel gas system	[t/d]	
Electricity - Stabilizer	185	I	Electricity generation and imports	[MWh/d]	
Stabilized crude to storage	10	O	Crude oil storage	[t/d]	
Stabilizer gas	32	O	Gas gathering	[t/d]	

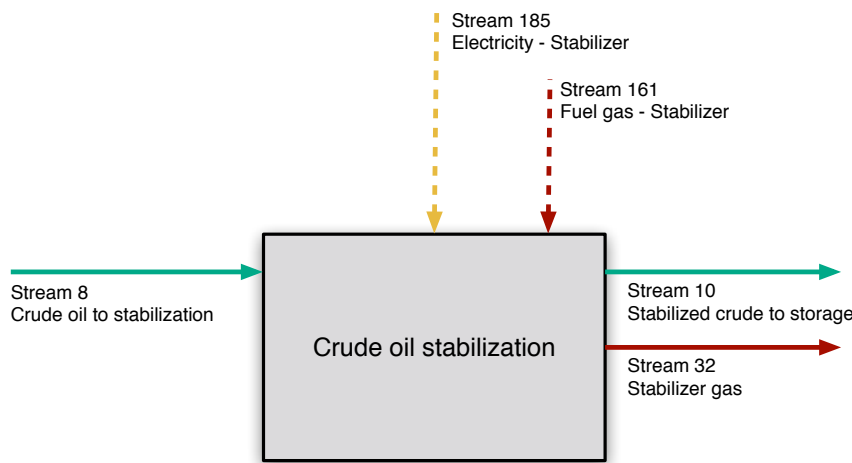


Figure 7.17: Streams flowing into and out of the '*Crude oil stabilization*' worksheet. All streams measured in tonnes per day excepting electricity which is measured in MWh/d.

Table 7.24: Secondary parameter inputs to the '*Crude oil stabilization*' worksheet.

Parameter name	Cell	Eqn. term	Default value	Units	Source	Notes
Stabilizer pressure	M42	p_S	100	[psi]	[4]	-
Stabilizer temperature	M43	T_S	344	[°F]	[4]	-
Heat loss	M44	ϵ_S	2	[%]	[4]	-
Type of heater	M45	-	1	[option]	Assumption	1=NG, 2=e-
Heater fuel use factor - Gas	M46	η_S	1.25	[Btu/Btu]	Assumption	-
Heater fuel use factor - Elec.	M47	η_S	0.37	[kWh/Btu]	Assumption	-
Campbell eq. - a1	M49	a_1	1.390e-6	-	[4]	-
Campbell eq. - a2	M50	a_2	1.847e-3	-	[4]	-
Campbell eq. - a3	M51	a_3	6.320e-4	-	[4]	-
Campbell eq. - a4	M52	a_4	3.520e-1	-	[4]	-
Solution GOR eq. - a1	M54	a_4	5.527	-	[55?]	-
Solution GOR eq. - a2	M55	a_4	-1.841	-	[55?]	-
Solution GOR eq. - a3	M56	a_4	0.784	-	[55?]	-

Table 7.25: Streams flowing into and out of the heavy oil upgrading process. I/O denotes input or output stream

Flow name	Stream	I/O	Source/Destination	Units	Notes
Bitumen from mine to upgrader	5	I	Mining	[t/d]	
Crude to upgrading	19	I	Crude oil dewatering	[t/d]	
Fuel gas - Heavy oil upgrading	164	I	Fuel gas system	[t/d]	
Electricity - Heavy oil upgrading	190	I	Electricity generation and imports	[MWh/d]	
Upgraded crude to storage	11	O	Crude oil storage	[t/d]	
Process gas export from upgrader	83	O	Sales product	[t/d]	
Petcoke from upgrader	15	O	Petcoke handling and transport	[t/d]	

7.9 Heavy oil upgrading

Very heavy crude oils ($\text{API}^\circ \leq 12$) are often upgraded before transport. This is due to the heavy, viscous character of the crude which prevents flow at ambient conditions. This also results from the need to align heavy crude characteristics more closely to refinery input specifications. As a result, significant capacity in crude heavy oil and bitumen upgrading exists. Approximately 1 million bbl/d of bitumen upgrading capacity exists in Canada, while ≈ 0.5 million bbl per day of upgrading capacity exists in Venezuela.

The streams flowing into and out of the heavy oil upgrading are shown in Figure 7.18 and are listed in Table 7.25.

Heavy crude oil and bitumen upgrading is modeled OPGEE using results from the OSTUM model, supplemented with reported data from Canadian regulators [132]. The results for crude upgrading in OPGEE are most applicable to the case of Canadian bitumen upgrading, as data from these operations was used in the development of OSTUM. Applying the OPGEE upgrading module to other heavy crude upgrading operations is subject to greater uncertainty.

Crude oil upgrading operations are illustrated in process flow form in Figure 7.19

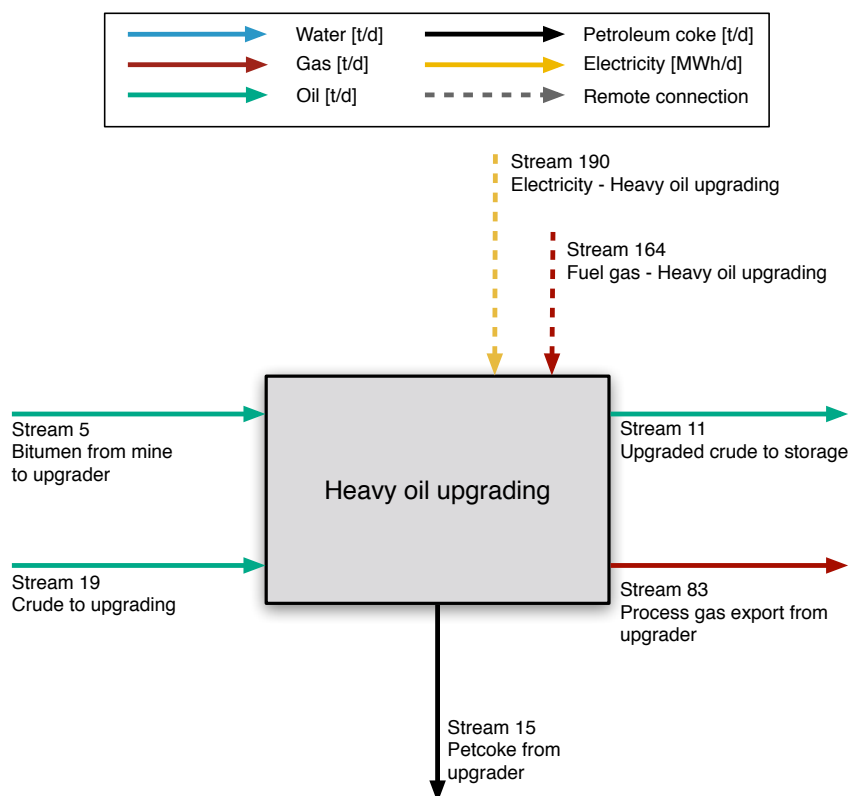


Figure 7.18: Streams flowing into and out of the heavy oil upgrading process. All streams measured in tonnes per day excepting electricity which is measured in MWh/d.

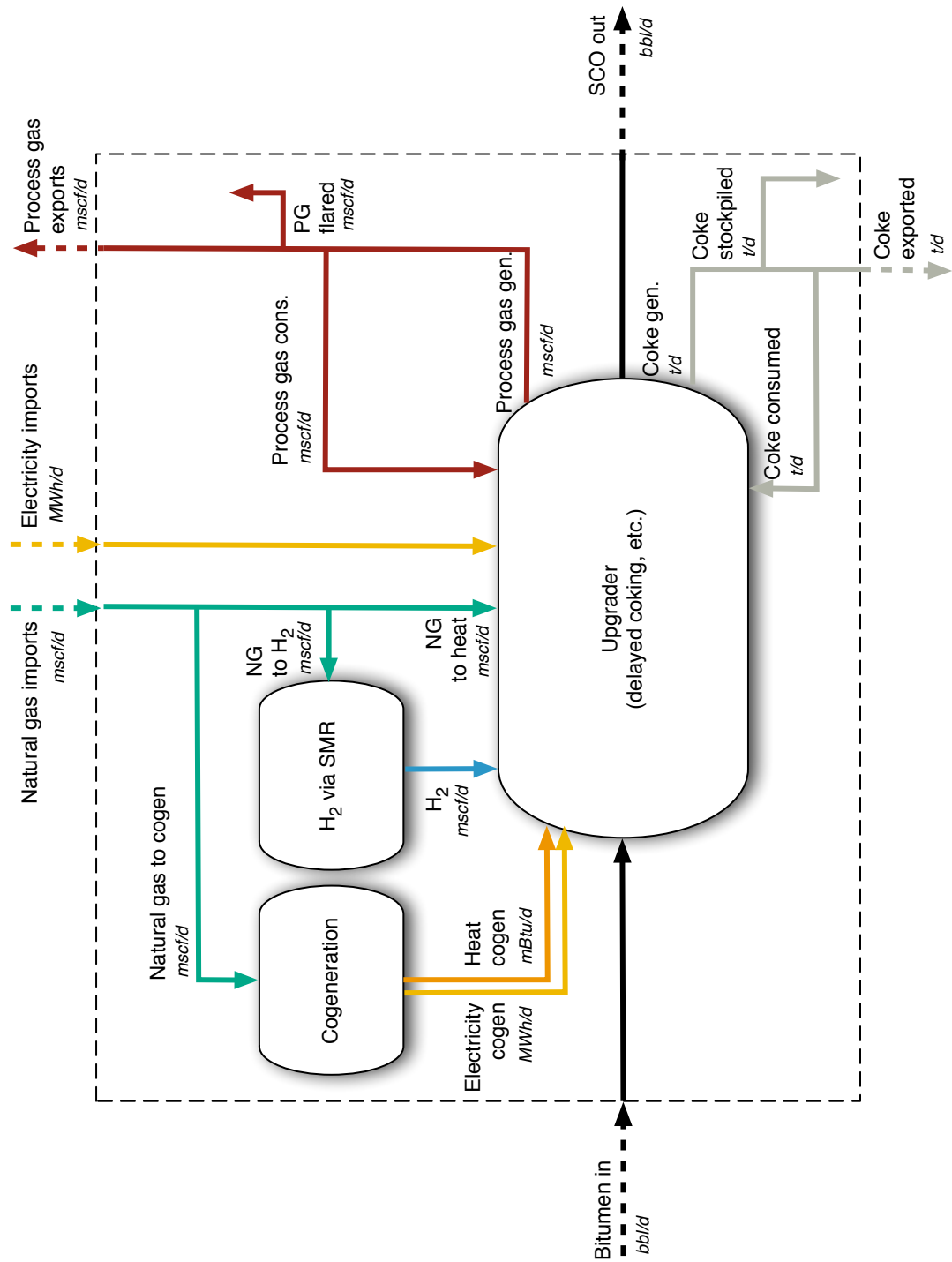


Figure 7.19: Process flow diagram for OPGEE upgrading module

The quantity "SCO out", or Q_{sco} is given by user in the inputs sheet. The required bitumen input rate Q_{bit}^{in} is determined using the SCO yield factor:

$$Q_{bit}^{in} = \frac{Q_{sco}}{Y_{sco}} \quad (7.47)$$

where Y_{sco} is the volumetric yield of SCO per volume of bitumen input [bbl SCO/bbl bitumen].

In addition to SCO, two other by-products are generated during upgrading of bitumen: process gas and coke. The generation of process gas is given by a process gas yield factor:

$$Q_{pg} = Q_{sco} Y_{pg} \quad (7.48)$$

where Y_{pg} is the process gas yield factor [scf process gas per bbl of SCO output]. The generation of coke is given by a coke yield factor:

$$Q_{ck} = Q_{sco} Y_{ck} \quad (7.49)$$

where Y_{ck} is the coke yield factor [kg coke per bbl of SCO output].

These two byproducts can be handled in one of three ways:

- Self-use in processing and upgrading facilities
- Disposal or rejection on site (flaring of process gas and stockpiling or land-filling of coke)
- Sales on secondary fuels markets

These uses are computed using three disposition fractions. Terms f_{pg}^{su} , f_{pg}^{fl} , and f_{pg}^{sl} for the case of process gas self-use, flaring, and sales, respectively. For coke, the equivalent terms are f_{ck}^{su} , f_{ck}^{sp} , and f_{ck}^{sl} , corresponding to self-use, stockpiling, and sales, respectively. For each by-product these terms must sum to 1.

Hydrogen consumption by the upgrader is given by a hydrogen intensity factor:

$$Q_{H2} = Q_{sco} I_{H2} \quad (7.50)$$

where I_{H2} is the H₂ intensity [scf H₂ per bbl of SCO]. The natural gas consumption associated with generating H₂ is therefore given by:

$$Q_{ng,H2} = \frac{Q_{H2} LHV_{H2}}{\eta_{H2} LHV_{ng}} \quad (7.51)$$

where LHV_{H2} is the lower heating value of hydrogen [Btu LHV/scf H₂], η_{H2} is the lower-heating-value-basis efficiency of H₂ generation [Btu LHV H₂/Btu LHV NG], and LHV_{ng} is the lower heating value of natural gas [Btu LHV/scf NG].

Similarly, the electricity requirement of upgrading is given by an electricity intensity factor:

$$Q_{el} = Q_{sco} I_{el} \quad (7.52)$$

where I_{el} is the electricity intensity [Btu e- per bbl of SCO]. This electricity is either generated on site using cogeneration, or purchased externally. The fraction of electricity generated on site f_{el} is entered by the user on the 'Inputs' sheet.

The need for process steam for upgrading is met by a combination of heat generated during co-generation of electricity (if used) and through a steam boiler. The need for steam is given by a steam intensity factor:

$$Q_{ws} = Q_{sco} I_{ws} \quad (7.53)$$

where I_{ws} is the steam intensity [Btu steam enthalpy per bbl of SCO produced]. This steam need is therefore met by steam cogeneration and conventional steam boilers:

$$Q_{ws} = Q_{el} f_{el} \frac{\eta_{HRSG}}{\eta_{GT}} + Q_{ng,ws} \eta_{ws} \quad (7.54)$$

where η_{HRSG} is the efficiency of steam generation from cogeneration HRSG [Btu steam enthalpy per Btu LHV NG input to turbine], η_{GT} is the efficiency of gas turbine [Btu e- per Btu LHV NG input to turbine], and η_{ws} is the efficiency of a supplemental steam boiler [Btu steam enthalpy per Btu LHV of NG input].

The inputs for these values, derived from the OSTUM model and public data sources, are described below in the discussion of the '*Upgrading*' worksheet. The '*Upgrading*' supplemental worksheet contains tabulated data on upgrading operations that are used in the '*Surface Processing*' worksheet to compute the energy use and emissions from crude hydrocarbon upgrading. The values of energy consumption for upgrading are estimated using the Oil Sands Technology Upgrading Model (OSTUM) produced by the University of Toronto and University of Calgary [132].

The OSTUM model is run for three different upgrading configurations. These three refinery configurations include:

- Delayed coking
- Hydroconversion
- Hydroconversion and fluid coking

These three refinery configurations resemble real-world refinery configurations used at the Suncor, Scotford, and Syncrude upgraders respectively.

In each upgrading configuration, a bitumen blend modeled as the Borealis Heavy Blend (BHB) is modeled as the input hydrocarbon feedstock. In each upgrading configuration, a light-sweet synthetic crude oil is produced, with characteristics similar to the premium SCO product produced by real-world upgraders. The properties of the output SCO blends are as follows:

- Delayed coking: Sweet SCO with API gravity = 33.2 °API, S = 0.18 wt%, and N = 692.3 ppm by mass. This SCO is similar to Suncor Synthetic A.
- Hydroconversion: Sweet SCO with API gravity = 31.1 °API, S = 0.03 wt%, and N = 77.6 ppm by mass. This SCO is similar to Premium Albion Synthetic.
- Hydroconversion and fluid coking: Sweet SCO with API gravity = 31.1 °API, S = 0.11 wt%, and N = 623.2 ppm by mass. This SCO is similar to Syncrude Sweet Premium.

The assumed heating value of process gas in OSTUM is nearly identical to the heating value of natural gas assumed by default in OPGEE (982 Btu/ft³ LHV).

The resulting intensities in OSTUM are given below in Table 7.26

Table 7.26: Inputs to OPGEE upgrading module from the Oil Sands Technology Upgrading Model (OSTUM)

	Delayed coking	Hydroconversion	Hydroconversion and fluid coking	Units
Process gas (PG) yield per bbl SCO output	501	341	650	[scf/bbl SCO]
- Fraction PG to self use	0.650	0.800	0.943	[0-1]
- Fraction PG exported	0.300	0.190	0.032	[0-1]
- Fraction PG flared	0.050	0.01	0.025	[0-1]
Coke yield per bbl SCO output	43	0	30	[kg/bbl SCO]
- Fraction coke to self use	0.106	0.000	0.207	[0-1]
- Fraction coke exported	0.000	0.000	0.000	[0-1]
- Fraction coke stockpiled	0.894	1.000	0.793	[0-1]
Electricity intensity	5.451	17.25	19.98	[kWh/bbl SCO]
- Fraction electricity self generated w/ cogent	-	-	-	[0-1]
Hydrogen (H2) intensity	845	1644	1283	[scf H2/bbl SCO]
- H2 generation efficiency	0.7	0.7	0.7	[LHV H2/LHV NG]
- NG requirements for H2	323.6	629.6	491.2	[scf NG/bbl SCO]
Cogen turbine efficiency	0.31	0.31	0.31	[Btu e-per Btu NG LHV]
Cogeneration steam efficiency	0.40	0.40	0.40	[Btu steam enthalpy per Btu NG LHV]
Steam requirements of upgrading	113.8	247.1	240.8	[lbm Btu steam enthalpy/bbl SCO]
Steam boiler efficiency	0.8	0.8	0.8	[Btu steam enthalpy/Btu NG LHV]
SCO/bitumen ratio	0.834	1.02	0.865	[bbl SCO/bbl bitumen]

7.10 Heavy oil dilution

The streams flowing into and out of the heavy oil dilution process are shown in Figure 7.20 and are listed in Table 7.27. The secondary input parameters are listed in Table 7.28.

The API gravities of bitumen and diluent are used to compute the specific gravities of the products. For raw bitumen:

$$\boxed{\text{M59}} \quad \gamma_{RB} = \frac{141.5}{131.5 + API_{RB}} \quad [\frac{\text{kg}}{\text{l}}] \quad (7.55)$$

with a similar equation for diluent **M60**. The volume fraction of dilbit as diluent f_{DI} is taken from the '*Active Field*' worksheet **M62**.

The mass inflow of heavy oil and bitumen are summed, $m_{\bar{o},RB} + m_{\bar{o},SO}$, and this total mass is converted to volume in (Q_{SO} or Q_{RB} [bbl/d]) using specific gravities of heavy oil and bitumen, depending on the source of the diluted heavy feedstock **M67**.

The total volume of diluent to be required is then computed using the expected final volume of diluted bitumen or crude oil:

$$\boxed{\text{M68}} \quad Q_{DO} = \frac{Q_{RB}}{f_{DI}} \quad [\frac{\text{bbl}}{\text{d}}] \quad (7.56)$$

which is then used to compute required volumes of diluent **M69**. Diluent specific gravity is used to convert diluent volume to diluent mass ($m_{\bar{o},DI}$) **M70**. Diluent mass plus heavy crude or bitumen mass equals the total mass outflow of diluted bitumen of heavy oil or bitumen ($m_{\bar{o},DO}$) **M71**.

Table 7.27: Streams flowing into and out of the '*Heavy oil dilution*' module. I/O denotes input or output stream

Flow name	Stream	I/O	Source/Destination	Units	Notes
NGL/diluent to dilution	16	I	NGL production and imports	[t/d]	
Bitumen from mine to dilution	6	I	Mining	[t/d]	
Crude to dilution	20	I	Crude oil dewatering	[t/d]	
Diluted crude or bitumen to storage	12	O	Crude oil storage	[t/d]	

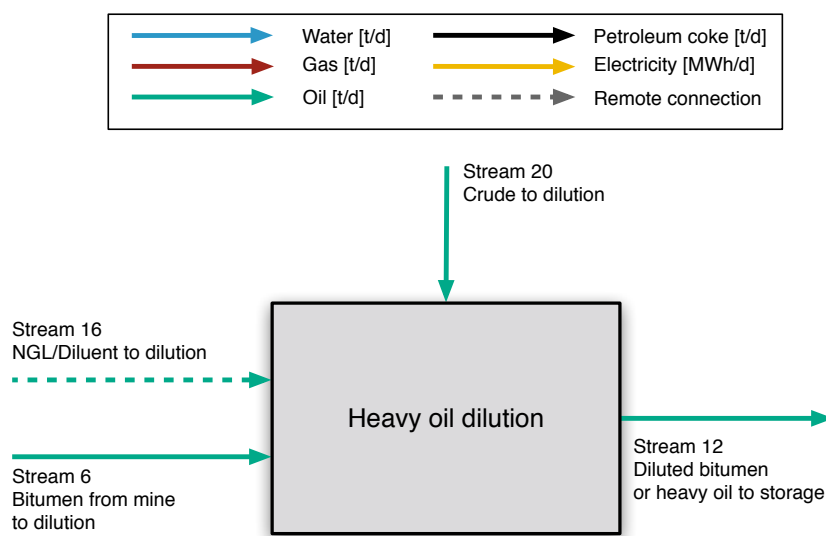


Figure 7.20: Streams flowing into and out of '*Heavy oil dilution*' worksheet. All streams measured in tonnes per day excepting electricity which is measured in MWh/d.

Table 7.28: Secondary parameter inputs to the '*Heavy oil dilution*' worksheet.

Parameter name	Cell	Eqn. term	Default value	Units	Source	Notes
Crude bitumen API grav.	M43	API_{RB}	8	[°API]	Assumption	-
Diluent API grav.	M44	API_{DI}	55.2	[°API]	Assumption	-
Diluent temperature	M47	T_{DI}	80	[°F]	Assumption	-
Diluent pressure	M48	p_{DI}	14.7	[psi]	Assumption	-
Final diluted crude mix temp.	M49	T_{DO}	60	[°F]	Assumption	-
Final diluted crude mix pressure	M50	p_{DO}	14.7	[psi]	Assumption	-

Table 7.29: Streams flowing into and out of the crude oil storage module. I/O denotes input or output stream

Flow name	Stream	I/O	Source/Destination	Units	Notes
Crude oil to storage	9	I	Crude oil dewatering	[t/d]	
Stabilized crude oil to storage	10	I	Crude oil stabilization	[t/d]	
Upgraded crude oil to storage	11	I	Heavy oil upgrading	[t/d]	
Diluted bitumen to storage	12	I	Heavy oil dilution	[t/d]	
NGL to blend with crude	17	I	NGL production and imports	[t/d]	
Storage vapors to flare	81	O	Storage vapor destruction flare	[t/d]	
Storage vapors to VRU	82	O	VRU compressor	[t/d]	
Fugitives from HC storage tank	279	O	Emitted to atmosphere	[t/d]	

7.11 Crude oil storage

The streams flowing into and out of the heavy oil dilution process are shown in Figure 7.20 and are listed in Table 7.29. The secondary inputs entered on the ‘Crude oil storage’ worksheet are given in Table ??.

The amount of vapor leaving solution into the tank headspace (the gas “flashed”) is a key driver of emissions from tank storage of crude oil. For crude oils that are not stabilized, the solution GOR at storage tank input conditions is drawn from the value computed in the ‘Separation’ worksheet. For crude oils that are stabilized, the minimum solution GOR is taken from the ‘Stabilization’ worksheet or the ‘Separation’ worksheet.

M68'

M68'

The crude oil in the storage tank has lower temperature and pressure than crude oil entering the tank. The new solution GOR is computed at these new conditions, using the methods described above in section ???. The difference in the solution GOR at inlet conditions and the solution GOR at tank conditions is the amount of gas flashed from the crude oil [scf/bbl]. Multiplying this difference in solution GOR by the crude oil flow rate, we compute the amount of flashed gas. This flashing mass is converted to tonnes per day using the gas composition and divided between flaring, recovery, and venting using the following relationship:

M69'

M70'

M71'

$$f_{vn} = 100 - f_{fl} - f_{VRU} \quad [\text{mass \%}]$$

$$'M71' = 100 - 'M68' - 'M69'$$

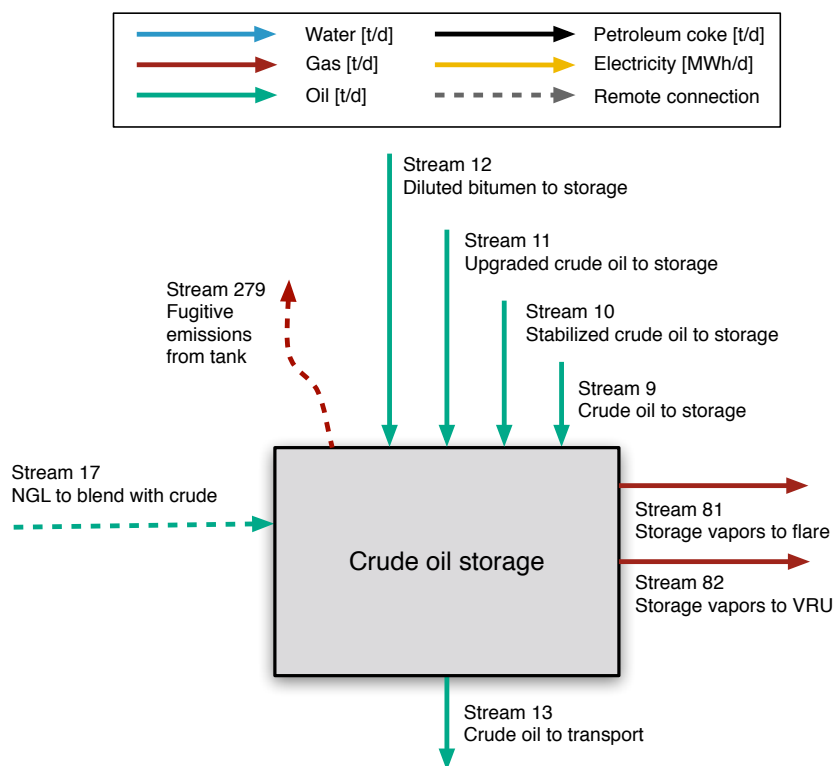


Figure 7.21: Streams flowing into and out of crude oil storage module. All streams measured in tonnes per day excepting electricity which is measured in MWh/d.

Table 7.30: Secondary inputs for crude oil storage.

Param.	Description	Eq. no.	Cell	Default	Lit. range	Unit	Sources	Notes
f_{fl}	Fraction of tank vapor flared	-	M44	0.0	0.0 – 1.0	[tonne/tonne]		a
f_{VRU}	Fraction of tank vapor sent to VRU	-	M45	0.0	0.0 – 0.95	[tonne/tonne]		a

a - This is a user input. No defaults are available and empirical practice at the field should be included if data are available.

Table 7.31: Streams flowing into and out of the produced water treatment process. I/O denotes input or output stream

Flow name	Stream	I/O	Source/Destination	Units	Notes
Water after separator to produced water treatment	103	I	Separator	[t/d]	
Water from crude oil dewatering to produced water treatment	115	I	Crude oil dewatering	[t/d]	
Electricity - Produced water treatment	186	I	Electricity generation and imports	[MWh/d]	
Treated produced water to steam generation	111	O	Steam generation	[t/d]	
Treated produced water to reinjection	113	O	Water reinjection	[t/d]	
Produced water to surface disposal	112	O	Environment	[t/d]	
Produced water to sub-surface disposal	114	O	Environment	[t/d]	

7.12 Produced water treatment

Oil production generates a significant amount of produced water, which can be contaminated with hydrocarbons, salts, and other undesirable constituents; Table 7.32 [10, p. 59] presents a typical profile. The pollutant profile varies with factors such as reservoir geology [10]. The fraction of water produced is determined by the WOR. After cleaning, produced water is reinjected, discharged to the local environment, or injected into aquifers. Streams flowing into and out of the '*Produced water treatment*' worksheet are outlined in Table ??

Process water from oil production can be treated in a variety of different ways. The technologies in OPGEE are grouped into 4 different treatment stages according to the categorization of water treatment technologies as shown in Table 7.33 [133]. This categorization and the energy consumption of each technology in kWh per m³ of water *input* (converted to kWh per bbl of water) was adopted from Vlasopoulos et al. [10].

The user can set up a water treatment system composed of 1-4 stages of treatment with one option from each treatment stage as shown in Table 7.33, which also describes the pollutants targeted by each stage. The technology combinations are selected according to the target water qualities that must be achieved.

The model scheme has two treatment trains: (i) one for the treatment of process water generated from oil production and (ii) another for the treatment of imported water, such as sea water, if applicable.

The user can set up a treatment train by switching on/off the treatment tech-

Table 7.32: Typical concentrations of process water pollutants. Table from Vlasopoulos et al [10].

Pollutants	Concentration (mg/l)
Oil and grease	200
Boron	5
Total dissolved solids (TDS)	5000
Sodium	2100

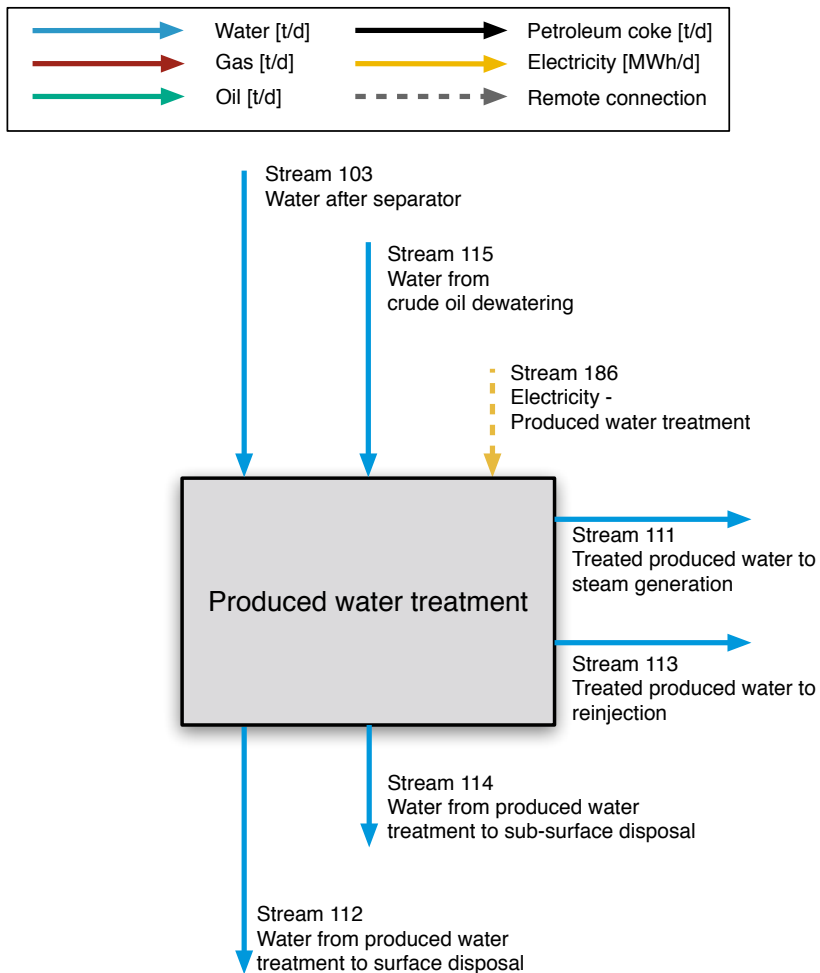


Figure 7.22: Streams flowing into and out of produced water treatment process. All streams measured in tonnes per day excepting electricity which is measured in MWh/d.

Table 7.33: Categorization of water treatment technologies. Table based on table from Vlasopoulos et al. [10], with minor modifications

Name	Signifier
Stage 1	
Dissolved air flotation	DAF
Hydrocyclones	HYDRO
Stage 2	
Rotating biological contactors	RBC
Absorbents	ABS
Activated sludge	AS
Trickling filters	TF
Air stripping	AIR
Aerated lagoons	AL
Wetlands	CWL
Microfiltration	MF
Stage 3	
Dual media filtration	DMF
Granular activated carbon	GAC
Slow sand filtration	SSF
Ozone	OZO
Organoclay	ORG
Ultrafiltration	UF
Nanofiltration	NF
Stage 4	
Reverse osmosis	RO
Electrodialysis reversal	EDR
Warm lime softening	WLS

nologies listed under each treatment stage. One option is allowed for each treatment stage. Based on the user selections, OPGEE retrieves the corresponding electricity consumption and calculates the total electricity consumption:

$$E_{tot} = e_{s1}Q_{w1} + e_{s2}Q_{w2} + e_{s3}Q_{w3} + e_{s4}Q_{w4} \quad \left[\frac{\text{kWh}}{\text{d}} \right] \quad (7.57)$$

*'Surface
Processing
2.3.1'*

where E_{tot} = total electricity consumption [kWh/d]; $e_{s,N}$ = electricity consumption of stage N [kWh/ bbl of water input]; and $Q_{w,N}$ = water feed into stage N [bbl of water/d].

For the produced water treatment train the water feed of stage 1 is equal to the water flow in the well stream as calculated in eq. (7.58). The default volume losses are assumed 0% for all treatment technologies except for wetlands which is assumed to be 26% [10]. The water feed of stages 2-4 is calculated as:

$$Q_{w,N} = Q_{w,(N-1)}[1 - \epsilon_{V,(N-1)}] \quad \left[\frac{\text{bbl of water}}{\text{d}} \right] \quad (7.58)$$

*'Surface
Processing 2.3.1
Figure'*

where $\epsilon_{V,(N-1)}$ = volume loss in stage $N - 1$ [fraction].

For the imported water treatment train, if applicable, the same calculations apply but the water feed is calculated backwards starting from stage 4 where the output is equal to the amount of water supplied to the process in excess of the output from the produced water train. The volume losses are set to be direct user inputs in the mass balance to avoid circular references.

The energy consumption value for warm lime softening (WLS) is taken from documents outlining the processing configurations for Canadian SAGD operations [134].

[TBD: CONSIDER HOW EQUATIONS LINE UP WITH FLOWS AND CELLS.
NEED TO FINALIZE AND STANDARDIZE]

7.12.1 Defaults for water treatment

Defaults for surface operations are shown in Table 7.34.

Table 7.34: Default inputs for surface processing.

Param.	Description	Eq. no.	Default	Literature range	Unit	Sources	Notes
E_{tot}	Total electricity consumption	(7.57)	-	-	[Kwh/d]		
$e_{s1} \dots e_{s4}$	Electricity consumption by stage	-	-	-	[Kwh/d]		
$\epsilon_{V,(N-1)}$	Fraction of volume loss in stage $N - 1$	-	var.	-	[L]	[10]	a
Q_w	Volume of produced water	(7.58)	-	-	[bbl/d]		
$*Q_{w1} \dots Q_{w4}$	Water feed by stage	(7.58)	-	-	[bbl water/d]		

a - This is a user input. No defaults are available for most of the treatment technologies. The default for wetlands (CWL) where volume losses are significant is 26% [10].

Table 7.35: Streams flowing into and out of the makeup water treatment process. I/O denotes input or output stream

Flow name	Stream	I/O	Source/Destination	Units	Notes
Makeup water to treatment	104	I	Makeup water source	[t/d]	
Electricity - Makeup water treatment	188	I	Electricity generation and imports	[MWh/d]	
Treated makeup water to steam generation	105	O	Steam generation	[t/d]	
Treated makeup water to reinjection	106	O	Water reinjection	[t/d]	
Makeup water waste to disposal	107	O	Environment	[t/d]	

7.13 Makeup water treatment

Makeup water treatment is modeled identically to produced water treatment. See Section 7.12 for calculation details. Table 7.35 gives the streams flowing into and out of the makeup water treatment process. Figure ?? illustrates these flows.

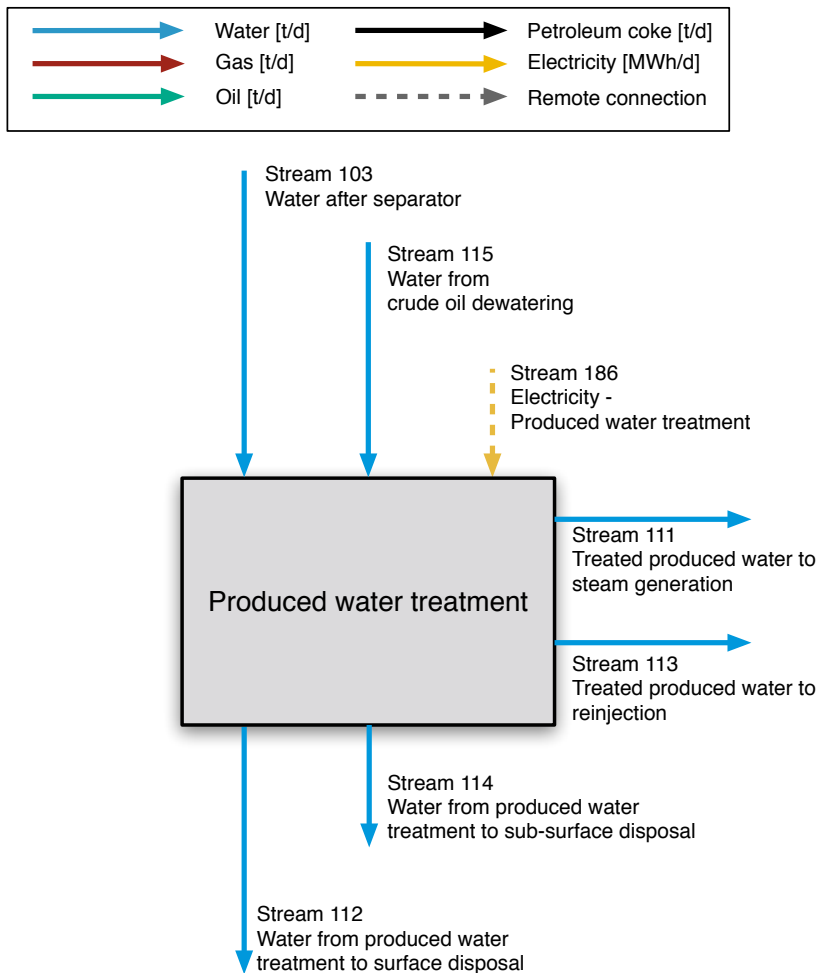


Figure 7.23: Streams flowing into and out of makeup water treatment process. All streams measured in tonnes per day excepting electricity which is measured in MWh/d.

Table 7.36: Streams flowing into and out of the water injection process. I/O denotes input or output stream

Flow name	Stream	I/O	Source/Destination	Units	Notes
Treated makeup water to reinjection	106	I	Makeup water treatment	[t/d]	
Water from produced water treatment to reinjection	113	I	Produced water treatment	[t/d]	
Electricity - Water injection	189	I	Electricity generation and imports	[MWh/d]	
Water to reinjection wells	116	O	Reservoir	[t/d]	

7.14 Water injection

Water injection requires energy if the pressure of the water to be injected is not sufficient to induce it to flow into the injection reservoir. For example, if the reservoir pressure is high, energy will be required to induce the water to flow into the reservoir.

The streams flowing into and out of the water injection process are outlined in Table 7.36 and Figure 7.24.

[TBD: ADD WATER TREATMENT EQUATIONS]

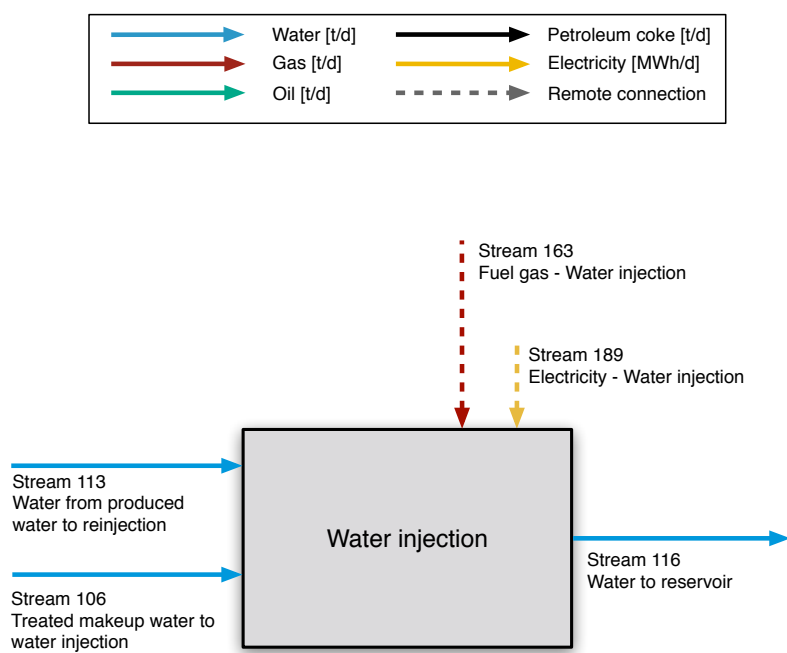


Figure 7.24: Streams flowing into and out of water injection process. All streams measured in tonnes per day excepting electricity which is measured in MWh/d.

Table 7.37: Streams flowing into and out of the steam generation process. I/O denotes input or output stream

Flow name	Stream	I/O	Source/Destination	Units	Notes
Treated makeup water to steam generation	105	I	Makeup water treatment	[t/d]	
Treated produced water to steam generation	111	I	Produced water treatment	[t/d]	
Fuel gas - Steam generation	162	I	Fuel gas system	[t/d]	
Electricity - Steam generation	187	I	Electricity generation and imports	[MWh/d]	
Steam to steam injection wells	108	O	Steam injection wells	[t/d]	
Steam gen. waste to waste rejection	109	O	Environment	[t/d]	
Electricity co-generated with steam	198	O	Electricity generation and imports	[MWh/d]	

7.15 Steam generation

The steam generation module is used to estimate energy use in generating steam for heavy projects.

The streams flowing into and out of the steam generation process are shown in Figure 7.25 and are listed in Table 7.37.

7.15.1 Introduction to steam generation

Steam injection for thermal enhanced oil recovery (TEOR) is practiced globally, with significant operations in California, Alberta, Indonesia, and Venezuela [135]. Steam injection reduces the viscosity of heavy crude oils by multiple orders of magnitude, even with relatively small temperature increases [23, 68, 71, 136, 137]. This viscosity reduction results in improved flow characteristics and improved reservoir sweep [71]. Many fields that would not produce economic volumes of hydrocarbons without steam injection become large producers after steam injection.

7.15.2 Calculations for steam generation

Steam generation for thermal oil recovery is modeled using three technologies: steam generation via once-through steam generators (OTSG) (Figure 7.26), and steam and electricity co-production via gas turbine and heat recovery steam generator (HRSG) combination (7.28), and steam generation via solar thermal technology.

'Steam Generation 1.1.6'

7.15.2.1 Steam system properties

The quantity of steam required is given by the oil production rate and the steam oil ratio:

$$Q_{ws} = SOR \rho_w Q_o \quad \left[\frac{\text{lbm water}}{\text{d}} \right] \quad (7.59)$$

'Steam Generation 2.1.1'

Where Q_{ws} = steam required to be generated per day [lbm water/d]; SOR = steam oil ratio [bbl steam as cold water equivalent/bbl oil]; ρ_w = density of water [lbm/bbl]; and Q_o = quantity of oil produced [bbl/d]. Steam quantities are measured as volume of cold water equivalent.

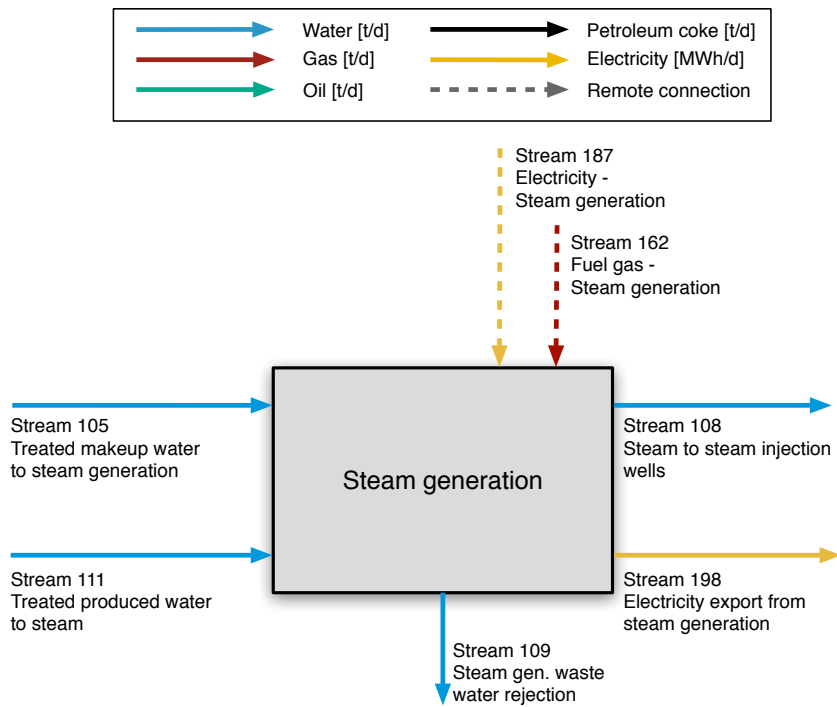


Figure 7.25: Streams flowing into and out of the steam generation process. All streams measured in tonnes per day excepting electricity which is measured in MWh/d.

The enthalpy of steam generated ($h_{ws} = h_{ws}(p_{ws}, T_{ws})$) at steam quality X_{ws} , steam pressure p_{ws} , saturated steam temperature T_{ws} is given by:

$$h_{ws} = h_{ws,g}X_{ws} + h_{ws,f}(1 - X_{ws}) \quad \text{where} \quad h_{ws} = h_{ws}(p_{ws}, T_{ws}) \quad \left[\frac{\text{Btu}}{\text{lbm}} \right] \quad (7.60)$$

'Steam Generation 2.1.11'

Steam temperature T_{ws} [$^{\circ}\text{F}$] is tabulated for saturated steam as a function of saturation pressure p_{ws} [psia] (assuming that pressure is the controlled variable) [138]. Because we are using steam tables rather than direct computation, steam pressure is rounded before lookup. $h_{ws,g}$ = enthalpy of vapor phase water at p_{ws} [Btu/lbm] while $h_{ws,f}$ = enthalpy of saturated water at p_{ws} [Btu/lbm].

Steam is generated at sufficient pressure to ensure that it will flow into the subsurface (eliminating the need for wellhead compressors). Due to friction and thermal losses in piping and wellbore, the steam pressure drops before reaching the reservoir:

$$p_{ws} = p_{res}\epsilon_p \quad [\text{psia}] \quad (7.61)$$

'Steam Generation 1.2.8'

where ϵ_p = pressure loss factor which is ≥ 1 [psia generator/psia reservoir]. Chilingerian et al. [51, p. 228] note that 10-50% of the pressure in the steam at steam generator outlet can be lost by the time the steam reaches the reservoir. The default assumption is loss of 10% of steam pressure, so $\epsilon_p = 1.1$. In addition, DOE guidebooks on practical implementation of EOR suggest that chokes are used at the wellhead to control steam flow-rate, and that the choke upstream pressure is about 1.7 times the choke downstream pressure. Both of these losses are incorporated in computing steam generator outlet pressure.

Pressure is provided by reciprocating positive displacement pumps with 90% mechanical efficiency and 97% volumetric efficiency (compressibility and slip through seals). [139, Fig. 27]. Thus, overall pressure provision has a default efficiency of 87.3%.

Steam quality X_{ws} [lbm vapor/lbm steam] is governed by the needs of the project. Higher steam qualities impart more energy into the formation, but steam quality is limited by the steam generator configuration. OTSGs cannot generate 100% quality steam because of deposition of solids in boiler tubes. In practice, $\approx 20\%$ of water mass is left in fluid state to carry solutes ($X_{ws} \approx 0.8$) [140].

The enthalpy increase of water is given by the difference between water inlet enthalpy and exit enthalpy:

$$\Delta h_{ws} = h_{ws} - h_{w,in} \quad \left[\frac{\text{Btu}}{\text{lbm water}} \right] \quad (7.62)$$

'Steam Generation 2.1.12'

Where $h_{w,in}$ is water inlet enthalpy [Btu/lbm] for compressed water enthalpy at inlet water pressure $p_{w,in}$ and inlet water temperature $T_{w,in}$ [138]. Inlet pressure is assumed equal to required steam outlet pressure (e.g., no pressure drop in boiler).

'Input Data Table 5.4'

7.15.2.2 Once-through steam generator modeling (OTSG)

Once-through steam generators are modeled [23, 140], as shown in Figure 7.26. Fuel inputs include pipeline quality natural gas, produced gas, or produced crude oil. A binary choice is required for gaseous or liquid fuels. For gaseous fuels, a mixture of produced gas and purchased gas is allowed.

'Steam Generation 2.2'

The operating conditions of combustion must be specified. These include the inlet air temperature $T_{a,in}$ [$^{\circ}\text{F}$], the outlet exhaust temperature $T_{e,out}$ [$^{\circ}\text{F}$] and the excess air in combustion $R_{a,comb}$ [mol O₂/ mol stoichiometric O₂].

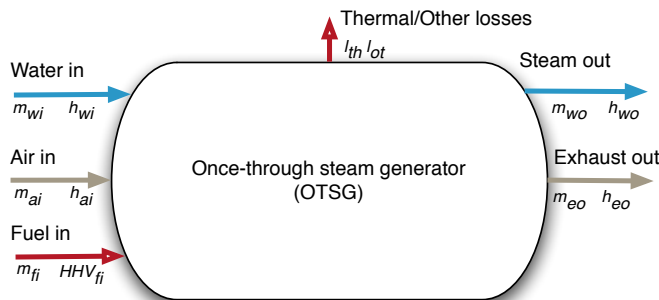


Figure 7.26: Once-through steam generator with mass and energy balance terms. Lower case terms are defined per lbmol of input fuel.

Gaseous fuel combustion for steam generation The gas species tracked in the OTSG are described below in Section 10.4. For an arbitrary fuel makeup, the composition, average molar mass, and lower heating value (LHV) are calculated.

OTSG inlet air composition, combustion stoichiometry, and excess air ratio are used to compute the mass of air required per lbmol of fuel consumed. For each reactive species, the reactants needed per mol of input fuel are computed:

$$N_i = \frac{x_{a,i}}{x_{a,O_2}} \left(x_{f,C} + \frac{x_{f,H}}{4} \right) \quad \left[\frac{\text{lbmol}}{\text{lbmol fuel}} \right] \quad (7.63)$$

where N_i = number of moles of air species i [mol]; $x_{a,i}$ = mole fraction of species i in air [mol/mol]; $x_{f,C}$ = mol of carbon per mol of fuel (e.g., 2 for C_2H_6) [mol/mol]; and $x_{f,H}$ = mol of hydrogen per mol of fuel [mol/mol]. The sum over all species i gives air required for stoichiometric combustion, which is multiplied by the excess air ratio $R_{a,comb}$ to get real air requirements:

$$N_a = R_{a,comb} \sum_{i=1}^n N_i \quad \left[\frac{\text{lbmol air}}{\text{lbmol fuel}} \right] \quad (7.64)$$

Where $R_{a,comb}$ = ratio of combustion air to stoichiometric air [lbmol air / min lbmol air for combustion]. In this case there are n species present in air.

At constant pressure the change in enthalpy with temperature is given as:

$$\delta h = C_p \delta T \quad \left[\frac{\text{Btu}}{\text{lbmol}} \right] \quad (7.65)$$

Specific heat capacity C_p as a function of T can be defined for gas species i as [141, Table A-2E]:

$$C_{p,i} = a_i + b_i T + c_i T^2 + d_i T^3 \quad \left[\frac{\text{Btu}}{\text{bmol} \cdot ^\circ\text{R}} \right] \quad (7.66)$$

Which can be integrated between outlet and inlet temperatures

$$h_i = \int_{T_{ref}=300}^T C_{p,i} dT = a_i T + \frac{b_i}{2} T^2 + \frac{c_i}{3} T^3 + \frac{d_i}{4} T^4 + e_i \quad \left[\frac{\text{Btu}}{\text{lbmol}} \right] \quad (7.67)$$

where e_i is a constant of integration. OPGEE sets $h = 0$ at $T_{ref} = 300$ K to solve for e_i . Terms a through d are given in OPGEE for N_2 , O_2 , CO_2 , SO_2 , air, $\text{H}_2\text{O}_{(v)}$ and fuel inputs (approximated as CH_4) [141].

For example, inlet air enthalpy is computed using the inlet air temperature:

'Steam Generation 2.2.3'

'Fuel Specs Table 2.3'

'Steam Generation 2.2.4'

'Input Data Table 4.1 - 4.6'

$$h_{a,in} = \sum_{i=1}^n \left(a_i T_{a,in} + \frac{b_i}{2} T_{a,in}^2 + \frac{c_i}{3} T_{a,in}^3 + \frac{d_i}{4} T_{a,in}^4 + e_i \right) \quad \left[\frac{\text{Btu}}{\text{lbmol air}} \right] \quad (7.68)$$

where again we have $i \in 1 \dots n$ components in air.

The outlet lbmol of all gases per lbmol of fuel consumed are computed assuming complete combustion (e.g., no unburned hydrocarbons, no CO produced), and no reactions with nitrogen.

'Steam Generation 2.2.3'

The enthalpy of OTSG outlet exhaust $h_{e,out}$ is computed with eq. (7.68), using user input OTSG exhaust outlet temperature $T_{e,out}$. In practice, efficient steam generation is achieved by reducing $T_{e,out}$ to as low as practicable, thus removing as much heat as possible from OTSG combustion products. $T_{e,out}$ has a lower limit due to the need to avoid condensing corrosive flue gas moisture onto heat transfer tubes [140].

'Steam Generation 2.5.1.4'

A wide range of exhaust gas temperatures is cited. Buchanan et al. cite ideal (minimum) exhaust gas temperatures of 266 °F [130 °C] or higher [142, p. 78]. Other sources cite temperatures of 350 °F [137, p. 36], 400 °F [51, p. 227] and even greater than 550 °F for older Russian units [136, p. 181].

In some cases, the exhaust gas temperature is limited by the approach to the inlet water temperature. In SAGD operations hot produced water is used as inlet water, and $T_{e,out}$ comes to within 15 °C of the inlet water temperature. An air pre-heater would allow utilization of this excess energy if hot produced fluids are used for water source [142].

'Steam Generation 2.2.7.2'

In addition to losses from flue gas exhaust, other losses occur in an OTSG. We lump all thermal losses into a thermal shell loss term. For simplicity, it is assumed that 4% of fuel enthalpy is lost as thermal shell loss ϵ_{th} [Btu/lbmol fuel consumed]. Other losses (start up inefficiencies, fouling, etc.) ϵ_{ot} are assumed $\approx 1\%$ of the fuel LHV [Btu/lbmol fuel consumed]. These total losses are supported by references, which cite losses of approximately 4% [140].

The enthalpy available for transfer to the incoming water is given by the difference between incoming enthalpy sources (incoming combustion air, fuel inputs) and outgoing enthalpy sources (hot exhaust, shell losses, other losses):

'Steam Generation 2.6.3'

$$\Delta h_{comb} = LHV + h_{a,in} - h_{e,out} - \epsilon_{th} - \epsilon_{ot} \quad \left[\frac{\text{Btu to water}}{\text{lbmol fuel}} \right] \quad (7.69)$$

The efficiency of steam generation η_{OTSG} (LHV basis) can be computed by comparing the enthalpy imparted on steam to the higher heating value of the fuel inputs:

'Steam Generation 2.2.7.4'

$$\eta_{OTSG} = \frac{\Delta h_{comb}}{LHV} \quad \left[\frac{\text{Btu to steam}}{\text{Btu fuel}} \right] \quad (7.70)$$

Using the enthalpy provided to steam and Δh_{comb} , the total fuel consumption rate required per day can be computed.

'Steam Generation 2.2.8.1'

$$m_f = \frac{Q_{ws} \Delta h_{ws}}{\Delta h_{comb}} \quad \left[\frac{\text{lbtol fuel}}{\text{d}} \right] \quad (7.71)$$

Liquid fuels for steam generation Liquid fuels can be used for steam generation. In general, these are produced heavy crude oils that are consumed on site for steam generation. This was common practice in California TEOR developments until the 1980s, when air quality impacts stopped the practice.

Because liquid fuels do not have consistent molar compositions, computations generate lbm of fuel consumed. The heating value of crude oil as a function of API

'Fuel Specs Table 1.1'

Table 7.38: Hydrogen constant a_H as a function of API gravity.

API gravity	a_H
0 - 9	24.50
10 - 20	25.00
21 - 30	25.20
31 - 45	25.45

gravity is tabulated [116]. The bulk chemical composition of crude oil is calculated [116, p. 41]. The mass fraction hydrogen w_H as a function of crude specific gravity sg is given as:

$$w_H = a_H - 15\gamma_o \quad [\text{mass frac. H}] \quad (7.72)$$

*'Fuel Specs
Table 1.2'*

Where a_H is a constant that varies with crude API gravity (and therefore specific gravity) as shown in Table 7.38.

The mass fraction of sulfur and other contaminants decreases with increasing API gravity, as seen in Figure 7.27 [143, Ch. 8, tables 3, 4] [143, Ch. 7, tables 2, 3, and 19] [144]. We therefore include default values of w_S that vary with API gravity from 5 wt.% (API gravity 4-5) to 0.5 wt.% (API gravity greater than 35). Nitrogen and oxygen content $w_N + w_O$ is assumed constant at 0.2 wt.% and in element balance it is assumed to be entirely made up of N. Mass fraction carbon w_C is calculated by difference using above mass fractions. Using the relative molar proportions of C, H, S, and N, the stoichiometric oxygen demand per carbon atom is computed assuming complete combustion.

*'Fuel Specs
Table 1.2'*

Using the oxygen requirement for combustion and the excess air ratio $R_{a,comb}$, the lbmol of air required is computed similarly to eq. (7.64) above. The inlet air enthalpy for combustion is computed using eq. (7.68) above. The outlet exhaust composition is computed via element balance assuming complete oxidation (including S to SO₂). The outlet exhaust enthalpy is computed as in eq. (7.68) for gaseous fuels combustion. The energy balance for combustion of liquid fuels is computed as in eq. (7.69).

'Steam Generation 2.2.3'

Forced air blower in OTSG Combustion air is forced through the OTSG unit with a blower. The power rating of the default OTSG blower is taken from COSIA documents outlining energy consumption and mass balances of a moderate-sized Steam-Assisted Gravity Drainage (SAGD) facility. The COSIA OTSG has a combustion duty rating of 1488 mmBtu/h and an air blower power consumption rate of 3.7 MW. This results in a consumption intensity of 0.139 bhp per mmBtu/d of OTSG consumption capacity.

'Steam Generation 2.2.8.3'

High and medium pressure boiler feedwater pump The OTSG boiler must generate steam at pressures high enough to overcome frictional loss in the surface and subsurface piping as well as to allow flow into the reservoir. The required pressure is supplied to the recycled produced water and makeup water depending on the mass fraction of each water stream. This pressure is assumed supplied by an electrically-driven pump of large capacity. For fields with low producing pressure, this consumption term is small.

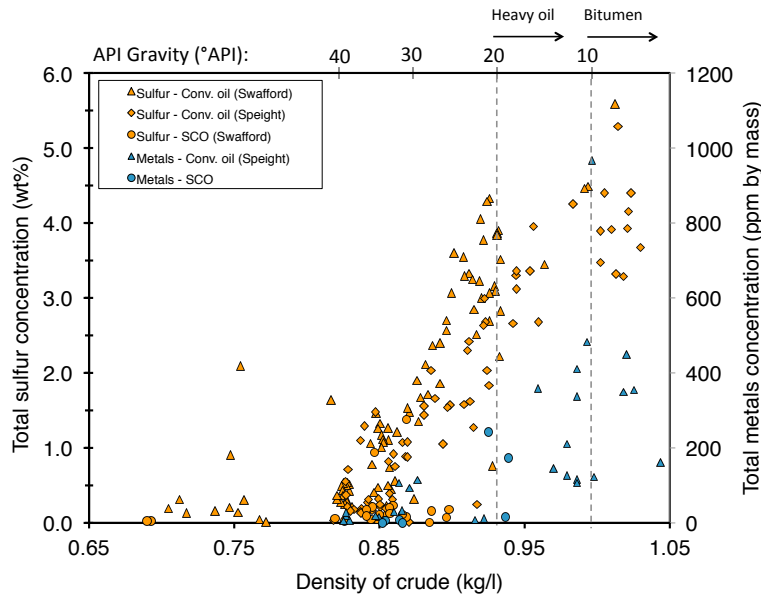


Figure 7.27: Increase of crude contaminant load with increase in crude specific gravity (decrease in API gravity). Data from: Speight (1994) and Swafford (2009).

7.15.2.3 Gas turbine with heat recovery steam generator

Cogeneration is used to co-produce electricity and steam for thermal oil recovery. These systems combine a gas turbine (GT) with a heat recovery steam generator (HRSG) to produce steam from the exhaust gas of the gas turbine (see Figure 7.28). OPGEE allows the usage of supplemental gas firing in the post-turbine exhaust stream, sometimes called “duct firing”, to allow for increased steam generation per unit of power output.

'Steam Generation 2'

Gas turbine modeling The chemical kinetics software tool Cantera [145] is used with MATLAB to compute the efficiency, losses, and turbine exit temperature for four hypothetical gas turbines labeled A, B, C, and D. The general method is as follows:

- Fuel and air compositions are specified in OPGEE for purchased natural gas (95% CH₄, 3% C₂H₆, 1.5% C₃H₈, and 0.5% inert) and air (dry air with 2% moisture).
- The LHV of the fuel is computed assuming complete combustion.
- Using the excess air fraction for a given turbine, the amount of O₂ (and therefore air) required relative to stoichiometric air requirements is used to compute relative air and fuel inputs into a mixture. The masses of fuel inputs $m_{f,in}$ and air inputs $m_{a,in}$ are normalized to a 1 kg mixture, as is default in Cantera.
- The fuel and air mixture is equilibrated using the assumption of adiabatic combustion.

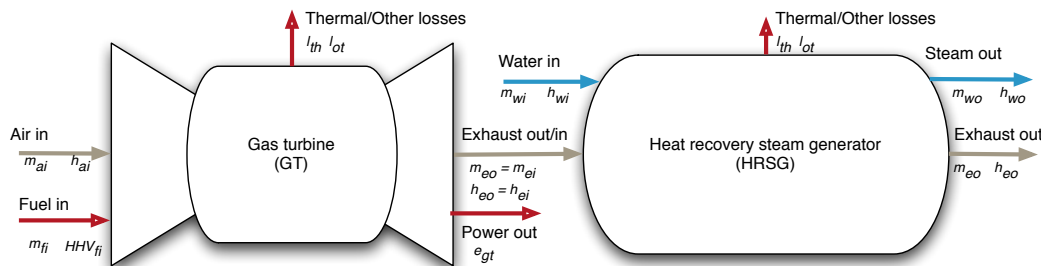


Figure 7.28: Gas turbine plus heat recovery steam generator model. Mass flows represented by m and energy flows represented by fuel lower heating value (LHV), electric power out (e) and enthalpy of gases (h).

- The enthalpy of products of adiabatic combustion is recorded as h_e , or the mass-specific exhaust enthalpy after combustion.
- The enthalpy of products of combustion is computed when returned to initial conditions (300 K, 101.325 kPa) to compute the reference enthalpy $h_{e,atm}$.
- The difference between the enthalpy of hot combustion products and the reference enthalpy of completely cool exhaust is partitioned into losses (pressure and temperature losses due to real machine imperfections), work provided by turbine (W_{GT}), and enthalpy of hot exhaust ($h_{e,out}$).
- The resulting temperature of hot exhaust gases is computed.

The gas turbine model was tested against reported gas turbine data. Data for turbine heat rate, power output, turbine exhaust mass flow rate, and turbine exhaust temperature were collected for commercial turbines from Siemens, GE, and Hitachi [146–148]. The code assumes consistent 4% thermal and other losses ($\epsilon_{th} + \epsilon_{ot}$) for each turbine. Results show excellent agreement between predicted turbine exhaust temperature and manufacturer-reported turbine exhaust temperatures (Figure 7.29).

The GT model is used to model four hypothetical turbines A - D, using characteristics similar to those specified by Kim [149]. The results from our code are used to generate required inputs for turbines A-D including turbine exhaust temperature [F], turbine efficiency [Btu e- per Btu LHV fuel input], turbine specific power [Btu e-/lb exhaust], turbine excess air [lbmol O₂ / lbmol stoichiometric O₂], and turbine loss factor [Btu/Btu LHV fuel input]. These results are shown in Table 7.39.

Using turbine efficiency and turbine loss from Table 7.39, energy balances for each turbine are computed. Using turbine excess air ratios from Table 7.39, total air requirements per lbmol of fuel input to gas turbine are computed. Inlet air enthalpy is computed as shown in eq. (7.68). Moles of combustion products are computed via stoichiometric relationships. Using turbine exhaust temperature, turbine exhaust composition, and relationships from eq. (7.68), the enthalpy of gas turbine exhaust is computed.

The enthalpy of the gas turbine exhaust is the useful energy input to the HRSG. Steam production via the HRSG is modeled analogously to that of the OTSG.

'Input data'

'Table 3.1'

'Steam Generation 2.3.1'

'Steam Generation 2.3.5'

'Steam Generation 3.3.5.1'

'Steam Generation 2.3.5'

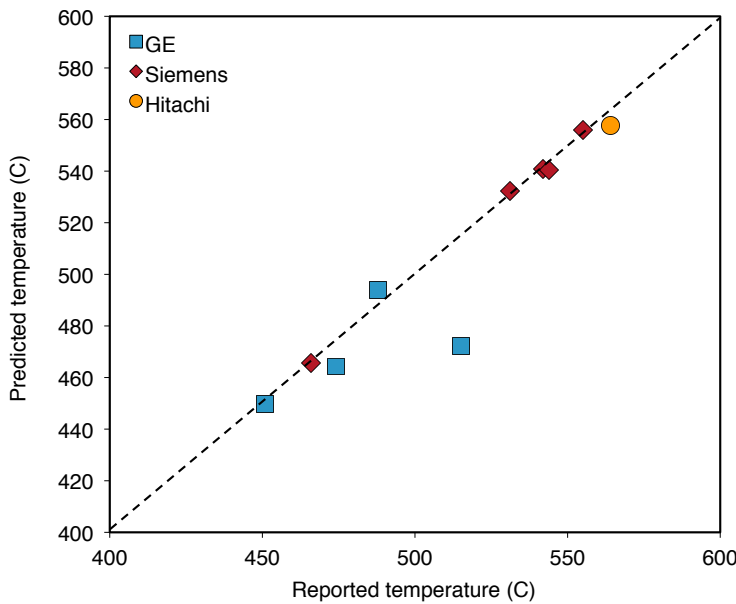


Figure 7.29: Predicted turbine exit temperatures for variety of turbines from literature (y-axis) as compared to reported value from the literature (x-axis).

Table 7.39: Gas turbine model results for hypothetical turbines A-D. These results serve as input data to OPGEE GT model.

Parameter	Unit	Turb. A	Turb. B	Turb. C	Turb. D
Turbine exhaust temp.	[°F]	932.0	947.9	950.0	1074.1
Turbine efficiency	[$\frac{\text{Btu e-}}{\text{Btu LHV}}$]	0.205	0.237	0.280	0.324
Turbine specific power	[$\frac{\text{lb exhaust}}{\text{lb e-}}$]	69.5	85.4	108.0	155.7
Turbine excess air	[$\frac{\text{Mol O}_2 \text{ real}}{\text{Mol O}_2 \text{ stoich.}}$]	4.00	3.75	3.50	2.80
Turbine loss	[$\frac{\text{Btu loss}}{\text{Btu LHV}}$]	0.041	0.036	0.032	0.027

Forced air blower in HRSG It is assumed that no forced air blower is required in an HRSG due to the high exit velocities of turbine exhaust.

Duct firing Duct firing increases the amount of steam generated from the gas turbine exhaust stream by heating the exhaust stream through supplemental combustion in the inlet of the HRSG. Because GTs operate with large amounts of excess air (air input = 2-3 times stoichiometric requirement), large amounts of residual oxygen remain the GT exhaust.

Duct firing is turned on at the top of the steam generation sheet.. If duct firing is selected, the GT exhaust temperature remains as selected from input data, but the effective HRSG inlet temperature is assumed to increase to 1300 °F [150, Table 5, Case 2]. The computed additional fuel required to duct fire to the desired temperature is computed using the composition of HRSG inlet gas to compute the effective heat capacity of the gas, which gives an approximate additional fuel needed to raise temperature (thus avoiding an iterative calculation). If very different conditions are selected (e.g., turbine or post-duct firing temperature), this approximate fuel consumption factor should be adjusted by the user.

'Steam Generation 1.2.7.2.3'

'Steam Generation 2.3.8.4'

Duct firing increases the efficiency of the HRSG, but this efficiency gain is somewhat offset by the loss of exported electricity per unit of steam generated. This reduces the co-production credit received by the cogeneration system and negates some of the potential GHG intensity reductions associated with duct firing.

7.15.2.4 Solar thermal steam generation

Solar thermal steam generation is modeled to allow for partial displacement of natural gas in steam generation thermal needs. The fraction of steam generated using solar thermal is provided by the user on the '*Inputs*' sheet. That fraction of steam is then provided by the solar thermal system at no cost of natural gas. Solar thermal pumping work for solar HTF circulation is calculated assuming that HTF pumping scales similarly to air blower work for OTSG steam generation (personal communication, John O'Donnell GlassPoint energy).

'Steam Generation 2.4'

'Inputs 1.4.13'

Reasonable fractions of energy displaced by solar thermal are around 15-25% in the absence of thermal storage or modification of steam injection schedule [151-153]. If steam injection schedule is modified to only inject steam during daytime solar hours, then the fraction of steam generated with solar thermal can approach complete NG displacement.

'Steam Generation 2.4.2.2'

7.15.3 Defaults for steam injection

7.15.3.1 General default parameters

Parameters and variables in the steam injection model are listed below in Table 7.40.

7.15.3.2 Defaults for SAGD operations

Default data for Canadian SAGD operations are taken from a variety of public sources. The overall approach to collecting data inputs for OPGEE is to use the COSIA template (Base case, warm lime softening- OTSG) [134] wherever possible to provide default input data to OPGEE to estimate emissions for SAGD operations [134]. When the template does provide the required data, we supplement that data with AER company reported data including statistical reports [121] and in situ performance presentations [154] and expert feedback when no public data is available.

Production method SAGD and CSS projects use gas lift or mechanical lift (downhole pump) and steam flooding for oil production. In mechanical lift, electric submersible pump (ESP), progressive cavity pump (PCP) and rod pump are used. OPGEE calculations can be modified based on the characteristics of these pump types. In the COSIA SAGD reference facility, mechanical lift via ESP, with down-hole pressure of 2.2 MPa, is used [134].

Gas handling properties: GOR, flaring, and venting These gas volume parameters are reported as a dimensionless value in AER statistical reports [121]. We assume that the value is in m³ gas per m³ bitumen, and convert to the desired unit (scf/bbl bitumen). The resulting values for all three gas volumes are much lower than conventional defaults, which is expected due to small quantities of associated gas in

bitumen deposits.

Field properties: productivity index, pressure, depth The difference between reservoir pressure and the injection downhole pressure is reported around 350 kPa for the Firebag project [154]. Using this value and other Firebag project data, productivity index (PI) is calculated around 22 bbl/(psi-d). This default is reasonable for SAGD projects in general due to the fact that at SAGD conditions, even large changes in PI do not affect the results significantly. The default high pressure steam system operates at 1400 psia [134]. Field depth of in situ extraction in current SAGD operations is 1300-2000 ft [134].

Steam generation technology Default steam generation technology from the COSIA template is a once-through-steam generator fired with (primarily) purchased gas. The OTSG requires forced air blowers and boiler feedwater pumps to increase pressure of both produced water and makeup water. The water is treated before boiling in a warm lime softener/evaporator.

Table 7.40: Default inputs for steam injection calculations.

Param.	Description	Eq. no.	Default	Lit. range	Unit	Sources	Notes
a_H	Crude hydrogen fraction constant	-	Table 7.38	-	[lbm H / lbm crude oil]	[116]	
$a_i \dots e_i$	Species-specific heat capacity constants	-	var.	-	[various]	[141]	
C_p	Heat capacity at constant pressure	(7.66)	-	-	[Btu / lbmol · °R]	[141]	
η_{OTSG}	OTSG efficiency	(7.70)	-	-	[Btu steam / Btu LHV fuel]	[140]	
ϵ_{th}	Thermal losses from OTSG	-	0.04	-	[Btu/BtuL fuel]	[140]	c
$\epsilon_{ot,ng}$	Other losses from OTSG fueled with natural gas	-	5000	-	[Btu/lbmol fuel]	[140]	c
$\epsilon_{ot,co}$	Other losses from OTSG fueled with crude oil	-	250	-	[Btu/lbmol fuel]	[140]	c
ϵ_{ws}	Steam pressure loss factor	-	1.25	0.1 - 0.5	[frac.]	[51]	d
λ_{rg}	Fraction natural gas	-	1	0 - 1	[frac.]	-	b
λ_{pg}	Fraction processed associated gas	-	0	0 - 1	[frac.]	-	b
$h_{a,in}$	Inlet air enthalpy	(7.68)	-	-	[Btu/lbmol]	[140]	
$h_{e,out}$	Enthalpy of OTSG exhaust	(7.68)	-	-	[Btu/lbmol]	[140]	
$h_{ws,f}$	Enthalpy of liquid phase water in steam	-	var.	180 - 730	[Btu/lbm]	[140]	
$h_{ws,g}$	Enthalpy of vapor phase water in steam	-	var.	1090 - 1205	[Btu/lbm]	[140]	
h_{ws}	Enthalpy of injected steam (< 100% quality)	(7.60)	-	-	[Btu/lbm]	[140]	
Δh_{tus}	Inlet water enthalpy	-	9.8	-	[Btu/lbm]	[140]	
Δh_{tcomb}	Change in water enthalpy upon boiling	(7.62)	-	-	[Btu/lbm]	[140]	
h_i	Heat available from combustion to water	(7.69)	-	-	[Btu / lbmol fuel]	[140]	
LHV	Enthalpy of species i	(7.67)	-	-	[Btu/LHV / 1bmol fuel]	[140]	
N_i	Lower heating value of fuel	-	var.	-	[lbmol]	[140]	
N_a	Number of moles of air species i	(7.63)	-	-	[lbmol]	[140]	
	Number of moles of air for real (non-stoichiometric) combustion	(7.64)	-	-	[lbmol]	[140]	
$p_{w,in}$	Inlet water pressure	-	$= p_s$	-	[psia]	[140]	
p_{ws}	Steam pressure	(7.61)	-	-	[psia]	[140]	
Q_o	Quantity of oil produced	-	1000	-	[bbl oil/d]	[140]	
Q_{ws}	Steam required	(7.59)	-	-	[lbm water/d]	[140]	
$R_{a,comb}$	Excess air combustion ratio	-	1.2	1.075 - 1.25	[lbmol air / lbmol air stoich.]	[155]	e
ρ_w	Density of water	-	350.4	-	[lbm/ft³]	[140]	f
γ_o	Crude specific gravity	(7.24)	-	-	[-]	[140]	
SOR	Ratio of steam injected to oil produced	-	3.0	2.5 - 6	[bbl water/bbl oil]	[91, 103]	g

Continued on next page...

Continued from previous page

Param.	Description	Eq. no.	Default	Lit. range	Unit	Sources	Notes
$T_{a,in}$	Inlet air temperature	-	540	500 - 560	[°R]	[various]	h
$T_{a,out}$	Temperature of OTSG exhaust	-	810	725 - 910	[°R]	[various]	i
$T_{w,in}$	Inlet water temperature	-	40	-	[°F]	[various]	j
T_{ws}	Steam temperature	-	var.	-	[°F]	[various]	j
w_H	Mass fraction hydrogen in crude	(7.72)	-	-	[lbm H / lbm oil]	[various]	j
$x_{a,i}$	Mole fraction of species i in air	-	var.	-	[lbmol/lbmol]	[various]	m
x_C	Moles of carbon per mole of fuel	-	var.	-	[lbmol/lbmol]	[various]	a
x_H	Moles of hydrogen per mole of fuel	-	var.	-	[lbmol/lbmol]	[various]	a
X_s	Steam quality	-	0.8	-	[lbm vap./lbm steam]	[71]	k
y_{ng}	Binary variable: gaseous fuel in OTSG	-	1	0 or 1	[y/n]	-	l
y_{co}	Binary variable: crude oil in OTSG	-	0	0 or 1	[y/n]	-	l

a - See 'Fuel species' Table 2.3 for combustion factors for gas inputs.*b* - Assumption: Gas is purchased due to typical low GORs for heavy crudes.*c* - Assumption to account for incomplete combustion, fouling, warm up and cool-down, and other real-world inefficiencies.*d* - Piping friction losses can represent 10-50% of the steam pressure developed at the outlet of the steam generator." [51, p. 228]*e* - Conservative assumption for input excess air. Can be lower with special combustion equipment.*f* - Fresh water input*g* - Common SOR for efficient TEOR project. Range is quite variable, especially in early years of steam injection.*h* - Equal to 300 K. Chosen for ease of gas turbine modeling.*i* - Equal to 350 °F. Reported range is wide in literature. See [51, 136, 137, 142].*j* - Assumption for cool water inlet.*k* - Most commonly cited steam quality. Other qualities cited include 75%.*l* - Assumption: Most steam generation in California and Alberta is natural gas fired.*m* - See 'Input Data' Table 2.4 for air composition.

Table 7.41: Streams flowing into and out of the flaring process. I/O denotes input or output stream

Flow name	Stream	I/O	Source/Destination	Units	Notes
Gas after separator	28	I	Separator	[t/d]	
Mine offgas to flare	84	I	Mining	[t/d]	
Gas consumed in flare	29	O	Environment	[t/d]	
Post-flare gas to vent	30	O	Venting	[t/d]	

Table 7.42: Sources of flaring data and construction notes

	Flaring volumes	Oil production volumes
2010	OPGEE 1.1e, 'Flaring' worksheet	BP 2016 Statistical Review of World Energy. If unavailable, EIA International Petroleum Production, data series "Total Petroleum and Other Liquids"
2011	OPGEE 1.1e, 'Flaring' worksheet	<i>ibid.</i>
2012	Dataset obtained from Chris Elvidge via Jim Duffy, California Air Resources Board, July 21st, 2015. Contains country-level totals from NOAA analysis	<i>ibid.</i>
2013	World Bank Global Gas Flaring Reduction Partnership, website accessed 5/30/2017	<i>ibid.</i>
2014	<i>ibid.</i>	<i>ibid.</i>
2015	<i>ibid.</i>	<i>ibid.</i>

7.16 Flaring

Flaring is used to dispose of associated natural gas produced during bulk separation (see Section ??) when it cannot be used economically. Gas flaring resulted in emissions of 0.28 Gt CO₂ eq. in 2008, or about 1% of global GHG emissions [27]. Since 1994, NOAA National Geophysical Data Center has estimated flaring volume using satellite imagery [27]. The distribution of estimate flaring volume by country is highly skewed; in 2008 Russia, Nigeria, Iran, and Iraq were the country with the highest flaring volumes [27].

The streams flowing into and out of the flaring process are shown in Figure 7.30 and are listed in Table 7.41.

7.16.1 Calculation of flaring emissions

For the calculation of flaring emissions, the key input parameter is the flaring-to-oil ratio, or FOR [scf/bbl]. The FOR is converted into flaring volume using the volume of oil produced:

$$Q_F = \frac{FOR \cdot Q_o}{10^6} \quad [\text{MMscf/d}] \quad (7.73)$$

where Q_F = flaring volume [MMscf/d]; FOR = flaring-to-oil ratio [scf/bbl of oil]; and Q_o = volume of oil produced [bbl/d].

The OPGEE default FOR is given by country-level flaring data [156] and production volumes [157] for the years 2010 to 2015. A detailed listing of sources and compilation notes for flaring data is given in Table 7.42. The default flaring rate is retrieved from the 'Flaring' worksheet based on the field location specified in the 'Active Field' worksheet. The flaring rate in a specific oil field could be significantly higher or lower than the country-average. In the case no default is available for the specified field location, the world average is taken as the default value.

'Flaring'

1.3'

'Flaring'

Table 4.1'

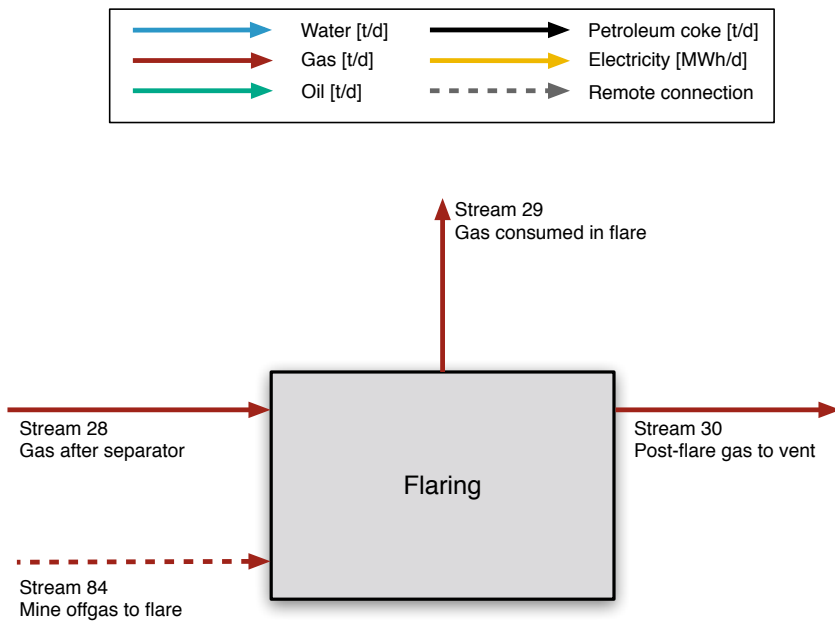


Figure 7.30: Streams flowing into and out of the flaring process. All streams measured in tonnes per day excepting electricity which is measured in MWh/d.

Table 7.43: Data requirements for utilizing field-specific flaring calculation.

Data requirement	Units
Oil production	[bbl/d]
Flaring intensity	[scf/bbl]
Number of flares	[#]
Number of flare tips per flare	[#]
Flare tip diameter	[in]
Lower heating value of gas (LHV)	[MJ/kg] or [Btu/scf]
Average wind speed	[mph]

Carbon-dioxide-equivalent flaring emissions are calculated from the flaring volume using the flare efficiency η_F . The flare efficiency is the fraction of flared gas that is combusted. The remaining gas undergoes fuel stripping and is emitted as unburned hydrocarbons.

*'Flaring
3.1'*

Flare efficiency varies with flare exit velocities and diameters, cross wind speed, and gas composition [25, 26]. For example, flare efficiencies in Alberta were estimated to range from 55% to $\geq 99\%$, with a median value of 95%, adjusted for wind speed distributions [25].

If the user does not have field specific information about the flare system design and average ambient wind conditions, then OPGEE populates the model with a default flare efficiency of 95%. If the user has the full amount of required data (see Table 7.43) then the user can determine the field-specific flaring efficiency.

*'Flaring
1.1'*

The logical progression of the flaring worksheet is shown as a flow-chart in Figure 7.31.

OPGEE uses a flare efficiency equation developed by Johnson and Kostiuk

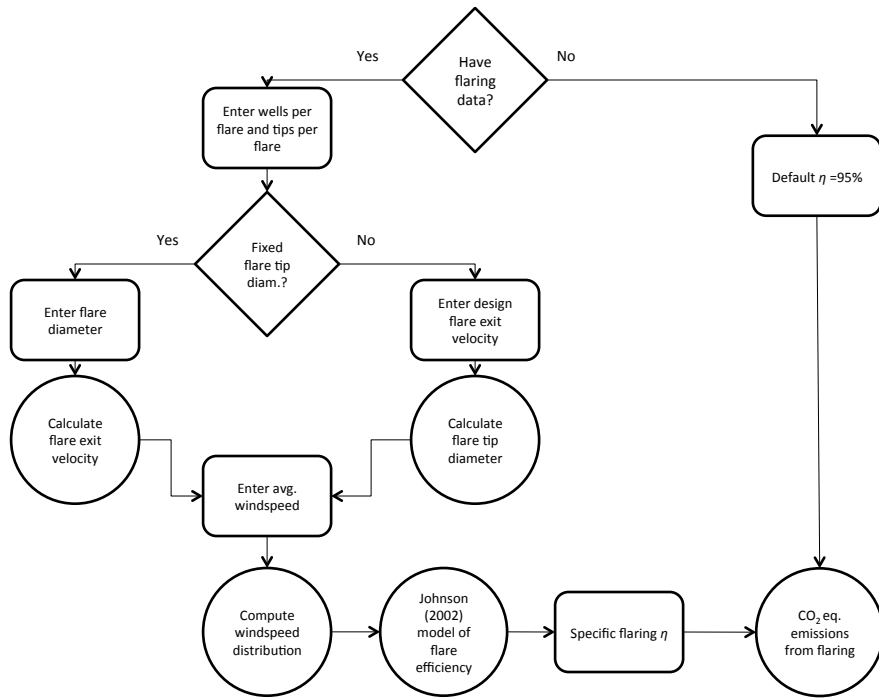


Figure 7.31: Flowchart illustrating the logic of the flaring computation worksheet.

[158]:

'Flaring 3.1'

$$\eta_F = 1 - \frac{A \exp \left[\frac{BU_\infty}{(gVd)^{\frac{1}{3}}} \right]}{LHV^3} \quad (7.74)$$

Where $A = 156.4$ [MJ/kg], $B = 0.318$ [dimensionless], U_∞ is the wind velocity [m/s], g is the gravitational constant [m/s²], V is flare gas exit velocity [m/s], d is flare pipe exit diameter [m], and LHV is the lower heating value of the flare gas [MJ/kg]. The most impactful parameters on flare efficiency are wind speed, gas exit velocity, and LHV. For completeness, all parameters are discussed below.

A second parametric model by Gogolek was explored [159], but for ease of integration into OPGEE, the Johnson model was selected.

7.16.1.1 Constants

The Johnson and Kostiuk model, contains different values for A and B given for methane flares and propane flares (the two flare gasses tested in the experiments). We implement the constants for methane flares for two reasons: first, the primary gas component in most flares is methane, and second, there is no simple direct linear relationship that can be used to interpolate the A and B values when non-pure gas mixtures are flared.

7.16.1.2 Lower heating value

The flare gas LHV is calculated by multiplying the LHV for each component of the gas by that component's mass fraction. The mass fraction of each gas species is taken from the '*Gas Balance*' worksheet, and the LHV for each species is taken from the '*Fuel Specs*' worksheet. If the flare gas has significant non-combustibles like N₂ and CO₂, the LHV of the gas, and thus the flare efficiency, will be reduced.

*'Flaring
1.4'*

7.16.1.3 Flare gas exit velocity and diameter

There are cases where multiple wells feed to a single flare. There are also cases where each flare stack has multiple openings (flare tips) out of which gas exits. To calculate an efficiency, we are interested in the velocity of the gas coming out of each individual flare tip. As such, the user is asked to enter the number of wells per flare and the number of flare tips per flare. The volumetric flowrate of gas exiting through each opening is found by dividing the total flowrate for the field by the number of flare tips in the field.

*'Flaring
2.1.2'
'Flaring
2.1.4'*

Some flare tips have a variable orifice diameter, to allow for more even combustion properties under varying flow conditions. The user therefore first chooses whether they have a fixed diameter flare or a variable diameter flare. If the user chooses a variable tip diameter, then they choose a flow rate to size the flare to. Suggested maximum regulated flare exit velocity are given in the notes section of this entry. A US EPA regulatory standard is used. For onshore U.S. production, the EPA 60.18 40 CFR Ch.1 [160] regulation states that for flares with a LHV of between 200 and 1,000 btu/scf, the maximum allowable gas exit velocity is 122 feet/sec. For flares with a LHV above 1,000 btu/scf, the maximum allowable gas exit velocity is 400 feet/sec [160].

*'Flaring
2.2.1'*

Users with pipe diameter information can enter that information. The flare pipe exit diameter is used directly in the Johnson and Kostiuk model, and is also used to calculate the flare gas exit velocity. Flare gas exit velocity is calculated by dividing the mass flux of gas by the cross sectional area of the pipe.

*'Flaring
2.2.2.1'
'Flaring
2.2.3.2'
'Flaring
2.2.3.3'*

7.16.1.4 Volume of gas flared

If the user knows the volume of gas that is flared in their field, they can input these data. Otherwise, OPGEE estimates this number based on what country the user selected on the '*Active Field*' worksheet.

*'Flaring
1.3'
'Flaring
Table 4.1'*

7.16.1.5 Wind Speed

The user must enter an average wind speed for their field. If the user is onshore in the United States, the user can select a local area from the dropdown list, and this will populate the wind speed cell with an average local wind speed. National Oceanic and Atmospheric Administration data on the average wind speed for hundreds of locations across the United States.

*'Flaring
2.3'*

Because the efficiency of combustion (7.74) has an exponential dependence on wind speed, a seemingly small increase in wind speed can significantly alter flare efficiency and thus emissions as well. As such, using a yearly average wind speed to calculate flaring efficiency can yield an inaccurate result. To resolve this, the

*'Flaring
Table 4.2'*

Rayleigh probability distribution method has been adapted and applied from da Rossa [161]. Figure 7.32 illustrates the fit of the Rayleigh distribution to National Renewable Energy Laboratory wind data for 6 randomly chosen wind sites in the western United States.

The Rayleigh method estimates a wind velocity probability distribution based on what is known about wind speeds. In this case, the user input average (mean) wind speed. This method estimates a mode (most frequently occurring wind speed) using the relationship:

$$m_U = \frac{\mu_U}{\sqrt{\frac{\pi}{2}}} \quad (7.75)$$

where m_U is the mode of the windspeed [mph], and μ_U is the average (mean) wind-speed [mph].

The probability density curve for the Rayleigh distribution is calculated from the mode using the expression:

$$p(U) = \frac{U}{m_U} \exp \left[-\frac{1}{2} \left(\frac{U^2}{m_U^2} \right) \right] \quad (7.76)$$

where $p(U)$ is the probability of finding wind speeds of velocity U [mph].

To calculate an overall flaring efficiency, the efficiency of combustion at each wind speed along the probability density curve is calculated using (7.74), and efficiencies are summed by their fractional probability. Figure 7.33 shows the probability distribution for an average wind speed of 30 mph. Using the Johnson and Kostiuk (2002) model with these data, OPGEE calculates the flaring combustion efficiency.

*'Flaring
3.1'*

7.16.2 Emissions from flares

Emissions from non-combusted gas are calculated using the composition of associated gas from the '*Gas Balance*' worksheet:

$$EM_{F,str} = Q_F (1 - \eta_F) \sum_i x_i \rho_i GWP_i \quad [\text{tCO}_2\text{eq/d}] \quad (7.77)$$

*'Flaring
3.2.2.1'*

where $EM_{F,str}$ = flaring emissions from stripped, non-combusted gas [tCO₂eq/d]; η_F = flaring efficiency [%]; Q_F = flaring volume [MMscf/d]; i = index of gas species CO₂, CH₄, and volatile organic compounds C₂H₆, C₃H₈ and C₄H₁₀; x_i = molar fraction of gas component i [mol/mol]; ρ_i = density of gas component i [g/ft³]; and GWP_i = GWP of gas component i [g CO₂ eq. / g gas].

Emissions from flare combustion products assume complete combustion:

$$EM_{F,comb} = Q_F \eta_F \sum_i x_i \rho_i \Pi_i \quad [\text{tCO}_2\text{eq/d}] \quad (7.78)$$

*'Flaring
3.2.1.1'*

where $EM_{F,comb}$ = flaring emissions from combusted gas [tCO₂eq./d]; Π_i = stoichiometric relationship between component i and product CO₂ for complete combustion [g CO₂/g gas]. Combustion factors are listed in Table 7.44.

Total flaring emissions are the sum of stripped and combustion emissions:

$$EM_{F,tot} = EM_{F,str} + EM_{F,comb} \quad [\text{tCO}_2\text{eq/d}] \quad (7.79)$$

*'Flaring
3.2'*

Table 7.44: Stoichiometric relationships for complete combustion.

Fuel	Stoichiometric factor Π
CO ₂	1
CH ₄	44/16
C ₂ H ₆	88/30
C ₃ H ₈	132/44
C ₄ H ₁₀	176/58

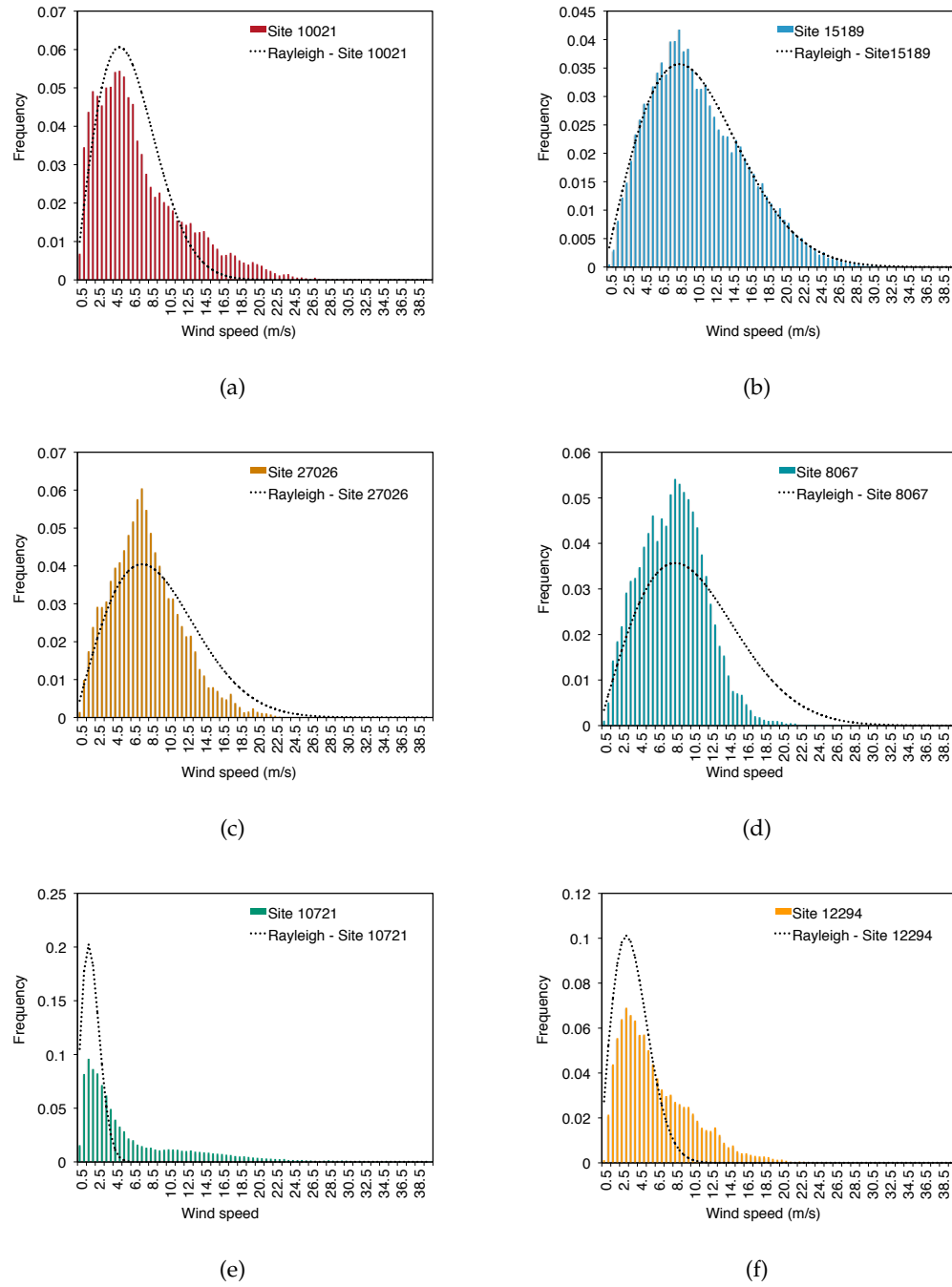


Figure 7.32: Rayleigh distribution fit to 6 wind speed datasets from western United States. Data source: NREL Western Wind Integration Dataset.

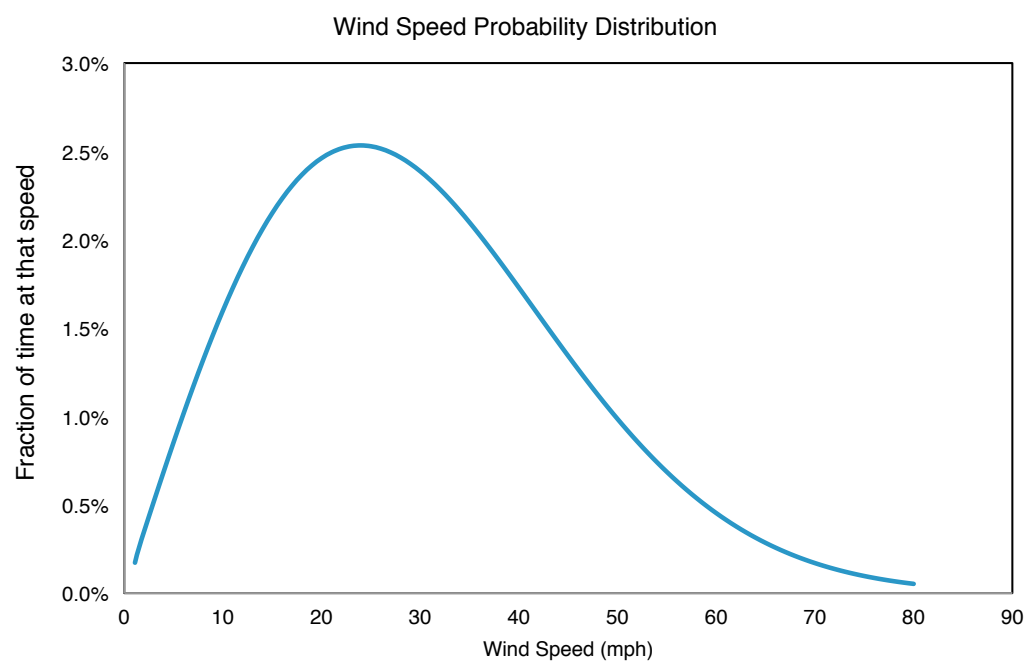


Figure 7.33: Example of OPGEE wind speed distribution for a 30 mph average windspeed input.

Table 7.45: Default inputs for venting, flaring, and fugitive emissions.

Param.	Description	Eq. no.	Default	Literature range	Unit	Sources	Notes
A	Flaring eff. pre-exponential constant	-	156.4	NA	[M]/kg]	[158]	
B	Flaring eff. growth constant	-	0.318	NA	[-]	[158]	
d	Flare diameter	-	3	0.25-24	[in]		
$EM_{F,comb}$	Flare combustion emissions	(7.78)	-		[tCO ₂ eq/d]		
$EM_{F,str}$	Flare stripping emissions	(7.77)	-		[tCO ₂ eq/d]		
η_F	Flaring efficiency	-	0.95	-	[scf/bbl]	[25, 26, 162]	a
FOR	Flaring-to-oil ratio	-	177	0.54 - ≥ 0.99 11-3010	[m/sec ²]		
g	Gravitational constant	-	9.8	-	[gCO ₂ eq./g]	[163]	b
GWP_i	Global warming potential for species i	-	'Input data' Table 2.1	-	[M]/kg]	[163]	b
LHV	Lower heating value of associated gas	-	-	-	[gCO ₂ /g]	-	c
Π_i	Stoichiometric combustion ratios	-	Table 7.44	-	[MMscf/d]	-	
Q_F	Flaring volume	(7.73)	-	-	[bbl/d]	-	
Q_o	Volume of oil production	-	1500	-	[g/ft ³]	-	d
p_i	Gas density for species i	-	'Input Data' Table 2.2	-	-	-	e
U_∞	Wind speed	-	NA	0-100	[mph]	-	f
V	Flare exit velocity	-	NA	0-100	[m/s]	-	
x_i	Mole fraction of gas composition	-	'Gas Balance' Table 1.1	-	[-]	[12]	g

a - Average efficiency for Alberta found to be ≈0.95 across 4 years of data using known wind distributions and flaring volumes [25]. Very low efficiencies are seen in high cross winds and with high fractions of non-combustible gas components (e.g., CO₂, N₂).

b - 100-year GWP's from the IPCC Fourth Assessment Report [163].

c - Standard combustion stoichiometry assuming complete combustion.

d - Standard gas densities [155]

e - The experimental wind conditions in the Johnson (2002) study only ranged from 4 to 38 mph. OPGEE presents a warning if a wind speed outside of this range is entered.

f - The flare exit velocities in the Johnson (2002) study only ranged from 0.5 to 4 m/s (low momentum flares). OPGEE presents a warning if a wind speed outside of this range is entered. For most flare design conditions, flare exit velocities (and momentum ratios) will be higher than this range, and flare efficiency will be at upper end of model results. Johnson suggest (pers. comm. 2012) that for conditions with momentum ratios above the experimental conditions, a default flaring efficiency of 99.8% be used.

g - Gas composition can vary. Default gas composition given from [12].

Table 7.46: Streams flowing into and out of the venting process. I/O denotes input or output stream

Flow name	Stream	I/O	Source/Destination	Units	Notes
Post-flare gas to vent	30	I	Flaring	[t/d]	
Gas to misc. venting and fugitives	253	O	Environment	[t/d]	
Gas to purposeful vent	252	O	Environment	[t/d]	

7.17 Venting

The streams flowing into and out of the venting process are shown in Figure 7.34 and are listed in Table 7.46.

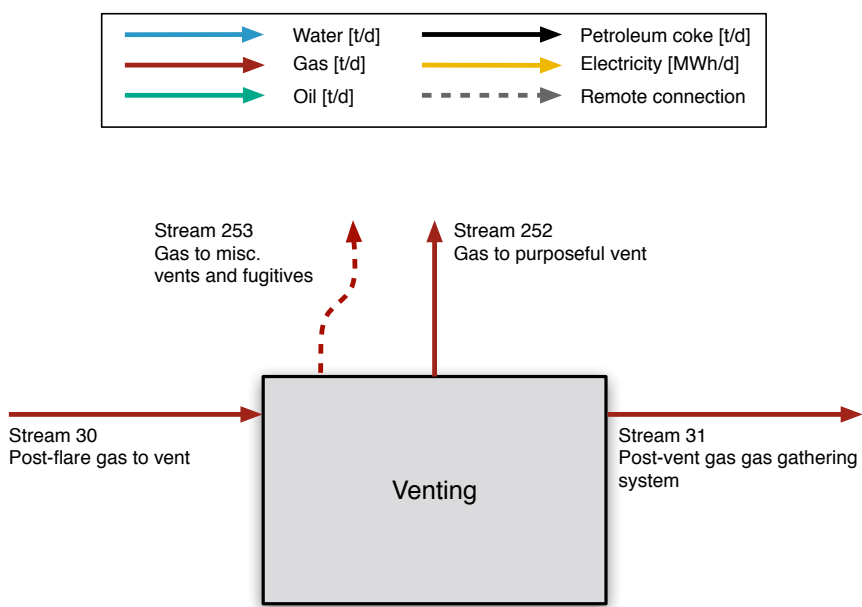


Figure 7.34: Streams flowing into and out of the venting process. All streams measured in tonnes per day excepting electricity which is measured in MWh/d.

Table 7.47: Streams flowing into and out of the gas gathering process. I/O denotes input or output stream

Flow name	Stream	I/O	Source/Destination	Units	Notes
Post-vent gas to gas gathering	31	I	Venting	[t/d]	
Stabilizer gas	32	I	Stabilizer	[t/d]	
VRU gas to gathering	33	I	VRU compressor	[t/d]	
Gathered gas to dehydration	34	O	Glycol dehydrator	[t/d]	
Fugitives from gathering	254	O	Environment	[t/d]	

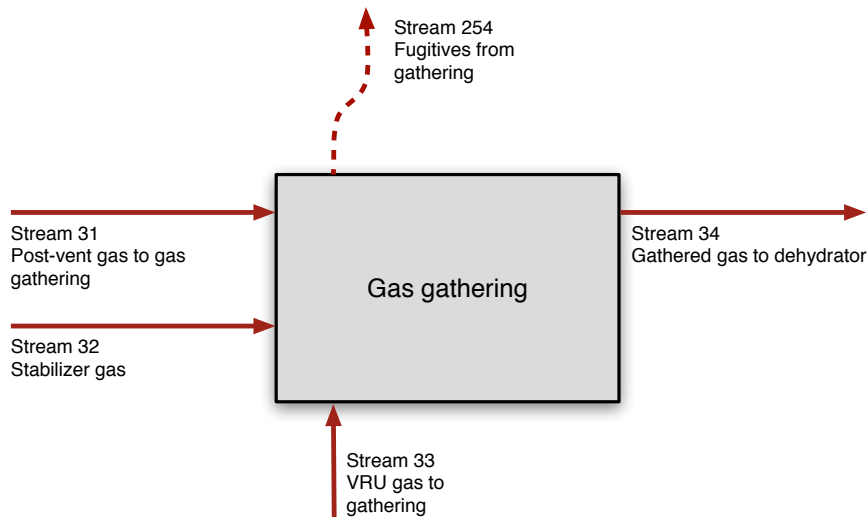
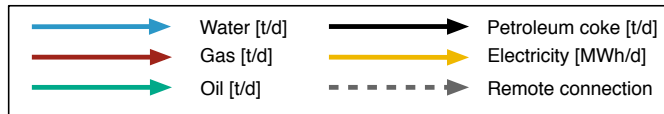


Figure 7.35: Streams flowing into and out of the gas gathering process. All streams measured in tonnes per day excepting electricity which is measured in MWh/d.

7.18 Gas gathering

The streams flowing into and out of the gas gathering process are shown in Figure 7.35 and are listed in Table 7.47.

Table 7.48: Streams flowing into and out of the glycol dehydrator process. I/O denotes input or output stream

Flow name	Stream	I/O	Source/Destination	Units	Notes
Gathered gas to dehydrator	34	I	Gas gathering	[t/d]	
Electricity - Dehydrator	176	I	Electricity generation and imports	[MWh/d]	
Fuel gas - Dehydrator	151	I	Fuel gas system	[t/d]	
Dehydrated gas to AGR	36	O	Acid gas removal	[t/d]	
Dehydrated gas to CO2-EOR pathways	35	O	Varies	[t/d]	

7.19 Glycol dehydrator

In addition to the sweetening process, natural gas often must be dehydrated to prevent issues such as condensation and hydrate formation that could negatively affect the gas processing and distribution process [4, p. 139]. This section discusses thermal and electrical energy demands from gas dehydration. The dehydration process also involves operational venting of some natural gas and water [4, p. 140]; dehydrator venting is discussed in the Venting & Fugitives section (see Section ??).

The streams flowing into and out of the glycol dehydrator process are shown in Figure ?? and are listed in Table 7.48.

The default dehydration method in OPGEE is liquid triethylene glycol (TEG) desiccant, which contacts the natural gas and absorbs water from it; heat is then applied to separate the water from the TEG [4, p. 140]. Two methods of modeling TEG units are used in OPGEE: (1) A method based on statistical analysis of results from process simulation software; and (2) A method based on methods from gas processing handbook. We strongly recommend use of method (1), while method (2) remains in OPGEE v3.0a primarily in order to maintain backward compatibility with earlier versions of OPGEE. We describe these two methods below.

7.19.1 TEG dehydration modeling using result from process simulation software

The simulations, and consequently OPGEE, model dehydration through the use of triethylene glycol (TEG). TEG is selected because of its ability to cheaply and easily regenerate to a concentration of 98–99.5% in an atmospheric separation unit [4]. Figure 7.37 illustrates the process flow diagram of a TEG dehydration process in Aspen HYSYS.

The modeled system works by combining the sweet gas and water in a mixer to create a wet natural gas entering the separator unit with moisture in equilibrium with the gas. The separator removes all liquid and solid impurities from the gas and sends it to a contact tower. In the contactor, the natural gas counter-currently flows against incoming TEG. The TEG dries the gas, which then gets passed through a heat exchanger and passed into the sales line. Meanwhile, the rich TEG leaves the contactor and passes into the regenerator. The gas rich TEG flows through the reboiler. Water is stripped, and the water vapor is vented from the top of the regenerator. The lean TEG is then passed through a make-up unit to be supplemented with fresh TEG. Finally, the lean TEG is pumped back to the contactor [4].

The goal of this research is to vary several different decision variables within

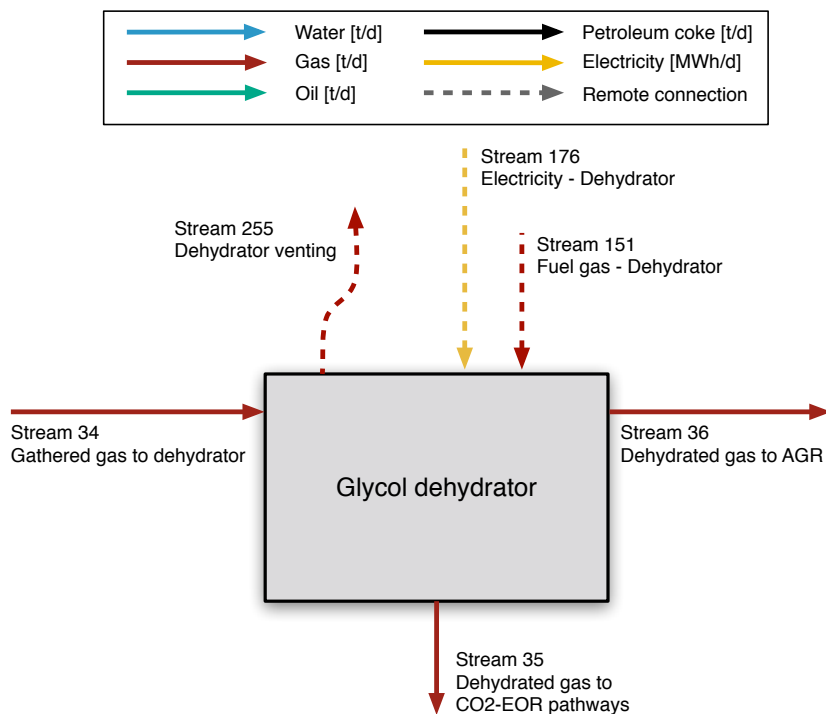


Figure 7.36: Streams flowing into and out of the glycol dehydrator process. All streams measured in tonnes per day excepting electricity which is measured in MWh/d.

the Aspen simulations in order to determine a model for energy consumption that can be utilized in OPGEE. The model will be used to adequately predict reboiler energy use, pump energy use, and cooler energy use. Meanwhile, the Aspen HYSYS simulations also allow for an ability to predict final water load in the sales gas, as long as it meets the 7 lb water / MMSCF or less standard. The variables that are adjusted are:

1. Pressure of the water and gas mixture entering the separator.
2. Temperature of the water and gas mixture entering the separator.
3. Water mass load of the water and gas mixture entering the separator.
4. Reflux ratio
5. Regenerator feed temp

The goal of the dehydration system will be to dry the sweet gas to a standard of 7 lb water/MMSCF, minimize required energy, and require minimal maintenance [4]. To be consistent with the OPGEE model, input parameters not being varied in the model are set to match parameters generated from OPGEE. Any parameters not generated from OPGEE are acquired from Manning and Thompson [4]. Non-variable process operating conditions are outlined in Table 7.49.

The number of stages in the contactor is selected as 2 based on exploration of model settings: additional trays do not contribute to the energy cost or final water

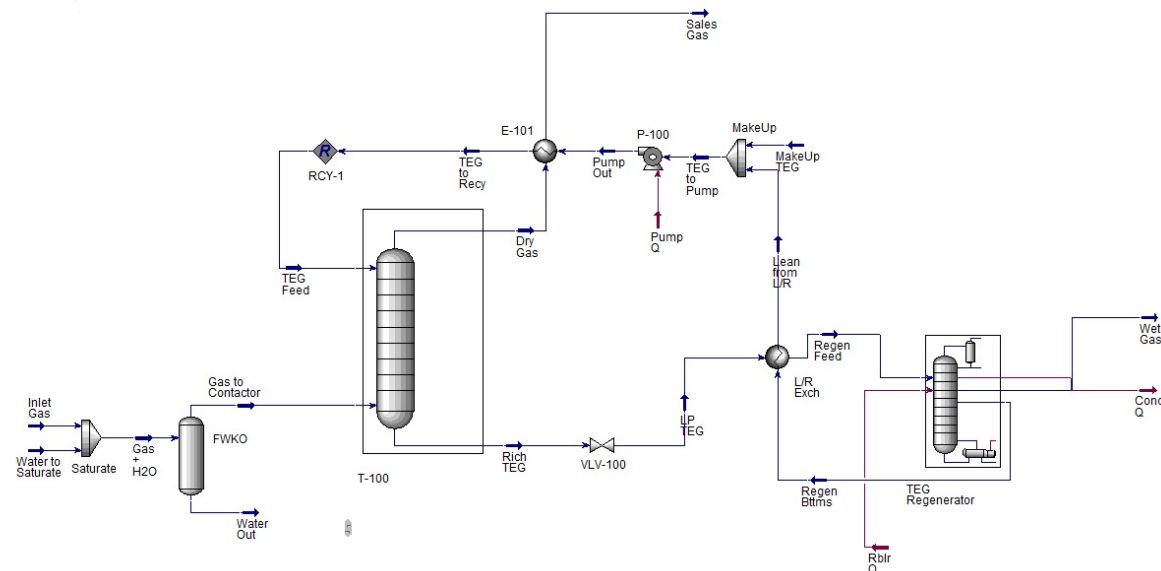


Figure 7.37: Glycol dehydrator process flow diagram from Aspen HYSYS model.

Table 7.49: Settings for non-varying operating parameters in Aspen HYSYS TEG dehydration unit simulations. Source “def.” is OPGEE assumed default from prior model versions.

Process unit	Parameter	Value	Unit	Source	Notes
Contactor	Operating pressure	800	psia	def.	
Contactor	TEG concentration	99	wt.%	def.	
Contactor	TEG-to-water ratio	2	gal TEG/lb H ₂ O	def.	
Contactor	TEG pressure	800	psia	[4]	
Contactor	Inlet moist gas flow rate	1.0897	MMscf/d	def.	
Contactor	Stages	2	stages	def.	
Pump	Discharge pressure	800	psia	def.	
Pump	Pump efficiency	75	%	def.	
Reboiler	Temperature	400	°F	[4]	

content beyond a negligible amount. Therefore, the number of effective stages is not considered an independent variable in the models.

The independent variables explored in the model are listed in Table 7.50.

In Aspen HYSYS a Box-Behnken sampling of 117 points are tested using the ranges shown in Table 2 for the inlet pressure, inlet temperature, inlet molar water flow rate, reflux ratio, and regenerator feed temperature. The values for TEG recirculation rate and TEG-to-contactor temperature are calculated from those 117 points as well. Those points are supplemented by a set of 10000 combinations generated from latin hypercube samplings in the same ranges. That combines to a total of 10117 different combinations. This set of randomly-selected settings of temperatures and flow rates is not likely to – in general – meet the required gas quality specifications. Therefore, after simulation, all points are vetted to ensure that they meet the 7 lb H₂O per MMSCF moisture content maximum, and samples that do not meet this standard are rejected. This leaves 1962 sampled points to be used to generate the prediction models.

Using these results, predictive equations are generated using MATLAB curve

Table 7.50: Ranges of independent variables explored in TEG dehydration Aspen HYSYS modeling.

Proc. unit	Variable	Low range	High range	Unit	Notes
Contactor	Inlet gas pressure	814.7	1014.7	psia	
Contactor	Inlet gas temperature	80	100	°F	
Contactor	Inlet water flow rate	5×10^{-4}	5×10^{-3}	MMSCFD	
Reboiler	Reflux ratio	1.5	3	-	
Reboiler	Reboiler feed temperature	190	220	°F	

fitting toolbox [164]. A set of four predictive equations were generated for the TEG dehydration unit. These equations predict (1) reboiler heat input, (2) pump work, (3) condenser cooling electrical load, and (4) residual moisture in lbs H₂O/MMSCF. Each dataset is split into a training dataset and a testing dataset. The testing set is a randomly selected subset of ≈10% of the observations which is removed from the dataset and held aside (i.e., not used to generate the statistical fit). The training set includes the remainder of the results (≈%90% of simulation runs). The training and testing sets are drawn independently for each predictive equation, so training n and testing n will vary for each predictive model. Each training dataset is fitted to a quadratic equation of all five independent variables. The quadratic equation includes all linear terms, interaction terms, and square terms. The quadratic model fits are of the general form:

$$P = \beta_0 + \sum_{i=1}^5 \beta_a x_i + \sum_{i=1}^5 \sum_{j=i+1}^5 \beta_b (x_i \times x_j) + \sum_{i=1}^5 \beta_c x_i^2 \quad (7.80)$$

where the coefficient β_0 is the intercept, β_a are linear coefficients, β_b are coefficients on interaction terms, and β_c are quadratic coefficients on squared terms. Each model is fit to the full quadratic model (21 β terms).

Terms without statistically significant coefficients are retained in the models due to the desire to avoid arbitrary “over-fitting” our models to simulated data. The raw fitting results are presented in OPGEE as a data appendix, which includes statistical fit and significance results for each term.

After the model is fit, the fitted model is fed the independent variables from the test dataset and asked to predict the dependent variables from the test dataset. The results from these testing runs are shown as parity charts in Figure 7.38. A perfect statistical model would exactly predict the results of Aspen HYSYS, and all test points would fall along 45-degree parity line. With one exception, the resulting models have extremely high adjusted-R² values of ≈ 1, suggesting that these models accurately capture the physics and chemistry modeled in Aspen HYSYS. The mean absolute deviation (MAD) for each model equation is the mean of the absolute values of the differences between model and data, and gives a sense of the quantitative magnitude of error in kW. The case of DGA pump power has a lower quality fit ($R^2 = 0.954$) and some visible residual artifacts, but no quadratic model resulted in a better quality fit. For simplicity and consistency, we keep the same quadratic functional form for DGA pump power, despite this somewhat poorer fit.

7.19.2 TEG dehydration modeling using gas handbook methods

A schematic of the glycol dehydrator is shown in Figure 7.39.

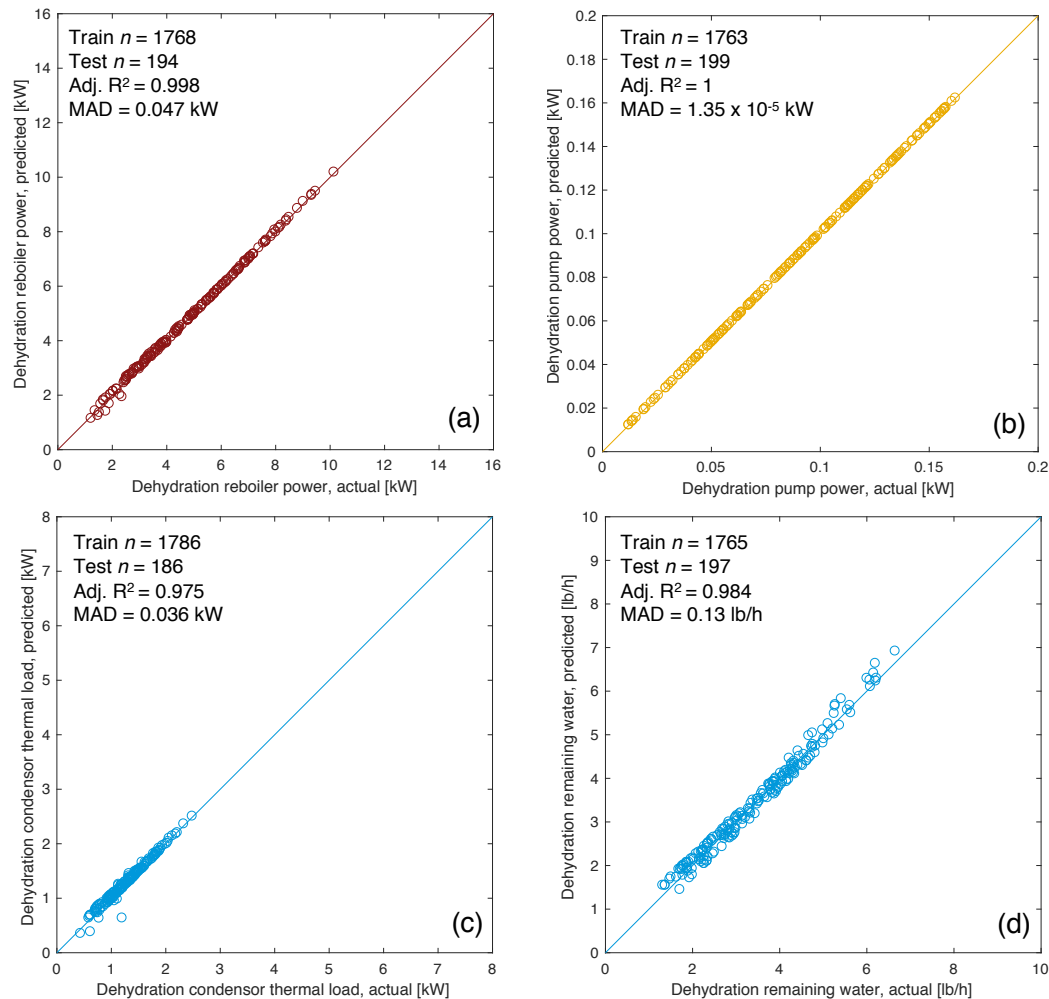


Figure 7.38: TEG dehydration energy use prediction parity chart. (a) Reboiler thermal inputs [kW]; (b) Pump work [kW]; (c) reflux condenser electrical load [kW]; (d) amine cooler thermal load [kW]. *x*-axis represents Aspen HYSYS simulation results, *y*-axis represents OPGEE statistical model predictions. MAD = mean absolute deviation.

The first step in the estimation of the TEG reboiler duty is the calculation of the rate of water removed using the assumed weight of water vapor in the inlet and exit gases as:

$$\Delta M_{w,rem} = M_{w,in} - M_{w,out} \quad \left[\frac{\text{lb H}_2\text{O}}{\text{MMscf}} \right] \quad (7.81)$$

*'Surface
Processing
2.2.2.1.3'*

where $\Delta M_{w,rem}$ = water removed [lb H₂O/MMscf]; $M_{w,in}$ = water in inlet gas [lb H₂O/MMscf]; $M_{w,out}$ = water in outlet gas [lb H₂O/MMscf]. The weights of water vapor in the inlet and exist gases are user inputs. The default values are 52 and 7 lb H₂O/MMscf, respectively [4, p. 160]. The weight of water removed is converted to rate of water removal ($\Delta Q_{w,rem}$) in lb H₂O/d by multiplying with the gas flow rate, MMscf/d.

The reboiler duty per weight of water removed is calculated as [4, p. 158]:

$$\Delta H_{GD} = 900 + 966 q_{TEG} \left(\frac{1}{10^6} \right) \quad \left[\frac{\text{MMBtu}}{\text{lb H}_2\text{O}} \right] \quad (7.82)$$

*'Surface
Processing
2.2.2.2.1'*

where ΔH_{GD} = specific reboiler heat duty [MMBtu/lb H₂O]; and q_{TEG} = TEG circulation rate [gal TEG/lb H₂O] removed. The heat duty is converted to MMBtu/d by multiplying by the rate of water removed, lb H₂O/d, as calculated in eq. (7.81).

The default TEG concentration assumed is 99 wt% [4, p. 155] and the default TEG circulation rate q_{TEG} is 2 gal TEG/lb H₂O removed [4, p. 147].

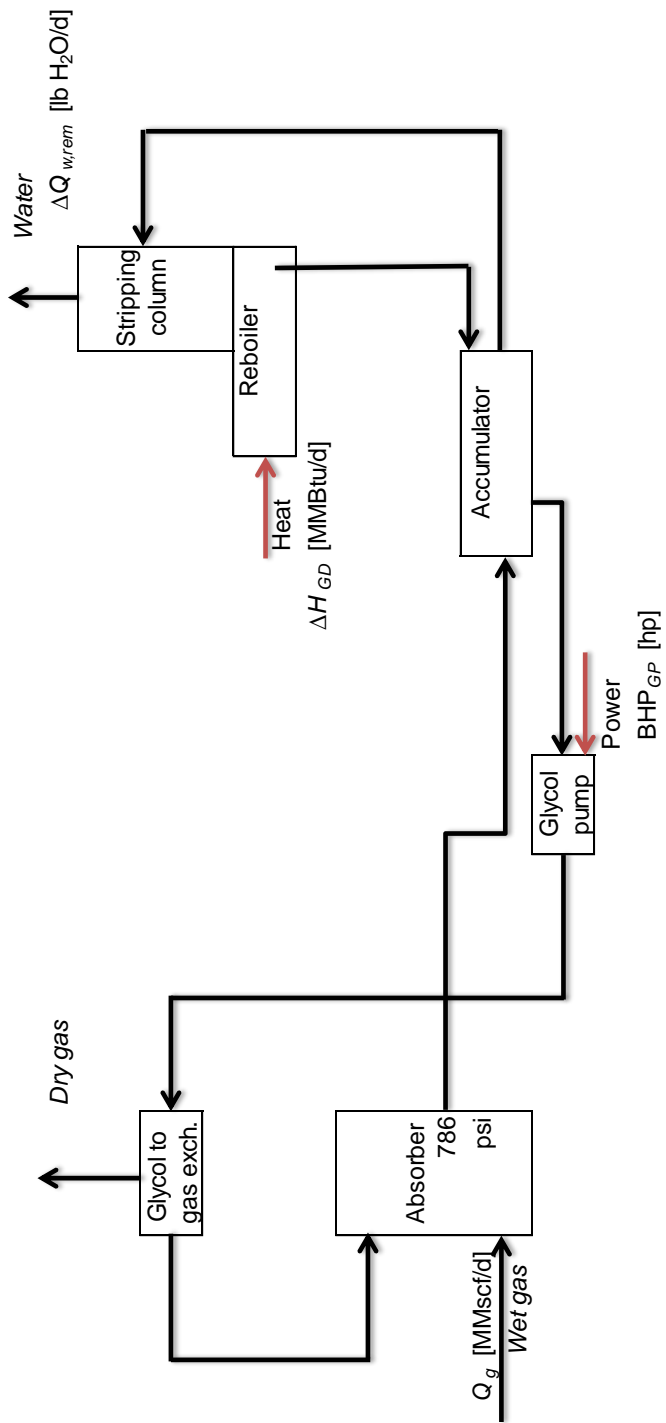


Figure 7.39: Glycol dehydrator simple process flow diagram [4, p. 141].

The glycol pump in the gas dehydration process is assumed to be electric by default. The horsepower is calculated using the conventional brake horsepower equation:

$$\text{BHP}_{TEG} = \frac{Q_{TEG} \cdot \Delta p}{1714\eta_{TEG}} \quad [\text{hp}] \quad (7.83)$$

*'Surface
Processing
2.2.2.3'*

where BHP_{TEG} = TEG pump brake horsepower [hp]; Q_{TEG} = TEG circulation rate [gpm]; Δp = pumping pressure [psi]; and η_{TEG} = TEG pump efficiency [-]. The pumping pressure is the difference between pump discharge and suction pressures. The default pump suction pressure is 0 psi. The TEG pump discharge pressure is equal to contactor operating pressure. The default contactor operating pressure is 786 psi [4, p. 160]. The TEG circulation rate in gpm is calculated as:

$$Q_{TEG} = q_{TEG} \Delta Q_{w,rem} \left(\frac{1}{24 \cdot 60} \right) \quad [\text{gpm}] \quad (7.84)$$

*'Surface
Processing
2.2.2.1.5'*

where q_{TEG} = TEG circulation rate [gal TEG/lb H₂O removed]; and $\Delta Q_{w,rem}$ = rate of water removal [lb H₂O/d]. The calculation of the rate of water removal is shown in eq. (7.81).

7.19.3 Defaults for surface processing

Defaults for surface operations are shown in Table 7.64.

Table 7.51: Default inputs for surface processing.

Param.	Description	Eq. no.	Default	Literature range	Unit	Sources	Notes
BHP_F	Fan brakehorse power	(7.93)	-	-	[hp]	[4, p. 118]	
BHP_{RP}	Reflux pump brakehorse power	(7.94)	-	-	[hp]	[4, p. 118]	
BHP_{BP}	Booster pump brakehorse power	(7.95)	-	-	[hp]	[4, p. 118]	
BHP_{CP}	Circulation pump brakehorse power	(7.96)	-	-	[hp]	[4, p. 118]	
BHP_{TEG}	TEG pump brakehorse power	(7.83)	-	-	[hp]	[9, p. 455]	
BHP_{RS}	Refrigeration brakehorse power	(7.98)	-	-	[hp]	[165]	
$C_{P_{\text{ho}}}$	Specific heat of oil	-	150	-	[Btu/bbl-°F]	[60, p. 136]	
C_{P_w}	Specific heat of water	-	350	-	[Btu/bbl-°F]	[60, p. 136]	
E_{tot}	Total electricity consumption	(7.57)	-	-	[Kwh/d]	[Kwh/d]	
$e_{s1} \dots e_{s4}$	Electricity consumption by stage	-	-	-	[-]	[60, p. 136]	a
e_j	Fraction of heat loss in unit j	-	0.02	-	[-]	[10]	
$e_{V,(N-1)}$	Fraction of volume loss in stage N – 1	-	var. 0.65	-	[-]	[-]	
η_P	Pump efficiency	-	0.4	-	[-]	[60, p. 136]	
$\lambda_{w,rem}$	Fraction of water removed below fire tube	-	Section 4.3.0.6	-	[scf/bbl]	[MMBtu/d]	
GOR	Gas-to-oil ratio	(7.90)	-	-	[MMBtu/d]	[4, p. 119]	
ΔH_R	Amine process reboiler heat duty	(7.82)	-	-	[MMBtu/d]	[4, p. 158]	
ΔH_{GD}	Glycol dehydrator reboiler heat duty	-	0	-	[MMBtu/d]	[165]	b
ΔH_{FR}	Fractionation reboiler heat duty	-	2.05	0.95-2.05	[gpm-d/100MMscf]	[4, p. 115]	
K	Amine solution K value	-	0.14	-	[-]	[60, p. 136]	
$\lambda_{w,ent}$	Fraction of water entrained in oil	-	2	-	[gal TEG/lb H ₂ O]	[4, p. 147]	
q_{TEG}	TEG circulation rate	-	786	-	[psi]	[4, p. 160]	
p_d	Pump discharge pressure	-	$Q_g \Delta M_{w,rem}$	-	[lb H ₂ O/d]	[4, p. 115]	
$\Delta Q_{w,rem}$	Rate of water removal	(7.91)	-	-	[gpm]	'Gas Balance'	
Q_{amine}	Amine flow rate	-	var.	-	[MMscf/d]	[60, p. 136]	
Q_{CO_2}	Volume of CO ₂ removed	(??)	-	-	[bbl/d]	'Gas Balance'	
$Q_{w,ent}$	Volume of entrained water	-	Section 7.16.1	-	[MMscf/d]	'Gas Balance'	
Q_F	Flaring volume	(7.89)	-	-	[MMscf/d]	'Gas Balance'	
Q_g	Inlet gas flow rate	-	var.	-	[MMscf/d]	'Gas Balance'	
Q_{H_2S}	Volume of H ₂ S removed	(??)	-	-	[bbl/d]	[60, p. 136]	
$Q_{w,heat}$	Volume of heated water	-	1500	-	[bbl/d]		
Q_o	Volume of oil production	-	-	-	-	-	

Continued on next page...

Continued from previous page

Param.	Description	Eq. no.	Default	Literature range	Unit	Sources	Notes
Q_{TEG}	TEG circulation rate in gpm	(7.84)	-	-	[gpm]		
Q_w	Volume of produced water	(7.58)	-	-	[bbl/d]		
$Q_{w1} \dots Q_{w4}$	Water feed by stage	(7.58)	-	-	[bbl water / d]		
ΔT_{CD}	Crude dehyd. temp. difference	-	75	-	[°F]	[60, p. 136]	
ΔT_S	Crude stabilizer temp. difference	-	224	-	[°F]	[60, p. 161, 163]	
$\Delta M_{w,rem}$	Weight of water removed	(7.81)	-	-	[lb H ₂ O /MMscf]		
$M_{w,in}$	Weight of water in inlet gas	-	52	-	[lb H ₂ O /MMscf]	[4, p. 160]	
$M_{w,out}$	Weight of water in outlet gas	-	7	-	[lb H ₂ O /MMscf]	[4, p. 160]	
WOR	Water-to-oil ratio	(4.5)	-	-	[bbl water / bbl oil]		
$Chiller_{IN}$	Temperature of feedstream entering chiller unit	-	59	-	[°F]		
$Chiller_{OUT}$	Temperature of feedstream exiting chiller unit	-	35	-	[°F]	[166]	
RH_{IN}	Temperature of feedstream entering Ryan-Holmes process	-	81	-	[°F]	[167]	
RH_{backup}	Usage rate of Ryan-Holmes backup engine	-	2.63	-	[hrs/d]	[167]	

a - This is a user input. No defaults are available for most of the treatment technologies. The default for wetlands (CWL) where volume losses are significant is 26% [10].*b* - It is assumed that heat exchange with the inlet stream provides the heat duty.*c* - The default is monothanolamine (MEA).

7.20 Acid gas removal

A major element of associated gas treatment is acid gas removal (AGR). Associated gas from petroleum may naturally contain CO₂ and H₂S, which are acidic gases. Their concentrations are limited by regulations and thus they must be removed if necessary [168, p. 211-213].

In addition to containing naturally-occurring acid gases, associated gas may contain additional CO₂ injected during carbon dioxide enhanced oil recovery operations. In the period immediately following commencement of carbon dioxide flooding, the produced fluids will not contain any additional, non-native carbon dioxide. But as CO₂ mixes with the reservoir fluids and proceeds away from injector wells it will eventually begin to be produced along with the other reservoir fluids. Associated gas from a mature CO₂ flood project may contain very high levels of carbon dioxide. An example of this process is provided by the flood at the SACROC unit in Texas' Permian Basin, which commenced in 1972. Based on the specifications of the initial acid gas processing units installed in 1973 and 1974, the associated gas contained approximately 24% CO₂. The CO₂ content of the associated gas stream rose to 40% twelve years after carbon dioxide flooding began [169]. By 2002 the carbon dioxide content had risen to 85% [170].

The large variation in the percentage of CO₂ and the overall volume of gas over the course of a carbon dioxide enhanced recovery project may require modifications to the separation process. The initial SACROC gas treatment facilities used monoethanolamine or potassium carbonate chemical separation processes [170]. As CO₂ percentage and gas volumes increased, the operators adopted a dual treatment process that added filtration through a selectively permeable membrane in addition to the chemical separation unit [169].

Besides chemical-based and membrane separation technologies, a refrigerated distillation method known as the Ryan-Holmes process is another means of removing CO₂ from associated gas streams. OPGEE incorporates three different acid gas separation modules: an amine-based process, a membrane-amine dual process, and the Ryan-Holmes refrigerative process.

The second step after the separation of individual phases is the treatment of associated gas. Treatment of associated gas starts with acid gas removal (AGR, also called gas sweetening). There are more than 30 natural gas sweetening processes. OPGEE assumes that the amine process is used. The batch and amine processes are used for over 90% of all onshore wellhead applications with amines being preferred when lower operating costs justifies the higher equipment cost. The chemical cost of batch processes may be prohibitive [4, p. 99].

Two methods of modeling AGR units are used in OPGEE: (1) A method based on statistical analysis of results from process simulation software; and (2) A method based on methods from gas processing handbook. We strongly recommend use of method (1), while method (2) remains in OPGEE v3.0a primarily in order to maintain backward compatibility with earlier versions of OPGEE.

The streams flowing into and out of the acid gas removal process are shown in Figure 7.40 and are listed in Table 7.52.

Table 7.52: Streams flowing into and out of the acid gas removal process. I/O denotes input or output stream

Flow name	Stream	I/O	Source/Destination	Units	Notes
Dehydrated gas to AGR	36	I	Glycol dehydration	[t/d]	
Hydrocarbon rich gas to AGR	64	I	CO ₂ membrane	[t/d]	
Fuel gas - Dehydrator	152	I	Fuel gas system	[t/d]	
Electricity - Dehydrator	177	I	Electricity generation and imports	[MWh/d]	
Gas to demethanizer	37	O	Demethanizer	[t/d]	
AGR CO ₂ to reinjection	73	O	CO ₂ reinjection compressor	[t/d]	
AGR venting and fugitives	256	O	Atmosphere	[t/d]	

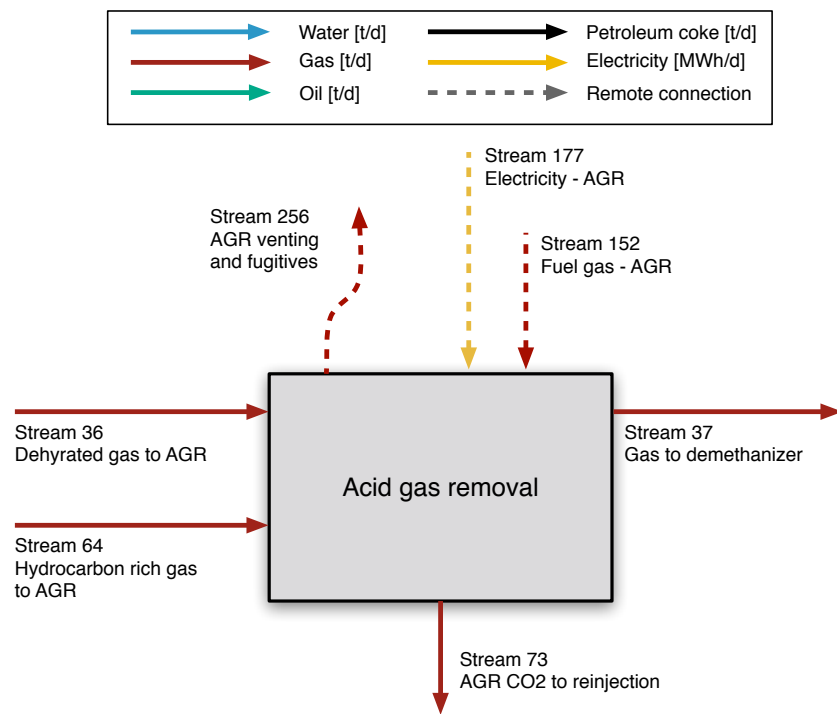


Figure 7.40: Streams flowing into and out of the acid gas removal process. All streams measured in tonnes per day excepting electricity which is measured in MWh/d.

7.20.1 AGR modeling using result from process simulation software

In order to generate accurate results for AGR energy consumption under a wide variety of operating conditions, commercial chemical process simulation software is used to simulate thousands of operating conditions, and statistical models are fit to the results. The resulting statistical models allow OPGEE to predict the results of chemical engineering software without the expense and challenge of running full AGR system simulations. OPGEE v3.0a uses Aspen HYSYS v.8.8, a commercial chemical simulation software, to model a total of 5 different AGR systems with differing solvents and solvent loadings [5].

AGR systems were modeled in Aspen HYSYS starting with default AGR template flowsheets. Some minor modifications to the default AGR flowsheet were made where necessary (described below). The AGR flowsheets used in Aspen HYSYS are generally modeled using the same connection patterns for absorption columns, regeneration units, pumps, and coolers. The major difference between AGR units is the selection of an alkanolamine to be used in the absorption columns. OPGEE v3.0a allows users to select one of five different amines for the AGR process:

- Diethanolamine (DEA) (30% wt.)
- Diethanolamine (DEA) High Load (35% wt.)
- Methyl-diethanolamine (MDEA)
- Diglycolamine (DGA)
- Monoethanolamine (MEA)

Most of these amines utilize the same process flowsheet in Aspen HYSYS. Figure 7.41 shows the process flowsheet in Aspen HYSYS for the DGE, DEA, DEA High Load, and MDEA simulations. The process flowsheet used in Aspen HYSYS for the MEA system is very similar to the flowsheet utilized by the other amines. The only difference is the addition of a second makeup unit that inputs a pure water stream into the absorber unit along with the lean amine coming from the primary makeup unit. Simulations of MEA-based systems without this secondary makeup system often fail to converge. Figure 7.42 illustrates the process flowsheet in Aspen HYSYS for an AGR unit that utilizes MEA.

The primary differences in the AGR solvent choices in OPGEE result from differing work of regeneration and differing usefulness for certain acid gas species. DEA is the most commonly used amine in current hydrocarbon processing, and therefore is the OPGEE default [4]. High-load DEA is favored when the partial pressures of acid gas are high. MDEA is favored in situations where recovery of H₂S is desired. DGA is very suitable for cold climates. MEA is a traditional choice in gas processing applications but has fallen out of favor due to its high corrosive potential and high regeneration energy requirements. It is still used in cases with dilute acid gas streams (i.e. low partial pressure) [4].

The flowsheets for all five AGR options contain the same fundamental units: an absorption unit and a regeneration unit. The absorption unit consists of an absorption tower and a separator. The absorption tower utilizes counter-current

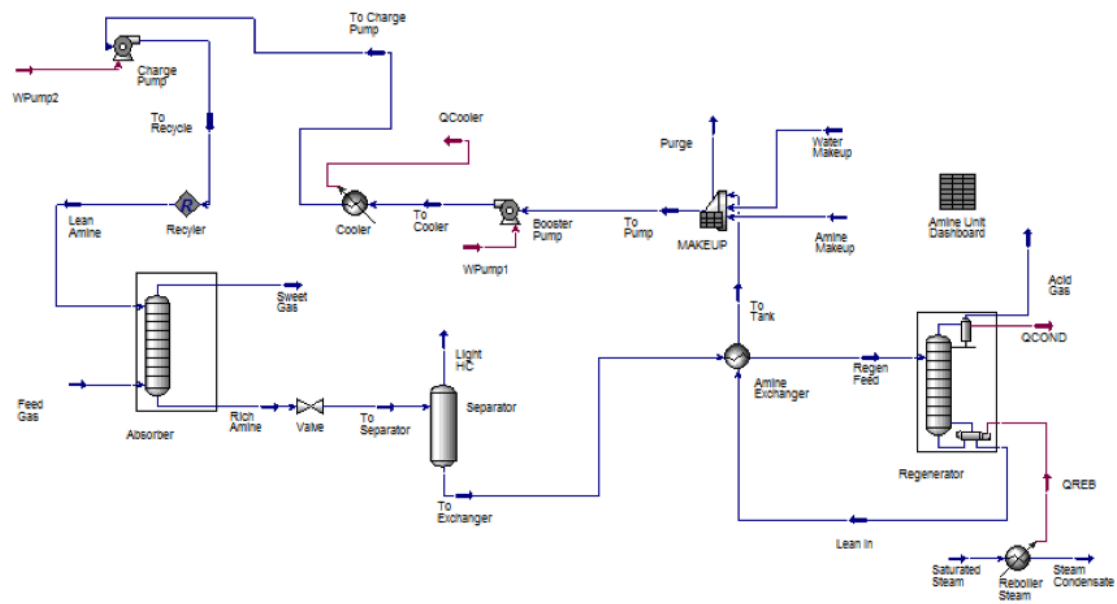


Figure 7.41: Amine process flow diagram from Aspen HYSYS as used in modeling DGA, DEA, DEA-High-Load, and MDEA [5].

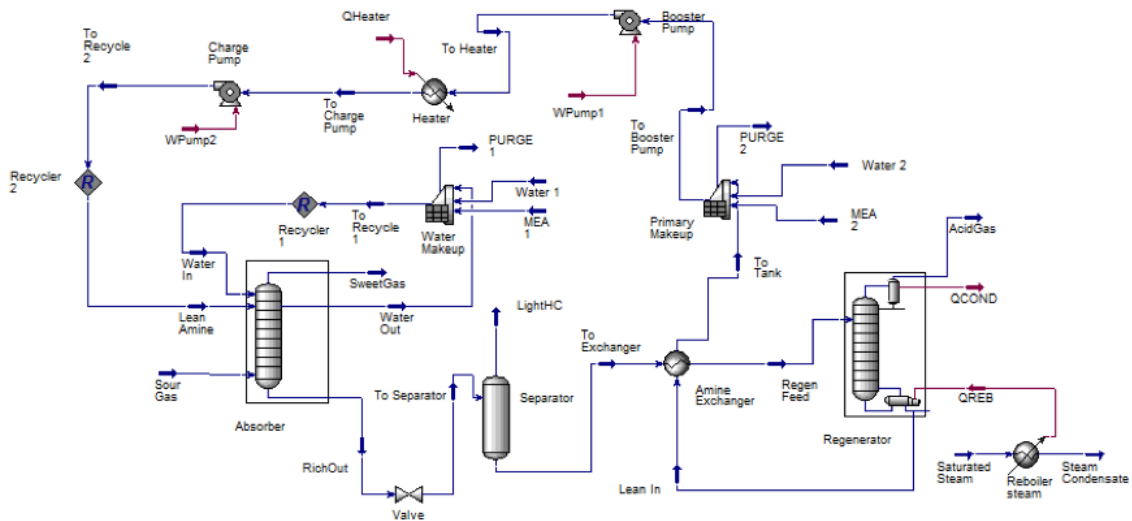


Figure 7.42: Amine process flow diagram from Aspen HYSYS as used in modeling MEA [5].

Table 7.53: Settings for non-varying operating parameters in Aspen HYSYS AGR unit simulations.
Source “def.” is OPGEE assumed default from prior model versions.

Process unit	Parameter	Value	Unit	Source	Notes
Absorber	Stages	20	[-]		
Absorber	Operating Pressure	364.7	psia	def.	
Absorber	Acid Gas Temperature	90	°F	[4]	<i>a</i>
Absorber	Lean Amine Temperature	105.2	°F	[4]	<i>b</i>
Absorber	Lean Amine Pressure	414.7	psia	[4]	<i>c</i>
Absorber	Acid Gas Flow Rate	1.0897	MMscf/d	def.	
Regenerator	Stages	20	[-]		
Regenerator	Booster Pump Discharge	50	psia	[4]	
Regenerator	Charge Pump Discharge	414.7	psia	[4]	<i>c</i>

a - Sweet gas temperature is 15-30 °F higher than acid gas temperature and/or 0-15 °F above lean amine temperature

b - Lean amine temperature is 100 ? 130 °F.

c - Lean amine pressure is 50 psi over absorber operating pressure

flow of amine solution against the acid gas, allowing reaction with CO₂ and H₂S with amines. The adsorption tower is modeled in Aspen HYSYS using sufficient number of theoretical trays to ensure converged simulations. From the absorption unit, two products are generated: sweetened gas and a rich amine solution loaded with CO₂ and H₂S. The sweetened gas is exported as product from the process, and the rich amine solution is circulated to the regeneration unit. After leaving the absorption unit the rich amine solution enters a separator which removes any residual gases carryover, preventing gas-phase H₂S and CO₂ from contaminating downstream systems.

The regeneration unit includes the heat exchanger, still, condenser, reboiler, primary make-up unit, cooler, and pumps. The rich amine is pre-heated using a heat exchanger crossed with outgoing hot-lean amine leaving the regeneration column. In the reboiler, acid gases are driven from the rich amine as it passes through the regeneration tower. The condenser cools the overhead stream of H₂S, CO₂, water vapor, and amine vapor, returning condensed water and amine back to the regeneration column. The lean amine is then supplemented by the amine makeup unit. Pumps and a cooler bring the lean amine back to the absorption tower at a specified temperature and pressure to be used again.

We use Aspen HYSYS to run thousands of cases for each amine across 5 different independent variables:

1. Carbon dioxide concentration [mol. fraction] (x_1)
2. Hydrogen sulfide concentration [mol. fraction] (presented as x_2 in equations and tables below)
3. Reflux ratio of the regeneration system [-] (x_3)
4. Temperature of regeneration feed from the heat exchanger into the still tower [°F] (x_4)
5. Pressure of the acid gas entering the absorption tower [psi] (x_5).

Settings for other non-varying operating parameters are given in Table 7.53. In the simulation, the temperature of the sweet gas is identical to the lean amine

Table 7.54: Ranges of independent variables explored in generating predictive equations for AGR energy use. DEA-HL = DEA-high-load

Variable	MEA	DGA	DEA	DEA-HL	MDEA
Reflux ratio [-]	1.5 – 3.0	1.5 – 3.0	1.5 – 3.0	1.5 – 3.0	6.5 – 8.0
Regen. feed temp. [°F]	190 – 220	190 – 220	190 – 220	190 – 220	190 – 220
Feed gas pressure [psia]	14.7 – 514.7	14.7 – 514.7	14.7 – 514.7	14.7 – 514.7	14.7 – 514.7
Amine loading [wt.%]	20	60	30	35	50
Amine circ. rate ^a	Var.	Var.	Var.	Var.	Var.
H ₂ S conc. [mol.%]	1 – 20	1 – 20	1 – 20	1 – 20	1 – 20
CO ₂ conc. [mol.%]	1 – 15	1 – 15	1 – 15	1 – 15	1 – 15

^a - Amine circulation rate is dependent on the concentration of the acid gas. The starting value is acquired from Manning and Thompson [4] based on the acid gas composition, and Aspen HYSYS varies the circulation rate to achieve convergence.

temperature; therefore, the acid gas temperature is selected to be 90 °F, since the sweet gas temperature is at least 15 °F hotter than the acid gas temperature. In OPGEE, the operating pressure of the absorber is 364.7 psia, so the 414.7 psia is selected as the lean amine pressure because the lean amine pressure is generally set 50 psi over the absorber pressure. Each unit has 20 separation trays to allow separation to achieve H₂S constraints. It was determined that the number of trays has a negligible effect on the total energy cost after the value is large enough to ensure convergence, so it is not considered as a decision variable in the linear models.

The independent variables are varied over ranges that are reasonable for the solvent of choice. The ranges of independent variables chosen are listed in Table 7.54.

As different mole fractions H₂S and CO₂ are explored, the remaining species are scaled proportionately by the OPGEE default molar ratios after removing N₂: 6.12% CO₂, 1.02% H₂S, 85.72% CH₄, 4.08% C₂H₆, 2.04 % C₃H₈, 1.02% C₄H₁₀.

The sampling strategy used combines deterministic and random sampling across our five independent variables x_1 to x_5 . Within each amine case, 16 different gas compositions are modeled, as the cross product of 4 H₂S concentrations (1 mol%, 5 mol%, 10 mol% and 20 mol%) and 4 CO₂ concentrations ((1 mol%, 5 mol%, 10 mol% and 15 mol%). For each gas composition, deterministic sampling is performed using Box-Behnken sampling across the remaining three variables (reflux ratio, regenerator feed temperature, and feed gas pressure). Box-Behnken sampling is a deterministic sampling strategy that explores a central point and extremal points in high variable space (e.g., corners and faces of high-dimensional variable bounds). Box-Behnken sampling returns 13 combinations of variables. Additionally, a random sampling of 100 additional points for each amine and gas composition is also performed using latin hypercube sampling methodology. Thus, per gas composition we have 113 samples, or 1808 samples for each amine. Therefore a total of \approx 9000 simulations of AGR systems were performed across all amine systems. All samples are generated using MATLAB [164] and run in bulk through Aspen HYSYS.

All points are required to meet the sweet gas specification of 4 ppmv H₂S in order to have a converged result (CO₂ concentrations are reduced to very low values in meeting this H₂S specification). For some solvents, all possible combinations did not converge, resulting in a smaller number of sample points.

A total of five outputs (dependent variables) for each run are recorded. These include (1) reboiler thermal load [kW], (2) booster pump horsepower [hp], (3)

charge pump horsepower [hp], (4) reflux condenser thermal load [kW], and (5) amine cooler thermal load [kW]. Additionally mole fractions of CO₂ and H₂S in sweet gas product stream are recorded for each simulation to ensure constraints are met.

Using these results, predictive equations are generated using MATLAB curve fitting toolbox [164]. A set of four predictive equations were generated for each amine. These equations predict (1) reboiler heat input, (2) total pump work (sum of booster and charge pumps), (3) reboiler reflux condenser cooling thermal load, and (4) amine cooling thermal load. Each dataset (i.e., for each amine) is split into a training dataset and a testing dataset. The testing set is a randomly selected subset of ≈10% of the observations which is removed from the dataset and held aside (i.e., not used to generate the statistical fit). The training set includes the remainder of the results (≈%90% of simulation runs). The training and testing sets are drawn independently for each predictive equation. Each training dataset is fitted to a quadratic equation of all five independent variables. The quadratic equation includes all linear terms, interaction terms, and square terms. The quadratic model fits are of the general form:

$$P = \beta_0 + \sum_{i=1}^5 \beta_a x_i + \sum_{i=1}^5 \sum_{j=i+1}^5 \beta_b (x_i \times x_j) + \sum_{i=1}^5 \beta_c x_i^2 \quad (7.85)$$

where the coefficient β_0 is the intercept, β_a are linear coefficients, β_b are coefficients on interaction terms, and β_c are quadratic coefficients on squared terms. Each model is fit to the full quadratic model (21 β terms).

Terms without statistically significant coefficients are retained in the models due to the desire to avoid arbitrary “over-fitting” our models to simulated data. The raw fitting results are presented in OPGEE as a data appendix, which includes statistical fit and significance results for each term.

After the model is fit, the fitted model is fed the independent variables from the test dataset and asked to predict the dependent variables from the test dataset. The results from these testing runs are shown as parity charts in Figures 7.43 to 7.47. A perfect statistical model would exactly predict the results of Aspen HYSYS, and all test points would fall along 45-degree parity line. With one exception, the resulting models have extremely high adjusted-R² values of ≈ 1, suggesting that these models accurately capture the physics and chemistry modeled in Aspen HYSYS. The mean absolute deviation (MAD) for each model equation is the mean of the absolute values of the differences between model and data, and gives a sense of the quantitative magnitude of error in kW. The case of DGA pump power has a lower quality fit ($R^2 = 0.954$) and some visible residual artifacts, but no quadratic model resulted in a better quality fit. For simplicity and consistency, we keep the same quadratic functional form for DGA pump power, despite this somewhat poorer fit.

The model coefficients are included in predictive equations in OPGEE. .

'Acid Gas Removal 4.1'

'Acid Gas Removal 1.2.9'

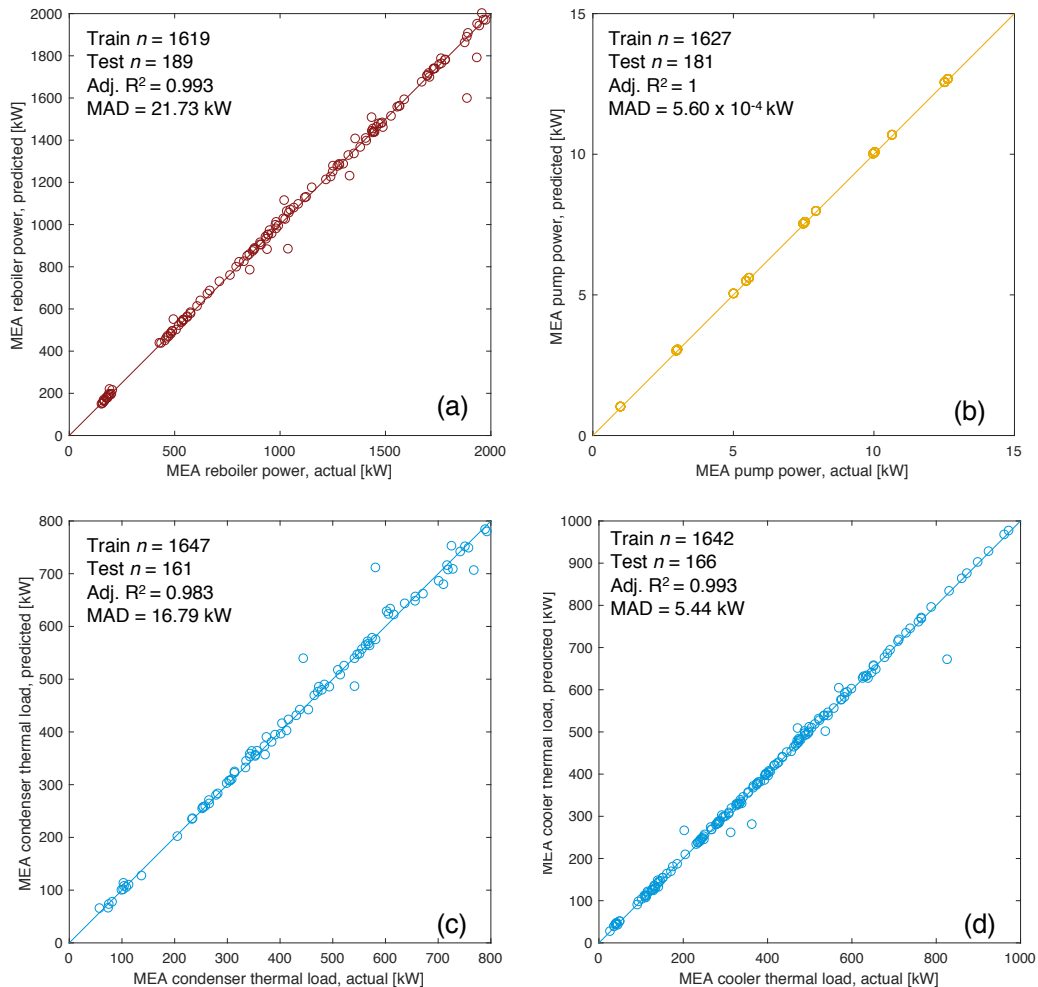


Figure 7.43: MEA-based AGR energy use prediction parity chart. (a) Reboiler thermal inputs [kW]; (b) Total pump work (charge+booster) [kW]; (c) reflux condenser thermal load [kW]; (d) amine cooler thermal load [kW]. x-axis represents Aspen HYSYS simulation results, y-axis represents OPGEE statistical model predictions. MAD = mean absolute deviation.

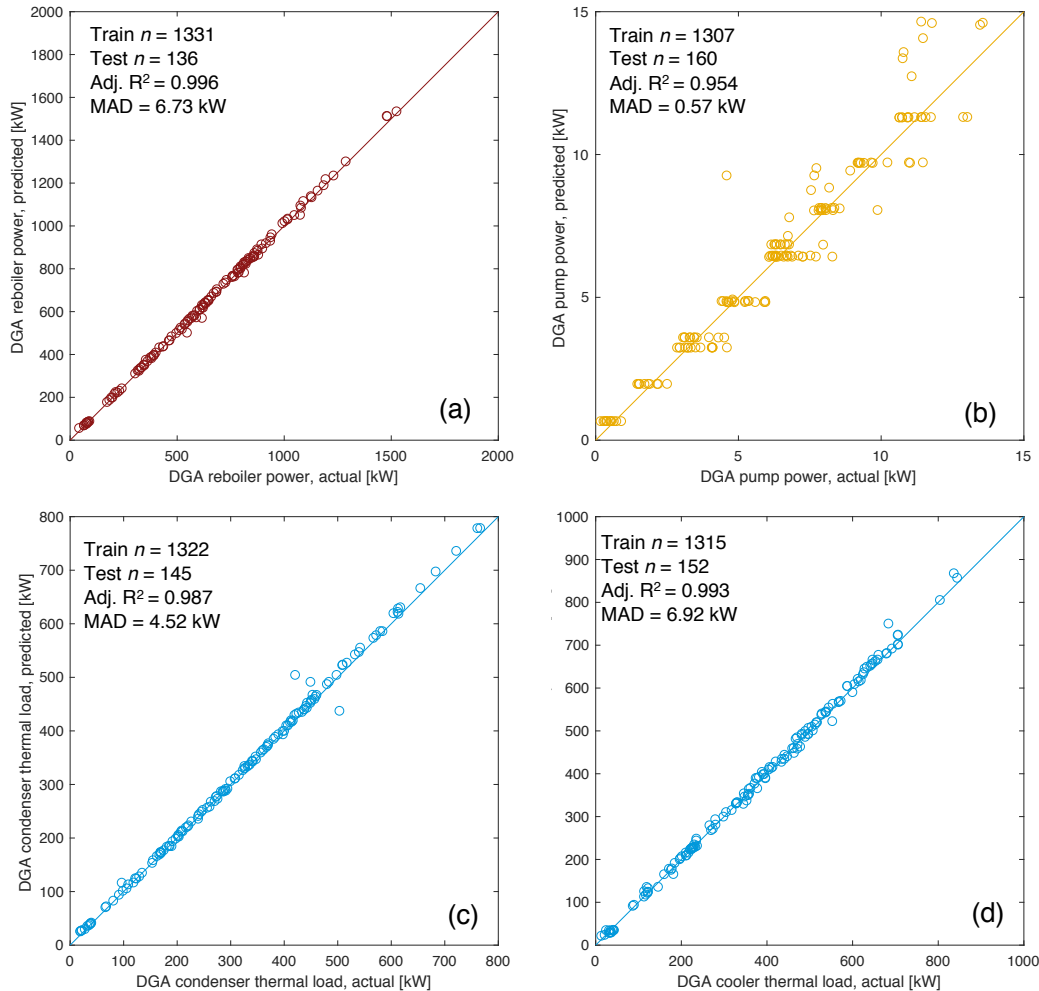


Figure 7.44: DGA-based AGR energy use prediction parity chart. (a) Reboiler thermal inputs [kW]; (b) Total pump work (charge+booster) [kW]; (c) reflux condenser thermal load [kW]; (d) amine cooler thermal load [kW]. *x*-axis represents Aspen HYSYS simulation results, *y*-axis represents OPGEE statistical model predictions. MAD = mean absolute deviation.

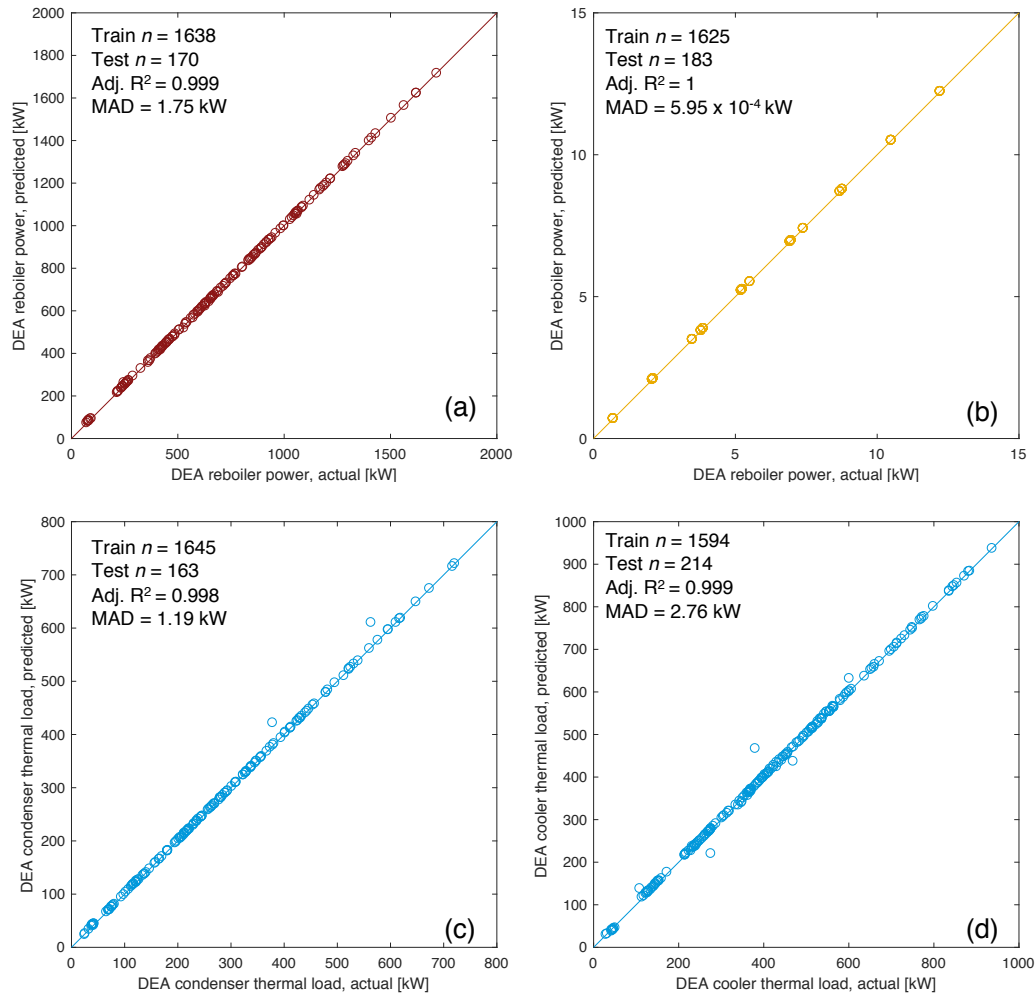


Figure 7.45: DEA-based AGR energy use prediction parity chart. (a) Reboiler thermal inputs [kW]; (b) Total pump work (charge+booster) [kW]; (c) reflux condenser thermal load [kW]; (d) amine cooler thermal load [kW]. x -axis represents Aspen HYSYS simulation results, y -axis represents OPGEE statistical model predictions. MAD = mean absolute deviation.

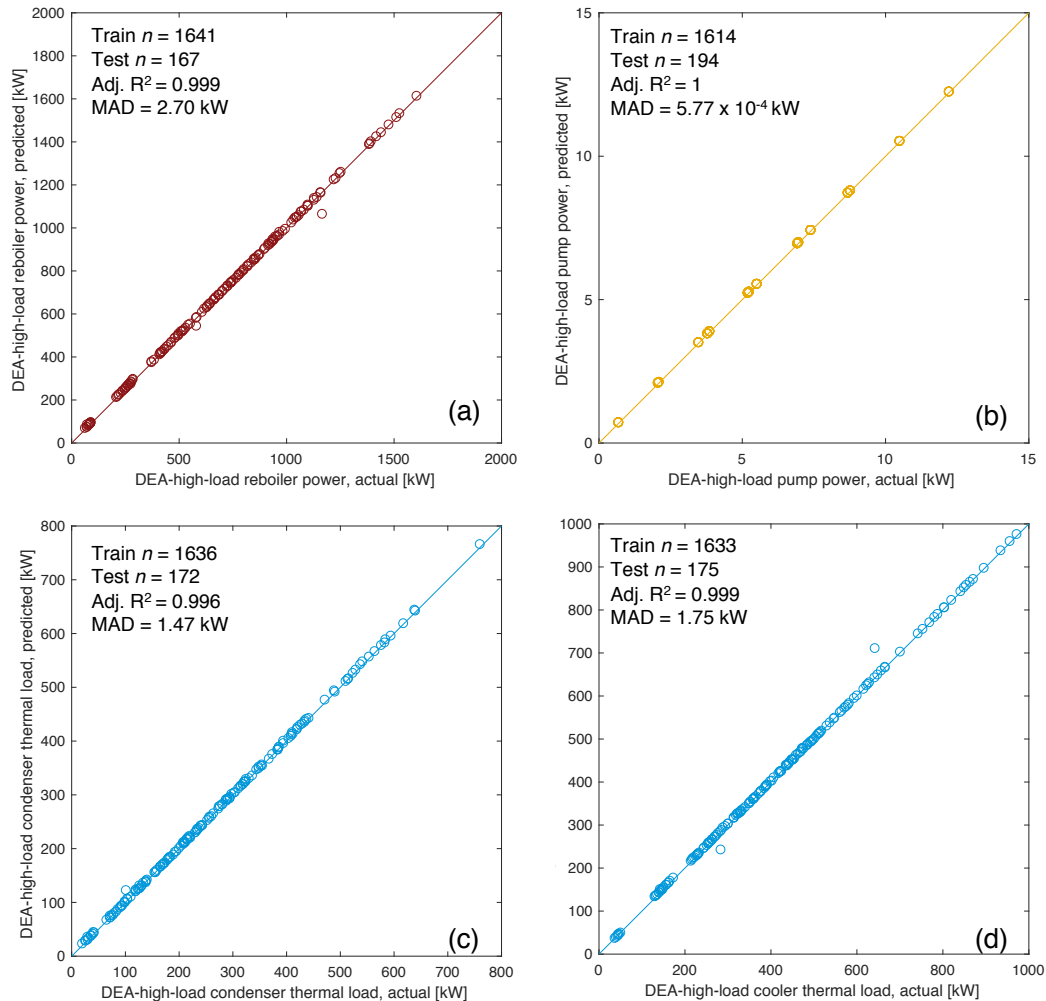


Figure 7.46: DEA-high-load-based AGR energy use prediction parity chart. (a) Reboiler thermal inputs [kW]; (b) Total pump work (charge+booster) [kW]; (c) reflux condenser thermal load [kW]; (d) amine cooler thermal load [kW]. *x*-axis represents Aspen HYSYS simulation results, *y*-axis represents OPGEE statistical model predictions. MAD = mean absolute deviation.

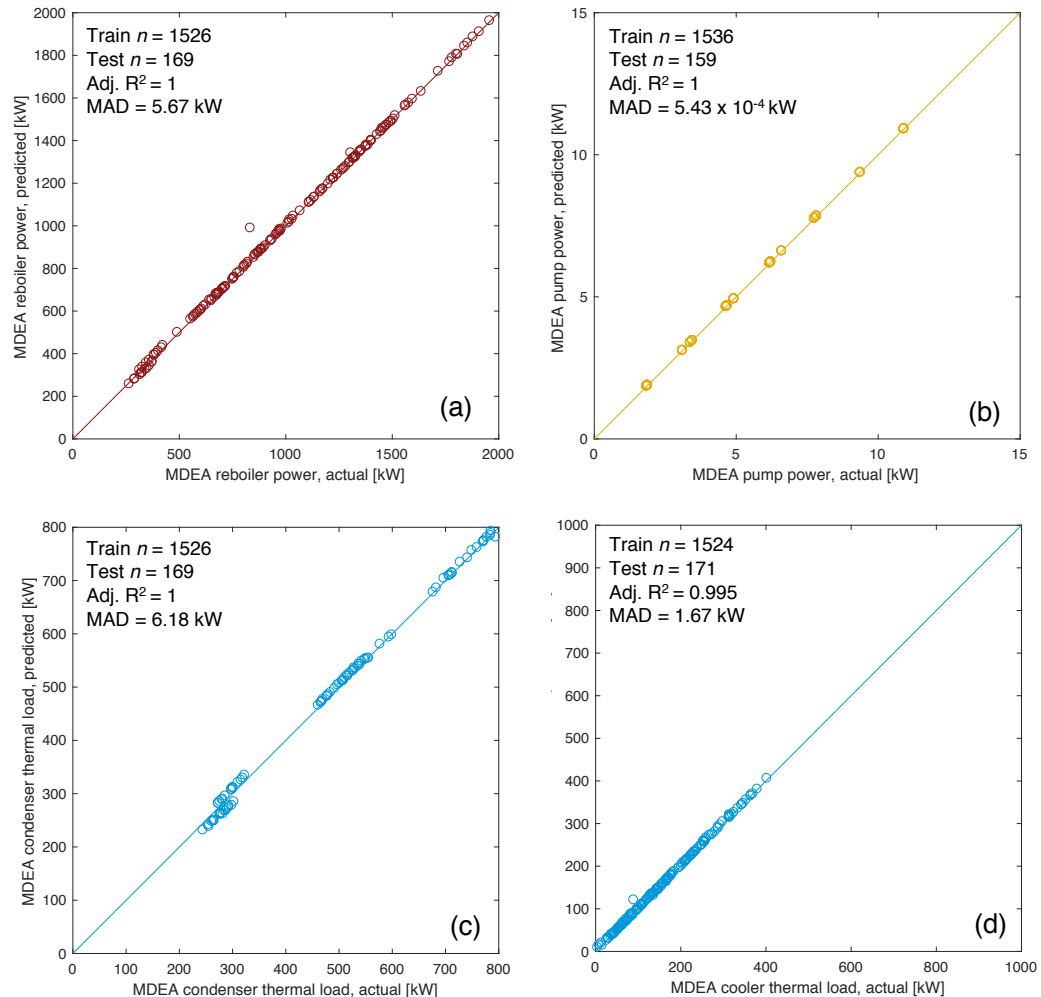


Figure 7.47: MDEA-based AGR energy use prediction parity chart. (a) Reboiler thermal inputs [kW]; (b) Total pump work (charge+booster) [kW]; (c) reflux condenser thermal load [kW]; (d) amine cooler thermal load [kW]. *x*-axis represents Aspen HYSYS simulation results, *y*-axis represents OPGEE statistical model predictions. MAD = mean absolute deviation.

Estimated thermal load for the reboiler is increased by a factor of 1.25 to account for boiler inefficiencies. Pump work is converted directly from reported kW in predictive equations.

Estimating the work of cooling systems from Aspen HYSYS outputs requires more effort. The two cooling loads for reflux condenser and amine cooler are presented by Aspen HYSYS as thermal loads to be removed from hot streams, in kW thermal load. We model cooling as performed via forced-draft air-cooled heat exchangers [4, 56]. The method from the Gas Processors Supplier's Association (GPSA) electronic databook is used to estimate blower electrical load. The load on fan in brake horsepower (bhp) is given as [56, p. 10-17]:

$$bhp = \frac{ACFM \times PF}{6356 \times 0.7 \times 0.92} \quad (7.86)$$

where $ACFM$ is the actual cubic feet per minute of air flow over the exchangers [ft.^3 per min], PF is the total fan back-pressure [in. H_2O], 6356 is a conversion factor from inches of water back pressure to horsepower, and 0.7 represents 70% fan efficiency. Additionally, the factor of 0.92 represents the efficiency of the motor-to-fan speed reducer.

For this work, air-cooler pressure drop is chosen to be conservative value of 0.6 in. of water. Detailed methods are available in GPSA handbook to compute pressure drop from heat exchanger geometry and surface area, as well as tube and fin geometry [56, Ch. 10]. $ACFM$ is estimated using the formula:

$$ACFM = \frac{W_a}{D \times 60 \times 0.0749} \quad [\text{ft}^3/\text{min}] \quad (7.87)$$

Where W_a is the air quantity in lbs. air, D is a air-density correction factor, and 60 and 0.0749 are conversion factors [56, p. 10-16]. OPGEE assumes standard conditions (70°F), so $D=1$. The quantity of air needed for heat exchange is equal to:

$$W_a = \frac{Q}{0.24 \times \Delta T_a} \quad [\text{lb}/\text{h}] \quad (7.88)$$

where Q is the thermal load (Btu/h), 0.24 is a conversion factor, and ΔT_a is the temperature increase of cooling air across the heat exchanger. OPGEE assumes for simplicity that $\Delta T_a = 40^\circ\text{F}$, while users can consult GPSA handbook for detailed methods of computing ΔT_a given geometry and temperatures of streams [56, Ch. 10].

7.20.2 AGR modeling using gas handbook methods

This method uses AGR modeling methods from a well-known gas processing handbook [4]. The user is advised to preferentially use the above method based on process simulation software.

In the amine process an aqueous *alkanolamine* solution is regenerated and used to remove large amounts of sulfur and CO_2 when needed. The model scheme allows the user to choose between the commonly used amine solutions (MEA, DEA, DGA, etc.). Each amine solution is characterized by a K value which is inversely proportional to both the acid gas removal rate (pick up) and amine concentration [4, p. 115]. When choosing an "other" amine solution, the user must enter a K

'Acid Gas Removal 1.2.8'
'Acid Gas Removal 2.1.8'

value. The default contactor operating pressure is the median value of the pressures reported in the calculation of the contact tower diameter [171] [4, p. 117]. A schematic of the amine process is shown in Figure 7.48. The user has the option of turning OFF the AGR unit in the gas processing scheme.

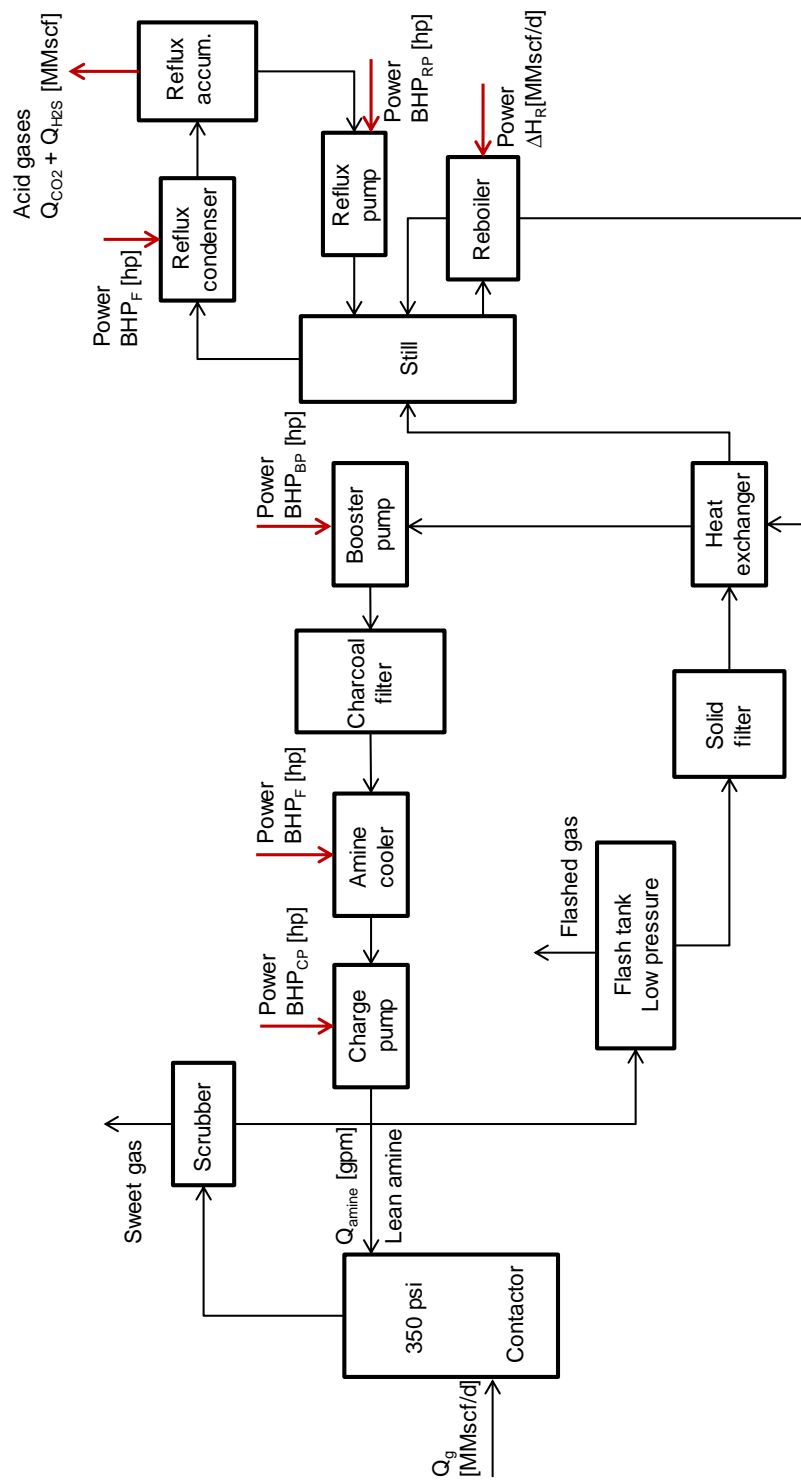


Figure 7.48: Amine simple process flow diagram [4, p. 112].

The inlet gas flow rate of the gas processing stage in the gas balance (see '*Gas Balance*' worksheet) is calculated as:

$$Q_g = Q_o \cdot \text{GOR} \left(\frac{1}{10^6} \right) - Q_F \quad \left[\frac{\text{MMscf}}{\text{d}} \right] \quad (7.89)$$

'Surface Processing 2.2.1 Figure'

where Q_g = inlet gas flow rate [MMscf/d]; Q_o = rate of oil production [bbl/d]; Q_F = flaring rate [MMscf/d]; and GOR = gas-to-oil ratio [scf/bbl]. The inlet gas flow rate is used in the calculation of the amine circulation rate in eq. (7.91). Although the accumulation of gases to flare likely occurs at various points throughout the process, OPGEE assumes that the gas flared is removed before gas processing occurs. This allows for OPGEE to account for "early field production" or production in locations without a gas market. For these situations, no surface processing exists and all produced gas is flared.

The amine reboiler in OPGEE is a direct fired heater that uses natural gas. The reboiler duty is: (i) the heat to bring the acid amine solution to the boiling point, (ii) the heat to break the chemical bonds between the amine and acid gases, (iii) the heat to vaporize the reflux, (iv) the heat load for the makeup water, and (v) the heat losses from the reboiler and still [4, p. 117].

The heat duty of the amine reboiler can be estimated from the circulation rate of the amine solution as [4, p. 119—originally Jones and Perry, 1973]:

$$\Delta H_R = \frac{24 \cdot 72000 \cdot Q_{\text{amine}}}{10^6} 1.15 \quad \left[\frac{\text{MMBtu}}{\text{d}} \right] \quad (7.90)$$

'Surface Processing 2.2.1.4'

where ΔH_R = heat duty [MMBtu/d]; and Q_{amine} = amine flow rate [gpm]. A gallon of amine solution requires approximately 72000 Btu for regeneration [172]. A safety factor of 15% is added for start up heat losses and other inefficiencies. The flow rate of the amine solution can be estimated using the following equation [4, p. 115]:

$$Q_{\text{amine}} = 100 K(Q_{H_2S} + Q_{CO_2}) \quad [\text{gpm}] \quad (7.91)$$

'Surface Processing 2.2.1.1'

where Q_{amine} = amine flow rate [gpm]; K = amine solution K value [gpm-d/100MMscf]; Q_{H_2S} = H_2S removal [MMscf/d]; and Q_{CO_2} = CO_2 venting from AGR unit [MMscf/d]. The venting of CO_2 from the AGR unit is calculated in the '*Gas Balance*' worksheet. The rate of H_2S removal is calculated as:

$$Q_{H_2S} = x_{H_2S} \cdot Q_g \quad \left[\frac{\text{MMscf}}{\text{d}} \right] \quad (7.92)$$

where x_{H_2S} = molar fraction of H_2S [-]; and Q_g = inlet gas flow rate [MMscf/d]. The calculation of the inlet gas flow rate is shown in eq. (7.89). The molar fraction of H_2S is determined from the composition of associated gas.

In OPGEE all H_2S remaining in the associated gas is removed in the AGR unit. Removed H_2S is calculated in eq. (7.92) by multiplying the inlet gas flow rate with the molar percent of H_2S . Also all the CO_2 removed is vented and that is calculated in the '*Gas Balance*' worksheet.

Other equipment in the amine regeneration system that consume power and energy include the reflux condenser and the amine cooler. There also are reflux, booster, and circulation pumps. The reflux condenser and the amine cooler are air-cooled, forced-draft heat exchangers. In OPGEE both services are combined into one structure with a common fan.

The motor size of the amine cooler fan can be estimated from the amine circulation rate as [4, p. 118]:

$$\text{BHP}_F = 0.36 \cdot Q_{\text{amine}} \quad [\text{hp}] \quad (7.93)$$

'Surface
Processing
2.2.1.3.1'

where BHP_F = fan brake horsepower [hp]; and Q_{amine} = amine circulation rate [gpm].

The heat duty of the reflux condenser is approximately twice the heat duty of the amine cooler [4, p. 117]. Therefore the motor size of the 'common' fan is estimated by multiplying the brake horsepower of the amine cooler by 3.

Similarly motor sizes of pumps can also be estimated from the amine circulation rate as [4, p. 118]:

$$\text{BHP}_{RP} = 0.06 \cdot Q_{\text{amine}} \quad [\text{hp}] \quad (7.94)$$

'Surface
Processing
2.2.1.2'

$$\text{BHP}_{BP} = 0.06 \cdot Q_{\text{amine}} \quad [\text{hp}] \quad (7.95)$$

$$\text{BHP}_{CP} = 0.00065 \cdot Q_{\text{amine}} \cdot p_d \quad [\text{hp}] \quad (7.96)$$

where BHP_{RP} = reflux pump brake horsepower [hp]; BHP_{BP} = booster pump brake horsepower [hp]; BHP_{CP} = circulation pump brake horsepower [hp]; and p_d = pump discharge pressure [psi]. The circulation pump discharge pressure = 50 psi over contactor operating pressure [4, p. 121]. The default contactor operating pressure as mentioned earlier is 350 psi.

7.20.3 Gas desulfurization modeling using result from process simulation software

Sulfur emission environmental regulations against H_2S toxicity are becoming increasingly stringent. Properly managing sulfur recovery units also improves the monetization of the unit. Thus, the acid gas out from the AGR regenerator unit (see Figure 7.41) needs to get desulfurized before tail gas treatment and final vent/incineration.

The Claus process is the most famous and well-established gas desulfurizing process, capturing elemental sulfur from gaseous hydrogen sulfide, carbonyl sulfide, carbon disulfide, sulfur dioxide, and other sulfur-containing species in a series of thermal and chemical reactions [173]. The majority of sulfur produced is byproduct sulfur from petrochemical plants. The elemental sulfur (S) is used for manufacturing sulfuric acid, medicine, cosmetics, fertilizers, pesticide, and rubber products.

In a Claus process, acid gases from the AGR unit (see Figure 7.41) is sent to a reaction furnace with air at high temperature. Rapid reactions at 1000-1400°C take place to convert one third of the total inlet H_2S to SO_2 at the outlet. Following heat recovery, elemental sulfur produced in the furnace is drawn out of the system using a low temperature condenser at about 130°C. The remaining gaseous effluent is sent through several (typically 2 or 3) catalytic sections in series operating at 170-370°C, which continue to convert the remaining SO_2 and H_2S to elemental sulfur and water (see below reactions). A cumulative sulfur recovery of >98% is typically targeted [173]. The gaseous effluent from the last catalytic stage condenser is low in sulfur compounds, but may require some additional treating to meet flare gas specifications. This gas is sent to tail gas treating processing, which can contain

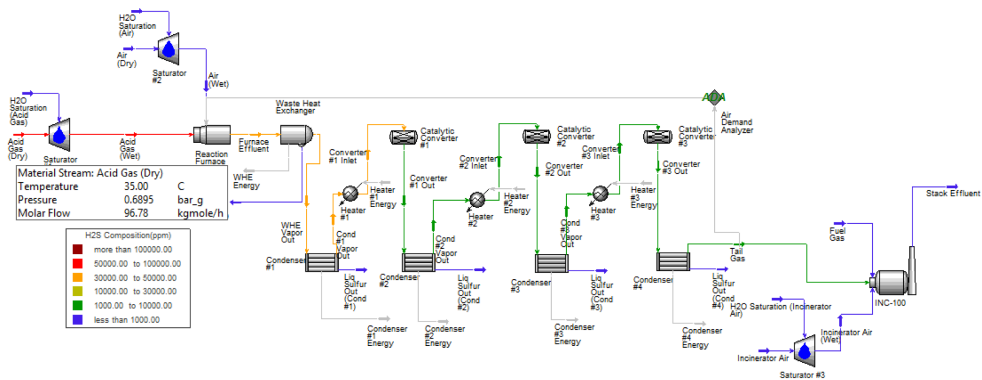
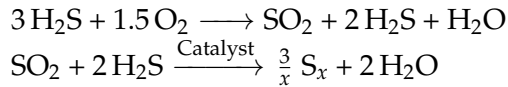


Figure 7.49: Claus unit modified process flow diagram from Aspen HYSYS as used in developing statistical proxy models.

process units such as a hydrogenation bed, reducing gas generator, quench tower, amine absorber, incinerator and flare.



As shown in Figure 7.49, a modified version of Aspen HYSYS default template flowsheet of *Sulsim (Sulfur Recovery) - 3 stage Claus process* is used for this analysis. Empirical models based on hundreds of sulfur plant test results are used by Aspen HYSYS to model the Reaction Furnace and predict the unit conversion efficiency, as well as quantities of COS, CS₂, H₂, CO, and H₂S at the outlet of the furnace. The concentrations of H₂S and CO₂ in the acid gas are the largest influencing factors upon the design and configuration of the Claus plant and have significant effects on the net reactions in the furnace, and thus, are the major independent variables of our system. For the cases with > 40% H₂S mole concentration in Acid Gas (Dry) stream, *Straight Through Amine Acid Gas* is selected as the Reaction Furnace empirical model, whereas for low H₂S concentration acid gas streams, *Lean Feed Acid Gas (Legacy)* model is utilized. Alumina catalyst bed is used for the Catalytic Converters. In all simulations, the Liq. Sulfur Out (Cond. 1) stream mass flow rate is adjusted and the Condenser 1 thermodynamic models are solved iteratively in order to obtain 99% sulfur recovery efficiency out of Condenser 1.

The fixed operating parameters are given in Table 7.55.

Table 7.55: Settings for fixed operating parameters in Aspen HYSYS desulfurization plant simulations.

Fixed variables	Value
Acid gas C ₁ , C ₂ , and C ₃ mole concentrations [mol. fraction]	0.005, 0.002, 0.001
Acid gas inlet temperature [°F]	95
Acid gas inlet pressure [psig]	10
H ₂ O saturation temperature [°F]	77
H ₂ O saturation pressure [psig]	0
Air dry temperature [°F]	95
Air dry pressure [psig]	10
Acid gas (wet) molar flow [kgmole/h]	100
Air (wet) [kgmole/h]	227.3
Furnace model [-]	Empirical: <i>Straight Through Amine Acid Gas Lean Feed Acid Gas (Legacy)</i>
Furnace, waste heat exchanger (WHE), condensers, catalytic converters, and incinerator pressure drop [bar]	0.03
Furnace residence time [s]	1
WHE type [-]	Single pass
WHE vapor out temperature [°F]	572
Condensers vapor out temperature [°F]	275
Sulfur recovery efficiency specified target value [%]	99
Catalytic converter catalyst [-]	Alumina
Catalytic converter space velocity [1/h]	1000
Incinerator fuel gas C ₁ , C ₂ , and C ₃ mole concentrations [mol. fraction]	0.95, 0.04, 0.01
Incinerator target outlet O ₂ mole concentration [mol. fraction]	0.02
Stack effluent temperature [°F]	1112
Stack effluent pressure [psig]	0.2905

Figure 7.50 shows the kJ energy duty per kg of sulfur produced as a function of the acid gas H₂S mole concentration for the condensers (1 to 4), heaters (1 to 3) and WHE. The corresponding best fit equations and R² are also shown in 7.50. In addition, other important output parameters trends versus the acid gas H₂S mole concentration are presented below (Figures 7.51 to 7.53). It should be noted that as ≈99% of total mole fractions of the Tail Gas and Stack Effluent streams are associated with H₂O, H₂, N₂, and CO₂ components, the other ultra-low concentration elements (i.e., Ar, CO, COS, CS₂, HCN, O₂, SO₂, and S₁-S₈) are excluded. Thus, the H₂O, H₂, N₂, and CO₂ concentrations are scaled to 100% and the scaled data are shown in Figures 7.51 and 7.52. The predictive best fit equations obtained in this analysis are used in OPGEE for estimating the energy consumptions and specification of different streams of the Claus unit.

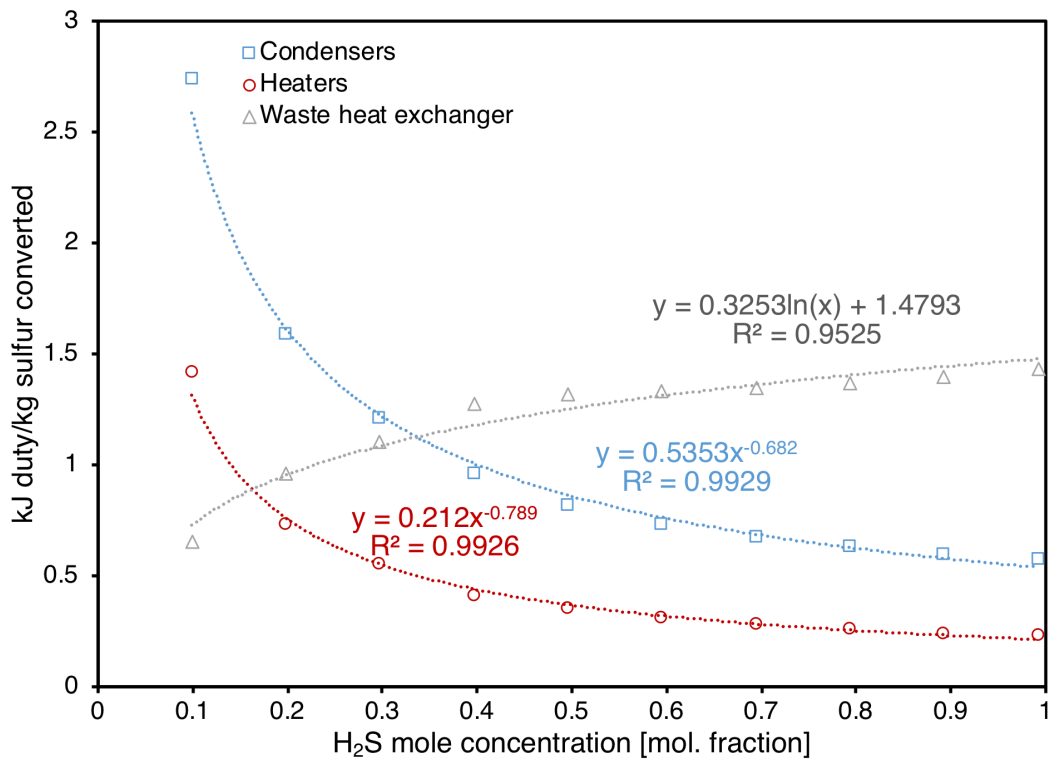


Figure 7.50: Desulfurization condensers, heaters, and waste heat exchanger heat duties per kilogram of sulfur produced in different acid gas H_2S concentrations.

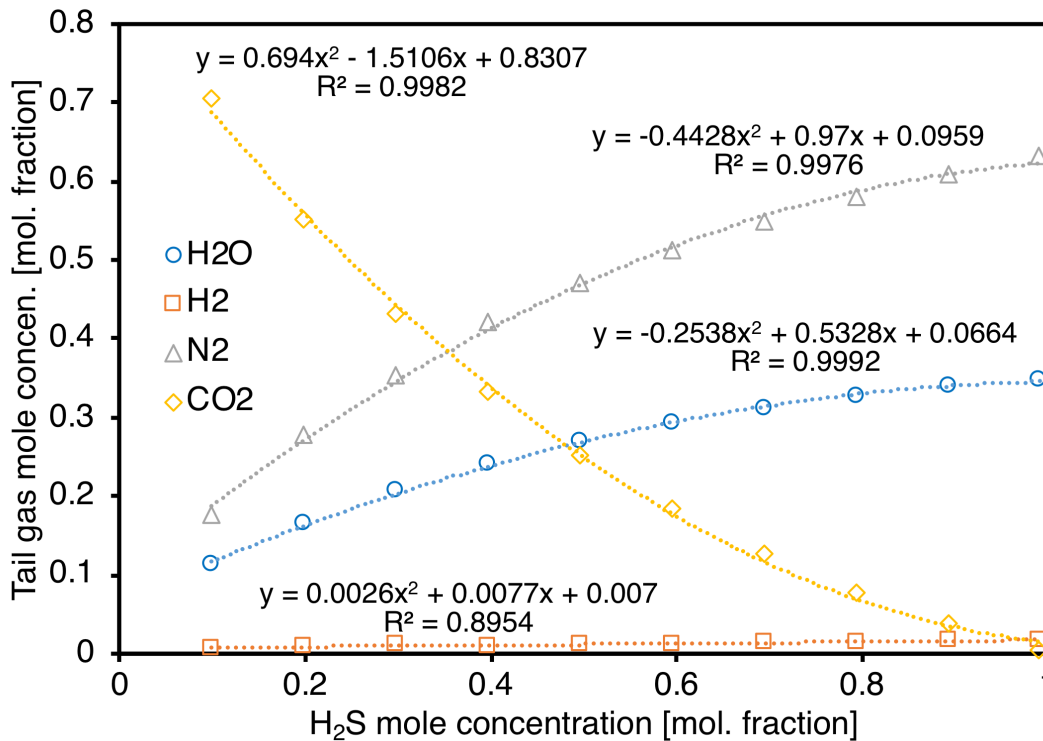


Figure 7.51: Tail gas H_2O , H_2 , N_2 , and CO_2 mole concentrations in different acid gas H_2S concentrations.

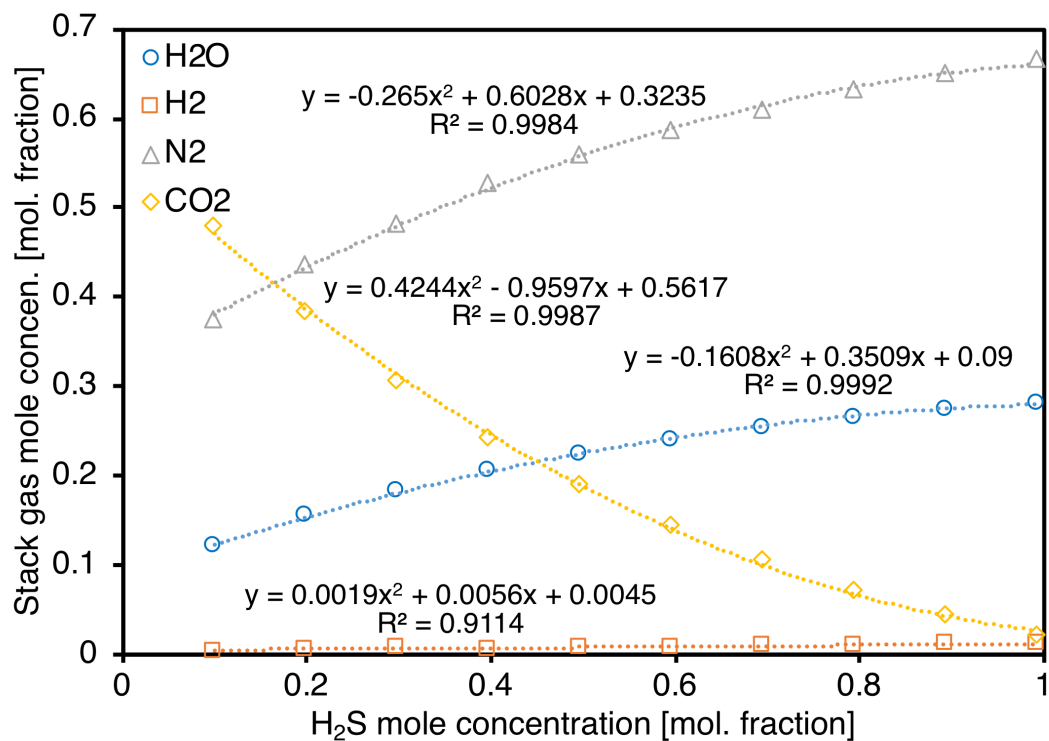


Figure 7.52: Stack gas H₂O, H₂, N₂, and CO₂ mole concentrations in different acid gas H₂S concentrations.

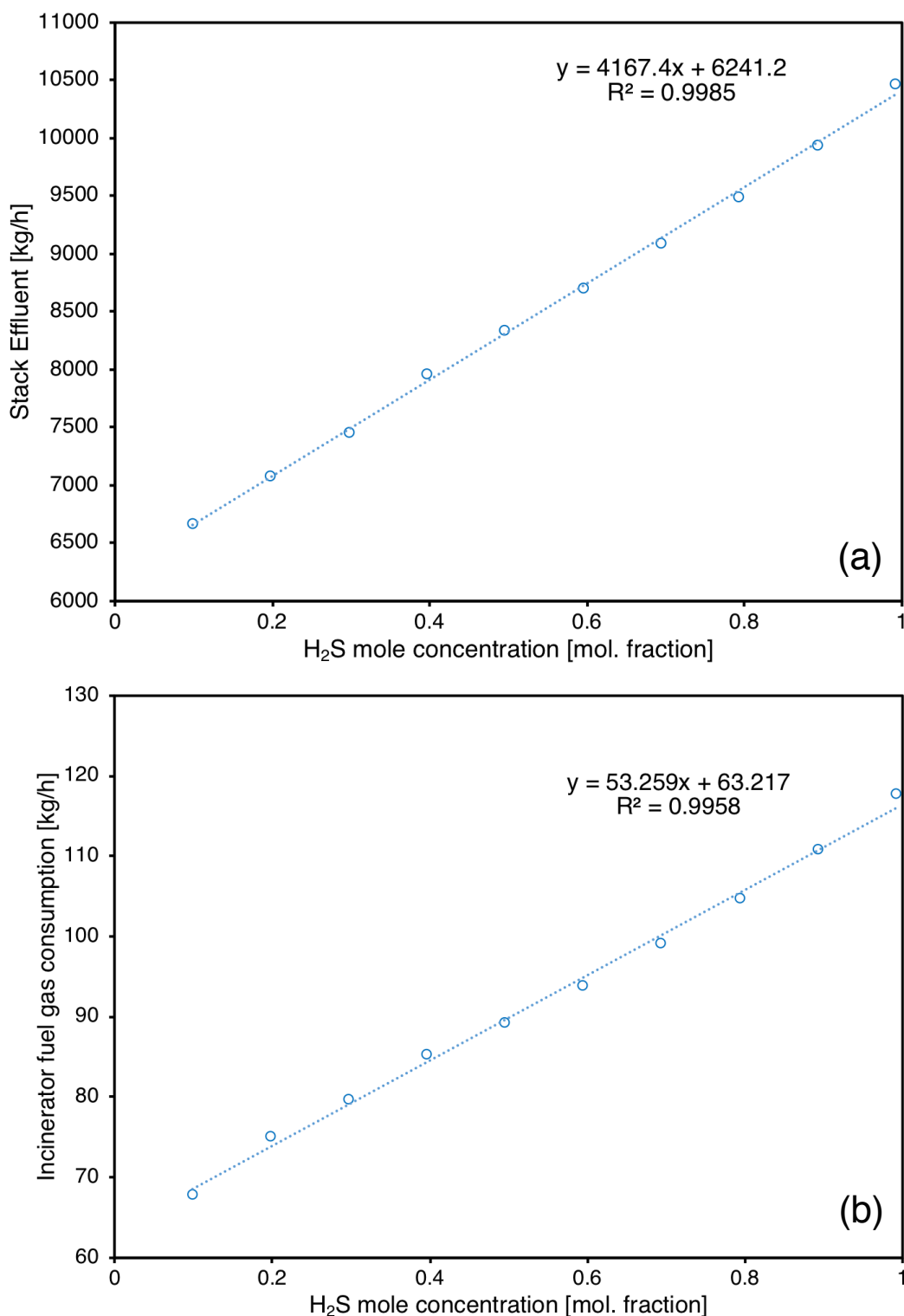


Figure 7.53: Desulfurization plant downstream mass flow rates vs. different acid gas H₂S concentrations
(a) Stack effluent mass flow rate (b) Incinerator fuel gas consumption.

7.20.4 Defaults for surface processing

Defaults for surface operations are shown in Table 7.64.

Table 7.56: Default inputs for surface processing.

Param.	Description	Eq. no.	Default	Literature range	Unit	Sources	Notes
BHP_F	Fan brakehorse power	(7.93)	-	-	[hp]	[4, p. 118]	
BHP_{RP}	Reflux pump brakehorse power	(7.94)	-	-	[hp]	[4, p. 118]	
BHP_{BP}	Booster pump brakehorse power	(7.95)	-	-	[hp]	[4, p. 118]	
BHP_{CP}	Circulation pump brakehorse power	(7.96)	-	-	[hp]	[4, p. 118]	
BHP_{TEG}	TEG pump brakehorse power	(7.83)	-	-	[hp]	[9, p. 455]	
BHP_{RS}	Refrigeration brakehorse power	(7.98)	-	-	[hp]	[165]	
C_{P_o}	Specific heat of oil	-	150	-	[Btu/bbl-°F]	[60, p. 136]	
C_{P_w}	Specific heat of water	-	350	-	[Btu/bbl-°F]	[60, p. 136]	
E_{tot}	Total electricity consumption	(7.57)	-	-	[Kwh/d]	[Kwh/d]	
$e_{s1} \dots e_{s4}$	Electricity consumption by stage	-	-	-	[scf/bbl]	[60, p. 136]	a
e_j	Fraction of heat loss in unit j	-	0.02	-	[scf/bbl]	[10]	
$e_{V,(N-1)}$	Fraction of volume loss in stage N – 1	-	var. 0.65	-	[MMBTu/d]	[4, p. 119]	
η_P	Pump efficiency	-	0.4	-	[MMBTu/d]	[4, p. 158]	b
$\lambda_{w,rem}$	Fraction of water removed below fire tube	-	Section 4.3.0.6	-	[MMBTu/d]	[165]	c
GOR	Gas-to-oil ratio	(7.90)	-	-	[gpm-d/100MMscf]	[4, p. 115]	
ΔH_R	Amine process reboiler heat duty	(7.82)	-	-	[gal TEG/lb H ₂ O]	[60, p. 136]	
ΔH_{GD}	Glycol dehydrator reboiler heat duty	-	0	-	[psi]	[4, p. 147]	
ΔH_{FR}	Fractionation reboiler heat duty	-	2.05	0.95-2.05	[lb H ₂ O/d]	[4, p. 160]	
K	Amine solution K value	-	0.14	-	[gpm]	[4, p. 115]	
$\lambda_{w,ent}$	Fraction of water entrained in oil	-	2	-	[MMscf/d]	'Gas Balance'	
q_{TEG}	TEG circulation rate	-	786	-	[bbl/d]	[60, p. 136]	
p_d	Pump discharge pressure	-	$Q_g \Delta M_{w,rem}$	-	[MMscf/d]	'Gas Balance'	
$\Delta Q_{w,rem}$	Rate of water removal	-	$Q_g \Delta M_{w,rem}$	-	[MMscf/d]	'Gas Balance'	
Q_{amine}	Amine flow rate	(7.91)	-	-	[MMscf/d]	[60, p. 136]	
Q_{CO_2}	Volume of CO ₂ removed	-	var.	-	[MMscf/d]	'Gas Balance'	
$Q_{w,ent}$	Volume of entrained water	(???)	-	-	[MMscf/d]	'Gas Balance'	
Q_F	Flaring volume	-	Section 7.16.1	-	[MMscf/d]	'Gas Balance'	
Q_g	Inlet gas flow rate	(7.89)	-	-	[MMscf/d]	'Gas Balance'	
Q_{H_2S}	Volume of H ₂ S removed	-	var.	-	[MMscf/d]	'Gas Balance'	
$Q_{w,heat}$	Volume of heated water	(???)	-	1500	[bbl/d]	[60, p. 136]	
Q_o	Volume of oil production	-	-	-	[bbl/d]		

Continued on next page...

Continued from previous page

Param.	Description	Eq. no.	Default	Literature range	Unit	Sources	Notes
Q_{TEG}	TEG circulation rate in gpm	(7.84)	-	-	[gpm]		
Q_w	Volume of produced water	(7.58)	-	-	[bbl/d]		
$Q_{w1} \dots Q_{w4}$	Water feed by stage	(7.58)	-	-	[bbl water / d]		
ΔT_{CD}	Crude dehyd. temp. difference	-	75	-	[°F]	[60, p. 136]	
ΔT_S	Crude stabilizer temp. difference	-	224	-	[°F]	[60, p. 161, 163]	
$\Delta M_{w,rem}$	Weight of water removed	(7.81)	-	-	[lb H ₂ O /MMscf]		
$M_{w,in}$	Weight of water in inlet gas	-	52	-	[lb H ₂ O /MMscf]	[4, p. 160]	
$M_{w,out}$	Weight of water in outlet gas	-	7	-	[lb H ₂ O /MMscf]	[4, p. 160]	
WOR	Water-to-oil ratio	(4.5)	-	-	[bbl water / bbl oil]		
$Chiller_{IN}$	Temperature of feedstream entering chiller unit	-	59	-	[°F]		
$Chiller_{OUT}$	Temperature of feedstream exiting chiller unit	-	35	-	[°F]	[166]	
RH_{IN}	Temperature of feedstream entering Ryan-Holmes process	-	81	-	[°F]	[167]	
RH_{backup}	Usage rate of Ryan-Holmes backup engine	-	2.63	-	[hrs/d]	[167]	

a - This is a user input. No defaults are available for most of the treatment technologies. The default for wetlands (CWL) where volume losses are significant is 26% [10].*b* - It is assumed that heat exchange with the inlet stream provides the heat duty.*c* - The default is monothanolamine (MEA).

Table 7.57: Streams flowing into and out of the demethanizer process. I/O denotes input or output stream

Flow name	Stream	I/O	Source/Destination	Units	Notes
Gas to demethanizer	37	I	Acid gas removal	[t/d]	
Fuel gas - Demethanizer	153	I	Fuel gas system	[t/d]	
Demethanizer light product	38	O	Gas partition A	[t/d]	
Demethanizer heavy product	39	O	NGL production and imports	[t/d]	
Demethanizer fugitives	257	O	Atmosphere	[t/d]	

7.21 Demethanizer

Recovery of natural gas liquids (NGL) from natural gas stream is a quite common practice in gas processing and has great economic importance. High volumes of associated gas produced from crude oil used to be flared routinely, and phasing out this wasteful and high emitting practice [174] has required greatly increased NGL recovery. The demethanizer splits the natural gas stream into a pipeline quality natural gas stream and a NGL stream. NGL recovery is however not totally an economic matter and regardless of economics, production of gas that meets stringent sales specifications may require NGL extraction. In addition, it may be desirable to produce a gas that can be pipelined without HC condensate formation which NGL unit becomes necessary [4].

The main sources of GHG emissions from the demethanizer unit are the refrigeration system and compressor shaft power and the heat duty of the fractionation column reboiler, if supplemental heat is required. These are calculated using energy factors which are generated from a default configuration [165]. The independent demethanizer unit described below is included in Gas Processing Paths 4 and 5. Gas Processing Path 7 (Ryan-Holmes) includes an integrated demethanizer.

The streams flowing into and out of the demethanizer process are shown in Figure 7.54 and are listed in Table 7.57.

7.21.1 Demethanizer modeling using result from process simulation software

Cryogenic processing and absorption methods are some of the ways to separate methane from NGLs. The cryogenic method is better at extraction of the lighter liquids, such as ethane, than is the alternative absorption method [175].

Similar to the AGR unit (see Section 7.20.1), in order to generate statistical proxy models to estimate energy consumption of the demethanizer plant under a wide variety of operating conditions, Aspen HYSYS commercial process simulation software is used to simulate thousands of conditions using different ranges of independent variables. The resulting open-source statistical models allow OPGEE to predict the results of commercial software without the expense and challenge of running full NGL simulations. Here Aspen HYSYS V10 is used to train the statistical proxy models.

A modified version of Aspen HYSYS default template flowsheet of *Deep Cut Turbo-Expander* plant is used for this analysis. As shown in Figure 7.55, in the cryogenic or turbo-expander NGL plant, the chiller is replaced by an expansion turbine (E-100) where the high pressure entering gas expands and supplies shaft work (en-

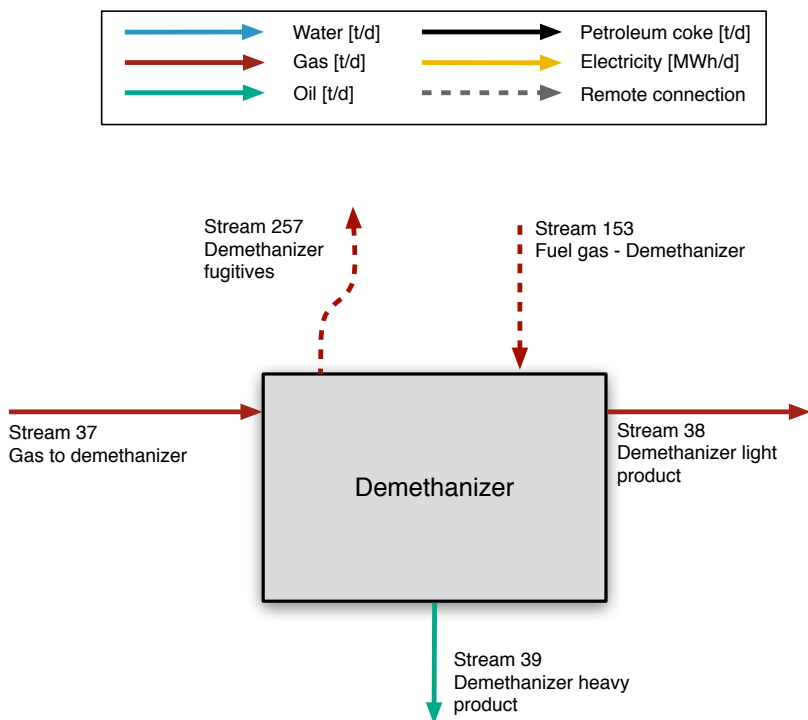


Figure 7.54: Streams flowing into and out of the demethanizer process. All streams measured in tonnes per day excepting electricity which is measured in MWh/d.

ergy steam 70) to the downstream turbine (K-100), thus reducing the gas enthalpy and large temperature drop. The quick drop in temperature that the expander is capable of producing condenses the hydrocarbons in the gas stream, but maintains methane in its gaseous form.

Feed gas is cooled first in the high-temperature, gas-to-gas heat exchangers. Condensate liquids then are removed in a separator (V-100). Gas from the cold separator expands through the expansion turbine to the pressure at top of the demethanizer. The demethanizer column (T-100) stabilizes the raw liquid product by reducing the methane content to a suitably low level. The molar ratio of methane to ethane in the bottom product of the column is typically 0.02-0.03 [4]. The demethanizer tower is modeled in Aspen HYSYS using sufficient number of theoretical trays (11 trays) to ensure converged simulations. The number of trays has a negligible effect on the total energy cost of the system. Horizontal cylindrical reboiler design is used for all simulations. All of the heat duty required for the demethanizer trays and reboiler (energy stream 80-82) are supplied from the cooler duty (stream Q-100) through a network of heat exchangers. From the demethanizer unit, two products are generated: methane gas (fuel gas) and a NGL product. The methane-rich fuel gas is exported as product from the process, and the NGL is exported for sale or to fractionation plant for further recovery.

As the gas is first processed with AGR unit (see Section 7.20), it is assumed that the inlet gas to the demethanizer plant is a H_2S and CO_2 free stream. High pressure gas is needed to pass through the turbo-expander. Here, the compressor and its energy duty needed to pressurize the inlet gas is excluded from the demethanizer

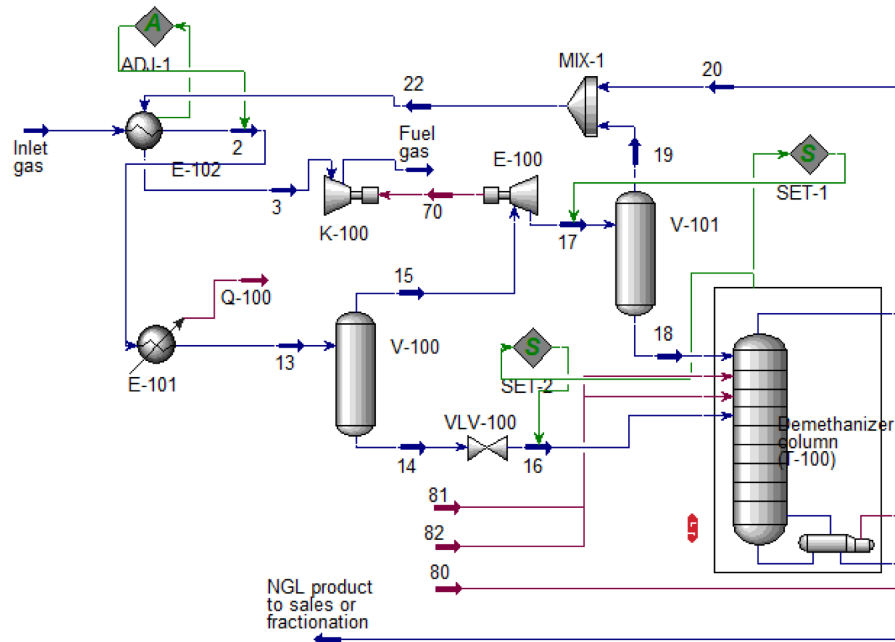


Figure 7.55: Demethanizer modified process flow diagram from Aspen HYSYS as used in developing statistical proxy models.

plant.

In this analysis, the heat exchanger network of the default template is simplified in order to be able to simulate the process under the variety of operating conditions. For each simulation, *Set* control blocks (Set-1 and Set-2 in Figure 7.55) are added to the flowsheet in order to dynamically set the outlet pressure of the expander and VLV-100 valve based on the determined pressure of the demethanizer column (T-100).

One of the major challenges of NGL simulation across range of operating conditions corresponds to the heat exchanger optimal design and performance. In particular, as the NGL column top outlet stream (i.e., stream 22 in Figure 7.55) temperature varies with different NGL column pressures, stream 2 temperature should also get adjusted in order to keep the heat exchanger (E-102) running at efficient condition. The total heat transferred between the tube and shell sides (heat exchanger duty) can be defined in terms of the overall heat transfer coefficient, the area available for heat exchange, and the log mean temperature difference (LMTD):

$$Q = UA\Delta T_{LM}F_t \quad \left[\frac{\text{MMBtu}}{\text{h}} \right] \quad (7.97)$$

where U is overall heat transfer coefficient, A is surface area available for heat transfer, ΔT_{LM} is the LMTD, and F_t is the LMTD correction factor. The heat exchanger correction factor (F_t) is selected as a design performance criterion. A F_t value lower than 75% generally corresponds to inefficient design in terms of the use of heat transfer surface. Thus, *Adjust* control block (ADJ-1) is added to the flowsheet in order to iteratively adjust stream 2 temperature to reach F_t target of >77% for each simulation.

We use Aspen HYSYS to run thousands of cases across 5 different independent

Table 7.58: Settings for fixed operating parameters in Aspen HYSYS demethanizer plant simulations.

Fixed variables	Value
H ₂ S concentration [mol. fraction]	0
CO ₂ concentration [mol. fraction]	0
Column pressure drop per tray [psi]	0.5
Number of trays [-]	11
Inlet gas temperature [°F]	100
Inlet gas flow rate [MMscf/d]	99.8
Expander (E-100) isentropic efficiency [%]	80
Compressor (K-100) adiabatic efficiency [%]	75

Table 7.59: Ranges of independent variables explored in generating predictive proxy models using Aspen HYSYS for demethanizer plant.

Fixed variables	Value
Inlet gas pressure [psi]	600-1000
Demethanizer column (T-100) pressure [psi]	155-325
Methane to ethane NGL composition molar ratio at NGL product stream [-]	0.01-0.05
Methane mole concentration at the inlet gas stream [mol. fraction]	0.5-0.95
Ethane mole concentration at the inlet gas stream [mol. fraction]	0.05-0.2

variables that are considered to be the major operating parameters in demethanizer plant:

1. Inlet gas pressure [psi] (x_1)
2. Demethanizer column (T-100) pressure [psi] (x_2)
3. Methane to ethane NGL composition molar ratio at NGL product stream [-] (x_3)
4. Methane mole concentration at the inlet gas stream [mol. fraction] (x_4)
5. Ethane mole concentration at the inlet gas stream [mol. fraction] (x_5).

As different mole fractions of methane and ethane are explored, the remaining species (N₂, C₃, C₄₊) are scaled proportionately by the OPGEE default molar ratios. Settings for other fixed operating parameters are given in Table 7.58.

The ranges of independent variables selected based on literature [4, 176, 177] are listed in Table 7.59.

Similar to the AGR predictive modeling approach (see Section 7.20.1), a combination of deterministic and random sampling strategy across the five independent variables x_1 to x_5 are used. In total 37 different gas compositions (C₁, C₂, C₃, C₄₊, and N₂) are modeled. For each gas composition, deterministic sampling is performed using Box-Behnken sampling across the remaining three variables (inlet gas pressure, column pressure, methane to ethane composition ratio). Box-Behnken sampling returns 15 combinations of variables. Additionally, Latin hypercube sampling methodology is employed for a random sampling of 100 additional points for each gas composition. In summary, per gas composition, we have 115

samples. Therefore, a total of 4,255 simulations of demethanizer systems were performed. All samples are generated using MATLAB [164] and run in through Aspen HYSYS 10 using *Case study* platform.

A total of 15 dependent variables as outputs for each run are recorded. These include (1) demethanizer reboiler thermal load (stream 80) [kW], (2) (3) demethanizer column trays 6 and 9 thermal loads (streams 81 and 82) [kW], (4) available thermal load from the heat exchanger E-101 (stream Q-100), (5) turbo-expander shaft work (stream 70) [kW], (6-10) NGL product N_2 , C_1 , C_2 , C_3 , and C_4+ mole concentrations [mol. fraction], (11-15) Fuel gas N_2 , C_1 , C_2 , C_3 , and C_4+ mole concentrations (steam 20) [mol. fraction].

Using these results, predictive equations are generated using MATLAB curve fitting toolbox [164]. A set of 15 predictive quadratic equations were generated. Similar to the AGR unit (see Section 7.20.1), each dataset is split into a training dataset and a testing dataset. The testing set is a randomly selected subset of 10% of the observations which is removed from the dataset and held aside (i.e., not used to generate the statistical fit). The training set includes the remainder of the results (90% of simulation runs). The training and testing sets are drawn independently for each predictive equation. Each training dataset is fitted to a quadratic equation of all five independent variables. The quadratic equation (similar to eq. (7.85)) includes all linear terms, interaction terms, and square terms. The raw fitting results are presented in OPGEE as a data appendix, which includes demethanizer fit and significance results for each term.

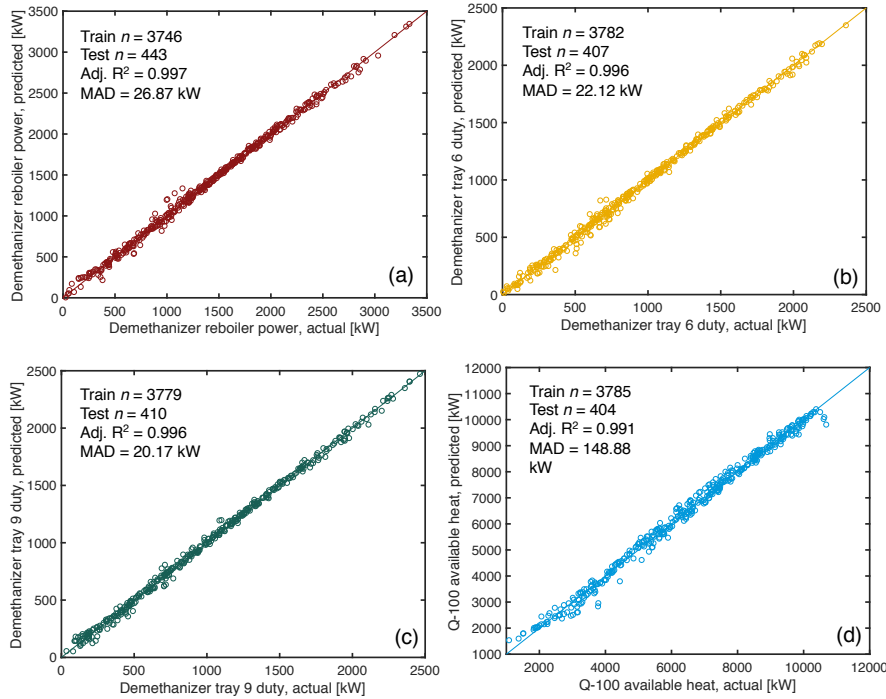


Figure 7.56: Demethanizer energy use prediction parity chart (a) Reboiler thermal inputs [kW]; (b) Demethanizer tray 6 duty [kW]; (c) Demethanizer tray 9 duty [kW]; (d) Demethanizer cooler Q-100 duty [kW].

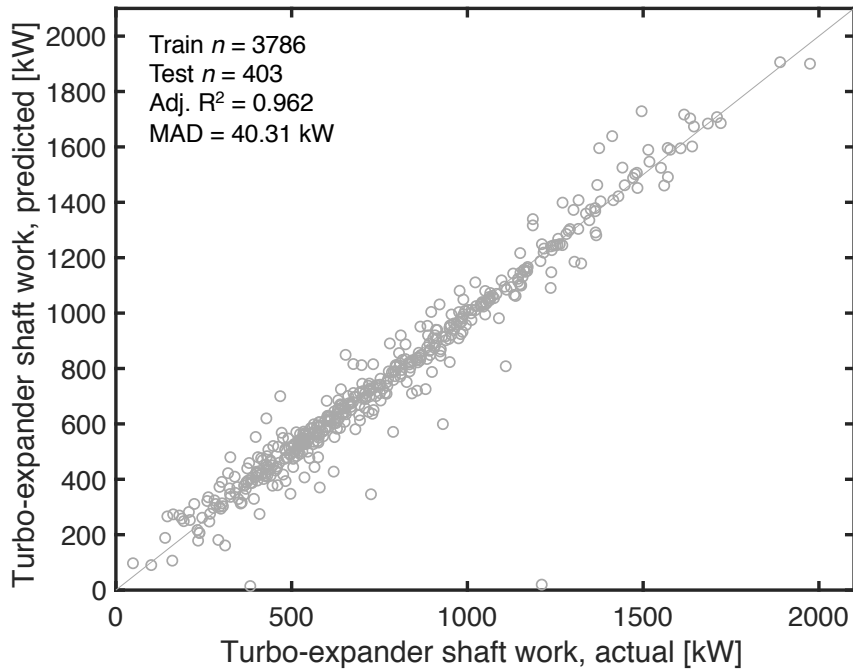


Figure 7.57: Demethanizer energy use prediction parity chart (a) Reboiler thermal inputs [kW]; (b) Demethanizer tray 6 duty [kW]; (c) Demethanizer tray 9 duty [kW]; (d) Demethanizer cooler Q-100 duty [kW].

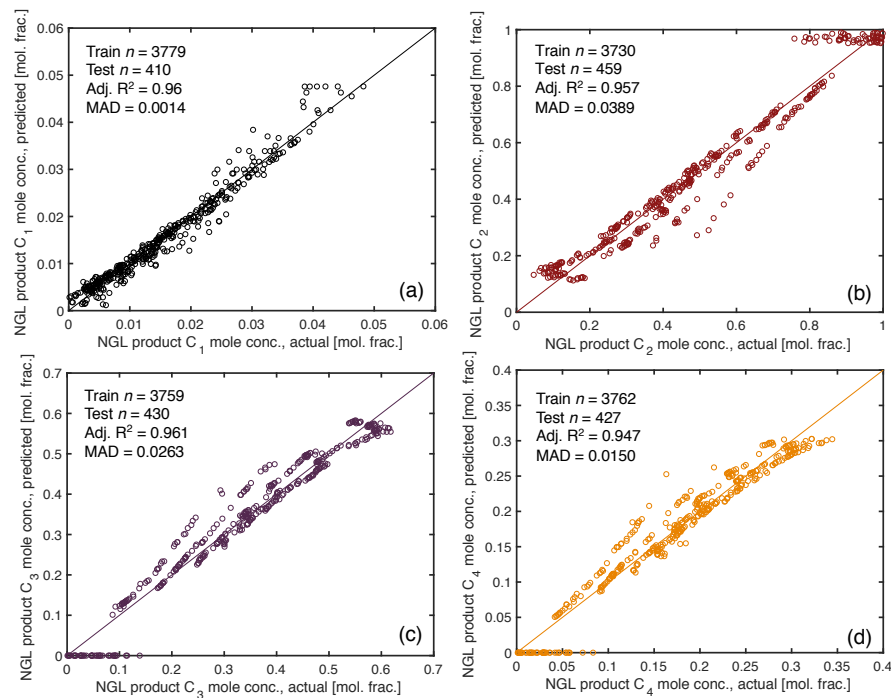


Figure 7.58: Demethanizer NGL stream mole concentration parity chart (a) C₁ [mol. frac.]; (b) C₂ [mol. frac.]; (c) C₃ [mol. frac.]; (d) C₄ [mol. frac.]

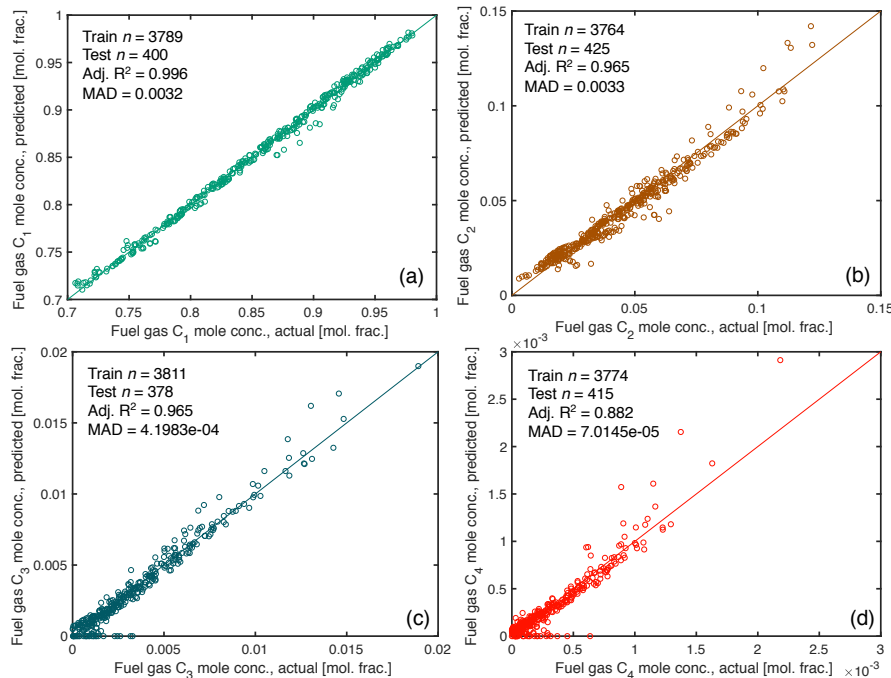


Figure 7.59: Demethanizer Fuel gas stream mole concentration parity chart (a) C₁ [mol. frac.]; (b) C₂ [mol. frac.]; (c) C₃ [mol. frac.]; (d) C₄ [mol. frac.]

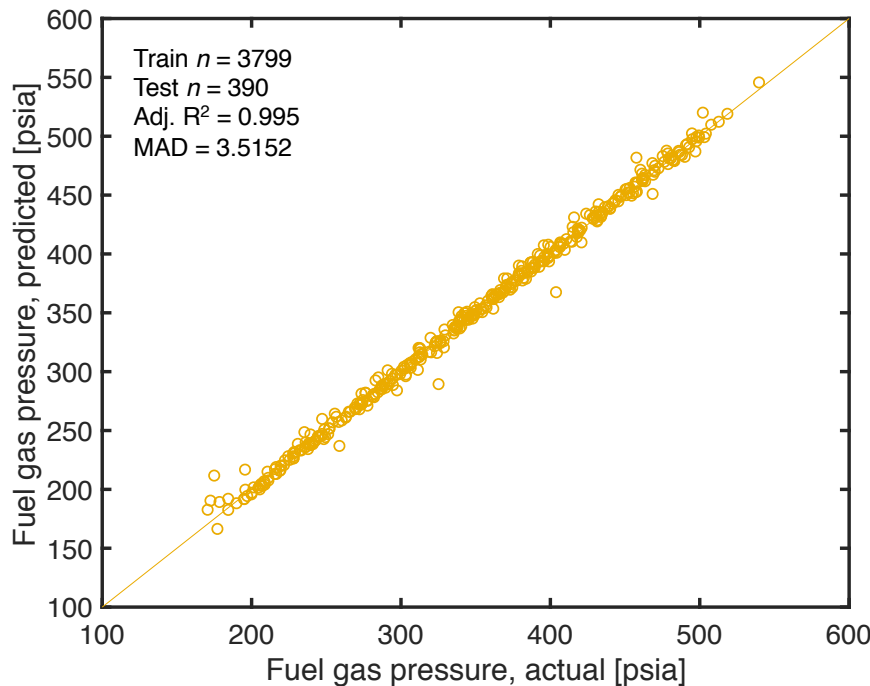


Figure 7.60: Demethanizer Fuel gas stream pressure parity chart.

After the model is fit, the fitted model is fed the independent variables from the test dataset and asked to predict the dependent variables from the test dataset. The results from these testing runs are shown as parity charts below (Figures 7.56 to 7.60). Almost all of the resulting models have extremely high adjusted-R² values of close to 1, suggesting that these models accurately capture what modeled in Aspen HYSYS. The Fuel gas C₄₊ concentration (Figure 7.59 (d)) resulted in adjusted-R² lower than 90% but the C₄₊ concentration is almost zero in the Fuel gas stream and the proxy model is not very important for this output component.

The model coefficients obtained in this analysis are incorporated in predictive equations in OPGEE and the fitting results are presented in OPGEE as a data appendix, which includes statistical fit and significance results for each term. In Aspen Hysys, the cooling load for E-101 cooler (see Figure 7.55) is presented as thermal duty (in kW) to be removed from stream 2 hot stream. Here similar to Section 7.20.1, forced-draft air-cooled heat exchanger is used to model the cooling system.

7.21.2 Demethanizer modeling using gas handbook methods

In the default OPGEE demethanizer configuration, the compressor system is assumed to operate upstream of the demethanizer; the resulting feedstream pressure is 60 bar [165]. The refrigeration duty is assumed to be proportional to the amount of gas condensed. A heat recovery system allows the cold gas that remains to be warmed back up in exchange with incoming gas. The energy factors of the compressor and refrigeration system are 0.58 [bhp-hr/kmol_{FEED}] and 3.6 [bhp-hr/kmol_{COND}], respectively. As seen in the demethanizer literature, OPGEE assumes that the reboiler heat duty is provided by heat exchangers from the in-

coming feed stream. Under this configuration the demethanizer is assumed to condense 90.2% of ethane and 100% of propane and butane [165], which is then assumed to be exported as LPG. These fractions can be changed on the '*Surface Processing*' worksheet. The gas feed measure is in gram moles as reported in the demethanizer unit synthesis report. The gas feed moles is calculated from the '*Gas Balance*' worksheet using the gas composition of the demethanizer feed. The refrigeration brake horse power is calculated as:

$$\text{BHP}_{RS} = \frac{1}{24} \cdot e_{RS} \cdot Q_{g_{in}} \quad [\text{hp}] \quad (7.98)$$

where BHP_{RS} = refrigeration system shaft brakehorse power [hp]; e_{RS} = energy factor [bhp-hr/kmol_{COND}]; and $Q_{g_{in}}$ = demethanizer gas condensed [kmol/d]. The compressor work is calculated similarly. The molar amount of the gas feed and gas condensed is calculated in the '*Surface Processing*' worksheet.

The energy consumption of the compression and refrigeration system is calculated using the fuel consumption of an appropriate NG turbine as determined by the power demand. GHG emissions are calculated using emissions factors of NG turbine from the '*Emissions Factors*' worksheet.

OPGEE allows flexibility in the gas processing scheme; the demethanizer unit can be turned OFF in fields with dry associated gas or where NGL recovery is not economic by selecting Gas Processing Paths 1, 2, or 3.

7.21.3 Defaults for surface processing

Defaults for surface operations are shown in Table 7.64.

'Surface Processing'
1.2.2.3.1'

'Surface Processing'
2.2.3.1'

Table 7.60: Default inputs for surface processing.

Param.	Description	Eq. no.	Default	Literature range	Unit	Sources	Notes
BHP_F	Fan brakehorse power	(7.93)	-	-	[hp]	[4, p. 118]	
BHP_{RP}	Reflux pump brakehorse power	(7.94)	-	-	[hp]	[4, p. 118]	
BHP_{BP}	Booster pump brakehorse power	(7.95)	-	-	[hp]	[4, p. 118]	
BHP_{CP}	Circulation pump brakehorse power	(7.96)	-	-	[hp]	[4, p. 118]	
BHP_{TEG}	TEG pump brakehorse power	(7.83)	-	-	[hp]	[9, p. 455]	
BHP_{RS}	Refrigeration brakehorse power	(7.98)	-	-	[hp]	[165]	
C_{P_o}	Specific heat of oil	-	150	-	[Btu/bbl-°F]	[60, p. 136]	
C_{P_w}	Specific heat of water	-	350	-	[Btu/bbl-°F]	[60, p. 136]	
E_{tot}	Total electricity consumption	(7.57)	-	-	[Kwh/d]	[Kwh/d]	
$e_{s1} \dots e_{s4}$	Electricity consumption by stage	-	-	-	[-]	[60, p. 136]	a
e_j	Fraction of heat loss in unit j	-	0.02	-	[-]	[10]	
$e_{V,(N-1)}$	Fraction of volume loss in stage N – 1	-	var. 0.65	-	[-]	[-]	
η_P	Pump efficiency	-	0.4	-	[-]	[60, p. 136]	
$\lambda_{w,rem}$	Fraction of water removed below fire tube	-	Section 4.3.0.6	-	[scf/bbl]	[MMBtu/d]	
GOR	Gas-to-oil ratio	(7.90)	-	-	[MMBtu/d]	[4, p. 119]	
ΔH_R	Amine process reboiler heat duty	(7.82)	-	-	[MMBtu/d]	[4, p. 158]	
ΔH_{GD}	Glycol dehydrator reboiler heat duty	-	0	-	[MMBtu/d]	[165]	b
ΔH_{FR}	Fractionation reboiler heat duty	-	2.05	0.95-2.05	[gpm-d/100MMscf]	[4, p. 115]	
K	Amine solution K value	-	0.14	-	[-]	[60, p. 136]	
$\lambda_{w,ent}$	Fraction of water entrained in oil	-	2	-	[gal TEG/lb H ₂ O]	[4, p. 147]	
q_{TEG}	TEG circulation rate	-	786	-	[psi]	[4, p. 160]	
p_d	Pump discharge pressure	-	$Q_g \Delta M_{w,rem}$	-	[lb H ₂ O/d]	[4, p. 115]	
$\Delta Q_{w,rem}$	Rate of water removal	(7.91)	-	-	[gpm]	'Gas Balance'	
Q_{amine}	Amine flow rate	-	var.	-	[MMscf/d]	[60, p. 136]	
Q_{CO_2}	Volume of CO ₂ removed	(??)	-	-	[bbl/d]	[bbl/d]	
$Q_{w,ent}$	Volume of entrained water	-	Section 7.16.1	-	[MMscf/d]	[bbl/d]	
Q_F	Flaring volume	(7.89)	-	-	[MMscf/d]	'Gas Balance'	
Q_g	Inlet gas flow rate	-	var.	-	[MMscf/d]	'Gas Balance'	
Q_{H_2S}	Volume of H ₂ S removed	(??)	-	-	[bbl/d]	[bbl/d]	
$Q_{w,heat}$	Volume of heated water	-	1500	-	[bbl/d]	[bbl/d]	
Q_o	Volume of oil production	-	-	-	-	-	

Continued on next page...

Continued from previous page

Param.	Description	Eq. no.	Default	Literature range	Unit	Sources	Notes
Q_{TEG}	TEG circulation rate in gpm	(7.84)	-	-	[gpm]		
Q_w	Volume of produced water	(7.58)	-	-	[bbl/d]		
$Q_{w1} \dots Q_{w4}$	Water feed by stage	(7.58)	-	-	[bbl water / d]		
ΔT_{CD}	Crude dehyd. temp. difference	-	75	-	[°F]	[60, p. 136]	
ΔT_S	Crude stabilizer temp. difference	-	224	-	[°F]	[60, p. 161, 163]	
$\Delta M_{w,rem}$	Weight of water removed	(7.81)	-	-	[lb H ₂ O /MMscf]		
$M_{w,in}$	Weight of water in inlet gas	-	52	-	[lb H ₂ O /MMscf]	[4, p. 160]	
$M_{w,out}$	Weight of water in outlet gas	-	7	-	[lb H ₂ O /MMscf]	[4, p. 160]	
WOR	Water-to-oil ratio	(4.5)	-	-	[bbl water / bbl oil]		
$Chiller_{IN}$	Temperature of feedstream entering chiller unit	-	59	-	[°F]		
$Chiller_{OUT}$	Temperature of feedstream exiting chiller unit	-	35	-	[°F]	[166]	
RH_{IN}	Temperature of feedstream entering Ryan-Holmes process	-	81	-	[°F]	[167]	
RH_{backup}	Usage rate of Ryan-Holmes backup engine	-	2.63	-	[hrs/d]	[167]	

a - This is a user input. No defaults are available for most of the treatment technologies. The default for wetlands (CWL) where volume losses are significant is 26% [10].*b* - It is assumed that heat exchange with the inlet stream provides the heat duty.*c* - The default is monooctanolamine (MEA).

Table 7.61: Streams flowing into and out of the pre-membrane chiller process. I/O denotes input or output stream

Flow name	Stream	I/O	Source/Destination	Units	Notes
Gas to pre-membrane chiller	61	I	Glycol dehydrator	[t/d]	
Electricity - pre-membrane chiller	180	I	Electricity generation and imports	[t/d]	
Gas to pre-membrane compressor	62	O	Pre-membrane compressor	[t/d]	
Fugitives - Pre-membrane chiller	271	O	Atmosphere	[t/d]	

7.22 Chiller

For the CO₂-EOR path based on membrane separation of CO₂, the incoming gas must be dehydrated before passing through the membrane system. In addition treatment in the glycol dehydrator, the associated gas stream is cooled in an electric chiller to preserve the functionality of the membrane [6].

The streams flowing into and out of the pre-membrane chiller are shown in Figure 7.61 and are listed in Table 7.61.

The default temperatures of the gas streams entering and exiting the chiller are 59 °F and 35 °F, respectively [166].

The electricity consumption rate of the chiller is calculated as [166]:

$$E_c = 3.44 \cdot \left(\frac{Q_c}{6.11} \right) \cdot \frac{(T_I - T_O)}{56} \quad [\text{MW}] \quad (7.99)$$

'Surface
Processing
2.2.6'

where E_c = chiller electricity consumption rate [kWh/d]; Q_c = mass flow rate of the chiller feed stream [mmkg/d]; T_I = temperature of the chiller feed stream [K]; and T_O = temperature of the chiller exit stream [K].

Equation 7.99 linearly scales the refrigeration compressor load in a gas separation process in the NETL chiller module [166] in which 6.11 mmkg/d is the mass flow rate of the feed stream, 56 K is the temperature drop resulting from the refrigeration process, and 3.44 [MW] is the compressor load.

Defaults for surface operations are shown in Table 7.64.

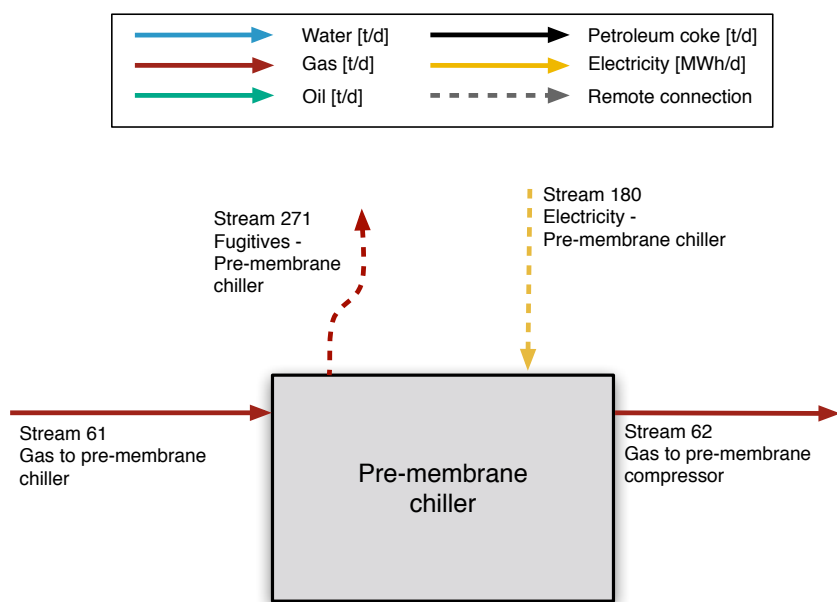


Figure 7.61: Streams flowing into and out of the pre-membrane chiller process. All streams measured in tonnes per day excepting electricity which is measured in MWh/d.

Table 7.62: Default inputs for surface processing.

Param.	Description	Eq. no.	Default	Literature range	Unit	Sources	Notes
Q_c	Mass flow rate into chiller	-	-	-	[mmkg/d]	-	
$*T_I$	Temperature of feedstream entering chiller unit	-	59	-	[°F]	[166]	
$*T_O$	Temperature of feedstream exiting chiller unit	35	-	-	[°F]	[166]	

a - This is a user input. No defaults are available for most of the treatment technologies. The default for wetlands (CWL) where volume losses are significant is 26% [10].
b - It is assumed that heat exchange with the inlet stream provides the heat duty.
c - The default is monothanolamine (MEA).

Table 7.63: Streams flowing into and out of the CO₂ separation membrane process. I/O denotes input or output stream

Flow name	Stream	I/O	Source/Destination	Units	Notes
Gas to CO ₂ separation membrane	63	I	Pre-membrane compressor	[t/d]	
Hydrocarbon rich gas to AGR	64	O	Acid gas removal	[t/d]	
CO ₂ rich stream from membrane	65	O	CO ₂ reinjection compressor	[t/d]	

7.23 Membrane

7.23.1 Defaults for membrane

The streams flowing into and out of the CO₂ separation membrane are shown in Figure 7.62 and are listed in Table 7.63.

Defaults for the CO₂ separation membrane are shown in Table ??.

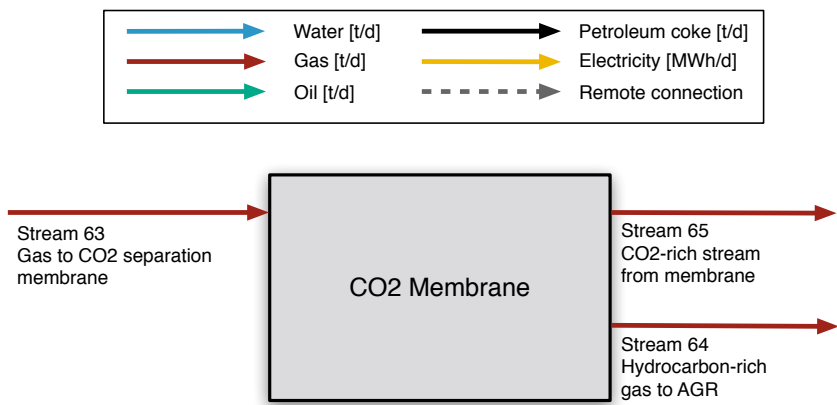


Figure 7.62: Streams flowing into and out of the CO₂ separation membrane process. All streams measured in tonnes per day excepting electricity which is measured in MWh/d.

Table 7.64: Default inputs for surface processing.

Table 7.65: Streams flowing into and out of the Ryan-Holmes separation process. I/O denotes input or output stream

Flow name	Stream	I/O	Source/Destination	Units	Notes
Gas to Ryan-Holmes process	66	I	Glycol dehydrator	[t/d]	
Fuel gas - Ryan-Holmes process	157	I	Fuel gas system	[t/d]	
Light HC stream from Ryan-Holmes process	67	O	Gas partition A	[t/d]	
Heavy HC stream from Ryan-Holmes process	68	O	NGL production and imports	[t/d]	
CO ₂ from Ryan-Holmes process	69	O	CO ₂ re-injection compressor	[t/d]	

7.24 Ryan-Holmes

Gas Processing Path 8 models the Ryan-Holmes separation process, which uses controlled compression and refrigeration to take advantage of the differing boiling points of the components of the feed gas stream; it includes a demethanizer. The process splits the feed stream into a CO₂ stream (assumed to be 100% pure), a natural gas stream, and a heavy product NGL stream [?]. OPGEE incorporates NETL's Ryan-Holmes process module which includes energy consumption for natural gas-fired compressors, a natural gas-fired oil heater, and a diesel-fired backup engine [167].

The streams flowing into and out of the Ryan-Holmes process are shown in Figure 7.63 and are listed in Table 7.65.

The default temperature of the feed stream entering the Ryan-Holmes process is 81 °F [167]. The energy consumption of each component of the Ryan-Holmes process is calculated as follows:

The natural gas consumption rate of the turbines is calculated as [167]:

$$E_t = \frac{Q_{RH}}{45} \cdot 25,800 \cdot \frac{24[\text{hrs}]}{1[\text{d}]} \cdot \frac{1[\text{Mscf}]}{1,000[\text{scf}]} \quad \left[\frac{\text{Mscf}}{\text{d}} \right] \quad (7.100)$$

'Surface
Processing
2.2.5'

where E_t = turbine natural gas consumption rate [Mscf/d] and Q_{RH} = volumetric flow rate of the Ryan-Holmes feed stream [MMscf/d]. Equation 7.100 linearly scales the turbine natural gas consumption rate based on the 45 MMscf/d feed stream throughput in the NETL Ryan-Holmes model, in which the turbines consume a total of 25,800 scf/hr [167].

The natural gas consumption rate of the compressors is calculated as [167]:

$$E_c = \frac{Q_{RH}}{45} \cdot 110,519 \cdot \frac{24[\text{hrs}]}{1[\text{d}]} \cdot \frac{1[\text{Mscf}]}{1,000[\text{scf}]} \quad \left[\frac{\text{Mscf}}{\text{d}} \right] \quad (7.101)$$

where E_c = compressor natural gas consumption rate [Mscf/d]; Q_{RH} = volumetric flow rate of the Ryan-Holmes feed stream [MMscf/d]. Equation 7.101 linearly scales the compressor natural gas consumption rate based on the 45 MMscf/d feed stream throughput in the NETL Ryan-Holmes model, in which the compressors consume a total of 110,519 scf/hr [167], [178].

The natural gas consumption rate of the oil heater is calculated as [167]:

$$E_h = \frac{Q_{RH}}{45} \cdot 14,589 \cdot \frac{24[\text{hrs}]}{1[\text{d}]} \cdot \frac{1[\text{Mscf}]}{1,000[\text{scf}]} \quad \left[\frac{\text{Mscf}}{\text{d}} \right] \quad (7.102)$$

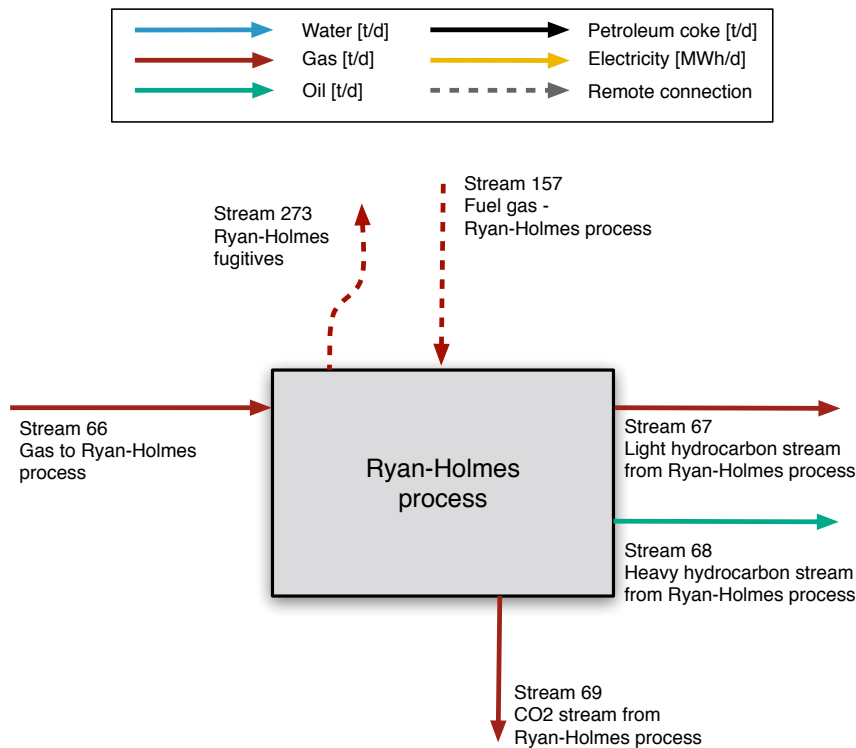


Figure 7.63: Streams flowing into and out of the Ryan-Holmes separation process. All streams measured in tonnes per day excepting electricity which is measured in MWh/d.

where E_h = oil heater natural gas consumption rate [Mscf/d]; Q_{RH} = volumetric flow rate of the Ryan-Holmes feed stream [MMscf/d]. Equation 7.102 linearly scales the oil heater natural gas consumption rate based on the 45 MMscf/d feed stream throughput in the NETL Ryan-Holmes model, in which the hot oil heater consumes 14,589 scf/hr [167].

The diesel consumption rate of the backup engine is calculated as [167]:

$$E_e = \frac{Q_{RH}}{45} \cdot 57 \cdot \frac{2.63}{24} \quad \left[\frac{\text{gal}}{\text{d}} \right] \quad (7.103)$$

where E_e = backup engine consumption rate [gal/d] and Q_{RH} = volumetric flow rate of the Ryan-Holmes feed stream [MMscf/d]. Equation 7.102 linearly scales the oil heater natural gas consumption rate based on the 45 MMscf/d feed stream throughput in the NETL Ryan-Holmes model in which the hot oil heater consumes diesel at a rate of 57 gal/d. The default usage rate of the backup engine is 2.63 hr/d [167].

7.24.1 Defaults for Ryan-Holmes unit

Defaults for the Ryan Holmes process are shown in Table 7.66.

Table 7.66: Default inputs for Ryan-Holmes process.

Param.	Description	Eq. no.	Default	Literature range	Unit	Sources	Notes
Q_{RH}	Volumetric flow rate into Ryan-Holmes feedstream	-	var. 81	-	[MMscf/d] [°F]	'Flow sheet'	[167]
RH_{IN}	Temperature of entering Holmes process	-	-	-	-		
RH_{backup}	Usage rate of Ryan-Holmes backup engine	-	2.63	-	[hrs/d]		[167]

Table 7.67: Streams flowing into and out of the gas flooding compressor. I/O denotes input or output stream

Flow name	Stream	I/O	Source/Destination	Units	Notes
CO2 from offsite for gas flooding	77	I	Offsite	[t/d]	
Hydrocarbon gas from offsite for gas flooding	78	I	Offsite	[t/d]	
N2 from offsite for gas flooding	79	I	Offsite	[t/d]	
Fuel gas - Gas flooding compressor	157	I	Fuel gas system	[t/d]	
Electricity - Gas flooding compressor	191	I	Electricity generation and imports	[t/d]	
Gas to gas flooding wells	80	O	Reservoir	[t/d]	
Fugitives - Gas flooding compressor	278	O	Atmosphere	[t/d]	

7.25 Gas flooding compressor

The streams flowing into and out of the gas flooding compressor are shown in Figure 7.64 and are listed in Table 7.67.

The energy consumed by gas flooding compressors is a function of the compression ratio between the compressor inlet pressure and the compressor outlet pressure, the volumetric gas flow rate, and the compressor efficiency.

7.25.0.1 Gas compression ratio

The total gas compression ratio is calculated using:

$$R_C = \frac{p_d}{p_s} \quad [-] \quad (7.104)$$

where p_d = discharge pressure [psia]; and p_s = suction pressure [psia].

Multi-stage compression applies when $R_C > 5$ [9, p. 295]. The compression of gas generates significant amount of heat, but compressors can only handle a limited temperature change. Multiple stage compressors allow cooling between stages making compression less adiabatic and more isothermal. OPGEE sets the compression ratio for each of the N stages equal to the N^{th} root of the total compression ratio [9, p. 295]:

$$\text{If } \frac{p_d}{p_s} < 5, \text{ then } R_C = \frac{p_d}{p_s}, \text{ otherwise if } \left(\frac{p_d}{p_s}\right)^{\frac{1}{2}} < 5, \text{ then } R_C = \left(\frac{p_d}{p_s}\right)^{\frac{1}{2}}, \dots \quad (7.105)$$

*'Production
& Extraction
2.5.1'*

where p_d = discharge pressure [psia]; and p_s = suction pressure [psia].

The number of stages is determined from the calculation of the compression ratio, as shown in eq. (7.105). OPGEE allows a maximum of 5 stages of compression.

7.25.0.2 Gas compressor suction temperature

When multiple stage compressors are used the gas must be cooled between stages to reduce the adiabatic work of compression. The discharge temperature at a given

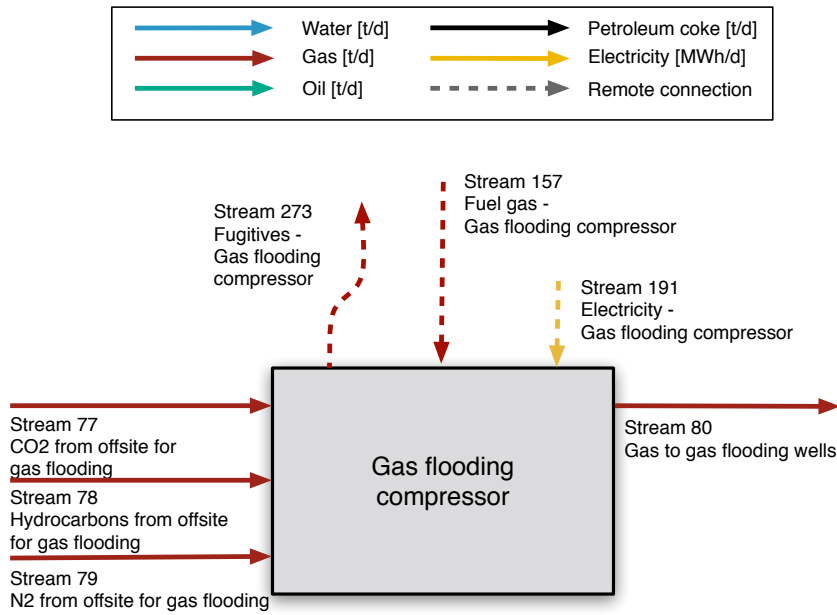


Figure 7.64: Streams flowing into and out of the gas flooding compressor. All streams measured in tonnes per day excepting electricity which is measured in MWh/d.

compressor stage is calculated using [67, p. 105]:

$$\frac{T_d}{T_s} = \left(\frac{p_d}{p_s} \right)^{\left[\frac{z_s(C_{p/v}-1)}{C_{p/v}} \right]} \quad [-] \quad (7.106)$$

where T_d = discharge temperature [$^{\circ}\text{R}$]; T_s = suction temperature [$^{\circ}\text{R}$]; $C_{p/v}$ = ratio of specific heats at suction conditions; and z_s = suction z-factor.

The suction temperature of the subsequent compressor is estimated assuming 80% interstage cooling (imperfect cooling) so that:

$$T_{s2} = \lambda_{\Delta T} (T_d - T_s) + T_s \quad [^{\circ}\text{R}] \quad (7.107)$$

where T_{s2} = suction temperature of stage 2 compressor [$^{\circ}\text{R}$]; and $\lambda_{\Delta T}$ = fraction of temperature increase remaining after cooling, 0.2 [fraction]. The default of $\approx 80\%$ interstage cooling is taken from an example of imperfect cooling in [179, Table 7].

7.25.0.3 Compressor brake horsepower

OPGEE assumes use of a reciprocating compressor. The ideal isentropic horsepower is calculated using [67, p. 105]:

$$-W_N = \left\{ \frac{C_{p/v}}{(C_{p/v}-1)} \right\} \left(3.027 \cdot \frac{14.7}{520} \right) T_s \left\{ \left(\frac{p_d}{p_s} \right)^{\frac{z_s(C_{p/v}-1)}{C_{p/v}}} - 1 \right\} \quad \left[\frac{\text{hp-d}}{\text{MMscf}} \right] \quad (7.108)$$

where W_N = adiabatic work of compression of N^{th} stage [hp-d/MMscf] (-W denotes work output); $C_{p/v}$ = ratio of specific heats [-]; T_s = suction temperature [$^{\circ}\text{R}$];

'Production
& Extraction
2.5.3'

'Production
& Extraction
2.5.6,2.6.5,2.7.6'

p_s = suction pressure [psia]; p_d = discharge pressure [psia]; and z_s = suction z-factor. The constant 3.027 has a unit of [hp-d/MMscf-psia]. Standard temperature (520 [$^{\circ}$ R]) and pressure (14.7 [psia]) are used as the initial values.

The total work of compression of the multiple stage compressor is multiplied by the compressor discharge rate and divided by the compressor efficiency to calculate the brake horsepower requirement as:

$$\text{BHP}_C = \sum_{N=1}^S \frac{W_N Q_d}{\eta_C} \quad [\text{hp}] \quad (7.109)$$

*'Production
& Extraction
2.5.8,2.6.7,2.7.8'*

where Q_d = compressor discharge rate [MMscf/d]; η_C = compressor efficiency [fraction]; and S = number of compressor stages.

[TBD: INSERT DEFAULTS TABLE]

Table 7.68: Streams flowing into and out of the gas lifting compressor. I/O denotes input or output stream

Flow name	Stream	I/O	Source/Destination	Units	Notes
Lifting gas to compressor	40	I	Gas partition A	[t/d]	
Electricity - Lifting gas compressor	178	I	Electricity generation and imports	[t/d]	
Fuel gas - Lifting gas compressor	154	O	Consumed in process	[t/d]	
Lifting gas to wellbore	42	O	Well/Downhole pump	[t/d]	
Fugitives - Lifting gas compressor	258	O	Atmosphere	[t/d]	

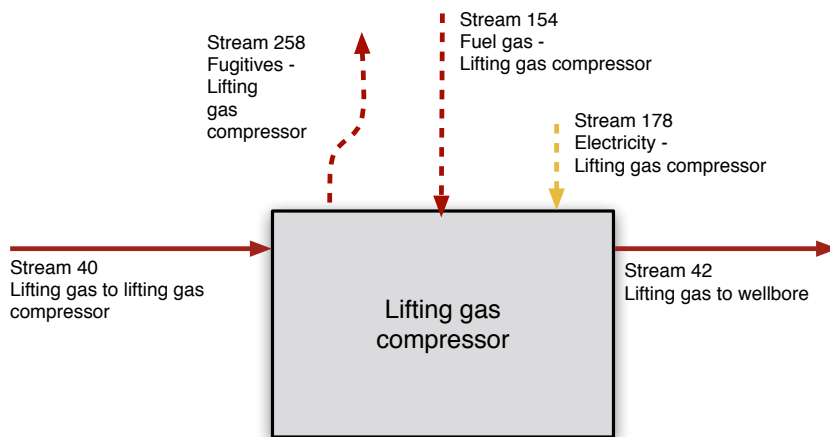


Figure 7.65: Streams flowing into and out of the gas lifting compressor. All streams measured in tonnes per day excepting electricity which is measured in MWh/d.

7.26 Gas lifting compressor

The streams flowing into and out of the gas lifting compressor are shown in Figure 7.65 and are listed in Table 7.68.

The treatment of gas lifting compressors uses a similar worksheet for the gas flooding compressor, described in detail in Section ??.

Differences in treatment of the gas lifting compressor include:

[TBD: EXAMINE ANY DIFFERENCES COMPARED TO GAS FLOODING COMPRESSOR SHEET]

Table 7.69: Streams flowing into and out of the gas reinjection compressor. I/O denotes input or output stream

Flow name	Stream	I/O	Source/Destination	Units	Notes
Gas to reinjection	46	I	Gas partition B	[t/d]	
Electricity - Lifting gas compressor	179	I	Electricity generation and imports	[t/d]	
Fuel gas - Lifting gas compressor	155	O	Consumed in process	[t/d]	
Gas to reinjection wells	47	O	HC gas reinjection wells	[t/d]	
Fugitives - Reinjection compressor	259	O	Atmosphere	[t/d]	

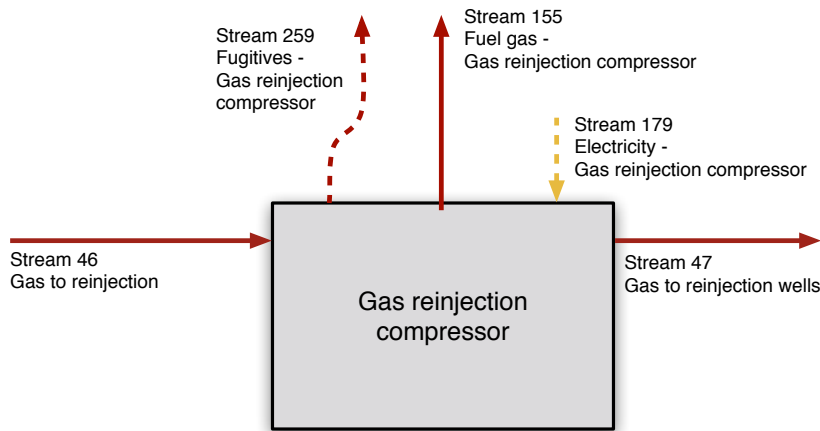


Figure 7.66: Streams flowing into and out of the gas reinjection compressor. All streams measured in tonnes per day excepting electricity which is measured in MWh/d.

7.27 Gas reinjection compressor

The treatment of gas reinjection compressors uses a similar worksheet for the gas flooding compressor, described in detail in Section ??.

Differences in treatment of the gas lifting compressor include:

[TBD: EXAMINE ANY DIFFERENCES COMPARED TO GAS FLOODING COMPRESSOR SHEET]

The streams flowing into and out of the gas reinjection compressor are shown in Figure 7.66 and are listed in Table 7.69.

Table 7.70: Streams flowing into and out of the CO₂ reinjection compressor. I/O denotes input or output stream

Flow name	Stream	I/O	Source/Destination	Units	Notes
AGR CO ₂ to reinjection	73	I	Acid gas removal	[t/d]	
CO ₂ -rich stream from membrane	65	I	CO ₂ separation membrane	[t/d]	
CO ₂ stream from Ryan-Holmes	69	I	Ryan-Holmes process	[t/d]	
Fuel gas - CO ₂ reinjection compressor	155	I	Fuel gas system	[t/d]	
Electricity - CO ₂ reinjection compressor	179	I	Electricity generation and imports	[t/d]	
CO ₂ to reinjection wells	47	O	CO ₂ reinjection wells	[t/d]	
Fugitives - CO ₂ reinjection compressor	259	O	Atmosphere	[t/d]	

7.28 CO₂ reinjection compressor

The treatment of CO₂ reinjection compressors uses a similar worksheet for the gas flooding compressor, described in detail in Section ??.

Differences in treatment of the gas lifting compressor include:

[TBD: EXAMINE ANY DIFFERENCES COMPARED TO GAS FLOODING COMPRESSOR SHEET]

The streams flowing into and out of the CO₂ reinjection compressor are shown in Figure 7.67 and are listed in Table 7.70.

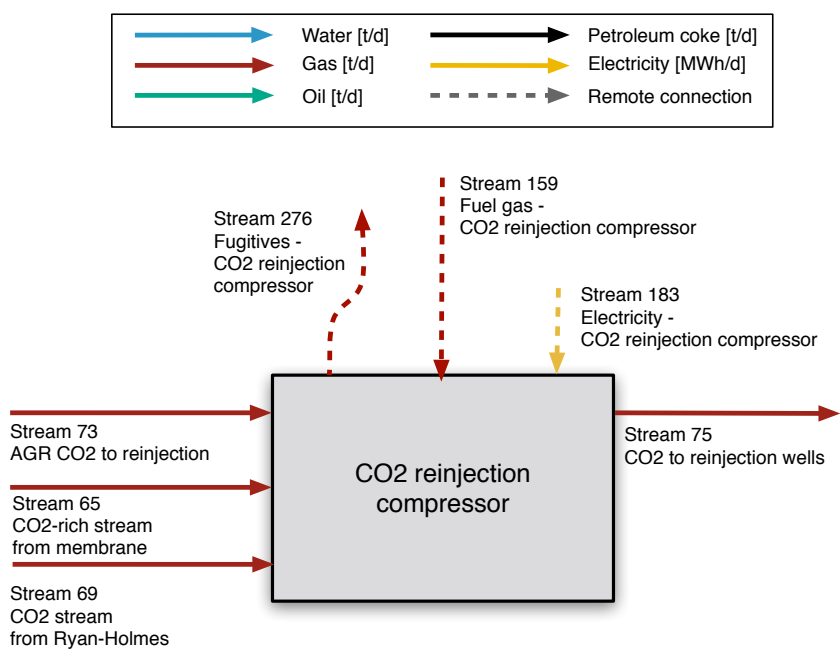


Figure 7.67: Streams flowing into and out of the CO₂ reinjection compressor. All streams measured in tonnes per day excepting electricity which is measured in MWh/d.

Table 7.71: Streams flowing into and out of the sour gas reinjection compressor. I/O denotes input or output stream

Flow name	Stream	I/O	Source/Destination	Units	Notes
Gas to sour gas reinjection compressor	70	I	Glycol dehydrator	[t/d]	
Fuel gas - Sour gas reinjection compressor	158	I	Fuel gas system	[t/d]	
Electricity - Sour gas reinjection compressor	182	I	Electricity generation and imports	[t/d]	
Sour gas to sour gas reinjection wells	71	O	Sour gas reinjection wells	[t/d]	
Fugitives - Sour gas reinjection compressor	274	O	Atmosphere	[t/d]	

7.29 Sour gas reinjection compressor

The treatment of sour gas reinjection compressors uses a similar worksheet for the gas flooding compressor, described in detail in Section ??.

Differences in treatment of the gas lifting compressor include:

[TBD: EXAMINE ANY DIFFERENCES COMPARED TO GAS FLOODING COMPRESSOR SHEET]

The streams flowing into and out of the sour gas reinjection compressor are shown in Figure 7.68 and are listed in Table 7.71.

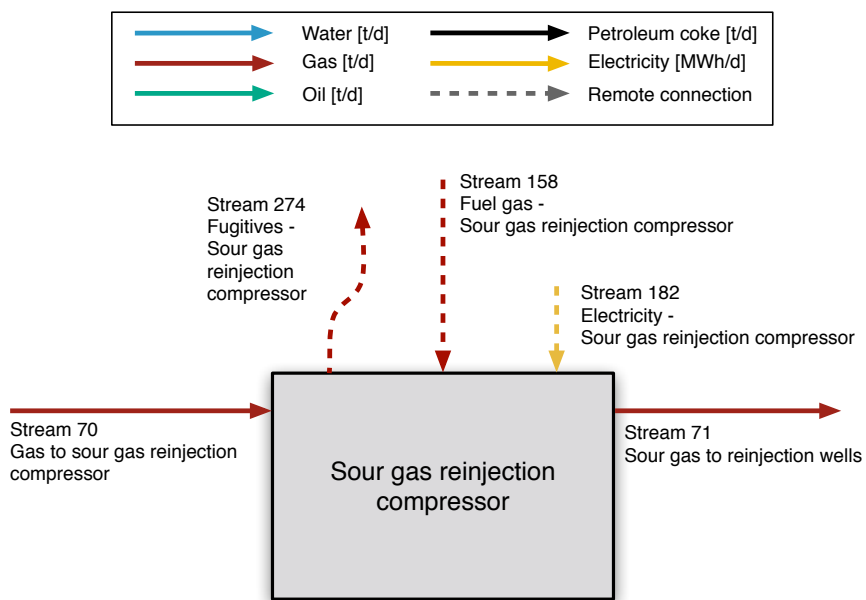
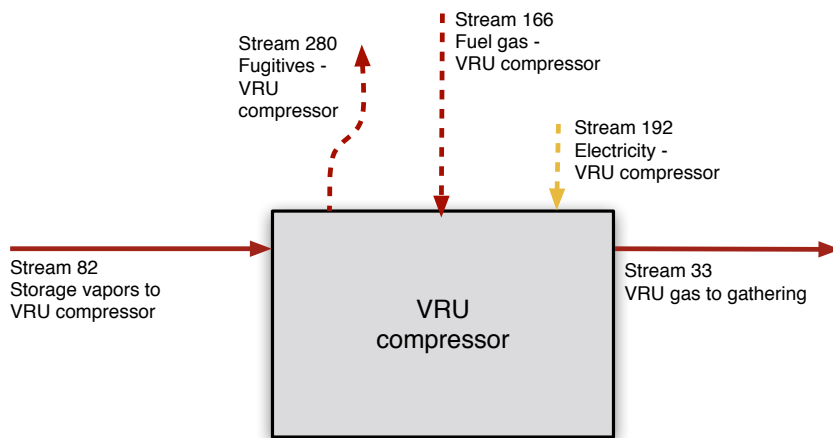
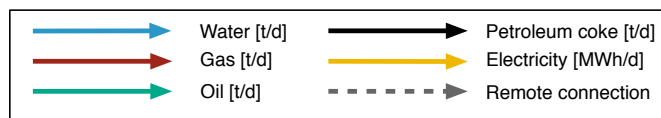


Figure 7.68: Streams flowing into and out of the sour gas reinjection compressor. All streams measured in tonnes per day excepting electricity which is measured in MWh/d.

Table 7.72: Streams flowing into and out of the VRU compressor. I/O denotes input or output stream

Flow name	Stream	I/O	Source/Destination	Units	Notes
Storage vapors to VRU compressor	82	I	Crude oil storage	[t/d]	
Fuel gas - VRU compressor	166	I	Fuel gas system	[t/d]	
Electricity - VRU compressor	192	I	Electricity generation and imports	[t/d]	
VRU gas to gathering system	33	O	Gas gathering	[t/d]	
Fugitives - VRU compressor	280	O	Atmosphere	[t/d]	

**Figure 7.69: Streams flowing into and out of the VRU compressor. All streams measured in tonnes per day excepting electricity which is measured in MWh/d.**

7.30 VRU compressor

The treatment of vapor recovery unit (VRU) compressors uses a similar worksheet for the gas flooding compressor, described in detail in Section ??.

Differences in treatment of the gas lifting compressor include:

[TBD: EXAMINE ANY DIFFERENCES COMPARED TO GAS FLOODING COMPRESSOR SHEET]

The streams flowing into and out of the VRU compressor are shown in Figure 7.69 and are listed in Table 7.72.

7.31 Pre-membrane compressor

The treatment of pre-membrane compressors uses a similar worksheet for the gas flooding compressor, described in detail in Section ??.

Differences in treatment of the gas lifting compressor include:

[TBD: EXAMINE ANY DIFFERENCES COMPARED TO GAS FLOODING COMPRESSOR SHEET]

7.32 Transmission compressor

The treatment of transmission compressors uses a similar worksheet for the gas flooding compressor, described in detail in Section ??.

Differences in treatment of the gas lifting compressor include:

[TBD: EXAMINE ANY DIFFERENCES COMPARED TO GAS FLOODING COMPRESSOR SHEET]

7.33 LNG liquefaction

7.34 LNG Regasification

7.35 LNG transport

7.36 Storage compressor

The treatment of gas storage compressors uses a similar worksheet for the gas flooding compressor, described in detail in Section ??.

Differences in treatment of the gas lifting compressor include:

[TBD: EXAMINE ANY DIFFERENCES COMPARED TO GAS FLOODING COMPRESSOR SHEET]

7.37 Post-storage compressor

The treatment of post-storage compressors uses a similar worksheet for the gas flooding compressor, described in detail in Section ??.

Differences in treatment of the gas lifting compressor include:

[TBD: EXAMINE ANY DIFFERENCES COMPARED TO GAS FLOODING COMPRESSOR SHEET]

7.38 HC gas injection wells

7.39 CO₂ injection wells

7.40 Sour gas injection wells

7.41 Steam injection wells

7.42 Gas storage wells

7.43 Storage separator

7.44 Gas partition A

7.45 Gas partition B

7.46 Fuel gas consumed

7.47 Maintenance

7.47.1 Introduction to maintenance operations

Emissions from maintenance include venting and fugitives associated with compressor blowdowns, well workovers and cleanups, separator cleaning and repair, and gathering pipeline maintenance and pigging. Other maintenance emissions are believed to be below the significance cut-off and are not included.

7.47.2 Calculations for maintenance operations

Emissions from maintenance operations are classified in Table C.5. Emissions from maintenance operations are either very small (e.g., embodied energy consumed in maintenance parts) or are tracked in the '*Venting & Fugitives*' worksheet (see Section ??). For this reason, OPGEE does not perform specific maintenance emissions calculations in the separate '*Maintenance*' worksheet.

7.47.3 Defaults for maintenance operations

Defaults used in the calculation of emissions from maintenance operations are discussed in Section ??.

7.48 Waste treatment and disposal

7.48.1 Introduction to waste treatment and disposal

Emissions from waste disposal occur during routine oilfield maintenance operations (e.g., disposal of residual hazardous waste products) due to clean up operations, or due to one-time events such as decommissioning of oilfield equipment. Emissions occur offsite due to the energy demands of waste disposal and the transport requirements for moving waste to waste treatment or disposal sites. A complete list of emissions sources, along with their categorization and estimated magnitude, is shown in Table C.6.

7.48.2 Calculations for waste treatment and disposal

Because waste treatment emissions only occur sporadically, they are likely to be small when amortized over the producing life of an oil field. For this reason, emissions from waste treatment are considered below the significance cutoff in OPGEE v3.0a.

Possible exceptions could be the treatment and disposal of fracturing fluids and fracturing flow-back water, due to the large volumes produced. Future versions of the model may include these factors.

7.48.3 Defaults for waste treatment

Waste treatment emissions default to 0 gCO₂/MJ. Any waste treatment emissions are assumed to be captured in the small sources emissions default parameter. *'Active Field 3.6'*

7.49 Crude oil transport

7.49.1 Introduction to crude oil transport

Crude oil transport includes all activities associated with moving crude oil from a production facility to a refinery. In the case of land transport, this generally involves transport via pipeline to the refinery. Pipelines are powered by natural gas, oil, or electric-powered drivers. In some instances, rail transport is used for overland transport. In the case of inter-continental trade, crude oil is transported to a loading dock, loaded onto a tanker or barge, transported via ship over water, unloaded at the destination, and finally transported to a refinery. Transport emissions occur due to energy consumption by transport equipment and due to fugitive emissions from loading and unloading operations. In OPGEE, transport emissions are modeled using methods and data from CA-GREET [111]. Transport emissions calculations allow for variations in transport modes, distance travelled, and fuel mix in each mode.

7.49.2 Calculations for crude oil transport

OPGEE crude oil transport calculations use sets of transport modes, transport propulsion technologies in each mode (most commonly one technology per mode), and transport fuels. Emissions are tracked per species of GHG. Transport modes include tanker (T), barge (B), pipeline (P), rail (R), and truck (TR). Pipelines include two propulsion technologies: turbines (GT) and reciprocating engines (RE). Fuels used in transport include diesel fuel (di), residual oil (ro), natural gas (ng), and electricity (el).

The effectiveness crude oil transport [Btu/ton-mi] is calculated for a variety of modes using a similar general form. Each mode has an effectiveness U . For example, tanker transport effectiveness U_T is calculated as:

$$U_T = \frac{\eta_T l_T P_T}{v_T C_T} \quad \left[\frac{\text{Btu}}{\text{ton-mi}} \right] = \frac{\left[\frac{\text{Btu}}{\text{hp-hr}} \right] [-] [\text{hp}]}{\left[\frac{\text{mi}}{\text{hr}} \right] [\text{ton}]} \quad (7.110)$$

*'Crude
Transport
2.2'*

where U_T = specific energy intensity of crude oil transport via tanker [Btu/ton-mi]; η_T = efficiency of tanker transport [Btu/hp-hr]; l_T = load factor of tanker (different on outbound and return trip) [-]; P_T = tanker power requirements [hp]; v_T = tanker velocity [mi/hr]; and C_T is tanker capacity [ton/tanker]. Barge and truck transport effectiveness U_B and U_{TR} are calculated in an analogous fashion.

For the case of pipeline and rail transport, the calculation is simpler. For pipeline transport the effectiveness is calculated as follows:

$$U_P = \sum_{j \in GT, RE} \lambda_{Pj} U_{Pj} \quad \left[\frac{\text{Btu}}{\text{ton-mi}} \right] = [-] \left[\frac{\text{Btu}}{\text{ton-mi}} \right] \quad (7.111)$$

*'Crude
Transport
2.2'*

where λ_{Pj} = fraction of each pipeline pumping technology j [-]; and U_{Pj} = effectiveness of pipeline transport for technology j [Btu/ton-mi]. For rail transport, only one technology exists, so no summation is required.

Back haul trips are calculated using GREET factors for the energy intensity of return trips [28]

The energy-specific transport energy intensity is calculated from the transport effectiveness using the energy density of crude oil. For example, in the case of tanker transport:

$$e_T = U_T \frac{1}{LHV_o} \rho_w \gamma_o \frac{1}{2000} \quad (7.112)$$

'Crude
Transport
2.4'

$$\left[\frac{\text{Btu}}{\text{MMBtu-mi}} \right] = \left[\frac{\text{Btu}}{\text{ton-mi}} \right] \left[\frac{\text{bbl}}{\text{MMBtu}} \right] \left[\frac{\text{lb}}{\text{bbl water}} \right] \left[\frac{\text{lb/bbl oil}}{\text{lb/bbl water}} \right] \left[\frac{\text{lb}}{\text{ton}} \right] \quad (7.113)$$

where UE_T = crude oil transport intensity per unit of energy transported [Btu/MMBtu-mi], LHV_o = crude lower heating value [MMBtu/bbl]; ρ_w = density of water [lb/bbl]; γ_o = crude specific gravity [-]; and 1/2000 = conversion factor between lb and ton.

Calculating emissions of GHG species associated with the consumption of a given energy type in a given device is performed via multiplication with the appropriate emissions factor. For example, in the case of tanker emissions:

$$EM_{Ti} = e_T \sum_k \lambda_{Tk} EF_{Tki}, \quad (k \in di, ro, ng) \quad (7.114)$$

'Crude
Transport
Table 2.4'

$$\left[\frac{\text{g}}{\text{MMBtu-mi}} \right] = \left[\frac{\text{Btu}}{\text{MMBtu-mi}} \right] [-] \left[\frac{\text{g}}{\text{Btu}} \right]$$

where EM_{Ti} = emissions of species i from tankers [g/MMBtu-mi]; λ_{Tk} = fraction of fuel k used in tankers [-]; and EF_{Tki} = emissions factor for fuel k , species i consumed in tankers [g/Btu]. Other modes are calculated similarly.

The total CO₂ equivalent emissions are then computed by weighting by gas global warming potential (GWP). Again, for the case of tanker transport:

$$EM_T = \sum_i EM_{Ti} GWP_i, \quad \left[\frac{\text{g CO}_2 \text{ eq.}}{\text{MMBtu-mi}} \right] = \left[\frac{\text{g}}{\text{MMBtu-mi}} \right] \left[\frac{\text{g CO}_2 \text{ eq.}}{\text{g}} \right] \quad (7.115)$$

'Crude
Transport
Table 2.4'

where GWP_i = GWP of species i .

The total energy consumption from transport is computed using the distances and fractions of transport, along with the mode-specific energy intensity of transport:

$$E_{TR} = \sum_j \lambda_j D_j UE_j \quad (j \in T, B, P, R) \quad (7.116)$$

'Crude
Transport
3.1'

$$\left[\frac{\text{Btu}}{\text{MMBtu}} \right] = [\text{mi}] \left[\frac{\text{Btu}}{\text{MMBtu-mi}} \right] [-]$$

where D_j = distance of crude oil transport in mode j [mi]; UE_j = energy-specific transport effectiveness for mode j [Btu/MMBtu-mi]; and λ_j = fraction of crude oil transported in mode j . The sum of fractional transport shares λ_j can be greater than 1, because some crude may be transported via both pipeline and tanker, for example.

The total emissions are calculated identically:

$$EM_{TR} = \sum_j \lambda_j D_j EM_j \quad (j \in T, B, P, R) \quad (7.117)$$

'Crude
Transport
3.2'

$$\left[\frac{\text{g CO}_2 \text{ eq.}}{\text{MMBtu}} \right] = [\text{mi}] \left[\frac{\text{g CO}_2 \text{ eq.}}{\text{MMBtu-mi}} \right] [-]$$

where EM_j are the emissions from mode j on a CO₂-equivalent basis.

7.49.3 Defaults for crude oil transport

Defaults for crude oil transport are generally taken from the CA-GREET model, with some modifications and simplifications applied. Defaults for surface operations are given below in Table 7.73.

Table 7.3: Default inputs for Transport.

Param.	Description	Eq. no.	Default	Literature range	Unit	Sources	Notes
C_j	Transport capacity of mode j	-	"Transport"	Table 2.1	[ton]	[Btu/MMBTu-mi]	[28]
e_n	Energy intensity of transport in mode j by energy unit transported	(7.112)	-	-	-	-	
EF_{ki}	Emissions factor for fuel k , species i , mode j	-	"Emissions Factors"	Table 1.5	[g/MMBTu]	[g /MMBTu-mi]	a
EM_{ji}	Emissions of species i by mode j	(7.114)	-	-	-	-	
EM_j	Emissions of all GHGs in CO ₂ eq. units by mode j	(7.115)	-	-	-	-	
ET_R	Total energy use in transport	(7.116)	-	-	-	-	a
EN_{TR}	Total emissions from in transport	(7.117)	-	-	-	-	a
η_j	Efficiency of transport mode j	-	"Transport"	Table 2.3	[Btu/hp-hr]	[Btu/hp-hr]	[28]
GWP_i	Global warming potential for species i	-	"Input data"	Table 2.1	[gCO ₂ eq./g]	[gCO ₂ eq./g]	[28]
γ_o	Specific gravity of crude oil	-	0.876	0.8-1.05	[-]	[-]	[116]
l_j	Load factor of mode j	-	"Transport"	Table 2.3	[%]	[%]	[28]
$\lambda_{j_1j_2}$	Fraction of technology j_2 used in mode j_1	-	"Transport"	Table 2.6	[%]	[%]	[28], Est.
λ_{ik}	Fraction of fuel k used in mode j	-	"Transport"	Table 2.7	[-]	[-]	Est.
P_j	Power consumption of mode j	-	"Transport"	Table 2.2	[hp]	[lb/bbl]	[28]
ρ_w	Density of fresh water	-	350.4	-	[Btu/ton-mi]	[Btu/ton-mi]	[155]
U_j	Transport effectiveness in mode m	(7.111), (7.110)	"Transport"	Table 2.5	[Btu/ton-mi]	[Btu/ton-mi]	[28]
$U_{j_1j_2}$	Transport effectiveness of propulsion tech j_2 used in mode j_1	-	"Transport"	Table 2.3	[mi-hr]	[mi-hr]	[28]
v_j	Velocity of mode j	-	"Transport"	Table 2.3	[mi-hr]	[mi-hr]	[28]

^a Default crude oil shipment distance in CA-GREET is 750 mi for a one-way trip [28].

7.50 Petcoke transport

??

[TBD: CHECK HOW PETCOKE TRANSPORT MODEL DIFFERS FROM OTHER
TRANSPORT SHEETS]

7.51 Gas distribution

??

7.52 Fuel gas inputs

??

7.53 Electricity generation and imports

??

The '*Electricity*' supplemental worksheet calculates the energy consumption of onsite electricity generation. The '*Electricity*' worksheet does not include electricity co-generation in steam generation system. Available generation technologies include natural gas generator set, natural gas turbine, and diesel generator set. The user enters the capacity of onsite electricity generation as a fraction of the electricity required. The fraction of electricity above 1.0 is exported. In the '*Electricity*' worksheet the amount of electricity generated onsite is calculated as:

$$E_{el,gen} = f_{el} \cdot E_{el,req} \quad \left[\frac{\text{MMBtu}}{\text{d}} \right] \quad (7.118)$$

where $E_{el,gen}$ = onsite electricity generation [MMBtu/d]; f_{el} = fraction of required electricity generated onsite; and $E_{el,req}$ = electricity required. The electricity required is calculated in the '*Energy Consumption*' worksheet.

The energy consumption of the generator is calculated from the appropriate driver in the '*Drivers*' worksheet as:

$$e_{GS} = \frac{e_D}{0.75\eta_G} \quad \left[\frac{\text{Btu}}{\text{kWh}} \right] = \frac{\left[\frac{\text{Btu}}{\text{bhp-hr}} \right]}{\left[\frac{\text{bkW}}{\text{bhp}} \right] [-]} \quad (7.119)$$

where e_{GS} = energy consumption of generator set [Btu/kWh]; η_G = efficiency of the electricity generator (not including driver) [-]; and e_D = driver energy consumption [Btu/bhp-hr]. The appropriate driver is determined by the required size based on the electricity generation capacity as calculated in eq. (7.118).

Once the onsite electricity generation, $E_{el,gen}$, and the energy consumption of the electricity generator, e_{GS} , are calculated the total energy consumption of onsite electricity generation is calculated as:

$$E_{EG} = E_{el,gen} \cdot 0.000293 \cdot e_{GS} \quad \left[\frac{\text{MMBtu}}{\text{d}} \right] = \left[\frac{\text{MMBtu}}{\text{d}} \right] \left[\frac{\text{kWh}}{\text{Btu}} \right] \left[\frac{\text{Btu}}{\text{kWh}} \right] \quad (7.120)$$

where E_{EG} = energy consumption of onsite electricity generation [MMBtu/d].

In addition to calculating the energy consumption of onsite electricity generation, this worksheet determines the grid electricity mix and the allocation method of credits from electricity export (see Section 8.2 on the '*Fuel Cycle*' worksheet). The user is allowed to choose between two allocation methods for credit from electricity export: (i) allocation by substitution of grid electricity, and (ii) allocation by substitution of natural-gas-based electricity. The default allocation method is the substitution of natural-gas-based electricity. This method prevents achieving unreasonably large credits from operations with significant power generation.

7.54 NGL or diluent production or imports

??

7.55 Gas flooding

Introduction to gas flooding Gas flooding can be performed with natural gas, molecular nitrogen (N_2), carbon dioxide (CO_2), air, or oxygen (O_2). Note that OPGEE v3.0a does not include air or oxygen flooding, so any parameters there are included for reference only. If gas flooding via N_2 injection is chosen, the work of air separation must be accounted for. Industrial capacity N_2 plants have specific work on the order of 0.25 kWh/Nm³ [180]. The largest N_2 separation plant in the world serves to provide N_2 for injection into the Cantarell field in Mexico [99]. This facility has compression horsepower of 500,500 hp to supply 1,200 MMSCF/d of N_2 at ≈ 1700 psia.

'Production & Extraction 2.8'

OPGEE computes gas flooding work to take gas from 125 psia to reservoir injection pressure.

'Production & Extraction 2.7.4'

Subtracting this work from the reported consumption at Cantarell, we arrive at specific work of ≈ 0.15 kWh/Nm³ for only the air separation component. Depending on the reservoir pressure, OPGEE will then add to this separation work the work to compress N_2 to required pressure. The work for gas injection compressors is modeled as noted above. If reinjected produced natural gas is assumed, then no separation work for N_2 production is required.

OPGEE calculates the reservoir injection pressure based on the choice of the flood gas. If a gas other than CO_2 is the flood gas, then the reservoir injection pressure is calculated as:

$$P_{inj} = P_{res} + 500 + 14.7 \quad [\text{psia}] \quad (7.121)$$

where P_{inj} = reservoir injection pressure [psia] and P_{res} = reservoir pressure [psig]. The term 14.7 converts [psig] to [psia].

CO_2 flooding and minimum miscibility pressure OPGEE assumes that CO_2 injection is performed to achieve a miscible gas flood. If CO_2 is the flood gas, then the reservoir injection pressure must reach the minimum miscibility pressure (MMP). The MMP is the minimum pressure necessary for CO_2 and oil to form a single fluid phase, which increases recovery rates and is the basis of miscible gas flooding. Many factors influence the MMP, such as reservoir temperature, the presence of other chemical species such as H_2S , and the density and composition of the oil [?].

'Production & Extraction 1.2.9'

The default MMP value is estimated using a correlation from the NPC (National Petroleum Council) based on the API gravity and reservoir temperature [11]. However, actual MMP values are usually available for miscible CO_2 flood projects and the actual data should be used whenever possible.

The API gravity of the oil is used to generate an initial estimate, as shown in Table 7.74. The reservoir temperature adjustment is then applied to the initial estimate as shown in table 7.75.

If CO_2 is the flood gas and the MMP is higher than the standard reservoir injection pressure determined in Equation (7.121), then the flood gas compressor injects at the MMP. If the standard reservoir injection pressure calculated in Equation (7.121) is higher than the MMP, then the flood gas compressor injects at the standard reservoir injection pressure.

Table 7.74: Minimum Miscibility Pressure and API Gravity Default Correlation. Source: [11].

API Gravity [°API]	Minimum Miscibility Pressure [psia]
<27	4,000
27-30	3,000
>30	1,200

Table 7.75: Temperature Adjustment to Minimum Miscibility Pressure Default Correlation Source: [11].

Reservoir Temperature [°F]	Adjustment [psia]
120	0
120-150	+200
150-200	+350
200-250	+500

7.55.0.1 CO₂ Enhanced oil recovery and sequestration parameters

CO₂ sequestration calculation In the early stage of a CO₂ flood project, newly acquired CO₂ will account for the entirety of the injected CO₂. As the injected CO₂ proceeds through the reservoir, a proportion of it will be trapped in the reservoir by factors such as blockage by surrounding rocks of low permeability or by trapping within water in the reservoir. The portion of CO₂ that is not immediately trapped will be produced and injected again following its separation from the oil and/or associated gas stream, if applicable, as described in the ?? section. Thus, following CO₂ breakthrough the injected CO₂ will consist of two portions: 1) a newly acquired, never-injected portion and 2) a previously-injected and recycled portion.

An individual molecule of CO₂ injected for EOR may thus transit the reservoir and the surface processing facilities multiple times before it is trapped within the reservoir. OPGEE assumes that a molecule of newly acquired CO₂ will ultimately be sequestered within the reservoir. An example demonstrating this process is the EOR project at the Denver Unit of the Wasson Field in the Texas Permian Basin, where Occidental Petroleum has injected CO₂ since the early 1980s [181]. In a presentation submitted to California's Energy Commission, Occidental Petroleum depicts an accounting of the volume of CO₂ acquired, injected, produced, trapped, recycled, and lost to venting and fugitive emissions during a 25-year period at the Denver Unit flood [182]. Occidental Petroleum indicates that 115 million metric tons of CO₂ were supplied to the project; their material balance calculations indicated that essentially an equivalent amount was sequestered in the reservoir. Venting and fugitives accounted for the loss of 0.3% of the cumulative volume of produced or recycled CO₂ [182].

OPGEE accounts for loss of CO₂ due to terminal blow-down operations or long-term leakage from the reservoir. These factors decrease the overall sequestration rate and are included in the 'GHG Emissions' gathering worksheet section. The gross (before deduction of aforementioned losses) daily CO₂ is calculated as follows:

First, the volumetric injection rate of CO₂ is calculated as:

$$Q_{CO_2} = R_{inj,fg} \cdot Q_o \cdot \frac{1[\text{Mscf}]}{1000[\text{scf}]} \left[\frac{\text{Mscf}}{\text{d}} \right] \quad (7.122)$$

where Q_{CO_2} = the volumetric injection rate of CO₂ [Mscf/d]; $R_{inj,fg}$ = the gas flood-

ing injection ratio [scf/bbl]; and Q_o = the oil production rate [bbl/d].

Second, the CO₂ gross sequestration rate S is calculated as:

$$S_{CO_2} = Q_{CO_2} \cdot f_{CO_2,new} \cdot \frac{1000[\text{scf}]}{1[\text{Mscf}]} \cdot \frac{0.117[\text{lb}]}{1[\text{scf}]} \cdot \frac{453.6[\text{g}]}{1[\text{lb}]} \quad [\frac{\text{g}}{\text{d}}] \quad (7.123)$$

*'Production
& Extraction
2.7.11'*

where S_{CO_2} = the gross sequestration rate of CO₂ [scf/d]; Q_{CO_2} = the volumetric injection rate of CO₂ [Mscf/d]; and $f_{CO_2,new}$ is the proportion of newly acquired CO₂ that has not previously been injected [-].

Long-term leakage rate of sequestered carbon CO₂ that is sequestered over the course of an EOR project must remain sequestered for long-term periods to have a significant impact on climate change mitigation. For this reason, considering the long-term stability of carbon storage is necessary for lifecycle assessment of CO₂-EOR. Many CO₂-EOR projects are located in extensively developed petroleum fields with large amounts of abandoned wells through which previously sequestered CO₂ could migrate and leave the reservoir. Research has investigated the role that these wells may play in allowing trapped CO₂ to leave the reservoir. For example, Kang et al. collected methane emissions data from abandoned wells in Pennsylvania; they concluded that the permeability of such wells was sufficiently low that they present only a "small" risk of allowing leakage of sequestered CO₂ [?].

Computational analyses of reservoir fluid flow have estimated long-term leakage rates through oil and gas wells of CO₂ sequestered by injection into saline aquifers. In one example, Celia et al. [?] used the properties of an area in Alberta, Canada with deep brine aquifers that have the potential to serve as CO₂ sequestration sites. The area also contains many oil and gas wells that could potentially allow the loss of trapped CO₂. After estimating the properties of the geological layers and the oil and gas wells in the target area, Celia et al modeled CO₂ injection into the deep aquifers and subsequent migration over 50 years. Celia et al. found that CO₂ leakage rates through the oil and gas wells were nearly always below 1% [?].

An Intergovernmental Panel on Climate Change's (IPCC) report by Benson, et al. [183] analyzed the general prospects of CO₂ sequestration and long-term leakage in underground geological formations, which include oil and gas reservoirs in the context of EOR operations. Benson et al. indicated — with the stipulation that sequestration sites must be "appropriately selected and managed" — that leakage rates are "likely" to be below 1% over a 1,000 year period; they defined "likely" as a 66%-90% probability [183]. During a 100 year period, Benson, Cook et al stated that is "very likely" (90%-99%) that CO₂ leakage rates would be below 1% [183].

Lastly, NETL's 2013 life-cycle analysis of CO₂ EOR assumes that 100-year leakage rates are between 0% to 1% and its base case value is a 0.5% leakage rate [6]. OPGEE adopts this value for its default long-term CO₂ leakage rate of 0.5%. OPGEE temporally collapses the proportion of CO₂ lost to long-term reservoir leakage and models it occurring at the time of injection.

Blow-down and venting of CO₂ in terminal stage of operation OPGEE allows the user to model an oilfield operator's decision to conduct a blow-down procedure on a CO₂ flood in the final stage of the project. Blow-down entails ceasing CO₂ injection and sealing the injector wells while maintaining production from the producer wells.

Additional oil would be recovered during this terminal-stage pressure decline; CO₂ could be vented following its separation from the produced oil [?].

Leach et al. [?] reviewed the literature to determine whether blow-down procedures are commonly used during the final stage of CO₂ EOR floods. While Leach et al. [?] found a handful of sources indicating that blow-down operations typically occur, their analysis of EOR-specific technical materials did not reveal references to blow-down. For this reason the OPGEE default is that 0% of sequestered CO₂ is lost because of terminal stage blow-down and venting. If the user chooses to select a positive blow-down percentage, then it is considered in the overall life-cycle calculations in the '*GHG Emissions*' gathering worksheet section. An actual blow-down procedure would be a process taking place over weeks and months. OPGEE temporally collapses the blow-down procedure and models it occurring at the time of injection.

*'Production
& Extraction
1.2.9.3'*

7.55.0.2 *Driver fuel consumption*

The total brake horsepower requirement (BHP) is used to determine the driver size. A database of drivers of different types and sizes (natural gas engine, diesel engine, electric motor, etc.) is built in the '*Drivers*' supplementary worksheet using technical worksheets of engine and motor manufacturers such as Caterpillar and General Electric [184, 185]. Natural gas fueled drivers, for example, range from 95 hp engine to 20,500 hp turbine. The appropriate driver is retrieved from a database based on the chosen driver type and the required driver size. Finally the fuel consumption of the component (pump, compressor, etc.) is calculated as:

'Production & Extraction 3.1'

$$E_j = \text{BHP}_j \cdot e_D \cdot \frac{24}{10^6} \quad \left[\frac{\text{MMBtu}}{\text{d}} \right] \quad (7.124)$$

where E_j = component fuel consumption [MMBtu/d]; and e_D = driver fuel consumption [Btu/hp-hr]. The type of fuel consumed (i.e. natural gas, diesel, etc.) is determined by the chosen type of driver.

The driver fuel consumption is required for the calculation of energy consumption of various production components. This includes sucker-rod pumps, electric submersible pumps, water injection pumps, and gas compressors.

7.55.1 Production and extraction defaults

Default values for production and extraction equations are shown in Table 7.76. The data basis for smart defaults for production and extraction modeling are described below.

Table 7.76: Default inputs for production and extraction.

Param.	Description	Eq. no.	Default	Literature range	Unit	Sources	Notes
${}^{\circ}\text{API}$	API gravity	(7.24)	-	-	[-]	[60, p. 47]	
A_p	Pipeline cross sectional area	-	$\pi \left(\frac{D_p}{2}\right)^2$	-	[ft ²]	[69, p. 27]	
BHP_P	Pump brakehorse power	(7.38)	-	-	[hp]	[hp]	
BHP_C	Compressor brakehorse power	(7.109)	-	-	[hp]	[hp]	
BHP_j	Component j brakehorse power	-	-	-	[hp]	[hp]	
C_{sd}	Concentration of dissolved solids	-	5000	-	[mg/L]	[10]	
$C_{p/v}$	Ratio of specific heats	-	1.28	1.16-1.40	[-]	[9, p. 320]	a
D_p	Well diameter	-	2.78	1.04-4.50	[in]	[54, p. 121]	b
η_P	Pump efficiency	-	65%	70%	[-]	[69, p. 27]	c
η_C	Compressor efficiency	-	70%	75-85%	[-]	[67, p. 105]	
E_j	Fuel consumption of component j	(7.124)	-	-	[MMBtu/d]	[Btu/hp-nr]	d
e_D	Driver fuel consumption	-	var.	Section 8.1	[-]	[116]	e
f	Friction factor	(7.30)	0.02	≤ 0.1	[-]	[116]	
γ_o	Oil specific gravity	-	0.84	0.8-1.05	[-]	[118, p. 10]	
γ_g	Gas specific gravity	(7.25)	-	-	[-]	[55, p. 1-481]	
γ_w	Water specific gravity	(5.33)	-	-	[-]	[118]	
γ_l	Liquid mixture specific gravity	(7.35)	-	-	[-]	[118]	
g_c	Gravitational constant	-	32.2	[lbm-ft/lbf-s ²]	[ft]	Figure 4.3	
h	Well depth	-	7240	-	[ft]	[ft]	
h_{tot}	Total head	(7.27)	-	-	[ft]	[ft]	
h_{el}	Elevation head	-	h	-	[ft]	[ft]	
h_f	Frictional head	(7.28)	-	-	[ft]	[9, p. 447]	
I_{MI}^{di}	Diesel intensity, integrated mine	-	-	-	[gal/bbl SCO]	[gal/bbl oilbit]	
I_{MN}^{di}	Diesel intensity, non-integrated mine	-	-	-	[kWh/bbl SCO]	[kWh/bbl oilbit]	
I_{MI}^{el}	Electricity intensity, integrated mine	-	-	-	[kWh/bbl SCO]	[kWh/bbl oilbit]	
I_{MN}^{el}	Electricity intensity, non-integrated mine	-	-	-	[scf/bbl SCO]	[scf/bbl oilbit]	
I_{MI}^{ng}	Natural gas intensity, integrated mine	-	-	-	[-]	[lbm/lbmol]	
I_{NG}^{MN}	Natural gas intensity, non-integrated mine	-	-	-	[-]	[4, p. 35]	f
λ_o	Volume fraction of oil	(7.36)	$1 - \lambda_o$	var.	[-]	[lbm/lbmol]	
λ_w	Volume fraction of water	-	$1 - \lambda_o$	-	[-]	[lbm/lbmol]	
MW_g	Gas molecular weight	-	-	-	[-]	[lbm/lbmol]	

Continued on next page..

Continued from previous page

Param.	Description	Eq. no.	Default	Literature range	Unit	Sources	Notes
μ_l	Fluid viscosity	-	var.	-	[cP] [unitless]	[119]	
Nre	Reynolds number	(7.29)	-	-	[-]	Section 4.3.0.3	
N_W	Number of producing wells	-	$\frac{Q_o [\text{bbl/d}]}{183[\text{bbl/well-d}]}$	-	[psi]	[4, p. 35]	
p_b	Base pressure	-	14.7	-	[psi] or [psia]		
p_d	Flow discharge pressure	-	var.	-	[psia]		
p_s	Compressor suction pressure	-	125	-	[psi]		
$p_{trav,tot}$	Total pressure traverse	(7.34)	-	-	[psi]	[9, p. 455]	
p_{lift}	Pressure for lifting	(7.37)	-	-	[psi]	[4, p. 80]	
p_{wh}	Wellhead pressure	-	1000	-	[psi]		
p_{res}	Reservoir pressure	-	$0.5 \left(\frac{h[\text{ft}]}{231[\text{ft/psi}]} \right)$	-	[psi]		
p_{wf}	Bottomhole pressure	-	-	[bbl liquid/psi-d]			
Pi	Well productivity index	(7.23)	3	-	[ft ³ /s]		
$Q_{l,W}$	Wellbore flow rate	(7.32)	-	-	[bbl/d] or [MMscf/d]		
Q_d^{MI}	Discharge flow rate	-	var.	-	[gal/d]		
$Q_{di,MN}$	Rate diesel fuel consumption, integrated mine	(7.39)	-	-	[gal/d]		
Q_{di}	Rate diesel fuel consumption, non-integrated mine	(7.39)	-	-	[ft ³ /s]		
Q_l	Total rate of liquid production	(7.33)	-	-	[bbl/d]		
Q_o	Total rate of oil production	-	1500	-	[bbl/d]		
Q_{db}	Rate of diluted bitumen production	-	1500	-	[bbl/d]		
Q_{SCO}	Rate of synthetic crude oil production	-	1500	-	[bbl/d]		
r	Relative pipe roughness	-	0.0006	-	[unitless]	[120]	
R_C	Compression ratio	(7.104)	-	-	[-]		
ρ_{gsc}	Gas density at standard conditions	(7.26)	-	-	[lbm/ft ³]	[4, p. 35]	
ρ_{asc}	Air density at standard conditions	-	0.0764	-	[lbm/ft ³]	[118, p. 10]	
T_b	Base temperature	-	520	-	[°R]	[4, p. 35]	
T_d	Compressor discharge temperature	(7.106)	-	-	[°R]	[67, p. 105]	
T_s	Compressor 1 suction temperature	-	656.7	-	[°R]		
T_{s2}	Compressor 2 suction temperature	(7.107)	-	-	[°R]		
$v_{l,W}$	Pipeline flow velocity	(7.31)	-	-	[ft/s]	[118]	
WOR	Water-to-oil ratio	-	Section 4.3.0.7	-	[bbl water/bbl oil]		
y^{MI}	Integrated mining operation?	(7.41)	0	-	[0-1]	[106], [107], [108], [109], [110], [93, p. 111], [104], [105], [2]	
y^{MN}	Non-integrated mining operation?	(7.41)	0	-	[0-1]		
Z	Compressibility factor	Section 5.2.5	-	-	[-]		

Continued on next page...

Continued from previous page

Param.	Description	Eq. no.	Default	Literature range	Unit	Sources	Notes
MMP	CO ₂ Minimum miscibility pressure	-	Section 7.55	-	[psia]	[11]	
LeakCO ₂	Long-term CO ₂ leakage rate	-	0.5%	-	[-]	[6]	
BlowCO ₂	CO ₂ proportion lost to terminal blow-down	-	0%	-	[-]	[?]	

a - The default of the ratio of specific heats for methane (not pure) is 1.28. In the case of nitrogen gas the default is 1.40.*b* - OPGEE default is slightly more conservative to account for wear, tear, older equipment, etc.*c* - OPGEE default is more conservative to account for wear, tear, older equipment, etc.*d* - For the calculation of the friction head a Moody friction factor of 0.02 is assumed.*e* - See 'Fuel specs'. Crude oil specific gravity varies between 0.8 and 1.05 in most cases.*f* - Calculated based on the molecular weights and molar fractions of gas constituents.*g* - Pressure traverse is calculated from the total head using the pressure gradient of fresh water.

Table 7.77: Description of OPGEE's Associated Gas Processing Schemes

Path #	Path Description	Path Components
1	None	None
2	Minimal	Glycol dehydrator
3	Acid gas	Glycol dehydrator + amine process
4	Wet gas	Glycol dehydrator + demethanizer
5	Acid wet gas	Glycol dehydrator + amine process + demethanizer
6	Dry acid gas reinjection	
7	CO ₂ EOR: Membrane/amine	Glycol dehydrator + compressor + membrane + amine process + demethanizer
8	CO ₂ EOR: Ryan-Holmes	Dehydrator + Ryan-Holmes process + demethanizer

7.55.2 Introduction to Surface processing

Surface processing of crude oil includes all production steps required after lifting the crude oil from the subsurface and before it is transported to the refinery. This includes oil-water-gas separation, treatment and stabilization of crude oil, and treatment of produced gas. The particular field processing scheme selected for an oilfield varies based on field parameters such as API gravity and operational factors such as limitations on energy inputs [60, p. 65]. The choice to conduct CO₂ EOR flooding will also affect the associated gas processing choice.

In OPGEE it is not possible to account for all variations in surface processing. The goal is to include frequently applied processes in the industry, while still retaining some flexibility to model varying operating modes and processing schemes.

After phase separation in the fluid separator, the associated gas is processed in a selected gas processing path. OPGEE allows the user to choose from eight gas processing paths to simulate a variety of field conditions and production choices, presented in Table 7.77.

Path 1 (None) is chosen in case the associated gas requires no processing. Path 5 (Acid wet gas) includes use of a glycol dehydrator, amine acid gas removal unit, and a demethanizer and is the default gas processing path. Paths 2, 3, and 4 allow the user to turn OFF one or more of the processing components of Path 5. Paths 6 and 7 represent processing of associated gas during CO₂ flooding for EOR. Paths 6 to 8 represent CO₂ EOR options. Path 6 is simple dehydration and reinjeciton of mixed acid gases and hydrocarbons. Pathways 7 and 8 adapt CO₂ EOR-related modeling performed by the Department of Energy's NETL [6, 166, 167, 186].

Figure 7.70 is a simplified depiction of the associated gas processing paths in OPGEE containing four main branches. The upper branch is the standard processing train and contains a glycol dehydrator, amine AGR unit, and a demethanizer — each of which can be turned ON or OFF. Gas processing paths 2-5 fall are contained wthin the upper trunk. The middle and lower trunks are the CO₂ EOR-specific paths. Pre-breakthrough CO₂ EOR separation is modeled using Processing Paths 1-5 within the upper branch (before breakthrough, injected CO₂ is not present in the associated gas stream).

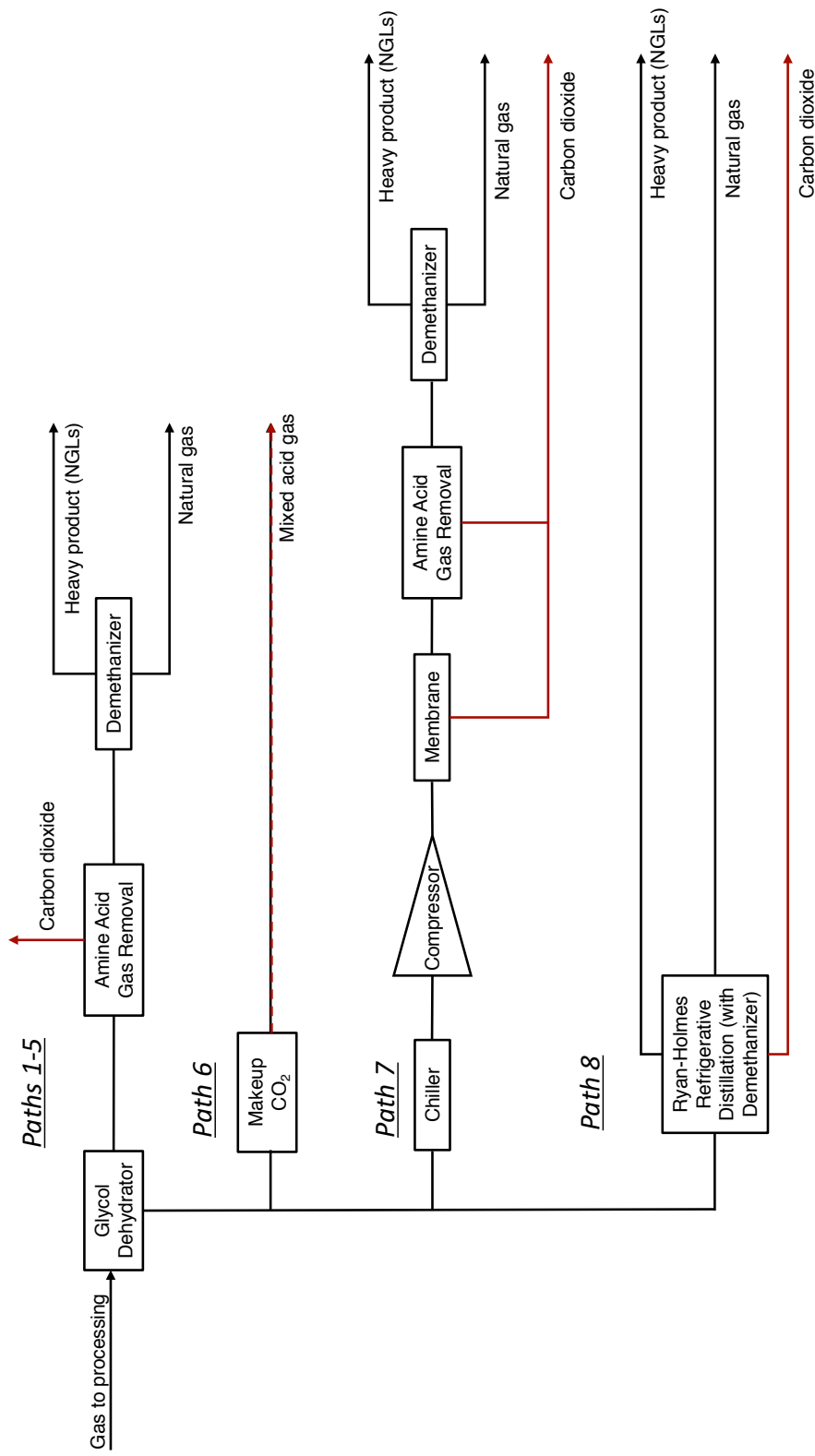


Figure 7.70: Schematic of associated gas treatment with four main branches. The lower 3 branches model post-breakthrough CO₂ enhanced oil recovery separation pathways [6].

7.55.2.1 *CO₂ Enhanced oil recovery pathway: membrane-amine dual process*

Gas Processing Path 7 includes the same amine-based AGR unit described in the Acid gas removal section, but also incorporates a selectively permeable membrane that reduces the CO₂ content of the gas stream prior to its transit through the amine process.

After exiting the chiller, the feed stream is compressed to reach a pressure sufficient to traverse the selectively permeable membrane. The compressor's energy calculations and operational assumptions are identical to the compressors described in the ?? section. The membrane removes 67% of the CO₂ in the feed stream; it is assumed that the post-membrane carbon dioxide stream is 100% pure [166]. The post-membrane natural gas-rich stream still contains 33% of the original CO₂, which then proceeds to an amine-based process which operates as described in the Acid gas removal section. The pure CO₂ streams exiting the amine-process and the membrane are united and ultimately reinjected into the reservoir.

8 Supplemental calculations worksheets

8.1 Drivers

Drivers (also known as prime movers) of pumps, compressors, and onsite electricity generators come in different types and sizes. Drivers in OPGEE include natural gas driven engines, natural gas turbines, diesel engines, and electric motors. The size and energy consumption of the driver is required to convert power requirements (e.g., downhole pump brake horsepower) into energy consumption as explained in Section 7.55.0.2. A database of drivers specifications of different types and sizes is included in OPGEE. Table 8.1 shows the types and size ranges of the drivers included in OPGEE.

Specifications of natural-gas-driven engines and diesel-driven engines are taken from Caterpillar technical worksheets [184]. Specifications of natural gas turbines are taken from Caterpillar-subsidiary Solar Turbines technical worksheets [187]. Specifications of electric motors are taken from General Electric technical worksheets [185]. Data were reported in original sources in different forms and with different levels of completeness.

The data for each driver model was converted into [bhp] for power and [Btu/bhp-hr] for energy consumption. In some cases the data on engine power was given in [bhp] and energy consumption is given in [Btu/bhp-hr], so no conversion is required. In other cases only data on the electricity generator set is given. The generator set includes an engine and an electricity generator. The brake horsepower of the engine is calculated from the electric power of the generator set as:

$$P_D = \frac{P_{GS}}{\eta_G} \cdot 1.34 \quad [\text{bhp}] = \frac{[\text{ekW}]}{[-]} \left[\frac{\text{bhp}}{\text{bkW}} \right] \quad (8.1)$$

where P_D = driver brake horsepower [bhp]; P_{GS} = electric power of the electricity generator set [ekW]; and η_G = efficiency of the electricity generator (not including engine) [-]. For the calculation of the electric power [ekW] of the electricity generator sets Caterpillar assume an electricity generator (without engine) of efficiency 96% [188, p. 4]. Accordingly η_G in eq. (8.1) is equal to 0.96 [-].

Table 8.1: Types and size ranges of the drivers embedded in OPGEE.

Type	Fuel	Size range [bhp]
Internal combustion engine	Natural gas	95 - 2,744
Internal combustion engine	Diesel	1590 - 20,500
Simple turbine	Natural gas	384 - 2,792
Motor	Electricity	1.47 - 804

In the case where the overall efficiency of the electricity generator set is given, but the energy consumption of the engine component is not, the latter is calculated as:

$$e_D = \frac{3.6}{\eta_{GS}} \eta_G \quad \left[\frac{\text{MJ}}{\text{bkW-hr}} \right] = \frac{\left[\frac{\text{MJ}}{\text{bkW-hr}} \right]}{[-]} \quad (8.2)$$

$$e_D = \frac{e_D \cdot 947.8}{1.34} \quad \left[\frac{\text{Btu}}{\text{bhp-hr}} \right] = \frac{\left[\frac{\text{MJ}}{\text{bkW-hr}} \right]}{\left[\frac{\text{bhp}}{\text{bkW}} \right]} \left[\frac{\text{Btu}}{\text{MJ}} \right]$$

where e_D = driver energy consumption [Btu/bhp-hr]; η_{GS} = efficiency of generator set (engine + generator) [-]; η_G = efficiency of generator (without engine) [-].

The diesel engines energy consumption is reported in the technical worksheets in the form of gallons per hour [gal/hr]. This is converted into [Btu/bhp-hr] by:

$$e_D = \frac{e_D \cdot 137,380}{P_D} \quad \left[\frac{\text{Btu}}{\text{bhp-hr}} \right] = \frac{\left[\frac{\text{gal}}{\text{hr}} \right] \left[\frac{\text{Btu}}{\text{gal}} \right]}{\left[\text{bhp} \right]} \quad (8.3)$$

where e_D = driver energy consumption [Btu/bhp-hr]; P_D = driver brake horsepower [bhp]. The driver brake horsepower, P_D , is calculated from the electric power [ekW] of the given generator set as shown in eq. (8.1).

The calculation used to convert the efficiency of electric motors from the General Motors technical worksheets into energy consumption in [Btu/bhp-hr] is very similar to the calculation of the energy consumption of the engine component from the overall efficiency of the generator set in eq. (8.2):

$$e_D = \frac{3.6}{\eta_M} \quad \left[\frac{\text{MJ}}{\text{kWh}} \right] = \frac{\left[\frac{\text{MJ}}{\text{kWh}} \right]}{[-]} \quad (8.4)$$

where e_D = driver energy consumption [Btu/bhp-hr]; η_M = electric motor efficiency [-]. The energy consumption is converted to [Btu/bhp-hr] as shown in eq. (8.2).

OPGEE retrieves the energy consumption of the appropriate driver based on the user input and the required size.

Table 8.2: Default inputs for drivers calculations.

Param.	Description	Eq. no.	Default	Literature range	Unit	Sources	Notes
e_D	Driver energy consumption	(8.2)	-	-	[Btu/bhp·hr]	[185]	a
η_M	Electric motor efficiency	-	var.	0.84-0.96	[-]	[184]	b
η_{GS}	Efficiency of electricity generator set	-	var.	0.36-0.40	[-]	[188, p. 4]	c
η_G	Efficiency of electricity generator (no engine)	-	0.96	-	[-]	[188, p. 4]	d
P_D	Driver brakehorse power	(8.1)	-	-	[bhp]	[184]	
P_{GS}	Electric power of elect. gen. set	-	var.	275-2000	[ekWh]	[184]	e

a The cited equation is for gas drivers. Energy consumption of diesel and electricity drivers is calculated in eq. (8.3) and (8.4), respectively.

b Motor efficiency ranges from 0.84 to 0.96 for commonly applied motor size ranges [185].

c Literature range cited only for gas generator sets with gas engine sizes ranging from 1535-2744 [bhp].

d Standard electricity generator efficiency [188, p. 4].

e Literature range cited for diesel generator sets [184].

8.2 Fuel cycle

For fuels consumed in OPGEE, the upstream or “fuel cycle” energy consumption and GHG emissions are required to calculate the indirect energy consumption and GHG emissions of imported fuel. For example, if purchased electricity is used on site, the emissions associated with generating and transporting that purchased electricity must be accounted for and added to the direct emissions burden. Similarly, any co-products that are sold separately from the produced oil (e.g., natural gas, electricity, NGL) must be assigned a co-production credit for emissions avoided from the system that they displace. The approach here can therefore be described as a co-product emissions assessment via system boundary expansion rather than via allocation between products [189, 190]. In all cases, the energy consumption and GHG emissions of the displaced production system is calculated from CA-GREET [111].

For the calculation of credit from the export of natural gas or natural gas liquid (NGL), the natural gas production system is displaced. For NGL export, the natural gas production system is displaced because NGL is a byproduct of gas production and does not have an independent fuel cycle. Credit is not given for avoided gas transport emissions, because it is assumed that the gas will be transported to a remote consumer.

For the calculation of credit from electricity exports, the boundary of the system is extended to the user “plug”: the displaced system includes electricity generation and transport to the end user. This choice was made because exported electricity will naturally flow to the nearest consuming entity and not require long-distance transport. OPGEE calculates the energy consumption and GHG emissions of electricity generation based on the grid electricity mix (entered in the ‘*Electricity*’ worksheet) using CA-GREET data of different electricity sources (natural gas, biomass, etc).

For regions with significantly different fuel cycle characteristics than those represented in CA-GREET, the user can and should modify the inputs on the ‘*Fuel Cycle*’ worksheet.

8.3 Embodied emissions

Embodied emissions are emissions that occur during the production, processing, and transport of materials used oilfields. In OPGEE, the following embodied emissions are included:

- Embodied emissions in wellbore steel
- Embodied emissions in wellbore cement
- Embodied emissions in surface piping
- Embodied emissions in surface processing equipment
- Embodied emissions in on-site storage infrastructure
- Embodied emissions in pipeline infrastructure
- Embodied emissions from fracturing sand and water procura
- Embodied emissions from transporting above materials to oilfield site

We first discuss the datasets used to determine embodied emissions per unit of each required material. We then discuss methods of calculating the amount of materials consumed in each of these sources below.

8.3.1 Datasets for calculating embodied emissions from consumed materials

Two datasets are used to determine the GHG intensity of materials consumed in oilfield operations. The resulting tabulated data are included in the '*Input data*' worksheet, and compiled into the '*Embodied Emissions*' worksheet depending on the dataset selected by the user. We include data from the EcoInvent v.3.0 dataset [191] and the GREET model, version GREET2_2012 [192].

*'Embodied
Emissions 1.3'*

8.3.1.1 EcoInvent v3.0

The EcoInvent v.3.0 dataset was used to determine emissions for a variety of materials consumed within oilfield construction and operation. The materials included in OPGEE are listed in the '*Input Data*' worksheet. The EcoInvent v.3.0 dataset was accessed in April 2014. For each material of interest, two datasets were accessed. First, the unit process data (UPR) dataset was accessed for each material. The UPR data represent direct flows between the process of interest and other processes in the "technosphere", as well as flows between that process and the natural environment (both flows into and out of the process from the environment).

*'Embodied
Emissions 1.3'*

Next, full life cycle impact data were gathered for each material, in the form of life cycle inventory (LCI) data. These data were gathered using the EcoInvent default co-product accounting scheme (allocation). For each material, LCI data represent 1000s of possible flows between the economy and the natural environment, summed across all processes in the economy.

Because the desired impacts to be measured include *all* impacts across the economy, we base OPGEE emissions intensities on the LCI results, not the UPR results. For each product, primary energy consumption in the form of crude oil, natural

gas, and hard coal are tabulated. For each product, the following gas emissions rates (mass basis) are tabulated: CO₂, CH₄, non-methane volatile organic compounds (NMVOC), and N₂O. For each gas flow rate, EcoInvent partitions emissions to air using the following emissions location categories:

*'Embodied
Emissions 1.3'*

- Urban air, close to ground
- Non-urban air, or from high stacks
- Lower stratosphere + upper troposphere
- Unspecified emissions location
- Non-urban air
- Unspecified

For each mass flow rate, emissions from all relevant atmospheric categories are summed. Each species tracked may also be partitioned into various sources. Because we do not want to include general non-fossil emissions sources, the following sources were summed for each species.

- CO₂: Fossil carbon dioxide and carbon dioxide from soil or biomass stock. Non-fossil carbon dioxide (e.g., CO₂ from ethanol manufacture) is not included.
- CH₄: Fossil methane and methane emissions from soil. Unlabeled methane sources are not included.
- NMVOC: Sum of NMVOC emissions. Origins not partitioned.
- N₂O: Sum of dinitrogen monoxide emissions. Origins not partitioned.

For each product included in OPGEE, a functional unit of 1 kg was used in EcoInvent. Emissions intensities are also converted to g/lbm of material.

In order to choose the material production process, by default we use ROW (rest of world) or GLO (global) processes where possible. Because OPGEE is a global model, we prefer to use these ‘generic’ values rather than country-specific values. Specifically, each material input is documented below:

- Sand: The “gravel and sand quarry operation ROW” with output of 1 kg of sand was used. No specific entry was available for hydraulic fracturing proppant sand.
- Cement: The “cement production, Portland, RoW” process is used, with a functional unit of 1 kg of cement. Mitchell suggests [35, p. 382] that “almost all drilling cements are made of Portland cement, a calcined (burned) blend of limestone and clay.” The types of cement included in SPE documents are ASTM type I, II, III, and IV, which correspond to API classes A, C, G, H.
- Pipe manufacture: the “drawing of pipe, steel, RoW” process is used, with a functional unit of 1 kg of pipe manufactured. Mitchell and Miska [36, p. 387] suggest that most casing is manufactured via seamless production, which is a drawing mechanism. In EcoInvent, the pipe drawing process is modeled as a multiple of the wire drawing process.

- Gravel: the “gravel production, crushed, RoW” process is used, with a functional unit of 1 kg of gravel.
- Hematite: the “iron mine operation, crude ore, 46% Fe’, GLO” is used. The functional unit is 1 kg of ore.
- Steel: the “steel production, converter, unalloyed, ROW” and “steel production, converter, low-alloyed, ROW” are used, with 1 kg of steel functional unit in each case. Mitchell suggests that “almost without exception, casing is manufactured of mild (0.3 carbon) steel, normalized with small amounts of manganese. Strength can also be increased with quenching and tempering.” [35, p. 288].
- Bentonite clay: the “bentonite quarry operation, RoW” process is used, with a functional unit of 1 kg bentonite.
- Calcium chloride: the “soda production, solvay process, RoW” is used, with a functional unit of 1 kg calcium chloride.
- Sodium chloride: the “market for sodium chloride, powder, GLO” is used, with a functional unit of 1 kg sodium chloride.
- Monoethanolamine: the “market for monoethanolamine, GLO” is used, with a functional unit of 1 kg MEA.
- Triethylene glycol: the “market for triethylene glycol, GLO” process is used, with a functional unit of 1 kg TEG.

8.3.1.2 *GREET2_2012*

The GREET vehicle emissions model, GREET2, contains embodied emissions for a variety of materials. We use version GREET2_2012, accessed in April 2014 [192]. From the GREET worksheet ‘Mat_Sum’, the energy intensity (mmBtu/lb of material product) and emissions intensity (g/lb of product) were collected. In addition, emissions from cement production are taken from the ‘Cement_Concrete’ worksheet, for the same model outputs. Because GREET2 focuses on materials used in automobile manufacture, some inputs are not available (e.g., bentonite clay for cementing). These missing materials are given emissions of 0 g/lb in the current version of OPGEE when GREET is selected as the source of data inputs.

*'Embodied
Emissions 1.3'*

Because OPGEE GWP-weighting values are taken from GREET, the aggregate GREET GHGs figure is used for each material input.

8.3.2 Embodied emissions in wellbore steel

In order to estimate the amount of steel required per foot of well constructed, three “illustrative” wells are modeled in OPGEE: a complex well, a moderate well, and a simple well. The complex well design scheme is from Mitchell and Miska [36], for a deepwater GOM well. The moderate and simple well designs are from Nguyen [193]. The default well configuration is the moderate well configuration, with depths for some casing strings drawn from the overall depth of the well. A blank ‘User defined’ well type is also included for cases where specific well casing

*'Embodied
Emissions
2.2.2'
'Embodied
Emissions
2.2.2'*

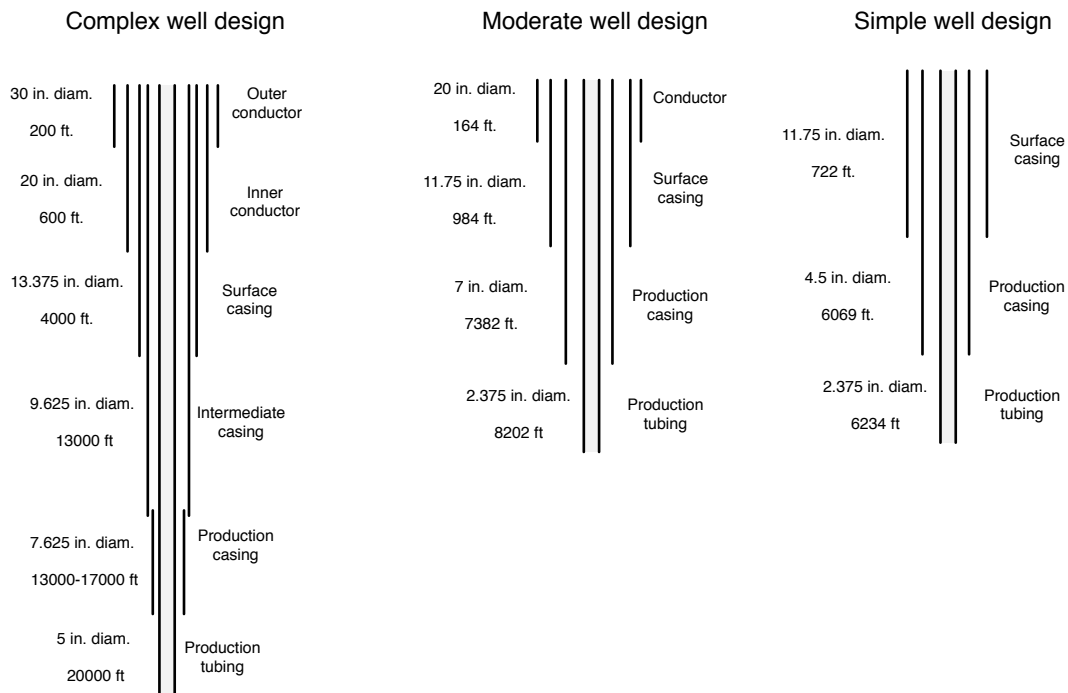


Figure 8.1: Casing plan for wells of complex, intermediate, and simple design. Well depths here are illustrative, and all steel consumption intensities are computed per unit length of well (per ft.). See text for sources.

geometry data are known (likely uncommon).

The casing plan for each of these wells is shown in Figure 8.1. For each casing diameter, the appropriate hole diameter was chosen from the literature [36, Figure 7.18]. Only commonly used bit/casing combinations were used, with tight clearance designs avoided. The smallest common bit diameter was used for each casing size. The diagram used does not give bit sizes for 24 or 30 inch casing, so we assume 6 inch excess hole diameter, as reported for 20 inch casing.

*'Embodied
Emissions
2.2.1'*

The mass of steel per unit length of casing is taken from Mitchell [35, Table 7.10]. Each casing outer-diameter size is listed in the literature with 1 to 10 inner diameters. The minimum, maximum, and average of all reported weights are used in OPGEE. OPGEE defaults to the average casing mass. No data were available on the mass per unit length of 30 in. diameter conductor casing, so data from GE were used [194], along with a steel density of 0.3 lbm/in³. Some casing sizes (e.g., 18.625 in. and 20 in.) only report one thickness, so min, max, and average value are identical.

*'Embodied
Emissions
2.3.1'*

Similarly, the production tubing mass per unit length is taken from the API tubing table for production tubing of nominal diameter 0.75 to 4.5 in [195]. For production tubing, many of the same grades have the same weight per unit length.

*'Embodied
Emissions
2.3.2'*

The resulting mass of steel per unit of well length [lbm/ft] is calculated for each casing and tubing layer. These per-unit length mass estimates are then compiled into aggregate steel use intensities per foot of simple, moderate, and complex well designs [lbm/ft]. The total steel used per production and injection well is also computed using these information.

*'Embodied
Emissions
2.3.3'
'Embodied
Emissions
2.3.6'*

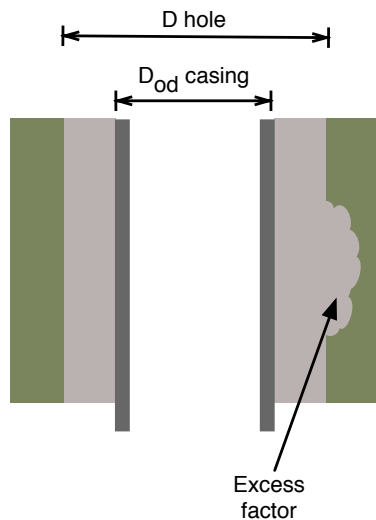


Figure 8.2: Diagram illustrating cement volume calculations (per unit depth). Cement is presented in grey, while earth is presented in green-brown.

8.3.3 Embodied emissions in wellbore cement

Wellbore diameters are collected for each casing diameter. The outer-diameter of each casing string, along with the drill bit diameter, are used to compute the volume of void space per unit length of the well [ft^3/ft] (see Figure 8.2) using the cross-sectional area to be filled:

$$A_{fill} = \pi \left(\left(\frac{D_{hole}}{2} \right)^2 - \left(\frac{D_{cas,out}}{2} \right)^2 \right) \quad (8.5)$$

The appropriate hole diameter for a given casing diameter was obtained from the literature [36, Figure 7.18]. Only commonly used bit/casing combinations were used, with tight clearance designs avoided. The nominal void volume is increased by a cement excess factor of 1.75, which represents additional cement required due to cement infiltration and excess hole enlargement or hole roughness created during drilling [36, Example 4.5], see Figure 8.2.

*'Embodied Emissions
2.2.1'*

*'Embodied Emissions
2.2.1'*

Four cement slurry compositions are modeled in OPGEE, based on API Class A cement [36, Table 4.2]. These compositions are low density, moderate density, high density, and high strength slurry blends. Slurry blend composition is calculated using method of Mitchell and Miska [36, Examples 4.3, 4.4, 4.5]. The properties of cement additives are provided by Mitchell and Miska, including data on bulk weight, specific gravity, and absolute volume [36, Table 4.4], as are water requirements per additive [36, Table 4.5]. Properties of these cement blends are presented in Table 8.3.

*'Embodied Emissions
2.4.1'*

The amount of cement required varies with the casing string being cemented. The following assumptions are applied to estimate the vertical extent of cementing in each well casing segment:

- Well conductor casing is cemented along its entire length (for stability and groundwater protection);

Table 8.3: Cement blends modeled in OPGEE.^a

Cement type:	Low density	Moderate density	High density	High strength
Additives:	16% bentonite, 5% NaCl	3% bentonite	5% hematite	2% CaCl
lb/sack of cement				
- Class A cement	94.00	94.00	94.00	94.00
- Bentonite	15.04	2.82	0.00	0.00
- Hematite	0.00	0.00	4.70	0.00
- Calcium chloride	0.00	0.00	0.00	1.88
- Sodium chloride	4.70	0.00	0.00	0.00
- Water	108.29	58.19	37.63	43.32
kg/kg slurry				
- Class A cement	0.42	0.61	0.69	0.68
- Bentonite	0.07	0.02	0.00	0.00
- Hematite	0.00	0.00	0.03	0.00
- Calcium chloride	0.00	0.00	0.00	0.01
- Sodium chloride	0.02	0.00	0.00	0.00
- Water	0.49	0.38	0.28	0.31
Slurry density				
- lb/gal	12.39	14.48	16.58	15.75
- kg/l	1.49	1.74	1.99	1.89
Slurry yield				
- ft ³ /sack cement	2.34	1.43	1.10	1.18
- l/kg cement	1.56	0.95	0.73	0.78

^a - See Mitchell and Miska [36, Example 4.3], Example 4.3 for overall methodology. Other composition data from [36, Example 4.4, 4.5]

- Surface casing is cemented along its entire length to prevent groundwater contamination;
- All other casing strings are assumed cemented to 300 ft. vertical fill-up (min), 600 ft. vertical fill-up (default), or filled in their entirety (max.). Minimum vertical extent of cementing is given in Mitchell and Miska [36, Section 4.5.11].

These assumptions are illustrated in Figure 8.3.

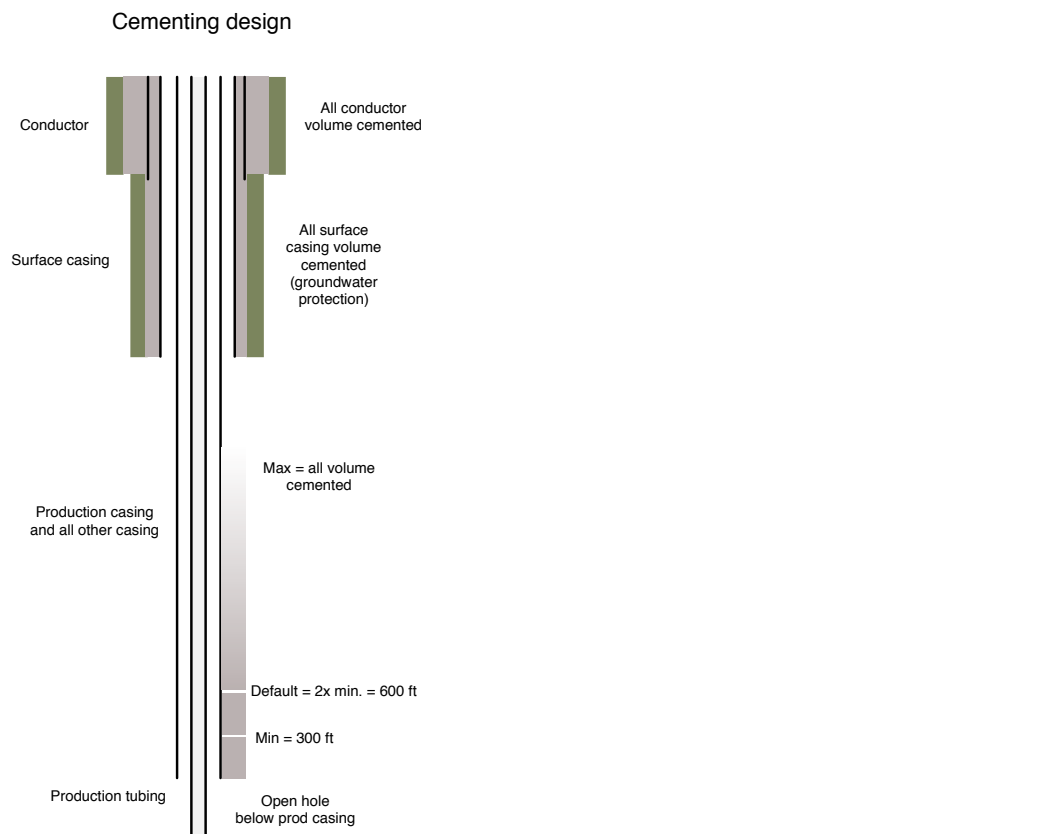


Figure 8.3: Default OPGEE cementing plan. Default non-conductor, non-surface casing fill-up is twice reported minimum, or 600 ft.

8.3.4 Embodied emissions in surface piping

Surface piping requirements will be highly dependent on the layout of the particular oilfield of interest. Data from the “Oilfield Data Handbook” [196, p.26] on surface pipe weight per unit length provide data on weight per pipe foot for standard (STD) and extra-strength (XH) pipes. Nominal diameters of 0.5 in. to 16 in. are included, with weights ranging from 0.8 to 80 lb/ft.

OPGEE defaults are set to 3 in. average diameter of surface piping, extra-strength (10.25 lbm steel/ft). OPGEE default surface piping per well is set to 2000 ft./well. If field-specific data are available on amounts of surface piping, these data should be used in preference to defaults.

8.3.5 Embodied emissions in fracturing materials

Materials requirements for fracturing are assumed (in the current version of OPGEE) to include only fracturing water and sand. We therefore currently neglect all other fracturing chemicals.

The water requirements of fracturing are set by default to 2 million gallons per well, a number near the median value observed in a recent study of the Bakken formation [?]. Across all studied Bakken wells, about 1.1 lb of sand was injected per gallon of fracturing water, which we use to estimate a default fracturing sand loading of 2.2 million lbs of sand per well. If well-specific data are available, or if regional or play-specific estimates for these quantities are available, those should be used in preference to defaults.

8.3.6 Embodied emissions in surface processing equipment

Three types of surface processing equipment are modeled to understand steel requirements: oil-water-gas separators, acid gas removal (AGR) units, and gas dehydration units.

8.3.6.1 Oil-water-gas separators

Horizontal, three-phase separators are assumed to be used to separate oil, water and gas . Three-phase separator data are tabulated from an equipment provider [197]. Working pressures of 720, 1000, 1200 and 1440 psig are tabulated, with liquid capacities ranging from 720 to 3170 bbl/d. Gas capacities range from 10.6 to 62.0 MMSCF/d, varying with the pressure of outlet gas, separator size and separator working pressure. The mass of each separator is tabulated from vendor specifications.

The wellhead pressure entered into the ‘Production & Extraction’ worksheet is used to select the proper separator working pressure. The number of separators needed is computed by dividing the total liquids production of the field (oil + water) by the liquid throughput capacity of each of the sizes of separators available at the desired pressure. It is assumed that the smallest number of large separators will be the most economical option, so by default this is selected. OPGEE checks to ensure that gas throughput capacity of these separators is sufficient to process the associated gas that is produced by the field. Given the number of separators and

'Embodied Emissions 3.1'

'Embodied Emissions 3.2.1'
'Embodied Emissions 3.2.4'

'Embodied Emissions 2.5.1'
'Embodied Emissions 2.5.4'

'Embodied Emissions 3.3.1'

'Embodied Emissions 3.3.2'

'Embodied Emissions 3.3.5'
- 3.3.7
'Embodied Emissions 3.3.8'

the required pressure and size of separators, the required total mass of separators is computed. Separator mass is assumed to be made of steel.

8.3.6.2 Acid gas removal

Acid gas removal contactor columns assume a 20-tray system, with a tray spacing of 18 in. [4, p.116], for a total contactor tower height of 30 ft. Correlations for sizing acid gas removal contacting towers are gathered from the technical literature [4]. For different gas pressures and gas flow rates, the required contactor tower diameter is computed using correlations from Manning and Thompson [4]. The log-log relationship plotted in the literature is converted to an exponential relationship, where for each operating pressure, the required contactor inner diameter is computed as:

$$D_{abs} = a_{abs} Q_{pg}^{b_{abs}} \quad (8.6)$$

Where D_{abs} is the absorber diameter [in.], a and b are fitting constants, and Q_{pg} is the flow rate of processed gas [MMscf/d], defined as associated gas less well-bore fugitives and flaring. The required inner diameter is combined with assumed steel thickness to compute the mass of the shell. The mass of contactor trays and auxiliary piping is assumed by default to equal the mass of the shell.

Detailed correlations for acid gas removal regenerator column sizing were not found in the public literature. Therefore, the mass of the desorber unit is assumed by default to equal the mass of the absorption column.

8.3.6.3 Gas dehydration

Vendor information on glycol dehydration absorption units is tabulated, with sizes (inner or outer diameter) given for various throughputs and operating pressures [198]. The required wall thickness is computed using ASME Standard B31.3 [50, eq. 9.27] for given diameters and pressures, and the required size of unit is computed using required gas processing throughput Q_{pg} (defined above). The estimated wall thickness is rounded up to the nearest 0.1 in. and used to compute the mass of steel required.

Glycol reboiler specifications are taken from vendor specifications [198]. The required wall thickness is computed using ASME Standard B31.3 [50, eq. 9.27] for given diameters, rated at assumed maximum operating pressure of 1000 psig. Given the glycol circulation rate the reboiler inner and outer diameters are computed. The required volume of steel is then computed, and doubled to estimate requirements for piping, support, exhaust, skid, and other auxiliary components.

8.3.7 Embodied emissions in on-site storage infrastructure

Crude oil and produced water storage tanks are assumed to meet API standard 12F specifications [199]. While larger custom tanks may be built on site in some instances, for simplicity, we assume standard tank dimensions. Tank capacity is chosen, which dictates height, outside diameter, shell and top/bottom steel thickness. From these parameters, assuming 0.25 in. thick steel (specific weight of 10.2 lb./ft²), the weight of each tank type is calculated.

To limit interrupted delivery due to equipment downtime, on-site storage of 3

'Embodied
Emissions
3.4.1'

'Embodied
Emissions
3.4.4'
'Embodied
Emissions
3.4.5'

'Gas Balance
M23'
'Embodied
Emissions
3.4.6'
'Embodied
Emissions
3.4.9-10'

'Embodied
Emissions
3.5.1'
'Embodied
Emissions
3.5.4-5'

'Embodied
Emissions
3.5.10'
'Embodied
Emissions
3.5.11-15'

'Embodied
Emissions
4.1.1'

'Embodied
Emissions
4.1.2-3'

days worth of produced oil and produced water is assumed. By default, the largest API 12F tank size is chosen (750 bbl, 15.5 ft. outside diameter, 24 ft. height). The user can select another tank size if desired.

8.3.8 Embodied emissions in long-distance transport infrastructure

Long-distance transport of crude in pipelines requires steel. The length of the US pipeline infrastructure is chosen as a model infrastructure, at 240,000 km [200]. The infrastructure is assumed to last 30 years, and transport 10×10^6 bbl/d averaged over its lifetime.

ANSI pipe schedules [50, Table 9.7] are used to tabulate thickness and weight per unit length for pipeline diameters from 12 to 48 in. (4 in. increments). Two standard thicknesses, designated STD and XH are tabulated, as these are available in all required sizes. By default, the assumed pipeline infrastructure is assumed to be made of 32 in. diameter, XH grade pipe (168 lb/ft).

The resulting default steel intensity is 278 bbl of oil transported per lbm of steel consumed in building long-distance pipelines.

We do not consider embodied emissions in oil tankers or trains in OPGEE v3.0a.

'Embodied Emissions'
'Embodied Emissions'
'Embodied Emissions'
'Embodied Emissions'
'Embodied Emissions'
'Embodied Emissions'

'Embodied Emissions'
'Embodied Emissions'

8.3.9 Shipment of oilfield capital equipment

All equipment and materials used to build oil and gas operations must be shipped from the site of production (e.g., well casing factory) to the oilfield site.

We first compute the total weight of oilfield equipment of four types modeled above:

- Steel;
- Cement;
- Fracturing sand;
- Fracturing water.

Default shipment distances assume that steel and fracturing sand are transported long distances (1000 mi) due to their specialized nature. Water and cement are assumed to be locally available (100 mi). If more specific information is available on the distances of material shipment, this should be used in place of defaults. further By default, steel products and fracturing sand are shipped by rail, while fracturing water and cement are moved by truck.

Using the energy intensity of transport used elsewhere in the OPGEE model, the energy requirements of transporting each material are computed. To compute emissions, all energy is assumed provided by diesel fuel consumed in the appropriate vehicle.

'Embodied Emissions'
'Embodied Emissions'

'Embodied Emissions'
'Embodied Emissions'

8.4 Emissions factors

Emissions factors are required for the calculation of GHG emissions from combustion (fuel combustion) and non-combustion (venting and fugitives) sources.

Table 8.4: Combustion technologies and fuels included in OPGEE.

	Natural gas	Diesel	Crude	Residual oil	Pet. coke	Coal
Industrial boiler	✓	✓	✓	✓	✓	✓
Turbine	✓	✓				
CC gas turbine	✓					
Reciprocating engine	✓	✓				

8.4.1 Combustion emissions factors

The emissions factors for fuel combustion are from CA-GREET [111]. Table 8.4 shows the technologies and fuels included. Gas species tracked include VOC, CO, CH₄, N₂O, and CO₂. Emissions are converted into carbon dioxide equivalent using IPCC GWP_s [163] as shown in eq. (8.7).

$$EM_{CO_2eq,i} = EM_i \cdot GWP_i \quad [\text{gCO}_2\text{eq}] \quad (8.7)$$

where $EM_{CO_2eq,i}$ = emissions of species i in carbon dioxide equivalent [gCO₂eq]; EM_i = emissions of species i [g]; and GWP_i = GWP of species i [gCO₂eq./g]. GWP_s are discussed in Section 10.1.

8.4.2 Non-combustion emissions factors

Section ?? describes how emissions factors for venting and some fugitives sources are generated from the ARB survey data [12]. Emissions factors from ARB are specified by gas component. The ARB survey data used to generate emissions factors for venting are shown in Table 8.5.

The emissions factors for venting by gas component were calculated using ARB survey data as:

$$EF_{CO_2Vent} = \frac{a_{EF_V}}{c_{EF_V}} 10^6 \quad \left[\frac{\text{g}}{\text{event}} \right], \text{ etc.} \quad (8.8)$$

$$EF_{CH_4Vent} = \frac{b_{EF_V}}{c_{EF_V}} 10^6 \quad \left[\frac{\text{g}}{\text{event}} \right], \text{ etc.}$$

where EF_{CO_2Vent} = emissions factor of CO₂ venting [g/event; g/mile-yr; g/MMscf]. For a description of a_{EF_V} , b_{EF_V} , and c_{EF_V} parameters see Table 8.5.

Similar calculations were performed for emissions factors for fugitives from the sources listed in Table 8.6. Emissions factors for fugitives from other sources (valves, flanges, etc) are taken from API [14, p. 20].

Emissions factors for gas dehydrators are calculated on volume basis (i.e., in grams of CO₂ or CH₄ per MMscf processed gas). These data are derived from an updated version of the ARB survey cited above [13]. In this improved version of the survey, ARB staff S. Detwiler and J. Duffy separated dehydration systems with and without vapor recovery systems (VRS) to determine emissions factors with and without VRS. See Table 8.7.

As described in Section 7.20, venting from the amine unit is calculated from the gas balance of OPGEE by assuming that all CO₂ left in the gas stream after flaring,

Table 8.5: ARB data used in the calculation of venting emissions factors (unit specified below).
Source: [12].

Source	Total CO ₂ emissions (tonne/yr) a_{EF_V}	Total CH ₄ emissions (tonne/yr) b_{EF_V}	# units (event/yr, otherwise noted) c_{EF_V}
Well workovers			
- Ultra-heavy	0	0	–
- Heavy	405	1,428	12,889
- Light	225	575	5,424
- Ultra-light	9	65	599
Well cleanups			
- Ultra-heavy	0	0	–
- Heavy	103	90	956
- Light	113	201	1977
- Ultra-light	3	21	187
Compressor startups	4	69	1071
Compressor blow-downs	172	3,238	1071
Gathering pipelines maintenance	2659	2490	2295 (mile)
Gathering pipelines pigging	104	5	1417

Table 8.6: ARB data used in the calculation of fugitives emissions factors (unit specified below).
Source: [12].

Source	Total CO ₂ emissions (tonne/yr) a_{EF_F}	Total CH ₄ emissions (tonne/yr) b_{EF_F}	# units (event/yr, otherwise noted) c_{EF_F}
Active wells			
- Ultra-heavy	0	0	–
- Heavy	66	155	36,619
- Light	459	1,415	14,261
- Ultra-light	19	139	1,323
Well cellars			
- Ultra-heavy	–	3	22
- Heavy	–	933	7,461
- Light	–	850	4,998
- Ultra-light	–	369	2,168
Gathering pipelines	327	867	2,295 (mile)
Separators	11	170	4,618
Sumps and pits	–	264	250

Table 8.7: ARB data for gas dehydrators, for systems with and without vapor recovery systems (VRS). Source: [13].

Source	CO ₂ emissions (g/MMscf)	CH ₄ emissions (g/MMSCF)	Gas input volume (MMscf)
Venting - No VRS	148	13,677	60,941
Venting - VRS	466	1,782	640,181
Venting - All dehyd.	439	2,816	701,123
Fugitives - No VRS	172	3,925	60,941
Fugitives - VRS	25,863	748	640,181
Fugitives - All dehyd.	23,630	1,024	701,123

Table 8.8: An example of EPA emissions factors for oil and gas production components (g/unit-yr). Source: [14].

Source	CH ₄	VOC emissions
Non-leaking components (< 10,000 ppmv)		
Valves		
Gas service	148	37
Heavy oil service	69	2
Light oil service	101	49
Connectors		
Gas service	60	15
Heavy oil service	62	2
Light oil service	52	25
Leaking components (> 10,000 ppmv)		
Valves		
Gas service	590,678	147,025
Heavy oil service	–	–
Light oil service	465,479	225,134
Connectors		
Gas service	159,029	39,584
Heavy oil service	–	–
Light oil service	141,668	68,519

fugitives, and other venting is vented. In Gas Processing Path 6 (membrane-amine CO₂ EOR) the vented CO₂ is reinjected into the reservoir. The emissions factor for CH₄ fugitives from the AGR unit is 965 scf CH₄/MMscf of gas throughput [201, p. 23].

EPA emissions factors for fugitives from the components listed in Table ?? are reported by API as total hydrocarbons (THC) by service type, i.e. gas service, heavy oil service [14, p. 20]. As explained in Section ?? the THC emissions factors are calculated assuming that 25% of the components are associated with gas service and the remaining 75% are associated with oil service. An example of EPA emissions factors for oil and gas production components after speciation is shown in Table 8.8 for valves and connectors [14, p. 20]. Fugitives from non-leaking components are negligible. The user determines the percentage of leaking components in the 'Venting & Fugitives' worksheet.

Emissions factors for land use change are discussed in Section 7.2. Table 7.6 shows the emissions factors per unit of crude oil produced for low, medium, and high intensity development in low, medium, and high ecosystem productivity environments [8].

9 Venting and fugitive emissions

9.1 Introduction to venting and fugitive emissions

Venting and fugitive (VF) emissions of CH₄, VOC, and CO₂ can be a significant source of GHG emissions from oil production operations. While literature definitions can vary, we use these definitions here:

Venting emissions: Purposeful release of non-combusted hydrocarbon gases to the atmosphere. Venting emissions generally occur during maintenance operations and other intermittent, infrequent activities. In some cases, gas is vented as a normal part of device operation (i.e., through pneumatics or rod-packing vents), but the amount of gas vented can increase if the device is functioning poorly.

Fugitive emissions: Non-purposeful or non-planned emissions of non-combusted hydrocarbon gases to the atmosphere. Fugitive emissions commonly result from leaking components or equipment. Component or equipment failure causing fugitive emissions can arise due to wear, thermal cycling, vibration, or stochastic failure.

Numerous sources of VF emissions exist. Intermittent sources include well workovers and cleanups, compressor startups and blowdowns, pipeline maintenance. Continuous sources can include process emissions from gas dehydrators, AGR units, as well as continuous leaks from failed components (valves, connectors, pump seals, flanges, etc.). The heterogeneous nature of these sources makes VF emissions difficult to monitor and track in practice.

OPGEE models VF emissions for sources classified as “on-site” differently from those sources that occur “off-site”. See Figure 9.1 for an illustration of the distinction between on-site and off-site VF emissions. On-site VF emissions are defined in OPGEE v3.0 as those that can be expected to occur within a field’s geographic boundary. OPGEE v3.0 assumes that on-site VF sources include production, gathering and boosting, and processing. Off-site emissions can be expected to occur outside of a field’s geographic boundary. In OPGEE v3.0, off-site emissions include transmission and storage, distribution, and end use stages.

These definitions of on-site and off-site are not likely unique nor correct in all cases. For example, in some regions, gas processing might occur off-site, and initial transportation compression might occur on-site if the pipeline terminus is co-located with the operations. However, for simplicity, these default geographic boundaries are assumed in OPGEE v3.0.

On-site and off-site emissions are modeled differently in OPGEE v3.0. On-site VF emissions can be modeled using two different, but complementary, methods, as selected by the user. The user chooses the method at the control panel on the top of the ‘Inputs’ sheet. In contrast, off-site VF emissions are modeled using a

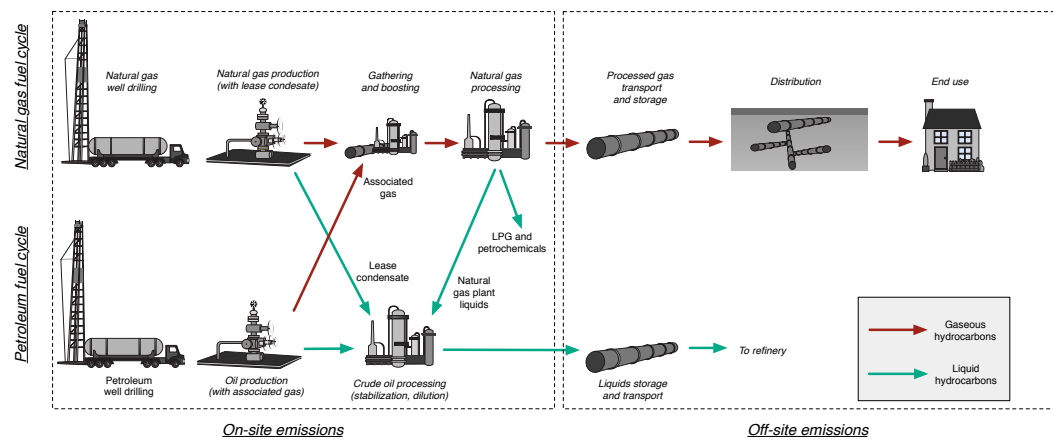


Figure 9.1: Boundary of venting and fugitive emissions accounting, dividing the process chains into “on-site” and “off-site” emissions.

single method. For backward compatibility, OPGEE v2.0 VF emissions estimation methods are retained in OPGEE v3.0, and can be selected, but these should be considered deprecated.

The ‘*Inputs*’ sheet methods for modeling VF emissions are as follows:

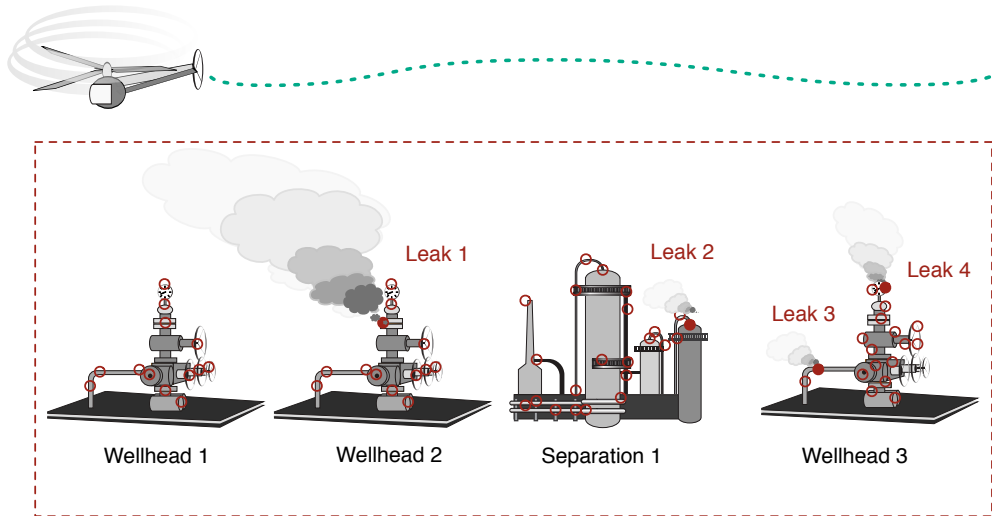
- **Site** Site-level methods used for on-site emissions and percentage loss fractions used for off-site emissions
- **Component** Component-level methods used for on-site emissions and percentage loss fractions used for off-site emissions
- **v2.0 (deprec.)** Deprecated OPGEE v2.0 methods are used for both on-site and off-site emissions. Maintained for backward compatibility only.

The differences between the two methods of modeling on-site VF emissions are largely due to the different field measurement methods used to generate the empirical basis for each model. We describe these differences below.

9.2 Site-level methods for on-site emissions

Site-level methods for estimating VF emissions leverage empirical data from site-level emissions measurement campaigns, typically performed at or beyond the facility “fence-line”. Figure 9.2 shows a schematic site containing four pieces of equipment: three wellheads and one separator. In a site-level study, a remote measurement is performed (in this illustration by drone) and total emissions from the site are estimated. No attempt is made to characterize the exact number of emissions points nor the exact location of the leaking components. Numerous site-level studies exist, and measurement has been performed via mobile ground vehicle [202–209], via instrumented aircraft measuring concentration [210–216], via aircraft-based imaging [217], and even via small drone aircraft [218].

We utilize two key site-level studies to generate site-level loss fraction estimation methods for (1) production sites and (2) gathering and processing sites.



Leakage estimate: Offsite measurement (e.g., concentration profile) converted to site-wide flux

Figure 9.2: Schematic of site-level quantification of methane emissions.

9.2.1 Production sites

Production sites include lifting of fluids from the sub-surface, basic separation of fluids, and storage of resulting hydrocarbon and water streams (in some cases). Production sites can contain compressors and (less commonly) simple processing equipment.

9.2.1.1 Statistical fit

Production site data are gathered from the Omara et al. 2018 data compilation [219]. The Omara paper is a synthesis of results from a number of site-level estimates of emissions from gas production sites. A total of 1009 sites were characterized across 8 producing regions in the U.S as measured in 7 prior studies. The Omara data also included 92 new site-level measurements that had not previously been reported. Omara et al. generated a linear relationship between the log-transformed natural gas production rate at a site and the log-transformed fractional loss rate of methane [219, Figure 3]. This relationship shows that as the gas production at a site increases, the fractional loss rate decreases.

Raw data underlying the Omara analysis was requested and received from M. Omara on October 11 2018. The following method was used for data analysis:

- Raw data are loaded into MATLAB.
- Data on loss rate are converted from % loss to loss fraction by dividing by 100.
- If the loss rate reported by Omara et al. is exactly 0, then the datum is removed to avoid log-transformation of 0. A total of 928 observations remain.

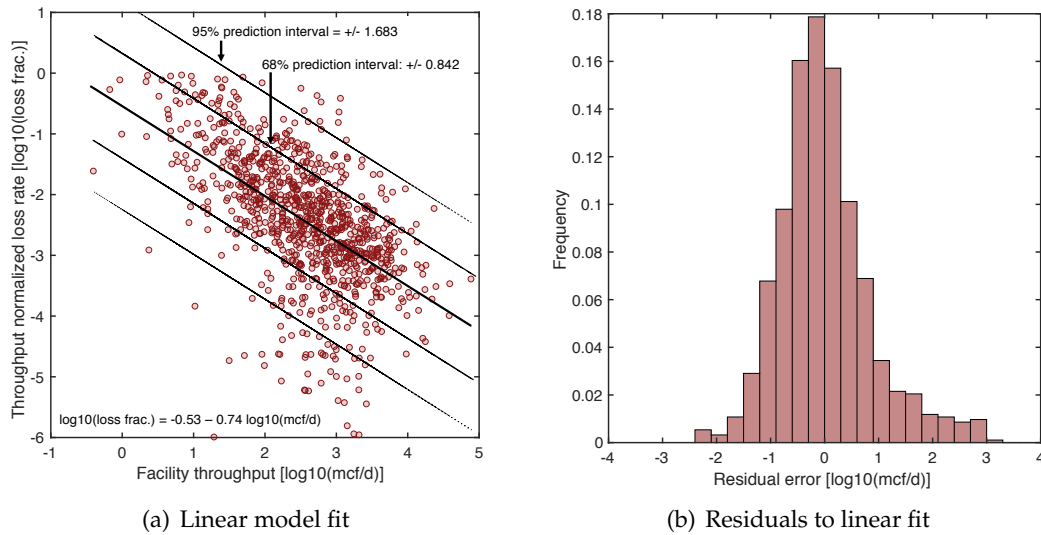


Figure 9.3: Results of fitting linear model to log-transformed leakage fraction as a function of log-transformed production facility throughput.

- Data for both production rate and loss fraction are log transformed using base-10 logarithm (MATLAB command `log10`).
- MATLAB command `fitlm` is used to generate linear fit between production rate (independent variable) and loss fraction (dependent variable).
- MATLAB commands `fit` with `Poly1` option (1st order polynomial, or linear fit) is used along with the `predint` command to develop prediction intervals for 68% ($\pm 1 \sigma$) and 95% ($\pm 2 \sigma$).

The resulting fit quality results are given below:

- Number of observations: 929, Error degrees of freedom: 927
- Root Mean Squared Error: 0.865
- R-squared: 0.328, Adjusted R-Squared 0.328
- F-statistic vs. constant model: 453, p-value = 3.36e-82
- Intercept param: -0.53723 (SE = 0.093586, p-value = 1.27E-8)
- Slope param: -0.74224 (SE = 0.034863, p-value = 3.35e-82)

The resulting fit and residuals are presented in Figure 9.3. Figure 9.3(a) shows the prediction intervals (PIs) for the resulting equation at the approximately $\pm 1\sigma$ and $\pm 2\sigma$ levels. The 68% PI is ± 0.842 , while the 95% PI is ± 1.683 . These PIs are used in OPGEE for drawing uncertainty realizations. Note that the residuals (Figure 9.3(b)) are reasonably evenly distributed about 0, with some over-weighting of the RHS residual (loss rate below that expected).

9.2.1.2 Default site counts for production sites

Omara et al. includes survey data from a number of sites in different producing regions. The number of wells per site can vary greatly between different regions with different drilling plans and well designs.

For this reason, we generate site counts as follows. The well count is divided by 2 to generate a production site count [212]. Further work could be performed to better characterize this value across producing basins or regions.

9.2.1.3 Default division between equipment types at production sites

The Omara et al. relationship gives the loss fraction for the entire site. This total-site emission must be apportioned into equipment-level loss for the purposes of OPGEE fugitives accounting. The default division of leakage between equipment is as follows:

- 50% of leakage is assigned to wellheads
- 50% of leakage is assigned to separators
- 0% of leakage is assigned to stabilizers

This default leakage assignment can be changed by the user.

9.2.2 Gathering and processing sites

Gathering and processing site data are gathered from the Mitchell et al. 2015 study of gathering and processing site emissions [220]. The Mitchell et al. characterized site-level emissions for sites containing gathering compressors, compressor/dehydration sites, compression/dehydration/sweetening sites, and full-featured gas processing plants. A total of 131 sites were characterized.

Raw data underlying the Mitchell analysis was digitized in October 2018 from online supporting information document associated with the paper. The following method was used for data analysis:

- Raw data are loaded into MATLAB.
- Data on loss rate are converted from % loss to loss fraction by dividing by 100.
- If the throughput rate reported by Omara et al. is 'NR', then the data are removed to avoid log-transformation of 'NaN' values. A total of 125 observations remain.
- Data for both production rate and loss fraction are log transformed using base-10 logarithm (MATLAB command `log10`).
- MATLAB command `fitlm` is used to generate linear fit between production rate (independent variable) and loss fraction (dependent variable).
- MATLAB commands `fit` with Poly1 option (1st order polynomial, or linear fit) is used along with the `predint` command to develop prediction intervals for 68% (± 1 SD) and 95% (± 2 SD).

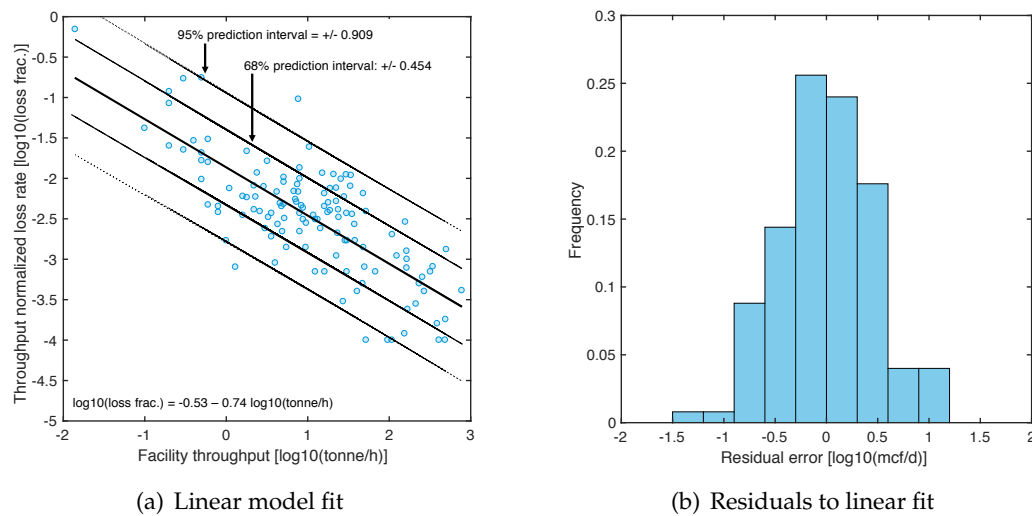


Figure 9.4: Results of fitting linear model to log-transformed leakage fraction as a function of log-transformed processing facility throughput.

The resulting fit quality results are given below:

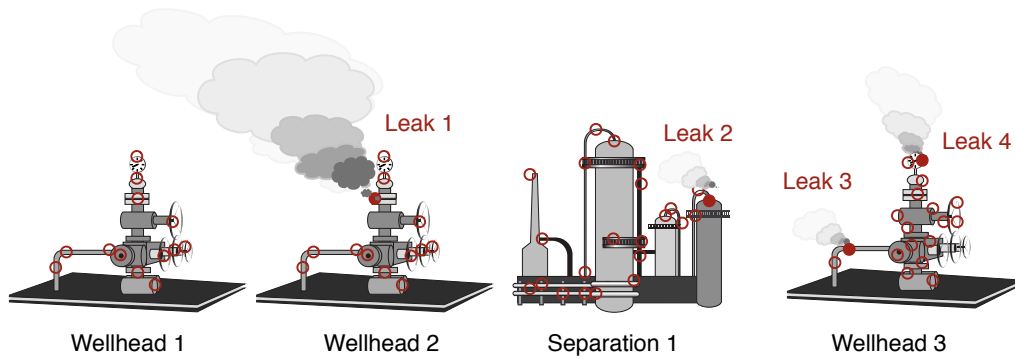
- Number of observations: 125, Error degrees of freedom: 123
- Root Mean Squared Error: 0.459
- R-squared: 0.582, Adjusted R-Squared 0.578
- F-statistic vs. constant model: 171, p-value = 4.93e-25
- Intercept param: -1.8618 (SE= 0.062499, p-value 4.3311e-58)
- Slope param: -0.59397 (SE = 0.045416, p-value = 4.9298e-25)

The resulting fit and residuals are presented in Figure 9.4. Figure 9.4(a) shows the prediction intervals (PIs) for the resulting equation. The 68% PI is ± 0.454 , while the 95% PI is ± 0.909 . The residuals (Figure 9.4(b)) are approximately evenly distributed around 0. The PIs are used by OPGEE to draw an uncertainty realization.

9.2.2.1 Default site counts for gathering and processing

EIA data show that in the U.S. in 2012, a total of 517 gas processing plants processed 65.5 billion cubic feet per day [?]. Thus, each processing plant handled 126.7 mmscf/d. This is used as the default gas processing plant capacity.

Marchese et al. 2015 [?] showed that the number of gathering facilities nationwide in the U.S. was 4459 [? , SI Table S12]. If we assume all of 2014 gross annual natural gas withdrawals of 31,405,381 mmscf [?] was apportioned evenly throughout time and across facilities, this amounts to average facility throughput of 19.3 mmscf/d. This is used as the default gas gathering plant capacity.



Equipment inventory: WH1, WH2, WH3, SE1

Component inventory: WH1: 12 TC ... 1 PRV
WH2: 14 TC ... 2 PRV
...

Leak inventory:
WH1: NA
WH2: Leak 1 (F)
WH3: Leak 3 (TC), Leak 4 (M)
SE1: Leak 2 (VL)

Leakage estimate: Leak 1 + Leak 2 + Leak 3 + Leak 4

Figure 9.5: Schematic of site-level quantification of methane emissions.

9.2.2.2 Default division between equipment types at gathering and processing sites

The default division of leakage between equipment is as follows:

- 50% of leakage is assigned to gas dehydration;
- 50% of leakage is assigned to acid gas removal;
- 0% of leakage is assigned to fractionation;
- 0% of leakage is assigned to the Ryan-Holmes process.

This default division can be changed by the user.

9.3 Component-level methods for on-site emissions

In contrast to the above-described site-level methods, component-level methods for estimating fugitive emissions start with a list of components present at a site. These components can include – for example – connectors, valves, flanges, or seals. Of these components, some fraction will be leaking. The leakage can be quantified by component and the total estimated volume of leakage can therefore be computed. This overall modeling philosophy is sketched in Figure 9.5, in contrast to the illustration for the site-level emissions in Figure 9.2.

The overall methodological approach to be used in the proposed tool is of the general family of “bootstrap resampling” methods, sometimes classified as a type of “non-parametric” approaches to uncertainty estimation.

Traditional statistical approaches to this problem would calculate overall properties (“parameters”) of sampled leaks from a given type of equipment or type of facility – such as mean μ and standard deviation σ and use these values to estimate leakage at non-sampled locations. For example, one might compute μ and σ of observed leakage for “connectors” based on measurements made at a set of facilities and then use these to model emissions from un-measured “connectors” by drawing from a classical distribution with these properties (e.g., Gaussian).

In contrast, bootstrap methods are computational in nature. The dataset of observed leaks is used to draw repeated instances of possible facilities by simulating facilities and drawing leaks from the available quantified leaks. These approaches are more computationally intensive, but are more useful in cases where properties of the dataset are highly skewed. Because of the “heavy tail” seen in empirical methane leak distributions [221], these resampling approaches should be favored compared to traditional parametric approaches.

We can first describe an “idealized” workflow that would generate emissions estimates if the user has complete information. The overall methodological approach is outlined in Figure 9.6. As shown in Figure 9.6, the basic steps are as follows:

1. Generate list of equipment at facilities. Each facility should contain a number of each generic equipment type in the model. If the user does not have an equipment inventory at each site, then defaults will be populated by the model.
2. Generate list of components for each piece of equipment. Each piece of equipment should contain a number of each general component type in the model. If the user does not have a component inventory for each piece of equipment, defaults will be populated by the model.
3. Generate a probability of leakage for a given component type, or the fraction of components that should be classified as leaking and non-leaking. If the user does not have a probability of failure for each component type, defaults will be populated by the model.
4. Construct the population of leaking components in a series of nested loops as follows:
 - (a) For each facility, examine the equipment types in order
 - (b) For each equipment type, examine the equipment pieces in order
 - (c) For each equipment piece, examine the component types in order
 - (d) For each component type, examine the components in order
 - (e) For each component, use the probability of leakage to assign the component to the leaking or non-leaking state
 - (f) Draw a leakage rate from the component from the appropriate section of the database (leaking or non-leaking).
 - (g) Add the component leakage to the component type total and iterate to the next component. Continue until all components in the component type are assessed.

- (h) Move to the next component type and repeat steps d-f.
 - (i) Move to the next equipment piece and repeat steps c-f.
 - (j) Move to the next equipment type and repeat steps b-f.
 - (k) Move to the next facility and repeat steps a-f.
5. After the population of leaking components is generated, analysis can be performed to understand a number of factors:
- (a) Number of total expected leaks, computed by counting the expected leaks across realizations
 - (b) Number of expected “super-emitters” at the facilities of interest, given various definitions of super-emitter
 - (c) Emissions distribution by size of leak, computed by plotting distributions and analyzing percentiles for resulting sets of leaks

Implementing such a tool would require and the following inputs:

1. Number of facilities
2. Equipment list for each facility
3. Component list of each piece of equipment
4. Probability of leakage by component type
5. Database of leakage volumes for measurements classified as leaks
6. Database of leakage volumes for measurements classified as “default 0” leaks.

In the case of implementing such a model in OPGEE, these data could be derived either from (1) user-supplied data particular to the facilities or equipment being modeled, as entered into OPGEE ‘Inputs’ or ‘Secondary Inputs’ sheets. Or, barring user inputs, (2) OPGEE defaults. Obviously, using user-supplied data in such a model is preferable due to the increased specificity allowed when data can be applied that are specific to the set of facilities being modeled. Some data are unlikely available in many cases. For example, the user may not have a list of components for each piece of equipment, so default component counts would be used in that case.

The method used in OPGEE differs somewhat from this idealized approach due to data challenges, as described below.

9.3.1 Literature review

To begin, we review the literature available below. The literature required for the component-level model is different from the literature required for site-level emissions estimates. For example, most site-level studies do not perform component-level emissions inventories.

9.3.1.1 Equipment lists by facility type

Few prior published studies include a complete list of equipment present at a given facility. The available data are challenging to standardize, as terminology and level of classification detail can differ significantly between studies. It is generally not clear in a given study whether the counts of equipment represent complete counts per site or the counts of surveyed equipment (if only a fraction of equipment is present). It is also generally not clear how equipment counts vary with throughput, nor often what the throughput is at a given facility that was studied.

Because of this general dearth of data on counts of equipment per facility type, users of OPGEE should ideally input equipment counts. This should be feasible for oil and gas operators as they will likely have detailed equipment inventories and know which sites contain which types of equipment and how many of each process unit is present. Depending on the regulatory jurisdiction, regulators or government agencies may have more or less data available on the counts and types of equipment per site. For example, Englander et al. [212] found that air quality permits from the North Dakota Environmental Protection Agency were generally of poor quality and the listed equipment very often differed from the equipment observable from field surveys or from remote sensing imagery (e.g., a site is listed as having 4 tanks but satellite imagery suggests that 8 tanks exist on the site).

Users can input component counts, if obtained, into OPGEE for direct use, overwriting the default equipment type component counts.

9.3.1.2 Component lists by equipment type

Each piece of equipment next needs a list of components that may leak. For example, rarely would a “separator” be considered leaking, but instead a component on a separator may be leaking (i.e., valve or flange).

Ideally, users of OPGEE will have detailed databases on the components present on a site, the age and manufacturer of the components, and repair records. The degree to which such data, as well as their quality assurance (QA) status or recency, exist may vary by operator. Given that OPGEE is often used with public domain data, it is not clear how many regulatory jurisdictions require information reported by operators on the components present at sites. We are not aware of regulatory datasets at the component level.

Absent detailed data on component counts for each piece of equipment, we describe literature sources for default component counts below. The same difficulty present in equipment datasets is present in component datasets: terminology is not standardized and different studies can use very different terms.

9.3.1.3 Fraction of components leaking

Next, OPGEE requires the fraction of components expected to be found leaking. For example, the user of the tool might enter that 2% of valves are expected to be leaking. An operator might have such data if extensive prior studies had been performed on the operator’s equipment and facilities so that a good baseline fraction of leaking components was understood.

In many cases, OPGEE users will not have specific information about the fraction of components expected to be leaking at a given site. In this case, OPGEE

populates defaults fractions of leaking components from the public domain literature.

Many, but not all, of the datasets that report component counts also report the fraction of components of a given type that were found leaking. Some caveats with regard to this data are worth noting here.

First, not all studies consider the same components to be part of the survey sample or even capable of leaking. For example, early studies largely neglect component counts and emissions rates of pneumatic controllers, as the design nature of these devices is to leak a certain amount of gas upon actuation.

Some studies only report the fraction of components leaking at a very aggregate or large-scale level. For example, Clearstone 2002 reports in detail the types of components at the site, but only give the fraction of components leaking for a given component type in the site as a whole (i.e., all connectors) not components at a given piece of equipment (i.e., connectors at compressors).

Each study uses a particular screening method to sort components into leaking and non-leaking components. While a few common screening methods predominate, these have changed over the years and will affect the fraction of components found leaking in a given survey. This also makes cross-comparison across studies performed over many years challenging.

OPGEE requires the fraction of components found to be leaking for the generic types of components described above. The literature, in general, lacks the data to assign frequency of leakage to a component/equipment pair, so we produce leakage probabilities by component type only (despite the fact that we generate counts on a component/equipment basis). For example, the data provide information that allow us to estimate a reasonable figure for the fraction of “connectors” leaking, but not the fraction of “connectors at compressors” leaking.

9.3.1.4 Database of component leakage or emission rates (leaking components)

The next piece of data required for OPGEE component-level VF estimates is a database of empirical leakage rates for each component type, ideally with each component type being measured at a variety of facilities. Most operators will not have such data, or would be interested in using the largest set of data possible, so we focus here on the publicly available data.

Leakage quantification data are the most widely available of our data requirements, and many of our reported studies include data on leakage volumes by quantified leak. We outline below a data gathering effort that resulted in more than 25,000 data entries for emission or leakage volume for each of a number of component failures.

9.3.1.5 “Default-zero” leakage or emission rates (non-leaking components)

The last data requirement is a default leakage rate to be applied to components classified in primary screening as “non-leaking”. Because any screening equipment used has a lower detection limit (LDL), there is some population of leakers which are emitting small amounts but are not classified as leaking by primary screening and are never measured.

For example, IR camera effectiveness was recently studied in a controlled environment [?]. It was found that at a distance of 3 m, the camera operator had a 90% chance of detecting leaks of size 10 gCH₄/h. Thus, if an IR survey is performed at such a distance, some “non-leaking” components might actually be leaking at some rate less than 10 gCH₄/h. For this reason, some studies measure emissions from components found to be “non-leaking” during screening and call these “default-zero” emissions factors.

Non-leaking emissions factors are generally less available than leakage databases. Also, non-leaking component emissions rates will differ greatly depending on the screening method use (i.e., local CH₄ concentration above 10 ppm vs. 10,000 ppm). Given the challenges in implementing non-leaking emissions factors and the small volumes of emissions involved, OPGEE by default does not include emissions from leakers.

9.3.2 Available datasets

Given the data needs discussed above, we now examine the available datasets that contain information on each required input.

Key questions include:

- Are available data sufficient in counts of equipment and counts of components to allow for generating expected lists components from facilities?
- How many studies include leakage fractions or other proxy-measures for the fraction of components that can be considered leaking?
- How robust are data on reported emissions estimates for leak? How many observations are available for each emission source? Do observations vary between studies or between different types of equipment?

We performed a thorough literature search, building on prior literature searches done for Brandt et al. 2014 [222] and Brandt, Heath, Cooley [221]. Over 200 papers were reviewed for Brandt et al. 2014, and since then many hundreds of potentially useful papers have been published.

The aim of our literature review was to identify papers containing original data collection. After collecting the initial papers, we removed papers falling into a number of categories:

- Re-analysis papers looking at prior datasets
- Methane emissions reduction policy analysis
- Methane-related climate impact analysis studies
- Assessments of new detector or estimation methods that lacked original field data gathering

Some studies included original data gathering, but data were not gathered at the correct scale for our analysis method. Many of these larger-scale studies informed the site-level method described above.

After these initial filters were applied, each paper – and any associated supporting documents and datasets – were analyzed for useful data. Papers that contained

useful information were “included”, while those that did not were “excluded”. In particular, a document was considered “included” if it contained any of the following information:

1. Data on activity counts (activity factors, AF) for oil and gas facilities, including:
 - (a) Activity counts for numbers of pieces of equipment per site, called *equipment quantification* (EQ) below
 - (b) Activity counts for numbers of components per piece of equipment or per site, called *component quantification* (CQ) below.
 - (c) Activity counts for number of activations, releases, or events in an intermittent release system, called *activation quantification* (AQ)
2. Data on fraction of components leaking found to be leaking in a survey, called *fraction leaking* (FL) data;
3. Data on quantified leak volumes per emitting component or source, called *leak quantification* (LQ) data;

While many of the resulting studies computed emissions factors, we did not make use of computed average emissions factors from studies. Our bootstrap approach aims to avoid use of average emissions factors and to instead draw empirical observations from complete datasets of all measured emissions within a study sample to better account for non-normally distributed leak sizes.

All studies which passed the initial screen are listed in Table 9.1.

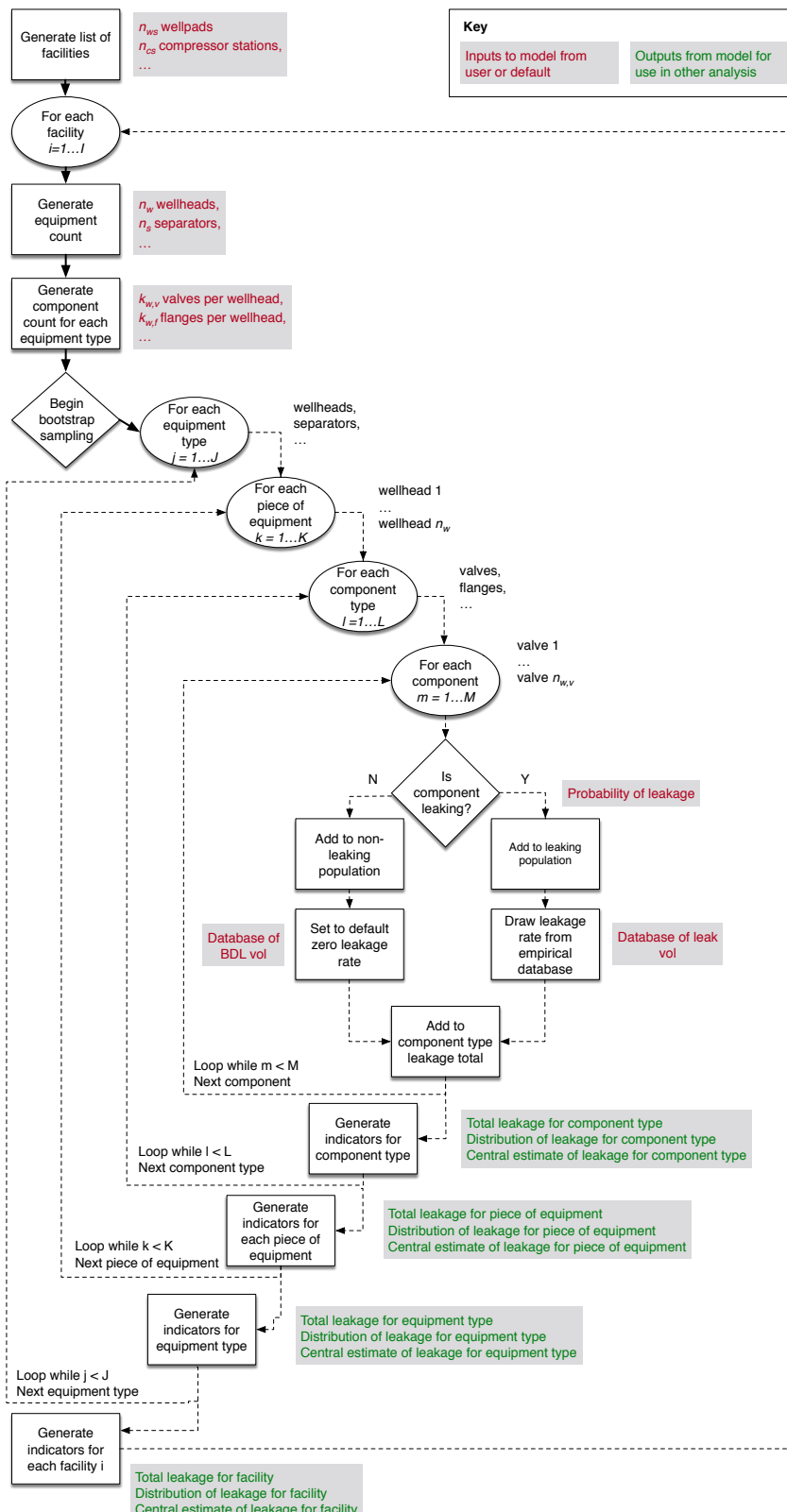


Figure 9.6: Schematic of method for generation of project-level fugitive emissions rates from component-level estimates.

Table 9.1: Studies considered for inclusion.

Study ID	Study Lead	Year	Location(s)	Seg.	Citation	Journal or publisher
Allen2013	D. Allen	2013	USA (various)	U	[223]	Proceedings of the National Academy of Sciences Environmental Science & Technology
Allen2014a	D. Allen	2014	USA (various)	U	[224]	American Petroleum Institute, Report Number API 4589
Allen2014b	D. Allen	2014	USA (various)	U	[7]	American Petroleum Institute, Report Number API 4615
API1993	Star Environmental	1993	USA (various)	U	[39]	American Petroleum Institute, Report Number API 4589
API1995	Star Environmental	1995	USA (various)	U	[40]	American Petroleum Institute, Report Number API 4615
API2004	T. Shires	2004	USA (various)	U/M/D	[30]	American Petroleum Institute
API2009	T. Shires	2009	USA (various)	U/M/D	[225]	American Petroleum Institute
Alvarez2018	R. Alvarez	2018	USA	All	[226]	Science Journal of Cleaner Production
Balcombe2018	P. Balcombe	2018	USA	All	[227]	Elementa Science of the Total Environment
Bell2017	C. Bell	2017	Fayetteville AR	U	[209]	Elementa Science of the Total Environment
Boothroyd2016	I. Boothroyd	2016	UK	U	[228]	CSIRO Energy Technology
Boothroyd2018	I. Boothroyd	2018	UK	M	[229]	Environ International for Texas Commission on Environmental Quality
CAPP2014	Clearstone Engineering	2014	Canada	U/M	[230]	Canadian Association of Petroleum Producers
Clearstone2002	Clearstone Engineering	2002	USA (Various)	M	[231]	Gas Technology Institute
Clearstone2015	Clearstone Engineering	2015	Mexico	U	[232]	Petroleum Technology Alliance Canada
Day2014	S. Day	2014	Australia	U	[233]	CSIRO Energy Technology
Environ2010	Environ International	2010	TX, USA	U	[234]	Environ International for Texas Commission on Environmental Quality
EPA1993	EPA	1993	USA (various)	M	[235]	US EPA, Report Number EPA-453/R-93-026
EPA1995	EPA	1995	US (Various)	All	[236]	US EPA, Report Number EPA-453/R-95-017
EPA1996	EPA	1996	US (Various)	All	[201]	US EPA, Report Number EPA-600/R-96-080A to EPA-600/R-96-080C
ERG2011	ERG	2011	Fort Worth TX	U/M	[237]	City of Fort Worth
ERG2012	ERG	2012	TX, USA	U	[238]	ERG, Eastern Research Group, Inc. Report Number 0292.01.011.001
Gidney2009	B. Gidney	2009	TX, USA	U	[239]	Hy-Bon Engineering Company, Ltd for Texas Commission on Environmental Quality
Greenpath2017	Greenpath Energy Ltd.	2017	Alberta/British Columbia	U/M	[240]	Greenpath Energy Ltd. For PTAC
Hendler2009	A. Hendler	2009	TX, USA	M	[241]	Texas Environmental Research Consortium
Harrison2011	M. Harrison	2011	TX, NM, USA	M	[242]	URS
Hendrick2016	M. Hendrick	2016	Boston, MA	D	[243]	Environmental Pollution
Johnson2015	D. Johnson	2015	TX, USA	M	[244]	Proceedings of the National Academy of Sciences
Kang2014	M. Kang	2014	Pennsylvania	U	[245]	California Energy Commission, PIER
Kuo2012	J. Kuo	2012	California	U/M/D	[246]	EPA, QAPP-1J16-019.R1, Revision 1
Jacobs2016	Jacobs Technology	2016	UT, USA	U	[247]	Environmental Science & Technology
Lamb2015	B. Lamb	2015	USA (various)	D	[248]	Environmental Science & Technology
Lyman2017	S. Lyman	2017	UT, USA	U	[249]	NGML, Clearstone Engineering Ltd., Innovative Environmental Solutions
NGML2006	NGML	2006	USA (various)	U/M	[250]	Air & Waste Management Association. Paper Number: 06-A-119-AWMA
Picard2006	D. Picard	2006	Canada	M	[251]	Environmental Science & Technology
Subramanian2015	R. Subramanian	2015	USA (various)	M	[252]	Journal of Environmental Protection
Thoma2017	E. Thoma	2017	Uintah Basin UT	U	[253]	Geophysical Research Letters
TownsendSmall2016	A. Townsend-Small	2016	USA (various)	U	[254]	Elementa
Vaughn2017	T. Vaughn	2017	Fayetteville AR	M	[255]	Environmental Science & Technology
VonFischer2017	J. Von Fischer	2017	USA (various)	D	[256]	Environmental Science & Technology
Zimmerle2015	D. Zimmerle	2015	USA (various)	M	[257]	Elementa
Zimmerle2017	D. Zimmerle	2017	Fayetteville AR	M	[258]	Elementa

After assessing each study in detail for whether it contains any of the required data types listed above (AF, LF, LQ), we grouped studies into included and excluded groupings.

Table 9.2 lists all studies that were examined for the above desired data and included in the study pool based on existence of one of the required three data types. Some studies contain all three data types, but a significant subset of the studies only include LQ data without a thorough CQ or assessment of LF.

Studies which were found upon close study to not contain useful data are not included in Table 9.2 and are not considered in future discussion. In most cases, these studies estimate emissions at the site-level or larger, typically via off-site monitoring and plume reconstruction and would inform site-level methods described above. In some cases, individual leaks were measured, but the leaks were not reported individually, making the results not usable with our methodology.

Table 9.2: Data types found in studies determined to contain original data of types activity factors (AF), leakage fraction (LF), leakage quantity (LQ), or default-zero (DZ). AF data include equipment quantification (EQ), component quantification (CQ), or activity quantification (AQ).

Study ID	Industry	Types of sites segment	Activity factor (AF) data available	Fraction leaking (FL) data available	Quantified leak (QL) data available
Allen2013 Allen2014a	U U	Wellsites Wellsites	- CQ: Pneumatic controllers, wells per site	- -	QL: 4 component types QL: Pneumatic controllers
Allen2014b API 1993	U U/M	Wellsites platforms, plants	AQ: Number of unloading events EQ: Equipment per site (incomplete) CQ: Components per equipment	FL: Fraction above 10 ppmv -	QL: Unloading events QL: 7 component types
API 1995	M	Gas plants	EQ: Equipment per site (incomplete) CQ: Components per equipment CQ: Components per facility	FL: Fraction above 10,000 ppmv -	QL: 7 component types
API 2009 Bell2017	U/M/D U	All Wellsites	- -	- -	QL: 18 component types for 7 pieces of equipment (Datafile)
CAPP2014	U/M	All	CQ: Components per equipment	FL: Fraction leaking by component type FL: Fraction leaking by component and site	-
Clearstone2002	M	Gas plants	CQ: Components per facility	- -	-
Environ2010 EPA1996 ERG2011	U U/M/D U/M	Tank batteries All Wellsites	- CQ: Component counts per site EQ: Wells, tanks, compressors per site CQ: Valves, connectors per site	FL: Customer meter leakage fraction Total number of leaks, but no fraction computable	QL: >50 component types (datafile)
Gidney2009 Greepath2017	U U/M	Wellsite tanks All	- -	- -	QL: 36 tank batteries QL: 8 component types, 17 different site types
HARC2009 Harrison2011	M M	Tank batteries Compressor stations Distribution Compressor stations	- - -	- -	QL: 33 tank batteries QL: 5 component types
Hendrick2016 Johnson2015	D M	Abandoned wells Various sites	- EQ: Average and ranges of component counts	- -	QL: 99 underground leaks QL: Named leaks, classified into categories QL: 7 component types
Kang2014 Kuo2012	U U/M/D	Distribution pipe and M & R Gas plants	- -	- -	QL: 19 abandoned wells QL: 10 types of facilities and 18 component or source types.
Lamb2015	D	Gas plant (fractionation) Compressor stations	CQ: Components per site	FL: Fraction leaking by component and site type	QL: 51 component types
NGML2006	U/M	Gas plant (fractionation)	CQ: Components per site	FL: Fraction leaking by component type and site	-
Picard2006	M	Compressor stations	-	FL: Fraction leaking by component type	-
Subramanian2011	M	Wellsites Abandoned wells Gathering and boosting stations Transmissions and storage sites Gathering systems	CQ: Pneumatic controllers per well	None, all were emitting by design FL: Fraction above screening value	QL: 20 source categories
Thomas2017a TownsendSmall2016 Vaughn2017	U M	- - - - -	- - - - -	QL: 80 pneumatic controllers QL: 165 abandoned wells QL: 7 types of sites and 18 types of components QL: 11 site types and 14 component/ emission types QL: 3 site types and 4 component/ emissions types	
Zimmerle2015 Zimmerle2017	M M	- -	- -	- -	-

9.3.3 Data sufficiency: Activity Counts

Activity count data specify “how many” of a given possible leak source are present. Activity counts can be performed at multiple levels of aggregation or scale. For example, activity counts may address any of the following questions:

- How many gas wellsites exist in a given field?
- How many separators are present at a typical wellsite?
- How many connectors exist per separator at a gas wellsite?

The first of these questions is primarily of interest in scaling up information from site-level studies as described above. For component-level estimates, the latter questions are applicable.

We assess activity counts at three levels:

Equipment quantification (EQ) How many pieces of equipment are at a typical facility of a given type? This is our equipment quantification, or EQ activity factor definition above.

Component quantification (CQ) How many components of a given type are present on a given piece of equipment or in a given facility? This is a component quantification or CQ activity factor defined above.

Activity quantification (AQ) How often does an intermittent or infrequent event occur? This is an activation quantification or AQ activity factor defined above.

We address these three types of activity factors below. The supplemental OPGEE VF shirworksheet contains details on the contributions from each study.

9.3.3.1 *Equipment quantification (EQ) counts per facility*

The first group of activity factors are equipment quantification counts per facility, (EQ), or equipment quantification activity factors (EQ-AF). A variety of studies include EQ data.

In compiling EQ data across studies, we face the challenge of non-standardized equipment type definitions. Equipment can be named differently in different studies, and not all studies cover all kinds of equipment. In some cases, equipment types are sub-divided by the type of process, fluid being treated, location, or type of resource being extracted. For example, API 2009 [225, Appendix B] presents default component counts for the same type of equipment used for “Light oil”, “Heavy oil”, etc. For example: a well in the light oil default contains 53 connectors, while a well in the heavy oil default contains 44 connectors. Other studies make distinctions are made between offshore and onshore oil [201, 225?], between deep oil and shallow oil [230], or between different chemical processes, such as gas sweetening with amine vs. gas sweetening with Sulfinol [230].

In order to compile EQ data across studies, we create a matrix that represents the correspondence between the equipment definitions used in a given study and a standardized equipment definition used for OPGEE.

The OPGEE standardized equipment definition was created by consulting reported datasets, with an emphasis on the following factors:

- Moderate level of disaggregation, to avoid too many equipment types (e.g., 98 equipment types of CAPP 2014) or too few equipment types (e.g., 3 equipment types for EPA 1996 gas processing estimates).
- Coverage of most of the classes of equipment outlined in two key historical documents, API 1993 and API 2009, due to the fact that many other studies apply similar categories.
- Alignment with as many references as possible to allow for multiple estimates of the same quantity.

Given these objectives, we arrive at the following standardized equipment list of 23 kinds of equipment (21 defined, 1 “other” and 1 “not recorded”):

- Well - Gas (WG)
- Well - Oil (WO)
- Header (HD)
- Heater (HE)
- Separator (SE)
- Chiller (CH)
- Stabilizer (ST)
- Meter (ME)
- Tank (TA)
- Compressor - Reciprocating (CR)
- Compressor - Centrifugal (CC)
- Compressor - Type unspecified (CM)
- Compressor - Balance of systems (CMBOS)
- Dehydrator (DE)
- Acid gas removal (AGR)
- Flare (FL)
- Vapor recovery unit (VRU)
- Fractionation (FRA)
- Metering & regulating (MR)
- Piping - Upstream (PU)
- Piping - Downstream (PD)
- Other (OTH)

- Not reported (NR)

While any categorization effort is inherently at least slightly arbitrary, we believe this moderate level of complexity is the best compromise given the currently available datasets and their groupings.

Some notes on particular categories: “Piping - upstream” and “Piping - Downstream” are currently unused in OPGEE. These are included as placeholders so that future development can include factors for these. These would need to be denominated in terms of unit distance instead of piece of equipment (i.e., connectors per kilometer of downstream piping). “Other” is included for cases where the piece of equipment is listed but does not readily fall into one of the listed categories. “Not recorded” is used where no equipment type is given (this is common in some datasets).

The correspondence matrix \mathbf{M} between the standardized equipment type and the listed study-specific equipment type is of dimension $i \times j$, where i is the row, or the equipment category from a study, and j is the column, or standardized OPGEE equipment category. Since $j = 23$, all correspondence matrices are of dimension $i \times 23$. In each element of the correspondence matrix M_{ij} , a value of 1 represents a match between the equipment type in row i to standardized equipment type j , while a value of 0 indicates no match.

The correspondence matrices are presented in the supplemental VF OPGEE worksheet. Due to the length of the full set of correspondence matrices, we do not present them in this report.

9.3.3.2 Component quantification (CQ) counts per equipment or facility

The second group of activity factors are component quantification (CQ) counts per piece of equipment or component counts per facility. We can classify these above as CQ-AF, or component quantification activity factors. A variety of studies include CQ data.

In order to aggregate the CQ-AF data from the various studies, a standardized set of components is required. Our proposed component structure is a 11-fold categorization scheme. All components from all studies will be grouped into 10 named categories and a category that combines “Other” and “Not recorded”:

- Connector (CN)
- Valve (VL)
- Open-ended line (OEL)
- Pressure-relief valve (PRV)
- Compressor seal (CS)
- Regulator (REG)
- Vent (VT)
- Pump (PM)
- Pneumatic controller/actuator (PC)

- Tank vent/hatch (TK)
- Other/Not recorded (OTH)

We generated the 11-fold categorization scheme by examining the frequency of data reporting and common levels of reported data granularity across the studies. As noted above, the range of details provided varies by study, so using too fine or too coarse of a classification scheme would be sub-optimal. If too fine of a classification scheme is used, data from studies where only coarse categorization is reported become challenging or impossible to use. If too coarse of a classification scheme is used, large amounts of possibly useful identifying information are lost. “Other” and “Not recorded” are combined into a single category at the component level due to the fact that “Not recorded” is very rare for component types.

Correspondence matrices for reclassification of component counts For each study we need to align the categories of components used by the authors of a study to generate CQ data into our common component definitions that can be used across all studies. In order to do this we create a correspondence matrix that converts the original CQ organization to the standardized CQ organization. This correspondence matrix is composed using the following procedure:

Assume that we have a component count matrix \mathbf{C} for a set of m equipment types and n component types, organized as follows for a given study:

	CM_1	CM_2	\dots	CM_n	
EQ_1	c_{11}	c_{12}	\dots	c_{1n}	
EQ_2	c_{21}	c_{22}	\dots	c_{2n}	(9.1)
\vdots	\vdots	\vdots	\ddots	\vdots	
EQ_m	c_{m1}	c_{m2}	\dots	c_{mn}	

For a given equipment type i ($i \in 1 \dots m$) and component type j ($j \in 1 \dots n$), the value of c_{ij} is the number of components of that type present in that equipment type.

However, each set of equipment and component types can vary between studies. That is, the values of m and n can differ (i.e., how many types of equipment or how many types of components) between studies. Also, the names of components and equipment can differ, as can their order of presentation between studies.

Given any given component count matrix \mathbf{C} in the form presented for a given study, we can create a standardization matrix \mathbf{P} that will permute and change the shape of \mathbf{C} such that it has the same set of components in a standard list of components $c^* = [c_1^*, c_2^*, c_3^* \dots c_n^*]$. We define the matrix \mathbf{P} as follows:

- An entry of \mathbf{P} at location $p_{ij} = 1$ if component type i in the study dataset should be included as part of component type j in the standardized component list
- An entry of \mathbf{P} at location $p_{ij} = 0$ if component type i in the study dataset should not be included as part of component type j in the standardized component list
- An entry of \mathbf{P} at location p_{ij} of between 0 and 1 means that component type i in the study dataset should be divided between component type j in the

standardized component type and another component type. The sum of p_{ij} across the row i should equal 1 so that all components from the source component type are allocated to the standardized component types.

As an example, the study dataset has two types of compressors ($m = 2$, reciprocating compressors and centrifugal compressors) with four possible types of components at each compressor: (1) centrifugal compressor seals, (2) reciprocating compressor seals, (3) threaded connections, and (4) flanges. However, in our standardized component set, we want to group compressor seals all together in a group called “compressor seals” (CS) and also call threaded connections and flanges both “connectors” (CN). If we have the following raw data \mathbf{C} from the study:

	Centr. CS	Recip. CS	Connectors	Flanges	(9.2)
Cent. compressor	6	0	6	7	
Recip. compressor	0	7	37	14	

We can create a standardization matrix \mathbf{P} as follows:

	CS	CN	(9.3)
Centr. CS	1	0	
Recip. CS	1	0	
Thread. Conn.	0	1	
Flanges	0	1	

Note that the standardization matrix has dimension of our starting set of components in the rows and our desired set of components in the columns. We can then create a new dataset \mathbf{F} with the component counts presented for each type:

$$\mathbf{F} = \mathbf{C} \times \mathbf{P} \quad (9.4)$$

Or, in our example, \mathbf{F} is equal to:

	CS	CN	(9.5)
Cent. compressor	6	13	
Recip. compressor	7	51	

The benefit of this approach is that the correspondence between the original data set and the final dataset is uniquely defined by \mathbf{P} . We do not reproduce the conversion matrices \mathbf{P} here, but they are available in the supplemental OPGEE VF worksheet.

In all cases, for simplicity we have avoided fraction values of \mathbf{P} . While in some cases the source dataset uses a coarser aggregation scale than our standardized component counts, the data about which underlying types are present is not available. Therefore, in these cases we assign all of the components to the most common type of our standardized component type.

The resulting component numbers for each of the standardized equipment types is given in Table 9.3. Construction of Table 9.3 occurs in the OPGEE VF worksheet.

Table 9.3: Component counts for standard equipment-component pairs, resulting from computations performed on OPGEE supplemental VF worksheet.

9.3.3.3 Activation counts for intermittent activities

The third and last possible type of activity factor is AQ, or activation quantification. These activity factors quantify the numbers of discrete activation events for intermittent emissions sources. For example, AQ data might present the number of liquids unloading events per year for a given site.

OPGEE v3.0 does not currently model intermittent activities using AF-AQ. Instead, intermittent activities are apportioned over the operating life of the well to instead result in a continuous release. For example, well completions and workovers are converted to a per-MJ emissions intensity using the estimated productivity of the wells. Also, liquids unloading events, though discrete in reality, are modeled as a continuous release.

9.3.4 Data sufficiency: Fraction of components leaking

The fraction of components leaking (FL) has been found to vary greatly by study. There are a number of potential reasons for such variation, including:

- Inherent inter-site variability (spatial, industry segment, sampling year/season, random variation)
- Sampling differences between studies
- Use of different screening methods (ppm threshold vs IR camera)
- Use of different screening sensitivity (leaker defined at local concentration above 10 ppmv vs. 10,000 ppmv)

Table 9.4 shows the source of leakage percentage data in relevant studies and the thresholds used in each study for classifying a component as leaking.

Table 9.5 shows the distribution of expected leakage fractions after alignment of the study components to the standardized component classifications as described above. The process by which the fraction of leaking components is computed for the standardized categories is the same as the method by which component counts are put into standardized categories with a transformation matrix. Instead, for the fraction of leaking components, both the numbers of components and the number of leaking components are converted into standard categories, then the ratio of these standardized counts is taken.

Table 9.4: Sources of data on fraction leaking components.

Study	Source of component count	Source of leakage count	Leakage screening method		Screening threshold
API 4589 (API1993)	Appendix B (digitized)	Appendix C (digitized)	HC sensor		>10 ppm, >10,000 ppm
API 4516 (API1995)	Appendix A (digitized)	Appendix B (digitized)	HC sensor		>10,000 ppm
Clearstone 2002	Table 6	Table 6	Bubble test or ultrasonic followed by HC sensor		>10,000 ppm
Kuo 2012	p. 123	Tables 5.2 various, Tables 5.4 various	RMLD followed by HC sensor		>10,000 ppm
NGML 2006	Table 5	Table 5	Bubble test or ultrasonic followed by HC sensor		>10,000 ppm

Table 9.5: Resulting fraction leaking (FL) data for the standardized component categories defined above.

	Connector	Valve	Open-ended line	Pressure-relief valve	Comp. seal	Regulator	Vents	Pump	Pneu. controller	Tank hatch	Other
	CN	VL	OEL	PRV	CS	REG	VT	PM	PC	TK	OTH
N study sites	34	34	31	25	10	7	17	0	0	0	30
N devices	441588	81241	7974	1884	819	1437	65	396	457	0	13701
N leakers	4333	4377	616	75	379	37	29	67	236	0	375
Overall fraction leaking	0.99%	5.39%	7.73%	3.98%	46.28%	2.57%	0.00%	16.92%	51.64%	0.00%	2.74%
Min	0.00%	0.00%	0.00%	0.00%	0.00%	0.00%	0.00%	0.00%	41.38%	0.00%	0.00%
Max	7.93%	16.86%	25.00%	50.00%	100.00%	9.52%	100.00%	61.36%	100.00%	0.00%	157.14%
Mean	1.38%	6.37%	8.48%	6.44%	36.87%	4.59%	64.19%	13.37%	-	-	35.06%
Median	1.14%	5.86%	6.93%	0.00%	26.92%	4.75%	100.00%	0.00%	-	-	23.49%
5%-ile	0.01%	0.07%	1.70%	0.00%	0.00%	0.00%	1.30%	0.00%	-	-	0.00%
25%-ile	0.59%	2.16%	4.86%	0.00%	0.00%	1.68%	24.67%	0.00%	-	-	9.46%
50%-ile	1.14%	5.86%	6.93%	0.00%	26.92%	4.75%	100.00%	0.00%	-	-	23.49%
75%-ile	1.70%	10.29%	11.92%	6.35%	58.82%	6.78%	100.00%	16.67%	-	-	37.89%
95%-ile	3.51%	15.24%	17.55%	39.29%	100.00%	9.33%	100.00%	46.12%	-	-	103.93%

9.3.5 Data sufficiency: Leakage quantification data (QL)

Emissions observations are reported for a larger number of studies than component quantification counts or fraction of components leaking. The emissions observations are grouped into our standard equipment type and standard component types using alignment matrices as above. The correspondence matrices are available in the attached worksheet.

9.3.5.1 *Grouping emissions observations with standard equipment and component types*

For each study, the following workflow was followed to generate lists of leaks in standard equipment and component types:

1. The equipment types listed in each dataset are sorted alphabetically and duplicates are removed to arrive at a standard list of equipment types used in the study. If trivially different duplicates exist (i.e., "SEPARATOR" and "Separator"), find-and-replace is used to generate the simplest list of equipment possible.
 2. Each equipment type in the dataset are matched to the list of standard equipment and a correspondence matrix is generated. If the listed equipment type is not included in the list of standard equipment, "other" (OTH) is used. If no equipment type is listed, "not reported" (NR) is used. This correspondence matrix is the same as matrix **M** described above.
 3. The component types listed in the dataset are sorted alphabetically and duplicates are removed to arrive at standard list of components for the study. If trivially different duplicates exist (i.e., "VALVE" and "Valve"), find-and-replace is used to generate the simplest list of components possible.
 4. Each component in the dataset is matched to the list of standard equipment. If the listed component type is not included in the list of standard equipment, "Other" (OTH) is marked.
- . This correspondence matrix is the same as matrix **P** described above.

In some cases, the original study did not list categories, but instead included text descriptions of the leakage point (for example, Allen 2013 [223]). In these cases the correspondence file contains many strings that are manually aligned with equipment and component types.

The details and logic involved in assigning the correspondence for each study are listed in the attached worksheet.

9.3.6 Summary of data sufficiency analysis

Data are available in the literature for all required pieces of our proposed workflow and tool. However, the data availability varies greatly between different required data inputs. Some pieces of information are widely available, such as the quantified leaks for different component types (i.e., tens of thousands of quantified leaks). Other data inputs are poorly represented in the literature.

Table 9.6: Properties of emissions distributions for component-level emissions.

	N [samples]	Minimum [kg CH4/d]	Maximum [kg CH4/d]	Mean [kg CH4/d]	Median [kg CH4/d]	Contr. of SE [top 5%]
Connectors	9323	0	732.3	2.7	0.5	0.61
Compressor seals	442	0	3172.7	70.4	7.9	0.72
Not recorded	44	0	7.8	1.0	0.2	0.40
OEL	3478	0	10834.1	60.5	3.9	0.82
Other	2665	0	3917.1	15.4	1.5	0.82
Pneu. controller	1050	0	139.4	4.5	0.6	0.50
Pump seal	181	0	127.9	5.7	0.7	0.65
PRV	292	0	4140.4	37.0	1.1	0.80
Regulator	372	0	331.2	3.7	0.7	0.56
Tank hatch	247	0	414.1	38.5	7.5	0.39
Valve	5918	0	4125.3	8.4	0.3	0.79
Vent	795	0	5579.3	66.0	3.6	0.66
All	24807	0	10834.1	17.6	0.7	0.83

Table 9.7: Properties of emissions distributions by originating study.

	N [samples]	Minimum [kg CH4/d]	Maximum [kg CH4/d]	Mean [kg CH4/d]	Median [kg CH4/d]	Contr. of SE [top 5%]
Allen 2013	645	0	133.0	4.1	1.2	0.42
Allen 2014a	377	0	66.2	2.3	0.0	0.58
API 1993	718	0	25.0	0.4	0.0	0.73
API 1995	240	0	74.0	2.0	0.2	0.64
Bell 2017	322	0	212.1	4.8	0.6	0.68
EPA 1995	775	7.5E-07	3.8	0.0	0.0	0.77
ERG 2011	2126	0	708.7	16.1	2.5	0.52
Greenpath 2016	13149	0	5520.6	6.6	0.8	0.69
Harrison 2011	176	0	7892.7	570.1	3.0	0.44
Kuo 2012	337	0.28	244.3	7.4	0.3	0.66
Lamb 2015	948	0	66.4	0.7	0.1	0.70
NGML 2006	1641	0	2988.6	8.5	0.4	0.72
Vaughn 2017	510	0	361.2	14.3	2.8	0.54
Zimmerle 2015	2665	0	10834.1	69.5	3.5	0.68
Zimmerle 2017	99	0	96.0	1.2	0.1	0.92
All	24807	0.0	10834.1	17.6	0.7	0.83

9.4 Statistical analysis of leakage datasets

From our datasets, we gather a total of 24,807 total measurements. These are categorized by the study name, equipment type, and component type. We can plot the empirical cumulative distributions as a function of rank-ordered leak size. In Figure 9.7 we see the cumulative distributions with the observations grouped by the type of component. In Table 9.6 we report the properties for each of these groups, including sample size, mean, median, minimum and maximum, and percentage contribution of the top 5% of leaks to the total leakage.

Similarly, one can group results by the originating study. Different studies can have quite different emissions distributions because of focus on a particular equipment or site type. The cumulative normalized distributions by study are listed in Figure 9.8. The properties of the distributions, including N , minimum, maximum, mean, median, and contribution of top 5%, are presented in Table 9.7.

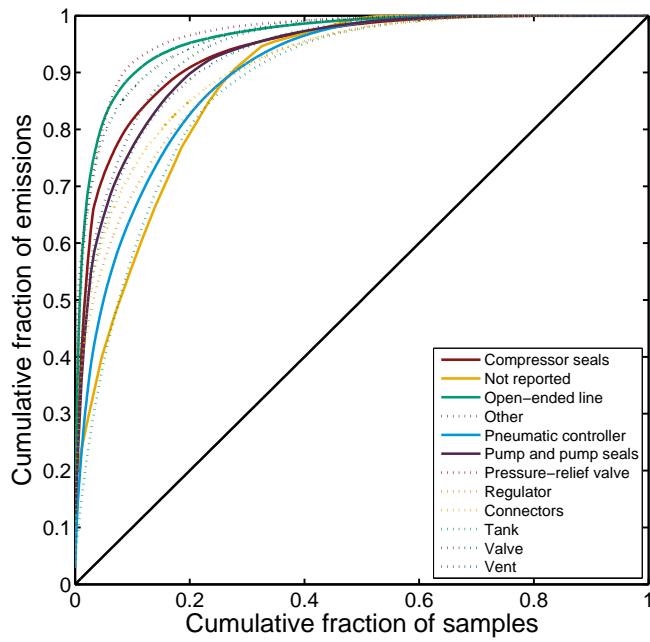


Figure 9.7: Cumulative contribution of rank-ordered normalized leakage volumes by 10 standard component classes and “other”.

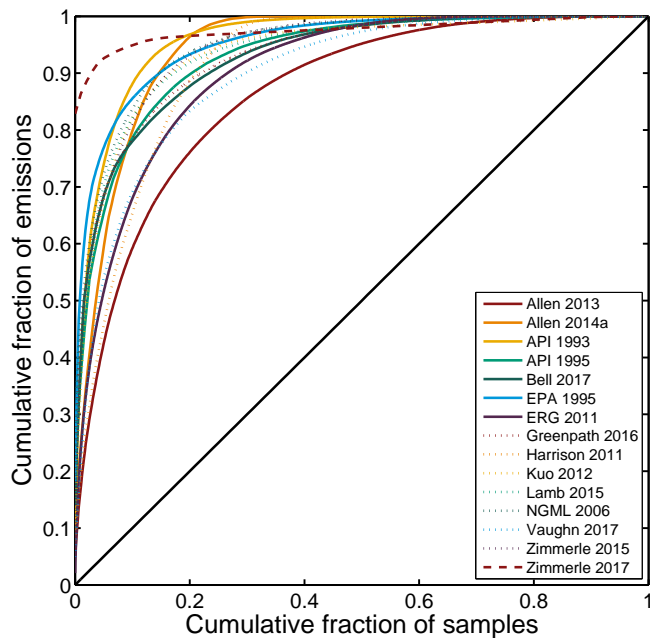


Figure 9.8: Cumulative contribution of rank-ordered normalized leakage volumes by originating study.

9.4.0.1 *Developing equipment-specific emissions distributions*

The resulting data from above are integrated into a MATLAB script for computing the emissions per piece of equipment. The steps are as follows:

1. Load data table of components per equipment type (see Table 9.3 above).
2. Load fraction of each component type expected to be leaking (see Table 9.5 above).
3. Load leakage database with leaking component, leaking equipment, and leak volume (see Table 9.6 and Figure 9.7 above).
4. Initialize a number of trials to analyze in Monte Carlo (MC) script. Default = 10,000 MC trials)
5. For each trial, iterate through the equipment list, assigning each component to leaker and non-leaker lists using fraction expected leaking for the particular component type of interest.
6. For each leak on the leaker list, draw a leak from the empirical distribution and add to the running sum of total equipment leakage.
7. At the end of the trial, save the total leakage and number of each leak type for that trial.
8. Iterate through MC trials to generate 10,000 realizations of equipment-level leakage.

The resulting equipment-specific percentiles are plotted in Figure 9.9 for 1,000 quantiles (0.1% fidelity). The resulting equipment specific mean and percentiles in 0.1% increments are loaded into OPGEE in the '*Leakage realizations - Component*' worksheet. For deterministic runs the mean leakage per piece of equipment is always used and is multiplied by the number of components. For uncertainty runs a random number is drawn and used to draw a leakage amount from the percentile table, which is multiplied by the number of pieces of equipment.

In future versions of the model, a feature may be added to draw each piece of equipment separately from the distribution, rather than drawing one value and multiplying it by the number of relevant equipment pieces.

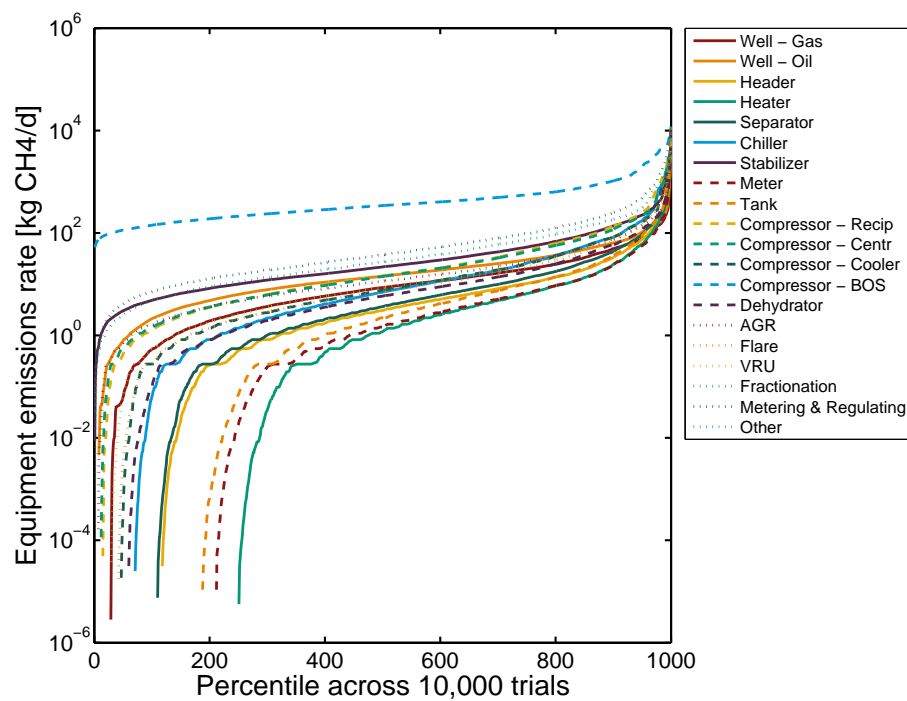


Figure 9.9: Absolute leakage (kg/d) percentiles (0.1% discretization giving 1000 steps) for equipment generated via 10,000 MC simulations of equipment given equipment component counts above.

9.4.1 Intermittent activities: Drilling and liquids unloading

Some activities release emissions at scattered points in time. For example, drilling and completions emissions occur during the the drilling and hydraulic fracturing of wells, but do not repeat over time. Workovers occur at discrete points in the life of the well, but are not common. And lastly, liquids unloading events occur at gas wells when liquid hydrocarbons and water build up in the wellbore and impede flow, which happens at varying frequency. We describe the methods to model these below.

9.4.1.1 Completions and workovers

We follow generally the method of Alvarez et al. [226] in modeling emissions from drilling and completions. While methane analysis work in the early 2010s found high emissions due to completions, regulations put into place around so-called “reduced emissions completions” (RECs) have greatly reduced completion methane emissions. Because operators are required to report GHG emissions to the Greenhouse Gas Reporting Program (GHGRP), we use these data in a similar fashion to Alvarez et al.

The methods to gather data for drilling completions and workovers are as follows

1. Access EPA custom GHG search site on October 19 2018. URL: <https://www.epa.gov/enviro/greenhouse-gas-customized-search>
2. Click on "Petroleum and natural gas systems"
3. Select reporting year 2017 and click "Go to step 2"
4. Click on appropriate tables for subject. Click first on "EF_W_COMP_WORKOVERS_FRAC" to obtain information for fractured well completions and workovers.
5. Click on step 3: Select Columns button
6. Select all columns
7. Click on "Go to step 4"
8. Do not select any narrowing criteria
9. Click on "output to CSV file"
10. Repeat steps 4-9 for second dataset "EF_W_COMP_WORKOVERS_NO_FRAC" to obtain information for non-fractured well completions and workovers.

These two datasets are then processed to generate per-well emissions rates and distributions.

For the dataset containing wells completed or worked over with hydraulic fracturing, the following processing workflow was followed:

1. Remove rows with no wells reported, as these rows are not useful in calculating per-well emissions rate

2. Compute per-well CO₂ and CH₄ emissions by dividing CO₂ and CH₄ emissions in tonne per year by well completion events per year
3. Remove rows where per-well emissions are zero (i.e., where wells are reported but no emissions are reported)
4. Separate results into sub-datasets depending on the activity pursued
 - (a) Split dataset into completion and workovers
 - (b) Further split dataset into completions with and without flaring and with and without RECs
 - (c) Further split dataset into workovers with and without flaring and with and without RECs
5. Compute mean and percentiles for each gas (CO₂ and CH₄) for the following categories
 - (a) Completions with flaring and RECs
 - (b) Completions with flaring only
 - (c) Completions with RECs only
 - (d) Completions with neither flaring nor RECs
 - (e) Workovers with flaring and RECs
 - (f) Workovers with flaring only
 - (g) Workovers with RECs only
 - (h) Workovers with neither flaring nor RECs
6. Plot box plots and cumulative distributions of resulting reported emissions

For the dataset containing wells completed or worked over without hydraulic fracturing, the following processing workflow was followed:

1. Remove rows with no wells reported, as these rows are not useful in calculating per-well emissions rate
2. Compute per-well CO₂ and CH₄ emissions by dividing CO₂ and CH₄ emissions in tonne per year by well completion events per year
3. Remove rows where per-well emissions are zero (i.e., where wells are reported but no emissions are reported)
4. Separate results into sub-datasets depending on the activity pursued
 - (a) Split dataset into completion and workovers
 - (b) Further split dataset into completions with and without flaring
 - (c) Further split dataset into workovers with and without flaring
5. Compute mean and percentiles for each gas (CO₂ and CH₄) for the following categories
 - (a) Completions with flaring

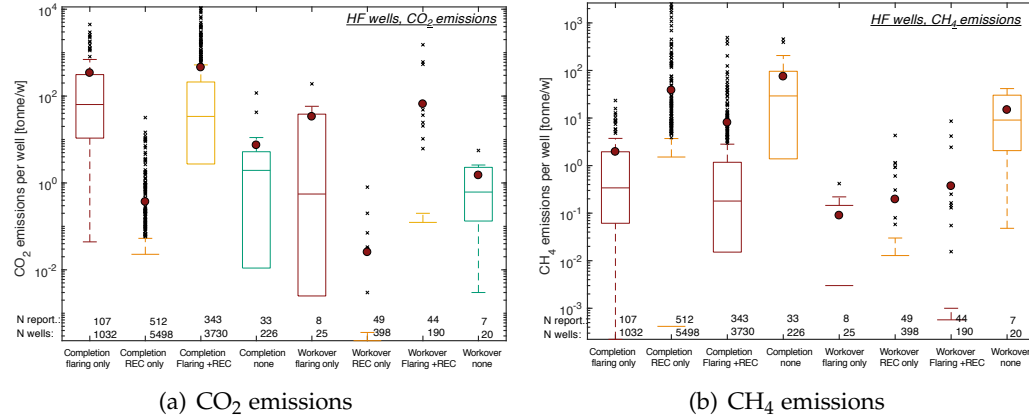


Figure 9.10: Emissions from completions and workovers performed on wells with the use of hydraulic fracturing, as reported to GHGRP datasets.

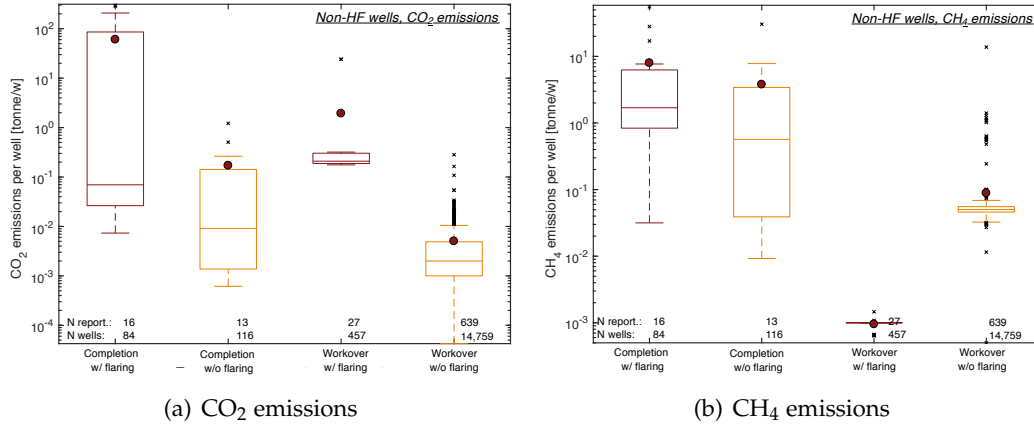


Figure 9.11: Emissions from completions and workovers performed on wells without the use of hydraulic fracturing, as reported to GHGRP datasets.

(b) Completions without flaring

(c) Workovers with flaring

(d) Workovers without flaring

6. Plot box plots and cumulative distributions of resulting reported emissions

The resulting box plots for wells with hydraulic fracturing and wells without hydraulic fracturing are presented in Figures 9.10 and 9.11 respectively. The resulting cumulative distributions are presented in Figure 9.12 and 9.13 for wells with and without hydraulic fracturing, respectively.

The resulting statistics are summarized in Table 9.8. If a deterministic OPGEE run is performed, the mean emissions per well are used for each well type. If uncertainty runs are performed, OPGEE picks an emissions value from the percentiles shown in the cumulative distribution (Figure 9.12 and Figure 9.13).

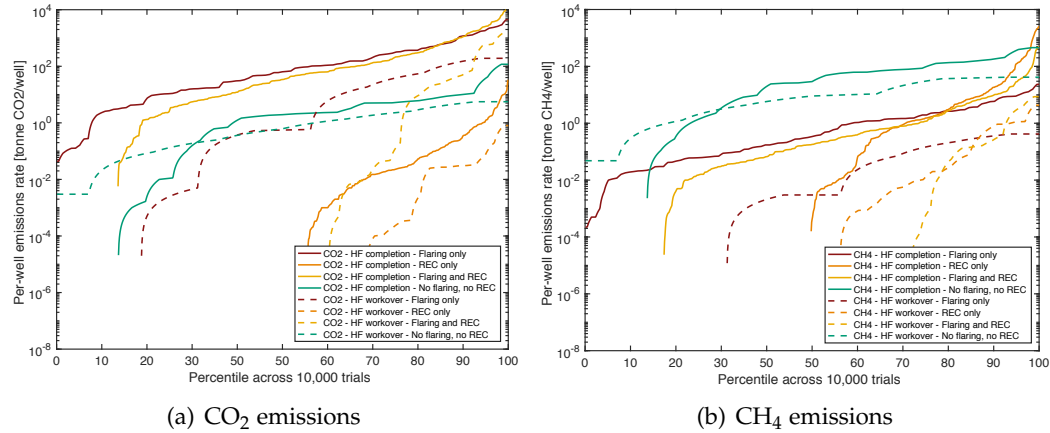


Figure 9.12: Cumulative distribution of emissions intensity for wells completed with the use of hydraulic fracturing.

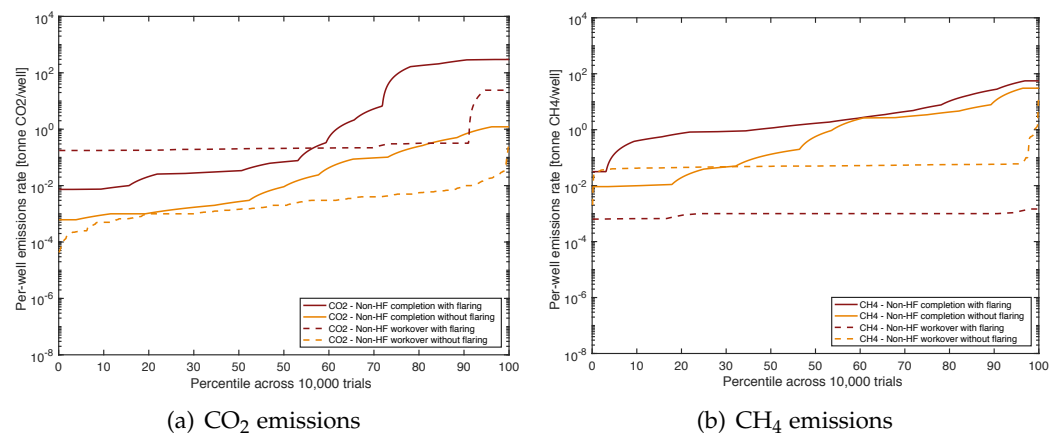


Figure 9.13: Cumulative distribution of emissions intensity for wells completed without the use of hydraulic fracturing.

Table 9.8: Properties of each category of gas well completion or well workover, sorted by application of hydraulic fracturing (HF) and application of emissions reduction method (flaring or reduced emissions completions (REC)).

Type	Number reporting companies [num rows]	Number of report- ing wells [num wells]	CO ₂ emissions to- tal [tonne CO ₂ /y]	Mean CO ₂ emis- sions per well [tonne CO ₂ /well]	CH ₄ emissions to- tal [tonne CH ₄ /y]	Mean CH ₄ emis- sions per well [tonne CH ₄ /well]
Completions with HF - Flaring only	107	1032	344538.5	333.9	1843	1.79
Completions with HF - REC only	515	5498	658.3	0.1	40948	7.45
Completions with HF - Flaring and REC	343	3730	1377711.2	369.4	10862	2.91
Completions with HF - No flaring or REC	33	226	624.9	2.8	4990	22.08
Workovers with HF - Flaring only	8	25	2757.5	110.3	6	0.25
Workovers with HF - REC only	49	298	1.5	0.0	14	0.05
Workovers with HF - Flaring and REC	44	190	16726.1	88.0	206	1.09
Workovers with HF - No flaring or REC	7	20	33.3	1.7	339	16.96
Completions without HF - Flaring	25	84	1917.3	22.8	169.3	2.0
Completions without HF - No flaring	45	116	2.8	0.02	201.6	1.7
Workovers without HF - No flaring	666	14759	66.6	0.0045	1264.3	0.1
Workovers without HF - Flaring	35	478	472	0.99	0	0.00

Table 9.9: Properties of reported liquids unloading fractional loss rates from Allen et al. 2014b [7].

Type	Num [N]	Prod-weighted mean [% loss]	5%-ile [% loss]	25 %-ile [% loss]	50 %-ile [% loss]	75 %-ile [% loss]	95 %-ile [% loss]
Automatic plunger	25	6.30	0.17	0.77	2.83	5.78	30.35
Manual plunger	50	0.37	0.00	0.06	0.36	1.53	5.79
No plunger	32	1.47	0.01	0.08	0.41	2.42	7.12
All wells	107	2.12	0.01	0.11	0.67	3.03	11.95

9.4.1.2 Liquids unloading

Liquids unloading emissions are intermittent events wherein liquids in the wellbore (oil and water) are removed to enable gas to flow more readily from the formation (reduce the pressure drop). Though liquids unloading events are discrete, for simplicity we model them here as if they occur continuously.

Liquids unloading data are obtained from Allen et al. 2014b [7]. Allen et al. characterize emissions from 107 wells, in a variety of regions and configurations (i.e., horizontal, vertical). Each well reports the gas production in scf/d as well as the annual methane emissions based on events per year reported by the operator and the measured emissions per event. These emissions per year are reported in mscf/y. We can then compute a fractional loss rate due to liquids unloading, as the total estimated annual liquids unloading loss divided by the extrapolated yearly production (i.e., assuming that gas production in scf/d is constant over the course of a year).

The resulting data are then categorized by the type of liquids unloading technology applied. The resulting mean, median, and emissions distributions are given in Table 9.9 and Figure 9.14 below. If a deterministic OPGEE run is performed, the mean emissions are used. If OPGEE uncertainty runs are performed, then a loss rate is drawn from the percentiles shown in Figure 9.14.

9.5 Off-site emissions

Off-site emissions are modeled using a simple overall loss-fraction approach in both site-level methods and component-level methods. Attempting to model mass loss rates from individual compression/transmission stations, for example, would lead to erroneous results because gas from many fields flows through each compressor stations and gas may flow through multiple compressor stations before arriving at end users.

For these reasons, D. Zimmerle and R. Subramanian, two authors of 2015 studies of transmission and storage sector emissions, recommended [?] taking overall fractional loss rates from Zimmerle et al. 2015 [257] and applying those to all gas flowing through the transport system. Zimmerle et al. estimate a total emissions amount of 1237 Gg CH₄/y (+36% / - 23% at 95% CI) [257, p. 9378]. Of this total loss, 75% was due to transmission and 25% was due to storage [257, Fig. 6]. Given a 2012 estimated transmission system throughput rate of 434 Tg CH₄, this amounts to a systemwide loss rate of 0.35% (0.28% – 0.45%, at 95% CI) of transported gas and a transmission-only loss rate of 0.263%. All transmission sector emissions are

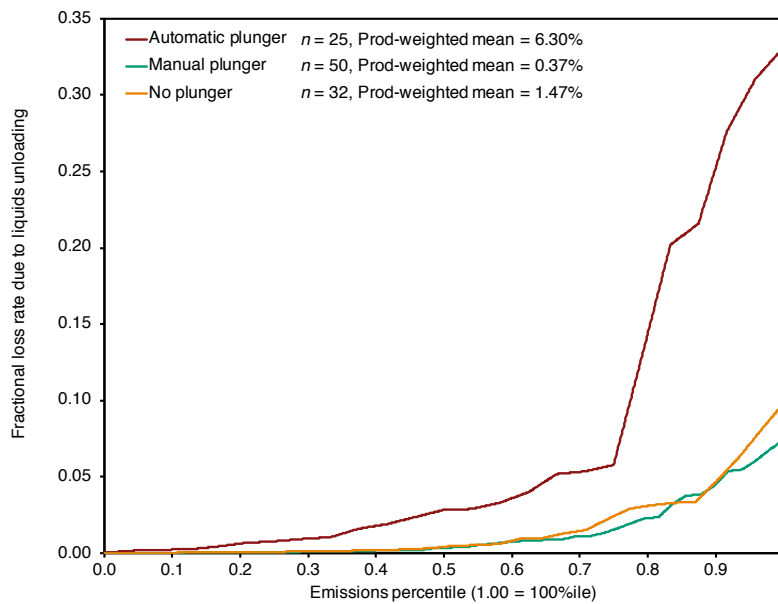


Figure 9.14: Fractional loss rates due to liquids unloading for 3 types of liquids unloading technologies from Allen et al. 2014b [7]. Sample size and mean emissions vary by technology.

assumed emitted at the transmission compressor.

A total of 25% of Zimmerle et al. [257] emissions are assumed from the storage sector (309 Gg CH₄/y (+36% / - 23% at 95% CI). Nationwide storage statistics for 2012 suggested injection of 2,825,427 million cubic feet and withdrawals of 2,818,148 million cubic feet for an average throughput rate of 2821 billion cubic feet [?]. Using the same assumptions as Zimmerle et al. for gas composition [257, SI section 16] of 95 wt% CH₄ and 19.2 g/scf, we estimate storage throughput of 51,455 Gg CH₄. Thus the fractional CH₄ loss rate for gas going into and out of storage is 309/51455 or 0.60%. This storage loss rate is applied only to gas that goes through the storage system and is applied in the storage compressor sheet.

Similarly, distribution emissions are modeled using loss rates from Alvarez et al. [226, SI p. 14], who estimate local distribution system losses of 0.16% before the customer meter. For simplicity, these are implemented as distribution system losses, with no loss at step-down or metering stations. Because little to no data are available on customer meter and end-use (e.g., homes or businesses) loss rates, nominal placeholders of 0.1% of gas throughput at each step is assumed.

These off-site loss rates are summarized in Table 9.10.

9.6 Deprecated OPGEE v2.0 VF modeling methods

See OPGEE v2.0 documentation (archived at Stanford University) for the methods to generate deprecated v2.0 VF emissions estimates.

Table 9.10: Loss rates for off-site emissions, all expressed in fraction of gas flow into the process stage of note.

Type	Sheet	Affected stream	Fugitive stream	Loss rate	Ref.
Transmission	'Transmission Compressor'	45	261	0.26%	[257]
Storage	'Storage Compressor'	50	262	0.60%	[257]
Distribution	'Gas Distribution'	58	268	0.16%	[226]
Cust. meter	'Gas Distribution'	59	269	0.10%	est.
End use	'Gas Distribution'	60	270	0.10%	est.

10 Fundamental data inputs

A variety of fundamental data inputs and conversions are required in OPGEE. These data inputs are included in the worksheets '*Input data*' and '*Fuel Specs*'. These inputs are described below, organized by broad class of property.

10.1 Global warming potentials

Global warming potentials (GWPs) for gases with radiative forcing are taken from the IPCC Fourth Assessment Report [163]. The GWPs used are the 100-year GWPs.

Input Data Table 2.1'

10.2 Properties of water and steam

The density of fresh water at 32 °F is used as the base density of water for lifting, boiling and other calculations in OPGEE. Thermodynamic properties of water and steam are required for steam generation calculations. The following data tables are required for use in steam generation calculations in OPGEE:

Input Data Table 5.1'

- Saturation properties as a function of temperature;
- Saturation properties as a function of pressure;
- Properties of compressed water and superheated steam.

10.2.1 Saturation properties as a function of temperature

Saturation properties of saturated water and steam as a function of saturation temperature are produced using Knovel steam tables [138, Table 1b]. Properties are derived for temperatures starting at 32 °F and in increments of 20 °F from 40 °F to the critical temperature of 705.1 °F. Properties included are liquid and vapor specific volume v [ft³/lb], specific enthalpy h [Btu/lbm], specific internal energy u (Btu/lbm), and specific entropy s [Btu/lbm °R]

Input Data Table 5.2'

10.2.2 Saturation properties as a function of pressure

Saturation properties of saturated water and steam as a function of saturation pressure are produced using Knovel steam tables [138, Table 1d]. Properties are derived for pressures starting at 15 psia in increments of 5 psia from 15 to 2500 psia. Identical properties are included as above.

Input Data Table 5.3'

10.2.3 Properties of compressed water and superheated steam

Properties of compressed water and superheated steam are compiled from Knovel steam tables [138, Table 2b]. Pressures are included from 100 to 1500 psia in increments of 100. The following temperatures are included: 32°F and in increments of 20 °F from 40 °F to 1500 °F. Identical properties are included as above.

*'Input
Data
Table 5.4'*

10.3 Properties of air and exhaust gas components

The composition of dry air and densities of gases required in OPGEE are derived from online tabulations [155]. Moisture in atmospheric air varies as a function of temperature and relative humidity. Assumed moisture content is 2 mol%.

*'Input
Data
Table 2.2'*

10.3.1 Enthalpies of air and exhaust gas components

The enthalpy of air and exhaust gas at various temperatures and atmospheric pressure is modeled as described above in the Steam Injection methods description (see Section ??). Coefficients for the specific heats of gases as a function of temperature are taken from literature tabulations [141, Table A2-E]. Specific heats are integrated to derive the enthalpy change between two temperatures for combustion products (exhaust gases) and inlet air/fuel mixtures.

*'Input
Data
Tables 4.1 - 4.7'*

10.4 Compositions and properties of fuels

10.4.1 Heating value of crude oil as a function of density

Crude oil heating values are a function of the chemical composition of the crude oil. Crude oil density can be used to determine the approximate heating value (gross and net heating value, or HHV and LHV) of crude oils. Gross and net crude oil heating values (in Btu per lb and Btu per gallon) are presented as a function of API gravity and are given for API gravities from 0 to 46 °API [116, Table 11]. These heating values are converted to SI units and specific gravity for broader applicability.

'Fuel Specs Table 1.1'

10.4.2 Crude oil chemical composition as a function of density

Crude oil chemical compositions (C, H, S, (O+N)) are given as a function of the density of crude oil [116, Table 9]. Values are interpolated between those given in the table using a relationship for fraction H as a function of API gravity. O + N contents are assumed to sum to 0.2 wt%. Sulfur content ranges from 5 wt% to 0.5 wt%, with approximate concentrations derived from Figure 7.27. Carbon mass fraction is computed by difference.

'Fuel Specs Table 1.2'

10.4.3 Heat of combustion of gaseous fuel components

A variety of properties were collected for gaseous fuel components, including N₂, Ar, O₂, CO₂, H₂O, CH₄, C₂H₆, C₃H₈, n-C₄H₁₀, CO, H₂, H₂S, and SO₂ [259, Chapter 17] [140]. For simplicity, N₂, Ar and all other inert species are lumped and given properties of N₂. The following properties were collected for each species:

'Fuel Specs Table 1.3'

- Molar mass [g/mol, mol/kg];
- Moles of C and H per mole of each species (for stoichiometric combustion calculations);
- Higher and lower heating value (HHV, LHV) on a volumetric [Btu/scf], gravimetric [Btu/lbm] and molar basis [Btu/mol, Btu/lbmol]. For completeness, gravimetric energy densities in SI units [MJ/kg] are also included.

10.4.4 Refined and processed fuels heating values

The heating values and densities of refined and processed fuels are taken from the CA-GREET model [111] for a variety of fuels.

'Fuel Specs Table 4.1'

11 OPGEE limitations

11.1 Scope limitations

OPGEE includes within its system boundaries over 100 emissions sources from oil and gas production. The current version of the model (OPGEE v3.0a) includes in the system boundaries emissions sources from all major process stages (e.g., drilling and development, production and extraction, surface processing). However, emissions are subject to significant cutoffs, wherein very small emissions sources are neglected as (likely) insignificant in magnitude. Therefore, some emissions sources from exploration, maintenance, and waste disposal are not explicitly modeled. This cutoff is applied because it would be infeasible (and counter-productive) for regulators or producers to model the magnitude of every emissions source.

Production technologies included in OPGEE are: primary production, secondary production (water flooding), and major tertiary recovery technologies (steam injection). Some production technologies are not included in the current version of OPGEE: polymer and chemical EOR, CO₂ EOR, miscible HC flooding, solar thermal steam generation, insitu combustion, subsurface electric heaters, and cold heavy oil production with sand (CHOPS) are not currently included.

11.2 Technical limitations

11.2.1 Production modeling

OPGEE assumes single phase fluid flow in the calculation of the pressure drop between the well reservoir interface and the well head. In reality, there is a simultaneous flow of both fluid (oil and water) and vapor (associated gas). Results show that pressure drop calculated using a two phase flow model can be significantly lower than that calculated using a single phase flow linear model [54]. The deviation of our single phase flow assumption from reality is expected to increase at high GOR.

In the modeling of TEOR, OPGEE does not model changes in viscosity of the oil in lifting calculations [71]. The concept of TEOR is based on reducing the viscosity of the oil, which decreases the lifting energy requirement. This effect is likely to be small because the bulk of the energy consumption in TEOR is from steam generation and not lifting.

11.2.2 Surface processing

It is infeasible in a model such as OPGEE to account for the many possible variations in surface processing. The goal is to include the most frequently applied processes in the industry, while still retaining some flexibility to model varying operating modes (e.g. placement of flow heater in the oil-water separation scheme).

The energy consumption of the demethanizer unit is calculated using energy factors that are generated from a default configuration [165]. Energy factors are calculated in unit energy per kmol of gas feed. Therefore, energy consumption is sensitive to inlet gas composition. However, the use of a default configuration does not allow accounting for the effect of changes in NGL recovery (e.g., 80% ethane recovery). The user can change the amount of NGL produced by changing the fractions of NGL recovered in the '*Surface Processing*' worksheet but this does not have an effect on the demethanizer energy consumption calculations. Emissions from a demethanizer unit are of small significance and therefore do not warrant a full engineering synthesis which can be reconfigured based on user inputs.

11.2.3 Data limitations

11.2.3.1 VFF data

Flaring rates (MMscf per bbl of oil) used in OPGEE are calculated using country level data, which cannot account for variations in field characteristics and practices [156, 157]. Most fugitive and venting emissions in OPGEE are calculated using emissions factors derived from California Air Resources Board (ARB) industry survey data [12]. Challenges include completeness and quality of data collected in the survey (as is common with all survey results). Also, the data are specific to California where environmental regulations and practices are different than other regions.

It was not possible to obtain operational venting and fugitives emissions factors for the chiller unit and the membrane unit. Operational venting and fugitives are not calculated for these units.

11.2.3.2 Default specifications

The accuracy of OPGEE results is fundamentally related to data inputs available. All inputs to OPGEE are assigned default values that can be kept as is or changed to match the characteristics of a given oil field or crude blend/MCON. If only a limited amount of information is available for a given field, most of the input values will remain equal to defaults. In contrast, if detailed-level data are available, a more accurate emissions estimate can be generated.

Some defaults require more flexible ("smart") default specifications. The water-oil ratio (WOR) is a major parameter in influencing GHG emissions. OPGEE includes a statistical relationship for water production as a function of reservoir age. The default exponential relationship is a moderate case parameterized with a variety of industry data. Nevertheless, this relationship does not work well in predicting WOR for giant fields with very high per well productivity (e.g., Ghawar in Saudi Arabia).

The GOR varies over the life of the field. As the reservoir pressure drops, increasing amounts of gas evolve from oil (beginning at the bubble point pressure if the oil is initially under-saturated). This tends to result in increasing producing GOR over time. Also, lighter crude oils tend to have a higher GOR. Because of this complexity, a static single value for GOR is not desirable. OPGEE uses California producing GORs to generate GORs for three crude oil bins based on API gravity. All data required to generate empirical correlations for GOR are not likely to be available.

11.3 Future work

In the future we will use more detailed engineering sub-models and more comprehensive data analyses to eliminate the limitations of OPGEE model. OPGEE will be expanded to include innovative production technologies such as solar steam generation. Larger data sets are collected to improve the correlations of WOR and GOR defaults. Another important initiative is the calculation of field-level flaring rates using high resolution satellite data [260]. This is believed to have significant impact on the accuracy of results from OPGEE. Work-in progress include generating and updating venting and fugitives emissions factors using technical reports.

A Terminology: Acronyms and abbreviations

Table A.1: Acronyms and abbreviations.

Acronym or abbreviation	Description
ABS	Absorbents
AGR	Acid gas removal
AIR	Air stripping
AL	Aerated lagoons
ANS	Alaska North Slope
API	American Petroleum Institute
ARB	California Air Resources Board
AS	Activated sludge
BHP	Brake horsepower
CHOPS	Cold heavy oil production with sand
CSS	Cyclic steam stimulation
CWL	Wetlands
DAF	Dissolved air flotation
DEA	Di-ethanol amine
DGA	Diglycolamine
DMF	Dual media filtration
DOGGR	State of California Department of Conservation Division of Oil, Gas and Geothermal Resources
EDR	Electrodialysis reversal
EGOR	Onsite electricity generation to oil ratio
EOR	Enhanced oil recovery
EPA	Environmental Protection Agency
ERCB	Alberta Energy Resources Conservation Board
FOR	Flaring to oil ratio
FWKO	Free-water knockouts
GAC	Granular activated carbon
GGFR	Global Gas Flaring Reduction Partnership at the World Bank
GHG	Greenhouse gases
GLR	Gas to liquid ratio
GOR	Gas to oil ratio
GREET	Greenhouse Gases, Regulated Emissions, and Energy Use in Transportation Model
GT	Gas turbine
GWP	Global warming potential
HHV	Higher heating value
HRSG	Heat recovery steam generator
HYDRO	Hydrocyclones
IPCC	Intergovernmental Panel on Climate Change
LCA	Life cycle assessment
LHV	Lower heating value
MEA	Monoethanolamine
MF	Microfiltration
NF	Nanofiltration
NGL	Natural gas liquid

Continued on next page...

Continued from previous page

Acronym or abbreviation	Description
NOAA	National Oceanic and Atmospheric Administration
OPGEE	Oil Production Greenhouse Gas Emissions Estimator
ORG	Organoclay
OTSG	Once-through steam generators
OZO	Ozone
RBC	Rotating biological contactors
RO	Reverse osmosis
RVP	Reid vapor pressure
SAGD	Steam assisted gravity drainage
SCO	Synthetic crude oil
SOR	Steam to oil ratio
SSF	Slow sand filtration
TDS	Total dissolved solids
TEG	Triethylene glycol
TEOR	Thermal enhanced oil recovery
TF	Trickling filters
THC	Total hydrocarbon
UF	Ultrafiltration
VFF	Venting, flaring and fugitives
VOC	Volatile organic compounds
VOR	Venting to oil ratio
W&S	Standing and working losses
WOR	Water to oil ratio
WTR	Well to refinery

B Mathematical terms and definitions

Mathematical terms and subscripts are defined in Table B.1. Parameters and variables serve as the key signifiers in the formulae. A variety of subscripts are used in the mathematics, and can be divided into:

1. Process stages, represented by a two- or three-letter capitalized symbol (e.g., DD = Drilling & Development)
2. Sub-processes, represented by two- or three-letter capitalized symbol (e.g. GP = Gas processing)
3. Process flows or environments, represented by lower-case symbols (e.g., a = air)
4. Technologies or technology components, represented by capitalized symbols (e.g., GD = glycol dehydrator)
5. Primary fuels and energy carriers, represented by one- to three-letter lower-case symbols (e.g., di = Diesel fuel)
6. Modifiers, represented by lower-case symbols or word fragments (e.g., avg = average)
7. Gas species, represented by capitalized species formulae (e.g., O_2 = oxygen)

In general, a term in the equation will follow the above order as in:

$$[Param][PROCESS][SUB-PROCESS][flow][TECHNOLOGY][fuel][modifier(s)][SPECIES] \quad (B.1)$$

if an element is not needed, it is simply excluded. To create a (relatively extreme) example, one might have: $p_{OTSG,ng,avg,in}$, which represents average inlet natural gas pressure to the once-through steam generator. Most equation elements will not require this many elements.

Table B.1: Mathematical symbols and subscripts.

Symbol	Description
Parameters and variables	
α	Solar absorbance
δ	Change
ϵ	Loss
η	Efficiency
γ	Specific gravity
λ	Fraction or share
ρ	Density
$a, b, c, d \dots$	Constants in fitting equations or from data
C	Capacity
C	Concentration
D	Diameter
API	Degrees API
e	Energy (per unit of something)
E	Energy quantity
EF	Emissions factor
EL	Energy loss
EM	Emissions
f	Friction factor
f	Fraction of a quantity
FOR	Flaring oil ratio
GOR	Gas oil ratio
GWP	Global warming potential
h	Height
h	Enthalpy
H	Head
I	Solar insolation
I	Process intensity factor
l	Load factor
m	Mass
MW	Molecular weight
N	Number of something
p	Pressure
P	Power
Q	Flow rate
R	Ratio
r	Radius
RVP	Reid vapor pressure
T	Temperature
U	Effectiveness
v	Velocity
V	Volume
W	Work
w	Mass fraction
WOR	Water oil ratio
x	Mole fraction
y	Binary variable
Y	Process yield factor
Process units or stages (Index = j)	
AGR	Acid gas removal
BM	Bitumen mining
CGW	CO ₂ gas injection wells
CH	Chiller
CRC	CO ₂ reinjection compressor
CS	Crude oil storage

Continued on next page...

Continued from previous page

Symbol	Description
<i>DD</i>	Drilling and Development
<i>DE</i>	Demethanizer
<i>EGI</i>	Electricity generation and imports
<i>EX</i>	Exploration
<i>FGC</i>	Fuel gas consumed
<i>FGI</i>	Fuel gas imports
<i>FL</i>	Flaring
<i>GD</i>	Gas dehydration (glycol dehydrator)
<i>GDI</i>	Gas distribution
<i>GFC</i>	Gas flooding compressor
<i>GG</i>	Gas gathering
<i>GLC</i>	Gas lifting compressor
<i>GPA</i>	Gas partition A
<i>GPB</i>	Gas partition B
<i>GRC</i>	Gas reinjection compressor
<i>GSW</i>	Gas storage wells
<i>HD</i>	Heavy oil dilution
<i>HGW</i>	Hydrocarbon gas injection wells
<i>HT</i>	Heater-treater (dewatering)
<i>HU</i>	Heavy oil upgrading
<i>LL</i>	LNG liquefaction
<i>LR</i>	LNG regasification
<i>LT</i>	LNG transport
<i>M</i>	Maintenance
<i>ME</i>	Membrane
<i>MWT</i>	Makeup water treatment
<i>NLI</i>	Natural gas liquids production and imports
<i>OT</i>	Oil transport
<i>PMC</i>	Pre-membrane compressor
<i>PSC</i>	Post-storage compressor
<i>PT</i>	Pet coke transport
<i>PWT</i>	Produced water treatment
<i>RE</i>	Reservoir
<i>RH</i>	Ryan-Holmes process
<i>S</i>	Stabilizer
<i>SE</i>	Separation
<i>SG</i>	Steam generation
<i>SGW</i>	Sour gas injection wells
<i>SIW</i>	Steam injection wells
<i>SRC</i>	Sour gas reinjection compressor
<i>SS</i>	Storage separator
<i>STC</i>	Storage compressor
<i>TRC</i>	Transmission compressor
<i>VRC</i>	Vapor recovery unit compressor
<i>VT</i>	Venting
<i>WD</i>	Waste disposal
<i>WI</i>	Water injection
<i>WO</i>	Wellbore and downhole pump
Solid process flow components	
<i>PC</i>	Petroleum coke
Liquid process flow components	
<i>DI</i>	Diluent
<i>DO</i>	Diluted crude oil
<i>PO</i>	Upgraded crude oil
<i>RB</i>	Raw bitumen
<i>SO</i>	Stabilized crude oil
<i>UO</i>	Unstabilized crude oil
<i>W</i>	Water

Continued on next page...

Continued from previous page

Symbol	Description
Gaseous process flow components	
C1	Methane
C2	Ethane
C3	Propane
C4	Butane
CO	Carbon monoxide
CO2	Carbon dioxide
EL	Electricity
H2	Hydrogen
H2O	Water
H2S	Hydrogen sulfide
N2	Nitrogen
O2	Oxygen
SO2	Sulfur dioxide
Technologies (Index = j)	
Amine	Amine-based process
B	Barge
BP	Booster pump
C	Compressor
CP	Circulation pump
D	Driver
DR	Drill rig
EG	Electricity generator
F	Fan
G	Generator
GP	Glycol pump
GS	Generator set
GT	Gas turbine
HRSG	Heat recovery steam generator
M	Motor
OTSG	Once-through steam generator
P	Pipeline
R	Roof
RE	Reciprocating engine
RP	Reflux pump
SMR	Steam-methane-reformer
T	Tanker
T	Tank
TR	Truck
V	Vent
W	Well
Modifiers	
avg	Average
atm	Atmospheric
b	Base
wf	Bottomhole (well-formation)
comb	Combusted
dir	Direct
d	Discharge
ent	Entrained
exp	Exported
gen	Generated
gr	Gross
heat	Heated
im	Imported
ind	Indirect
inj	Injected (as in an injected stream)

Continued on next page...

Continued from previous page

Symbol	Description
<i>in</i>	Input
<i>l</i>	Lost
<i>mu</i>	Make-up
<i>max</i>	Maximum
<i>min</i>	Minimum
<i>net</i>	Net
<i>new</i>	New
<i>ot</i>	Other
<i>out</i>	Output
<i>rem</i>	Removed
<i>req</i>	Required
<i>res</i>	Reservoir
<i>rec</i>	recovered
<i>ref</i>	refinery
<i>s</i>	Stages
<i>sc</i>	Standard conditions
<i>str</i>	Stripped
<i>s</i>	Suction
<i>th</i>	Thermal
<i>tot</i>	Total
<i>to</i>	Turn over
<i>wh</i>	Wellhead
<i>trav</i>	traverse
<i>lift</i>	lifting

C Tabulated sources for each production stage

The full classification of emissions sources for each production stage is given below in Tables C.1 to C.7.

Each emissions source is classified according to process, sub-process, and specific emissions source. Any variants of that emissions source are listed (if they have material effects on emissions or energy consumption). A sensitivity code is given from 1 to 4 stars (*) to ****) based on judgement of the likely magnitude of the source. Lastly, the table indicates whether or not an emissions source is included (incl. = 1 means that the source is included).

Table C.1: Emissions sources from exploratory operations. For inclusion: 0 = not included, 1 = included.

Main stage	Process	Sub-process	Emissions source	Variants	Sensitivity code	Estimated magnitude	Incl.
Seismic exploration	Terrestrial seismic	Vehicular emissions	-	*	<0.01 g	0	
		Data processing	-	*	<0.01 g	0	
		Consumed materials (charges etc.)	-	*	<0.01 g	0	
		Land use impacts	-	*	<0.01 g	0	
		Ship emissions	-	*	<0.01 g	0	
	Oceanic seismic	Data processing	-	*	<0.01 g	0	
		Consumed materials	-	*	<0.01 g	0	
		Prime mover emissions	-	*	<0.01 g	0	
		Land clearing and construction	-	*	<0.01 g	0	
		Vents and upset emissions	-	*	<0.01 g	0	
Exploration drilling	Terrestrial drilling	Drilling flares	-	*	<0.01 g	0	
		Casing and cement	-	*	<0.01 g	0	
		Other material consumption (e.g., frac sand)	-	*	<0.01 g	0	
		Land use impacts	-	*	<0.01 g	0	
		Indirect land use impacts (opening of inaccessible land)	-	*	<0.01 g	0	
	Offshore drilling	Prime mover emissions	-	*	<0.01 g	0	
		Drilling flares	-	*	<0.01 g	0	
		Vents and upset emissions	-	*	<0.01 g	0	
		Casing and cement	-	*	<0.01 g	0	
		Energy consumption (other than prime mover)	-	*	<0.01 g	0	
Waste handling and disposal	Mud and fluid handling	Fugitives from mud	-	*	<0.01 g	0	
		Disposal of mud	-	*	<0.01 g	0	
	Fracturing fluid disposal	Processing and disposal of fracturing fluid	-	*	<0.01 g	0	
		Processing of produced water	-	*	<0.01 g	0	
		Disposal of produced water (remote or on-site reinjection)	-	*	<0.01 g	0	

Table C.2: Emissions sources from drilling operations.

Main stage	Process	Sub-process	Emissions source	Variants	Sensitivity code	Estimated magnitude	Incl.
Developmental drilling	Terrestrial drilling	Prime mover emissions	-	**	0.1 g	1	
		Drilling flares	-	*	$\leq 0.01 \text{ g}$	0	
		Vents and upset emissions	-	**	0.1 g	0	
		Land use impacts	-	**	0.1 g	1	
		Clearing and construction	-	*	0.1 g	0	
	Oceanic drilling	Casing and cement embodied emissions	-	*	$\leq 0.01 \text{ g}$	0	
		Other materials consumption (e.g., frac sand)	-	*	$\leq 0.01 \text{ g}$	0	
		Prime mover emissions	-	**	0.1 g	1	
		Drilling flares	-	*	$\leq 0.01 \text{ g}$	0	
		Vents and upset emissions	-	**	0.1 g	0	
Drilling and development	Oil/gas/water separators	Casing and cement embodied emissions	-	*	$\leq 0.01 \text{ g}$	0	
		Separator assembly	-	*	$\leq 0.01 \text{ g}$	0	
		Separator fabrication	-	*	$\leq 0.01 \text{ g}$	0	
		Separator transport	-	*	$\leq 0.01 \text{ g}$	0	
		Raw materials manufacture	-	*	$\leq 0.01 \text{ g}$	0	
	Water wells	Various drilling emissions from reinjection wells (see above)	-	*	$\leq 0.01 \text{ g}$	0	
		Pump assembly	-	*	$\leq 0.01 \text{ g}$	0	
		Pump fabrication and raw materials manufacture	-	*	$\leq 0.01 \text{ g}$	0	
		Pump transport	-	*	$\leq 0.01 \text{ g}$	0	
		Tank assembly	-	*	$\leq 0.01 \text{ g}$	0	
Storage capital investment	Storage capital investment	Tank fabrication	-	*	$\leq 0.01 \text{ g}$	0	
		Tank transport	-	*	$\leq 0.01 \text{ g}$	0	
		Raw materials manufacture	-	*	$\leq 0.01 \text{ g}$	0	
		Land use impacts	-	*	$\leq 0.01 \text{ g}$	0	
		Pipeline assembly	-	*	$\leq 0.01 \text{ g}$	0	
Transport capital investment	Transport capital investment	Pipe fabrication	-	*	$\leq 0.01 \text{ g}$	0	
		Pipe transport	-	*	$\leq 0.01 \text{ g}$	0	
		Raw materials manufacture	-	*	$\leq 0.01 \text{ g}$	0	
		Land use impacts	-	*	$\leq 0.01 \text{ g}$	0	
		Other infrastructure fabrication and assembly	-	*	$\leq 0.01 \text{ g}$	0	

Table C.3: Emissions sources from production and extraction operations.

Main stage	Process	Sub-process	Emissions source	Variants	Sensitivity code	Estimated magnitude	Incl.
Lifting	Pumping		Combustion for pump driver	-	***	1 g	1.0
			Electricity for pump driver	-	***	1 g	1.0
	Gas lift		Casing and wellhead fugitive emissions	-	***	1 g	1.0
			Compressor prime mover emissions	-	***	1 g	1.0
	Gas injection		Compression electricity emissions	-	***	1 g	1.0
			Casing and wellhead fugitive emissions	-	***	1 g	1.0
	Water injection		External gas processing (e.g., N2 production)	-	***	1 g	1.0
			Gas compression energy	-	***	1 g	1.0
	OTSG fuel combustion		[I] Gas sequestration credit (CO2 flood)	-	***	1 g	0.0
			Water pumping energy	-	***	1 g	1.0
Production and extraction	Steam injection		Water pre-treatment	-	*	<= 0.01 g	0.0
			OTSG fuel combustion	NG, produced oil	****	10 g	1.0
	Injection		Turbine gas consumption (combined cycle)	Low, med, high efficiency	****	10 g	1.0
			HRSG duct firing (combined cycle)	-	***	1 g	1.0
			[I] Electricity co-production offsets (combined cycle)	Grid mix variation	****	10 g	1.0
			Steam pumping energy (if any)	-	*	<= 0.01 g	0.0
			Polymer embodied energy	-	*	<= 0.01 g	0.0
			Polymer mixing	-	*	<= 0.01 g	0.0
			Polymer/water mixture pumping energy	-	*	<= 0.01 g	0.0
			Surfactant/other embodied energy	-	*	<= 0.01 g	0.0
			Surfactant/other mixing	-	*	<= 0.01 g	0.0
			Surfactant/other mixture pumping energy	-	*	<= 0.01 g	0.0

Table C.4: Emissions sources from surface processing operations.

Main stage	Process	Sub-process	Emissions source	Variants	Sensitivity code	Estimated magnitude	Incl.
Separation and surface processing	Fluid separation	Oil-water-gas separation	Oil-water-gas separation	-	**	0.1 g	1
			Oil-water-gas separation with heater-treaters	-	***	0.1 g	1
			Associated gas venting	Variations in flare efficiency	****	10 g	1
	Solid/fluid separation	Solid separation from fluids	Associated gas flaring	Variations in flare efficiency	****	10 g	1
			Solids removal from separation	-	*	≤ 0.01 g	0
			Produced gas dehydration	-	*	≤ 0.01 g	1
	Gas processing	Gas processing	Produced gas venting and flaring	-	****	1 g	1
			Produced water cleanup	-	**	0.1 g	1
			Produced water handling and pumping	-	**	0.1 g	1
	Water treatment and disposal	Water treatment and disposal	Produced water reinjection	-	***	1 g	1
			Produced water disposal	-	**	0.1 g	1
			Storage pumping energy	-	*	≤ 0.01 g	0
Storage (as part of separation)	Storage	Tank assembly and installation	Tank assembly and installation	-	*	≤ 0.01 g	0
			Evaporative and fugitive emissions	-	**	0.1 g	1
			Tank materials manufacture	-	*	≤ 0.01 g	0
			Land use impacts	-	*	≤ 0.01 g	0

Table C.5: Emissions sources from maintenance operations.

Main stage	Process	Sub-process	Emissions source	Variants	Sensitivity code	Estimated magnitude	Incl.
Maintenance and workovers	Well workover	Terrestrial well workover	Workover rig energy use	-	*	≤ 0.01 g	0
			Fugitive emissions during workover	-	**	0.1 g	1
			Embodied energy in consumed replacement parts	-	*	≤ 0.01 g	0
	Offshore well workover	Offshore well workover	Workover rig energy use	-	*	≤ 0.01 g	0
			Fugitive emissions during workover	-	**	0.1 g	1
			Embodied energy in consumed replacement parts	-	*	≤ 0.01 g	0
	Other maintenance	Other maintenance	Solids removal from separation	-	*	≤ 0.01 g	0
			Land use impacts	-	*	≤ 0.01 g	0
			Water use impacts	-	*	≤ 0.01 g	0
			Soil use impacts	-	*	≤ 0.01 g	0

Table C.6: Emissions sources from waste treatment and disposal operations.

Main stage	Process	Sub-process	Emissions source	Variants	Sensitivity code	Estimated magnitude	Incl.
Waste treatment and disposal	Water processing waste	Water treatment waste disposal	Subsurface disposal of concentrated WW residuals	-	*	≤ 0.01 g	0
			Surface disposal of separated solids	-	*	≤ 0.01 g	0
			Surface disposal of concentrated WW residuals	-	*	≤ 0.01 g	0
	Other waste separation and processing	Other waste separation and processing	-	*	≤ 0.01 g	0	
	Other waste disposal	Other waste storage	-	*	≤ 0.01 g	0	
		Spills and other upsets	-	*	≤ 0.01 g	0	
		Other waste transport	-	*	≤ 0.01 g	0	
	Other waste disposal	Other waste disposal (non-hazardous)	-	*	≤ 0.01 g	0	
		Other waste disposal (hazardous)	-	*	≤ 0.01 g	0	
	Solid waste disposal and project decommissioning	Solid waste disposal	Solid waste separation and processing	-	*	≤ 0.01 g	0
		End of life and decommissioning	Solid waste transport and disposal	-	*	≤ 0.01 g	0
			Demolition and decommissioning	-	*	≤ 0.01 g	0
			Scrap and waste disposal	-	*	≤ 0.01 g	0
			[+/-] Credit for waste recycling (embodied energy)	-	*	≤ 0.01 g	0

Table C.7: Emissions sources from transport.

Main stage	Process	Sub-process	Emissions source	Variants	Sensitivity code	Estimated magnitude	Incl.
Crude product transport	Pipeline transport	Combustion for pump prime mover	-	***	1g	1	
		Electricity for pump use	-	***	1g	1	
		Process upsets (one-time events)	-	*	$\leq 0.01\text{ g}$	1	
		Leaks (pipeline losses)	-	***	1g	1	
		Construction equipment energy use	-	*	$\leq 0.01\text{ g}$	0	
	Tanker transport	Embodied energy in pipeline materials (cement and steel)	-	*	$\leq 0.01\text{ g}$	0	
		Land use impacts	-	*	$\leq 0.01\text{ g}$	0	
		Combustion in tanker prime mover (bunker fuels)	-	***	1g	1	
		Loading and unloading pumping	-	*	$\leq 0.01\text{ g}$	1	
		Flares	-	*	$\leq 0.01\text{ g}$	1	
Storage (as part of transport)	Storage	Vents, leaks and upsets	-	*	$\leq 0.01\text{ g}$	1	
		Embodied energy in tanker materials (steel)	-	*	$\leq 0.01\text{ g}$	0	
		Construction energy	-	*	$\leq 0.01\text{ g}$	0	
		Storage pumping energy	-	*	$\leq 0.01\text{ g}$	0	
		Tank assembly and installation	-	*	$\leq 0.01\text{ g}$	0	
	Storage	Evaporative and fugitive emissions	-	**	0.1g	1	
		Tank materials manufacture	-	*	$\leq 0.01\text{ g}$	0	
		Land use impacts	-	*	$\leq 0.01\text{ g}$	0	

D Bulk assessment macro error correction

The bulk assessment machinery is capable of fixing errors, performing iterative calculations and adjusting input parameters where necessary. It is not practical to perform these computational tasks manually when assessing a large number of projects (100+). The built-in macro ensures consistent treatment across all fields. Errors that are addressed in the macro include:

- Discrepancies between country-average default flaring rate and entered GOR (e.g., flaring module predicts more flaring than field has available);
- Discrepancies between default fugitive emissions of gaseous components and gas available from production;
- Requirement to iteratively solve for the gas composition in the wellbore in the case of gas lift;
- Error with productivity index resulting in negative bottomhole pressures;
- Error resulting from very large frictional lifting penalties due to too-small assumed wellbore;
- Requirement to iteratively solve for gas reinjected to result in 0 gas export.

Figure D.1 shows the logic of errors fixing and entry adjustments related to GOR and gas composition. Other errors and adjustments are shown in Figure D.2. One of the most common errors encountered in running OPGEE is the gas composition error which can result in more than one case of data inconsistency. First, the macro checks to ensure that GOR is at least 10 to satisfy the requirements for leaks in the other sections of the model (not shown in flow chart). Then, the macro tackles the most common gas-related errors are related to flaring and fugitive emissions. First, relying on country-average flaring rates in combination with field-specific GOR can result in flaring more gas than that which is produced. As shown in Figure D.1 the gas composition error is fixed by either increasing GOR to match flaring or decreasing flaring to match GOR. The choice between the two options is based on the input data quality. If flaring volume is default then flaring is adjusted. If GOR is default then GOR is adjusted. If both flaring volume and GOR are user inputs then GOR is adjusted because we assume that the flaring rate, being measured by satellite, is more likely to be accurate than the default GOR.

Another problem is having insufficient CO₂ and VOC in the gas stream to match default system losses from venting and fugitives (see Figure D.1 “Gas Comp Error?”). If this occurs, the GOR is increased by 10 scf/bbl until sufficient gas is available to provide emissions estimates.

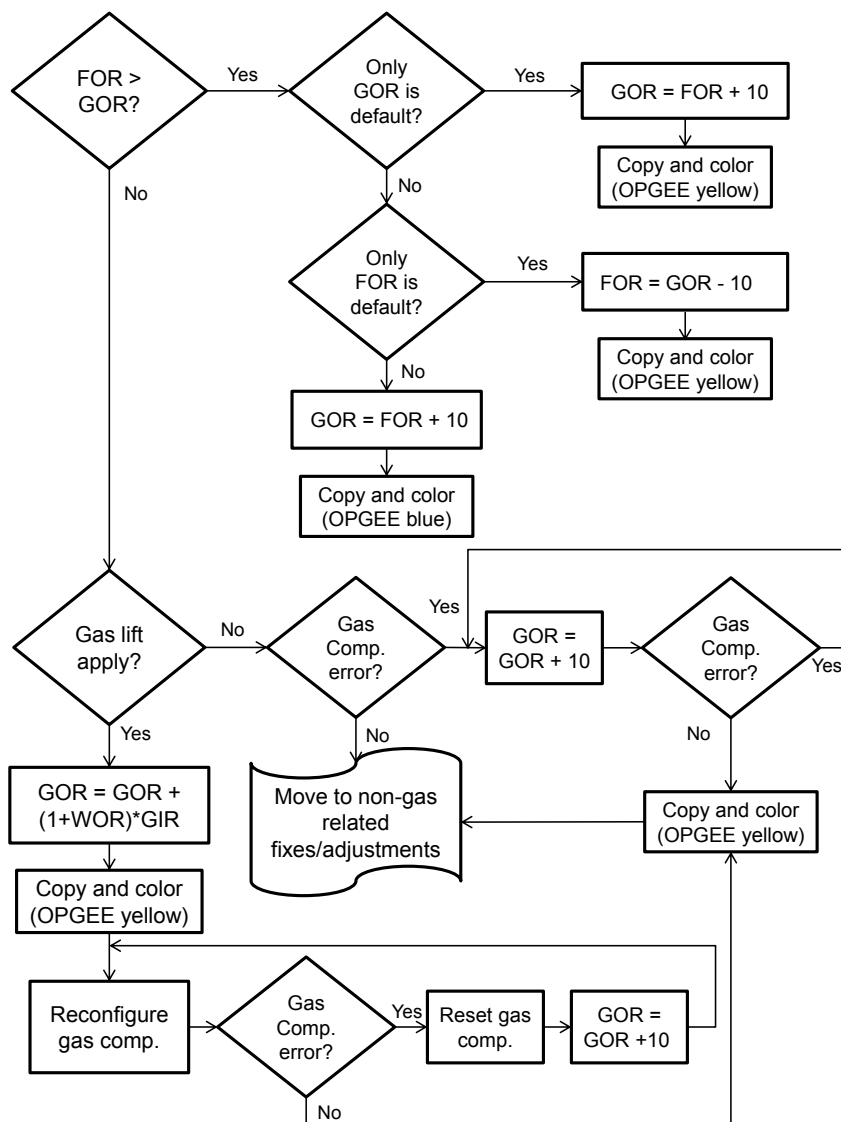


Figure D.1: The errors fixing/entries adjustment logic.

In the case of gas lift, the gas composition in the wellbore is not the reservoir gas composition. The product gas is injected into the well stream, re-processed and re-injected again in a continuous cycle. Therefore the gas at the wellhead separator is a mixture of both the reservoir and product gases. The bulk assessment machinery reconfigures the gas composition by combining the product and reservoir gases in consecutive iterations until the gas composition stabilizes. As shown in Figure D.1 before reconfiguring the gas composition the GOR is adjusted to add the amount of gas injected into the well stream.

Figure D.2 shows the error fixes and adjustments not related to GOR or gas composition.

The second most common error encountered in running OPGEE is the productivity index (PI) error which results when the user or default PI value does not satisfy the minimum bottomhole pressure requirement (0 psi). The bulk assessment

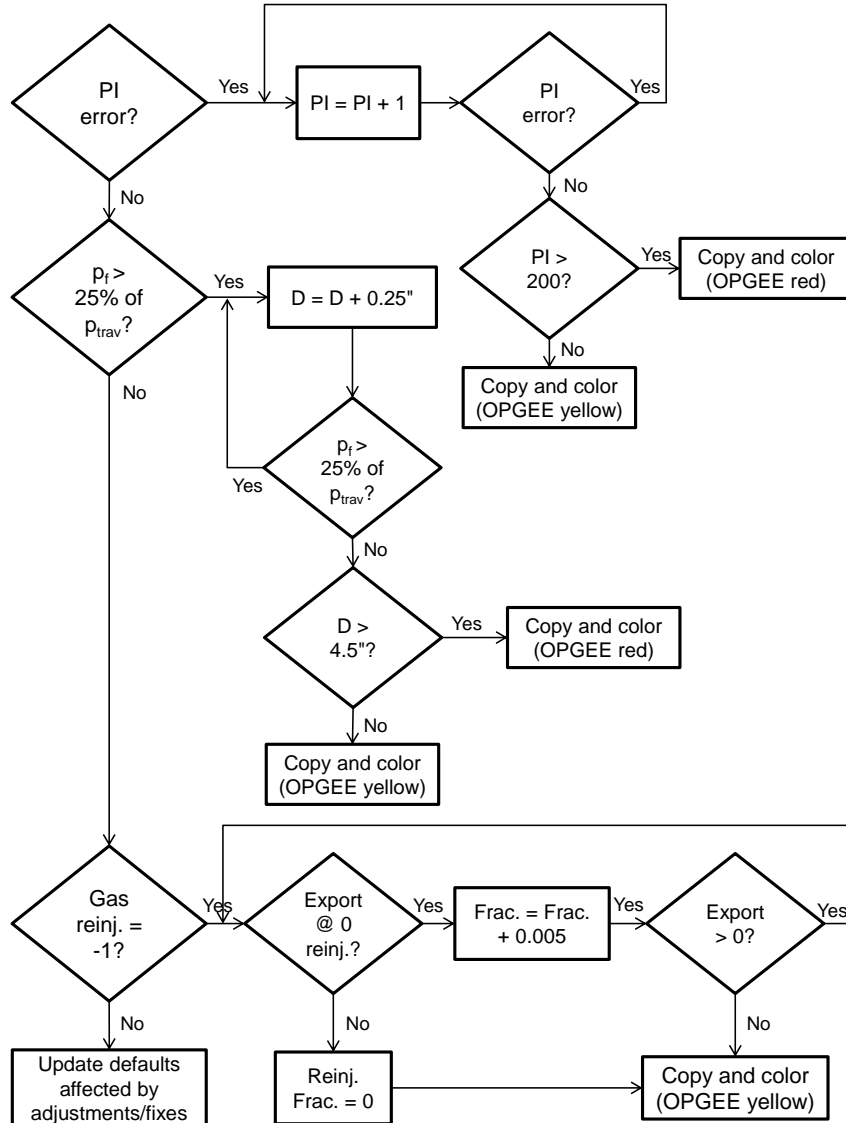


Figure D.2: The errors fixing/entries adjustment logic for non-GOR, gas composition related entries.

fixes the PI error by incrementally increasing the PI value until the error resolves.

After this, the macro checks for the friction pressure traverse (p_f) as a fraction of total pressure traverse (p_{trav}). In cases where the friction pressure traverse accounts for more than 25% of the total pressure traverse, it is assumed that this is not a realistic system design (e.g., designers would account for and reduce large friction penalties due to effects on lifting costs). Such assumptions are supported by the literature, where the nominal range of the friction pressure traverse is assumed not to exceed 25% of the total pressure traverse [118]. To address this problem, the bulk assessment macro widens the well diameter (D) in increments of 0.25 in. until the friction pressure traverse is $\leq 25\%$.

Finally, if the user chooses to set gas export to zero as opposed to default setting where remaining gas is exported, the bulk assessment machinery increases the gas reinjection fraction by increments of 0.5% until no remaining gas is exported. To

set gas export to ≈0 scf the user must enter -1 in the fraction of remaining gas reinjected.

Colors are used to highlight where the bulk assessment fills in or adjusts data. OPGEE *green color* represents default values. OPGEE *yellow color* represents adjusted parameters. And OPGEE *red color* represents warnings in case the adjusted parameter exceeds literature range / design standards (e.g., >4.5 inch production well diameter) [54, p. 106].

E Changes and updates from previous versions of OPGEE

E.1 Changes from OPGEE v2.0a to OPGEE v2.0b

- Flaring volumes are now updated for OPGEE 2.0b, including flaring volumes from 2010 to 2015. See worksheet "Flaring" for significant modifications.
 - Flaring volumes are updated using NOAA/GGFRP information for country-level flaring volumes over the years 2010-2015.
 - Oil production data is now updated to BP Statistical Review of World Energy, 2016 volume, for all available countries. Data are collected 2010-2015, in thousands of bbl per day.
 - Oil production data for countries not available in BP Statistical Review of World Energy (mostly minor producing countries) are updated using EIA international energy statistics for 2010-2015
- Solar thermal has now been implemented in OPGEE 2.0b as part of a re-implemented steam generation module. The user can now change the fraction of steam generated using solar thermal, on inputs sheet 1.4.13
- We have implemented duct firing in OPGEE 2.0b, as part of a re-implemented steam generation module. The user can now turn on duct firing on the Steam Generation worksheet, item 1.2.7.2.3 The comment about cogeneration crediting is unclear, will reach out to CAPP for more comments.

E.2 Changes from OPGEE v1.1 Draft E to OPGEE v2.0a

- Exploration emissions added
 - Added emissions from seismic exploration efforts, non-productive drilling ("dry holes") and scientific/exploratory wells
- Transport changes
 - Included transport energy use in "Energy consumption" gathering sheet
 - Included transport emissions in "GHG emissions" gathering sheet
 - Included indirect emissions associated with producing energy carriers used in transport, which were neglected in OPGEE 1.1 method of including transport outside of gathering sheets
 - Included truck transport using heavy-duty diesel vehicle from GREET1_2013 model

- Embodied energy added
 - Sheet which models embodied energy in oilfield materials and consumables is added.
 - Embodied emissions worksheet from A.R. Brandt (2015) "Embodied energy and GHG emissions from material use in conventional and unconventional oil and gas operations". Environmental Science & Technology. DOI: 10.1021/acs.est.5b03540
- CO₂ EOR feature added
 - Changes throughout model to include CO₂ EOR
 - New CO₂ accounting table on GHG emissions gathering sheet
 - New compressor work calculations on "Compressor" supplemental sheet
 - New gas balance pathways in "Gas Balance" worksheet
 - New gas processing technologies including membranes and Ryan-Holmes
- Heavy oil and bitumen upgrading added
 - "Upgrading" supplemental worksheet added
 - Upgrading section added to surface processing worksheet
- New analysis features added
 - Change start and end field to allow assessment of subset of fields

E.3 Changes from OPGEE v1.1 Draft D to OPGEE v1.1 Draft E

E.3.1 Steam Injection changes

- Feedwater temperature revised to 140°F to account for recycle of hot produced water
- HRSG exhaust temperature corrected to 350°F

E.4 Changes from OPGEE v1.1 Draft C to OPGEE v1.1 Draft D

E.4.1 Bulk assessment changes

- The overall error check in Bulk Assessment worksheet was not functional in previous versions. In this version, the Bulk Assessment macro checks for the overall error.
- The 'Bulk Assessment' worksheet has been split into two worksheets. Data for many fields should be entered in 'Bulk Assessment - Inputs' worksheet.
- The new 'Bulk Assessment - Results' worksheet reports results and allows monitoring of changes which are automatically applied to the user input variables entered in the 'Bulk Assessment - Data' worksheet.

- The Bulk Assessment macro is fixed to correctly solve for fraction of the remaining gas re-injected required to set the export gas to zero.
- In input data worksheet, row 1896, a new section 8 is added. This table works with the Bulk Assessment macro to verify that the Excel calculation mode is set to "Automatic" which is a requirement for Bulk Assessment worksheet to function correctly. This was overlooked in previous versions.

E.4.2 Fugitive emissions changes

- Modeling of gas dehydration system fugitives and venting are updated with improved California survey data. Now emissions factors are disaggregated depending on whether vapor recovery systems are applied.
- The number of valves, which are used to scale other components, are updated from new California survey data.
- The number of pump seals are updated using new California survey data.
- Pneumatic devices (controllers and chemical injection pumps) added as venting sources, using US EPA emissions intensities. Gas balance changes
- In 'Gas Balance' worksheet the rate of the fuel gas consumption (calculated in Energy Consumption worksheet) is added.
- A warning is added in 'User Inputs & Results' worksheet (I97). This warning is activated when the fraction of the remaining gas reinjected is adjusted to a value that causes the non-reinjected portion of the remaining gas become less than fuel gas demand for on-site use
- In the previous versions when gas lift is the method of recovery and FOR is higher than GOR then OPGEE gives error message on the gas composition.

E.4.3 Documentation and clarity improvements

- In 'Gas Balance' worksheet the 'Fuel Gas/Export' label is changed to 'Fuel gas consumed + export'.
- Typos in 'User Inputs & Results' are corrected: In row 297 and 298, AN19 and AN28 changed to AP19 and AP28

E.5 Changes from OPGEE v1.1 Draft B to OPGEE v1.1 Draft C

- Electricity module substantially revised to allow for variable power source efficiencies Drivers reworked with user-defined functions to greatly simplify calculation of driver energy use.
- Bitumen extraction and upgrading sheet updated to GHGenius version 4.03, utilizing GHGenius fuel use directly, or GHGenius LHV's where direct fuel consumption not available. This avoids incongruity between GREET and GHGenius LHV/HHV ratios.

- In bulk assessment macro, the location of ?Outputs.Range("J97").Value = 0? is changed . In the previous version (after revision of the electricity module), when the fraction of remaining gas re-injected was set to -1 in bulk assessment work sheet, a type mismatch error would occur.
- In gas balance work sheet ?Process fuel / Export? is changed to ?Process fuel consumed + Export?.

E.6 Changes from OPGEE v1.1 Draft A to OPGEE v1.1 Draft B

E.6.1 Gas balance and gas properties

- Gas balance sheet fixed so that gas compositions of C₄ = 0% do not trigger gas balance error. This required changing the accounting of fugitive emissions gas composition. Now, if the associated gas processing vents of C₄ are greater than the input of C₄ to gas processing, then no C₄ is assumed vented. Otherwise, the original C₄ venting equation holds. See cell 'Gas Balance' U14.
- Densities of gas changed: standard conditions are changed to 60F and 1 atm. The user can now select the definition of standard conditions. See 'Input Data' section 6: Definition of Standard Condition.
- Density of VOC is computed directly from VOC composition, rather than assuming density is equal to density of ethane (C₂). See 'Gas Balance' Table 1.4.

E.6.2 Production emissions

- Air separation unit work is now populated with literature data for N₂ separation for Cantarell field [99, 180]. The Cantarell field N₂ plant produces 1200 MMSCF/d of N₂ using 500,500 hp of compression power, resulting in power intensity of 417 hp/MMSCF/d. This includes both compression for air separation and compression to field pressure of 1685 psia. OPGEE calculations for compression from OPGEE default of 125 psia to 1685 psia is 185 hp/MMSCF/d. Thus, separation work is calculated as 232 hp/MMSCF/d, or 0.15 kWh/m³ N₂. See 'Production & Extraction' section 2.7.3. Any additional compression to take N₂ to field pressure is computed in 'Production & Extraction' section 2.7.4.
- A warning is now generated if no artificial lift is specified but reservoir pressure is not enough to provide artificial lift. See cell 'User Inputs & Results' N75.

E.6.3 Venting and fugitives

- Error corrected in 'Venting & Fugitives' section 1.2.8. Fraction of leaking components changed from 25% to a formula that provides a default based on API gravity. These defaults provided by API studies of leaking components [39]. The percentage of leaking components is outlined in 'Input Data'

section 7. From Tables 1-1 and 2-1 in API Standard 4589 [39], leaking components were found to be 0.86% in light crude oil service and 0.01% in heavy crude oil service. Because using these values directly causes a sharp discontinuity in crude carbon intensity at 20°API, OPGEE includes an intermediate case between 15°API and 25°API, with a leakage rate equal to the average of light crude oil and heavy crude oil service (0.43%).

- A conversion factor was fixed in computation of emissions from fugitive leaks. An error in ‘Venting & Fugitives’ cell F212:G212 resulted in division by 1,000,000 rather than division by 365. This effect offsets the reduction in leaking components.
- Corrected error in formula in ‘Venting & Fugitives’ cells F212 and G212. An offset error in these two cells was corrected so that cell reference H86 was changed to H87 and H87 was changed to H88.

E.6.4 Other corrections and error fixes

- GHG emissions worksheet error corrected. ‘GHG Emissions’ cell H22 previously called an incorrect emissions factor.
- Cells ‘Bitumen Extraction & Upgrading’ M38 and M40 were corrected to address error in VFF accounting. Cell M138 was changed to:

$$M52 * M57 * F288 / \mathbf{C240} + \dots \quad (\text{E.1})$$

from:

$$M52 * M57 * F288 + \dots \quad (\text{E.2})$$

where cell C240 scales the emissions per bbl of bitumen produced by the volumetric gain or loss upon upgrading to SCO. Cell M140 on the same sheet was changed similarly.

- Error in steam production calculations for default column fixed (did not affect user calculations). The function for default (not user) steam mixture fluid enthalpy in ‘Steam Injection’ section 1.2.11 referenced the wrong cell.

E.7 Changes from OPGEE v1.0 to OPGEE v1.1 Draft A

E.7.1 Overall model organization

- Added worksheet to track model changes
- Changed color themes to OPGEE custom color theme

E.7.2 User inputs & results worksheet

- Organized user inputs worksheet for the implementation of new macro for the bulk assessment
- Allowed removal of gas processing units on the user inputs worksheet

- Added ocean tanker size to user inputs worksheet
- Added volume fraction of diluent as a user input
- Added a separate emissions category for diluent life cycle emissions
- Removed the allocation of off-site GHG emissions (credits/debts)
- Added a separate emissions category for total off-site GHG emissions

E.7.3 Defaults and smart defaults

- Rounded no. of injection wells to the nearest 1 well

E.7.4 Data and input parameters

- Modified land use change emissions factors to account for 30 year analysis period
- Added petroleum coke life cycle energy consumption and GHG emissions

E.7.5 Error checks

- Corrected the '*Gas Balance*' gas composition overall error check
- Added error check to ensure that downhole pump and gas lift do not co-exist (results in miscalculation of required lifting work)
- Added error check to ensure that user input for volume fraction of diluent is not less than the volume fraction of NGL produced onsite as crude oil blend

E.7.6 New model functionality

- Added improved flaring efficiency calculation worksheet
- More detailed demethanizer model now includes energy consumed by demethanizer
 - Added demethanizer input data
 - Added N₂ and H₂S gas densities to input data worksheet
 - Calculated gas feed into demethanizer in kmol
 - Updated gathering worksheets to include energy consumption and emissions of demethanizer

E.7.7 Bulk assessment macro changes

- Developed a new macro which runs the bulk assessment for unlimited number of fields and has a built in logic for errors fixing
- Bulk assessment macro now has the following features:
 - Works with limited datasets, and fills in defaults or smart defaults where applicable

- Resolves errors by changing programmatically the well diameter, productivity index, GOR etc. See Section 3.7 for details.
 - Uses colors to highlight where the macro fills in or alters data
- Processing configuration flexibility
 - Dehydrator can be switched ON/OFF
 - AGR unit can be switched ON/OFF
 - Demethanizer can be switched ON/OFF
- Diluent blending and upgrading for non oil sands heavy crudes
 - Developed the option of diluent blending after production. The model now accounts for indirect GHG emissions associated with importing NGL for use as diluent. Added an ERROR check to make sure that the diluent volume fraction is the minimum as indicated by model inputs (minimum is NGL produced onsite as crude oil blend).
 - Calculated non-integrated upgrader emissions and energy consumption for non-bitumen pathways using upgrading data from bitumen worksheet
 - Added emissions and energy consumption of non-integrated upgrader (if applicable) to conventional oil GHG emissions

E.7.8 Corrections and improvements

- Changed heater/treater calculations using default oil emulsion (14% emulsified water)
- Corrected the AGR unit venting emissions calculation
- Heating value basis in Bitumen Extraction & Upgrading worksheet is changed from HHV basis to LHV basis to address error in emissions computation
- Fixed treatment of imported vs. on site energy at bitumen production facilities and clarified use of fuel cycle emissions for imported fuels
- Diluted bitumen pathways now exhibit sensitivity in flaring and fugitive emissions computations to level of diluent blending. Upstream flaring and fugitive emissions from diluent life cycle are tracked in the '*Fuel Cycle*' worksheet, and therefore should not be double counted in the '*Bitumen Extraction & Upgrading*' worksheet.
- Improved compressor model (compressor now between 1 and 5 stages)
- Corrected two typo mistakes in the bulk assessment worksheet (scf/bbl liquid for gas lift injection and C4+ instead of C4 for gas composition)
- Corrected flaring emissions calculations (use preprocessing gas composition)

E.7.9 Documentation and model explanation

- Highlighted changes to heater/treater calculations
- Improved description of offsite credits/debts
- Fixed error in documentation of small sources
- Labeling of '*Bitumen Extraction & Upgrading*' Table 4.10 fixed
- Fixed numbering in Bitumen Extraction & Upgrading worksheet

E.8 Changes from OPGEE v1.0 Draft A to OPGEE v1.0

Draft version A of the model was released on June 22nd, 2012 for public review and commenting. A public workshop which was held on the July 12th, 2012 at California Air Resources Board, Sacramento. In this appendix the comments received at this meeting and at other times are addressed as described below.

E.8.1 Major changes

- The version released to the public is now the same as the "pro" version of the model. The public version of the model now contains the macro to run up to 50 fields at one time. See worksheet '*Bulk Assessment Tool*', which allows the user to run multiple cases at once.
- Complex storage tank emissions calculations were removed from OPGEE v1.0 Draft A and replaced with a single parameter. At this time, it was judged that the scale of tank emissions (relatively small) and the complexity with which they were addressed (high complexity) were incommensurate. This is especially the case given the large numbers of parameters needed for the storage tank emissions model, many of which would not likely be available to users of the model. In place of the complex tank calculations, an average tank emissions factor from California data is included.
- The '*User Inputs & Results*' worksheet was significantly expanded to allow easier running of the model with less need to access the detailed calculation worksheets. Parameters added to the '*User Inputs & Results*' worksheet include: fraction of steam generated via cogeneration for thermal EOR; field productivity index; and well production tubing diameter.
- An option is now added to deal with the co-production of oil and other products (NGLs, gas, etc.): OPGEE v1.0 Draft A only treated co-production with system boundary expansion, while in OPGEE v1.0 Draft B, allocation of emissions by energy content is allowed. In system boundary expansion (also known as co-product displacement or co-product credit method), an alternative production method for the co-produced product is assessed and the resulting emissions are credited to the main product as if the co-product directly displaces material produced elsewhere. In allocation, the emissions are divided between products and co-products in proportion to some measure of output (often energy, mass, or monetary value). The user can now choose the co-product treatment method on the '*Fuel Cycle*' worksheet.

- OPGEE was updated with data from the CA-GREET variant of the GREET model. This update allows better congruence with other California LCFS calculations, which rely on the CA-GREET model. The data inputs changed include fuel properties and upstream (fuel cycle) emissions for use in co-product displacement calculations.
- All calculations were updated to use lower heating values instead of higher heating values. The user can still choose the heating value metric for the denominator energy content of the final result (e.g., g/MJ LHV or g/MJ HHV crude oil delivered to refinery).
- Water injection pressure is now calculated using reservoir pressure and an injectivity index (bbl/psi-well). This is more in line with the calculation of work to lift fluids.

E.8.2 Minor changes

- The user guide is expanded with additional descriptions of the input parameters on the '*User Inputs & Results*' worksheet to reduce uncertainty about the definitions of parameters. These descriptions are included in Section 3.6.1.
- More explanation is given in tables regarding parameters that are outside of literature ranges (e.g., pump and compressor efficiency).
- More attention is drawn to the overall model error check indicator to alert the user to possible errors in model inputs.
- An error is reported when a user puts in an incorrectly spelled country name. This prevents spurious default to average flaring emissions rates that might occur due to simple input errors.
- To address transmission losses between pumps and prime movers, pump efficiency is slightly reduced. This is believed to be a minor factor, and data are not currently available to separate transmission losses from other losses.
- The value for flaring emissions on the '*User Inputs & Results*' worksheet (J99 in OPGEE v1.0 Draft A) is now used to compute flaring emissions.
- The friction factor is now included as a 'User Free' cell instead of a fixed default. This will allow the user to reduce the friction factor in cases of very high well flow rates (flow character in turbulent regime).
- Water reinjection pump suction pressure is added as a parameter to allow for high pressure oil-water separation and resulting reduced pump work.
- Conversion factor from grams to pounds changed to 453.59 g/lb from 453.
- The units that accompanied cell '*Bitumen Extraction & Upgrading*' M164 in OPGEE v1.0 Draft A, are corrected from g/bbl to g/MJ.
- GWP values are allowed to vary for examining differences using 20 and 100 year GWPs.

Bibliography

1. Katz, D.L.; Standing, M.B. Density of Natural Gases. *Transactions of the American Institute of Mining, Metallurgical and Petroleum Engineers* **1942**, *146*, 140–149.
2. Standing, M.B. *Volumetric and phase behavior of oilfield hydrocarbon systems*; Society of Petroleum Engineers of AIME: Dallas, TX, 1977.
3. Beck, S.; Collins, R. Moody diagram. Technical report, University of Sheffield, 2008.
4. Manning, F.S.; Thompson, R. *Oilfield processing of petroleum, Volume 1: Natural gas*; PennWell: Tulsa, OK, 1991.
5. Inc., A. Aspen HYSYS v. 8.8.
6. Skone, T.J.; R., J.; Cooney, G.; Jamieson, M.; Littlefield, J.; Marriott, J. Gate-to-Gate Life Cycle Inventory and Model of CO₂-Enhanced Oil Recovery. Technical Report DOE/NETL-2013/1599, U.S. Department of Energy, National Energy Technology Laboratory, 2013.
7. Allen, D.T.; Pacsi, A.P.; Sullivan, D.W.; Zavala-Araiza, D.; Harrison, M.; Keen, K.; Fraser, M.P.; Daniel Hill, A.; Sawyer, R.F.; Seinfeld, J.H. Methane emissions from process equipment at natural gas production sites in the United States: Pneumatic controllers. *Environmental science & technology* **2014**, *49*, 633–640.
8. Yeh, S.; Jordann, S.M.; Brandt, A.R.; Turetsky, M.; Spatari, S.; Keith, D.W. Land use greenhouse gas emissions from conventional oil production and oil sands. *Environmental Science & Technology* **2010**, *44*, 8766–8772.
9. McAllister, E. *Pipeline rules of thumb handbook, 7th edition*; PennWell: Tulsa, OK, 2009.
10. Vlasopoulos, N.; Memon, F.; Butler, D.; Murphy, R. Life cycle assessment of wastewater treatment technologies treating petroleum process waters. *Science of the Total Environment* **2006**, *367*, 58–70.
11. Haynes, H.; Thrasher, L.; Katz, M.; Eck, T. An Analysis of the Potential for Enhanced Oil Recovery from Known Fields in the United States—1976 to 2000. Technical report, National Petroleum Council, 1976.
12. Lee, S. 2007 Oil and Gas Industry Survey Results: Draft Report. Technical report, California Environmental Protection Agency, Air Resources Board, 2011.
13. Detwiler, S. 2007 Oil and Gas Industry Survey Results - Final Report (Revised). Technical report, October 2013.
14. API. Calculation Workbook For Oil And Gas Production Equipment Fugitive Emissions. Workbook API publication number 4638, American Petroleum Institute, 1996.

15. Keesom, W.; Unnasch, S.; Moretta, J. Life cycle assessment comparison of North American and imported crudes. Technical report, Jacobs Consultancy and Life Cycle Associates for Alberta Energy Resources Institute, 2009.
16. Rosenfeld, J.; Pont, J.; Law, K.; Hirshfeld, D.; Kolb, J. Comparison of North American and imported crude oil life cycle GHG emissions. Technical report, TIAX LLC. and MathPro Inc. for Alberta Energy Research Institute, 2009.
17. Howarth, G. Carbon Intensity of Crude Oil in Europe Crude. Technical report, Energy-Redefined LLC for ICCT, 2010.
18. Skone, T.J.; Gerdes, K.J. Development of baseline data and analysis of life cycle greenhouse gas emissions of petroleum-based fuels. Technical Report DOE/NETL-2009/1346, Office of Systems, Analyses and Planning, National Energy Technology Laboratory, 2008.
19. Gerdes, K.J.; Skone, T.J. Consideration of crude oil source in evaluating transportation fuel GHG emissions. Technical Report DOE/NETL-2009/1360, National Energy Technology Laboratory, 2009.
20. Brandt, A.R. Variability and Uncertainty in Life Cycle Assessment Models for Greenhouse Gas Emissions from Canadian Oil Sands Production. *Environmental Science & Technology* **2011**, *46*, 1253–1261.
21. Charpentier, A.D.; Bergerson, J.; MacLean, H.L. Understanding the Canadian oil sands industry's greenhouse gas emissions. *Environmental Research Letters* **2009**, *4*, 14.
22. Charpentier, A.; Kofoworola, O.; Bergerson, J.; MacLean, H. Life Cycle Greenhouse Gas Emissions of Current Oil Sands Technologies: GHOST Model Development and SAGD Application. *Environmental Science & Technology* **2011**, *45*, 9393–9404.
23. Brandt, A.R.; Unnasch, S. Energy intensity and greenhouse gas emissions from California thermal enhanced oil recovery. *Energy & Fuels* **2010**, DOI: 10.1021/ef100410f.
24. (S&T)². GHGenius, model version 4.0c. Technical report, (S&T)² consultants, for Natural Resources Canada, <http://www.ghgenius.ca/>, 2012.
25. Johnson, M. Flare efficiency & emissions: Past & current research. Global Forum on Flaring and Venting Reduction and Natural Gas Utilisation, 2008.
26. Johnson, M.; Wilson, D.; Kostiuk, L. A fuel stripping mechanism for wake-stabilized jet diffusion flames in crossflow. *Combustion Science and Technology* **2001**, *169*, 155–174.
27. Elvidge, C.; Ziskin, D.; Baugh, K.; Tuttle, B.; Ghosh, T.; Pack, D.; Erwin, E.; Zhizhin, M. A fifteen year record of global natural gas flaring derived from satellite data. *Energies* **2009**, *2*, 595–622.
28. Wang, M. GREET Model 1.8d. Computer program, Argonne National Laboratory, <http://greet.es.anl.gov/>, 2010.
29. Abella, J.; Bergerson, J. Model to investigate energy and greenhouse gas emissions implications of refining petroleum: Impacts of crude quality and refinery configuration. *Environmental Science & Technology* **2012**, *46*.
30. Shires, T.M.; Loughran, C.J. Compendium of Greenhouse Gas Emissions Methodologies for the Oil and Gas Industry. Technical report, American Petroleum Institute, 2004.

31. Azar, J.; Samuel, G.R. *Drilling engineering*; PennWell: Tulsa, OK, 2007.
32. Devereux, S. *Practical well planning and drilling manual*; PennWell: Tulsa, OK, 1998.
33. Gidley, J.L.; Holditch, S.A.; Nierode, D.E.; Veatch, R.W.J. *Recent advances in hydraulic fracturing*; SPE Monograph Series, volume 12, Society of Petroleum Engineers: Richardson, TX, 1989.
34. Lapeyrouse, N.J. *Formulas and calculations for drilling, production and workover*, 2nd edition; PennWell: Tulsa, OK, 2002.
35. Mitchell, R.F. Volume II: Drilling Engineering. In *Petroleum Engineering Handbook*; Lake, L.W., Ed.; Society of Petroleum Engineers: Richardson, TX, 2006.
36. Mitchell, R.F.; Miska, S.Z. *Fundamentals of drilling engineering*; Society of Petroleum Engineers: Richardson, TX, 2011.
37. Wilson, M.J.; Frederick, J.D. *Environmental Engineering for Exploration and Production Activities*; SPE Monograph Series, Society of Petroleum Engineers: Richardson, TX, 1999.
38. API. An engineering assessment of volumetric methods of leak detection in above-ground storage tanks. Technical Report API Publication 306, American Petroleum Institute, 1991.
39. API. Fugitive hydrocarbon emissions from oil and gas production operations. Technical Report API Publication 4589, American Petroleum Institute, 1993.
40. API. Emissions factors for oil and gas production operations. Technical Report API Publication 4615, American Petroleum Institute, 1995.
41. API. Fugitive emissions from equipment leaks II: Calculation procedures for petroleum industry facilities. Technical Report API Publication 343, American Petroleum Institute, 1998.
42. API. Manual of petroleum measurement standards: Chapter 19 - Evaporative-loss measurement - Section 2 - Evaporative loss from floating-roof tanks. Technical Report Formerly API Publication 2517 & 2519, American Petroleum Institute, 2003.
43. API. Evaporation loss from low-pressure tanks. Technical report, American Petroleum Institute, 2006.
44. API. Flare details for general refinery and petrochemical service. Technical Report API/ANSI Standard 537, American Petroleum Institute, 2008.
45. API. Pressure-relieving and depressuring systems. Technical Report ANSI/API Standard 521, Fifth edition, American Petroleum Institute, 2008.
46. API. Compilation of air emission estimating methods for petroleum distribution and dispensing facilities. Technical Report API Publication 1673, American Petroleum Institute, 2009.
47. API. Specification for vertical and horizontal emulsion treaters. Technical Report API Specification 12L, American Petroleum Institute, 2009.
48. API. Specification for indirect type oilfield heaters. Technical Report API Specification 12K, American Petroleum Institute, 2009.

49. API. Specification for oil and gas separators. Technical Report API Specification 12J, American Petroleum Institute, 2009.
50. Arnold, K. *Petroleum Engineering Handbook, Volume III: Facilities and construction engineering*; Society of Petroleum Engineers: Richardson, TX, 2007.
51. Chilingarian, G.V.; Robertson, J.; Kumar, S. *Surface operations in petroleum production I*; Elsevier: New York, 1987.
52. Chilingarian, G.V.; Robertson, J.; Kumar, S. *Surface operations in petroleum production II*; Elsevier: New York, 1989.
53. Cholet, H. *Well production practical handbook*; Editions Technip: Paris, 2000.
54. Clegg, J.D. Volume IV: Production operations engineering. In *Petroleum Engineering Handbook*; Lake, L.W., Ed.; Society of Petroleum Engineers: Richardson, TX, 2007.
55. Fanchi, J.R. Volume I: General engineering. In *Petroleum Engineering Handbook*; Lake, L.W., Ed.; Society of Petroleum Engineers: Richardson, TX, 2007.
56. GPSA. *GPSA Engineering Data Book, 12th edition*; Gas Processors Suppliers Association: Tulsa, OK, 2004.
57. Holstein, E.D. Volume Va: Reservoir Engineering and Petrophysics. In *Petroleum Engineering Handbook*; Lake, L.W., Ed.; Society of Petroleum Engineers: Richardson, TX, 2007. OPGEE.
58. Holstein, E.D. Volume Vb: Reservoir Engineering and Petrophysics. In *Petroleum Engineering Handbook*; Lake, L.W., Ed.; Society of Petroleum Engineers: Richardson, TX, 2007.
59. Leffler, W.L.; Martin, R. *Oil and gas production in nontechnical language*; PennWell: Tulsa, OK, 2006.
60. Manning, F.S.; Thompson, R. *Oilfield processing, Volume 2: Crude oil*; PennWell: Tulsa, OK, 1995.
61. Stewart, M.; Arnold, K. *Gas-liquid and liquid-liquid separators*; Gulf Equipment Guides, Gulf Professional Publishing: Burlington, MA, 2008.
62. Stewart, M.; Arnold, K. *Emulsions and oil treating equipment: Selection, sizing, and troubleshooting*; Gulf Professional Publishing: Burlington, MA, 2009.
63. Stewart, M.; Arnold, K. *Produced water treatment field manual*; Gulf Professional Publishing: Waltham, MA, 2011.
64. Takacs, G. *Modern sucker rod pumping*; PennWell: Tulsa, OK, 1993.
65. Takacs, G. *Sucker rod pumping manual*; PennWell: Tulsa, OK, 2003.
66. Craig, F.F. *The reservoir engineering aspects of waterflooding*; SPE Monograph Series, volume 3, Society of Petroleum Engineers: Richardson, TX, 1993.
67. Jarrell, P.M.; Fox, C.; Stein, M.; Webb, S. *Practical aspects of CO₂ flooding*; SPE Monograph Series, volume 22, Society of Petroleum Engineers: Richardson, TX, 2002.
68. Prats, M. *Thermal recovery*; Henry L. Doherty Series, Volume 7, Society of Petroleum Engineers: Richardson, TX, 1985.

69. Rose, S.C.; Buckwalter, J.F.; Woodhall, R.J. *Design engineering aspects of waterflooding*; SPE Monograph Series volume 11, Society of Petroleum Engineers: Richardson, TX, 1989.
70. Warner, H. Volume VI: Emerging and peripheral technologies. In *Petroleum Engineering Handbook*; Lake, L.W., Ed.; Society of Petroleum Engineers: Richardson, TX, 2007.
71. Green, D.W.; Willhite, G.P. *Enhanced oil recovery*; Henry L. Doherty Memorial Fund of AIME, Society of Petroleum Engineers: Richardson, TX, 1998.
72. Khatib, Z.; Verbeek, P. Water to value - Produced water management for sustainable field development of green and mature fields, 2002.
73. Neff, J.M.; Hagemann, R.E. Environmental challenges of heavy crude oils: Management of liquid wastes. 2007 SPE E&P Environmental and Safety Conference, 2007, Vol. SPE 101973.
74. Reed, M.; Johnsen, S. *Produced water 2: Environmental issues and mitigation technologies*; Plenum Press: New York, NY, 1996.
75. Veil, J.A.; Puder, M.G.; Elcock, D.; Redweik, R.J.j. A white paper describing produced water from the production of crude oil, natural gas, and coal bed methane. Technical report, National Energy Technology Laboratory, 2004.
76. API. Correlation equations to predict reid vapor pressure and properties of gaseous emissions for exploration and production facilities. Technical Report API Publication 4683, American Petroleum Institute, 1998.
77. API. Fugitive emissions from equipment leaks I: Monitoring manual. Technical Report API Publication 342, American Petroleum Institute, 1998.
78. API. Manual of petroleum measurement standards: Chapter 19 - Evaporative loss measurement - Section 1 - Evaporative loss from fixed-roof tanks. Technical report, American Petroleum Institute, 2008.
79. API. Marine vapor control training guidelines. Technical Report API Recommended Practice 1127, American Petroleum Institute, 1993.
80. API. Venting atmospheric and low-pressure storage tanks. Technical Report ANSI/API Standard 2000, American Petroleum Institute, 2009.
81. API. Ship, barge, and terminal hydrocarbon vapor collection manifolds. Technical Report API Recommended Practice 1124, American Petroleum Institute, 1995.
82. API. Fugitive emission factors for crude oil and product pipeline facilities. Technical Report API Publication 4653, American Petroleum Institute, 1997.
83. Miesner, T.O.; Leffler, W.L. *Oil & gas pipelines in nontechnical language*; PennWell: Tulsa, OK, 2006.
84. Szilas, A. *Production and transport of oil and gas: Part B - Gathering and transport*; Elsevier: New York, NY, 1985.
85. O&GJ. 2010 Worldwide Oil Field Production Survey. Technical Report Microsoft Excel dataset, Oil & Gas Journal, PennWell publishers, 2009.
86. Simmons, M.R. *Twilight in the desert: The coming Saudi oil shock and the world economy*; John Wiley & Sons, 2005.

87. Simmons, M.R. The world's giant oilfields. Technical report, Simmons & Company International, 2006.
88. Deffeyes, K.S. *Hubbert's peak: The impending world oil shortage*; Princeton University Press: Princeton, NJ, 2001; p. 208.
89. Deffeyes, K.S. *Beyond oil: The view from Hubbert's peak*; Hill and Wang: New York, 2005.
90. O&GJ. A worldwide look at reserves and production. Technical Report Microsoft Excel dataset, Oil & Gas Journal, PennWell publishers, 2009.
91. CDC-DOGGR. 2010 Annual Report of the State Oil & Gas Supervisor. Technical report, California Department of Conservation, Department of Oil, Gas and Geothermal Resources, 2011.
92. AOGCC. Oil and Gas Pools - Statistics Pages. Technical Report http://doa.alaska.gov/ogc/annual/current/annindex_current.html, Alaska Oil and Gas Conservation Commission, 2012.
93. McCain, W.D. *Properties of Petroleum Fluids*, 2nd ed.; PennWell, 1990.
94. CDC-DOGGR. California Oil and Gas Fields, Volume III - Northern California. Technical report, California Department of Conservation, Division of Oil Gas and Geothermal Resources, 1982.
95. CDC-DOGGR. California Oil and Gas Fields, Volume II - Southern, Central Coastal, and Offshore California. Technical report, California Department of Conservation, Division of Oil Gas and Geothermal Resources, 1992.
96. CDC-DOGGR. California Oil and Gas Fields, Volume I - Central California. Technical report, California Department of Conservation, Division of Oil Gas and Geothermal Resources, 1998.
97. CDC-DOGGR. Online production and injection database. Technical report, California Department of Conservation, Division of Oil, Gas, and Geothermal Resources, <http://opi.consrv.ca.gov/opi/opi.dll>.
98. CDC-DOGGR. Monthly oil and gas production and injection report (January-December). Technical report, California Department of Conservation, Department of Oil, Gas and Geothermal Resources, 2010.
99. Kuo, J.; Luna-Melo, J.; Perez, P. World's largest N2 generation plant. *Oil & Gas Journal* 2001.
100. Malone, T.; Kuuskraa, V. CO₂-EOR Offshore Resource Assessment. Technical Report DOE/NETL-2014/1631, U.S. Department of Energy, National Energy Technology Laboratory, 2014.
101. CDC-DOGGR. 2009 Annual Report of the State Oil & Gas Supervisor. Technical report, California Department of Conservation, Department of Oil, Gas and Geothermal Resources, 2010.
102. ERCB. ST53: Alberta Crude Bitumen In Situ Production Monthly Statistics, 2009. Technical report, Energy Resources Conservation Board, 2010.
103. ERCB. ST53: Alberta Crude Bitumen In Situ Production Monthly Statistics, 2010. Technical report, Energy Resources Conservation Board, 2011.

104. Stewart, W.F.; Burkhardt, S.F.; Voo, D. Prediction of Pseudocritical Parameters for Mixtures **1959**. *Presented at the AIChE Meeting, Kansas City, MO*.
105. Wichert, E.; Aziz, K. Calculate Z's for sour gases. *Hydrocarbon Processing* **1959**, *51*, 119–122.
106. Span, R.; Lemmon, E.W.; Jacobsen, R.T.; Wagner, W.; Yokozeki, A. A Reference Equation of State for the Thermodynamic Properties of Nitrogen for Temperatures from 63.151 to 1000 K and Pressures to 2200 Mpa. *Journal of Physical and Chemical Reference Data* **2000**, *29*, 1361–1433.
107. Span, R.; Wagner, W. A New Equation of State for Carbon Dioxide Covering the Fluid Region from the Triple-Point Temperature to 1100 K at Pressures to 800 Mpa. *Journal of Physical and Chemical Reference Data* **1996**, *25*, 1509–1596.
108. Lemmon, E.W.; Jacobsen, R.T.; Penoncello, S.G.; Friend, D.G. Thermodynamic Properties of Air and Mixtures of Nitrogen, Argon, and Oxygen from 60 to 2000 K at Pressures to 2000 MPa. *Journal of Physical and Chemical Reference Data* **2000**, *29*, 331–385.
109. Schmidt, R.; Wagner, W. A New Form of the Equation of State for Pure Substances and its Application to Oxygen. *Fluid Phase Equilibria* **1985**, *19*, 175–200.
110. Lemmon, E.W.; Huber, M.L.; McLinden, M.O. *NIST Standard Reference Database 23: Reference Fluid Thermodynamic and Transport Properties - REFPROP*. National Institute of Standards and Technology, Standard Reference Data Program, Gaithersburg, MD, 9.1 ed., 2013.
111. Wang, M. CA-GREET Model v1.8b. Computer program, Argonne National Laboratory, 2009.
112. Vafi, K.; Brandt, A.R. GHGfrack: An open-source model for estimating greenhouse gas emissions from combustion of fuel in drilling and hydraulic fracturing. *Environmental Science & Technology* **2016**: In review.
113. Vafi, K.; Brandt, A. GHGfrack: Model documentation. Technical report, Stanford University, 2016.
114. Vafi, K.; Brandt, A.R., A.R. GHGfrack v.1.0 model code. Technical report, Stanford University, 2016.
115. Yeh, S. 2012 updates to calculations on land use emissions. Technical report, University of California, Davis, 2012.
116. Schmidt, P.F. *Fuel oil manual*, 4th ed.; Industrial Press: New York, 1985.
117. Vako, P.; McCain, W.D. Reservoir oil bubblepoint pressures revisited; solution gas-oil ratios and surface gas specific gravities. *Journal of Petroleum Science & Engineering* **2003**, *37*, 153–169.
118. Takacs, G. *Gas lift manual*; PennWell: Tulsa, OK, 2005.
119. Guo, B.; Lyons, W.C. *Petroleum production engineering, a computer-assisted approach*; Gulf Professional Publishing, 2007.
120. Cengel, Y.A.; Turner, R.H. *Fundamentals of thermal-fluid sciences*; McGraw-Hill, 2005.
121. AER. ST39: Alberta Mineable Oil Sands Plant Statistics. Technical report, Alberta Energy Regulator, 1970–2002, 2008–2012.

122. AER. ST43: Alberta Mineable Oil Sands Plant Statistics – Annual. Technical report, Alberta Energy Regulator, 2003-2007.
123. AER. Alberta Energy Regulator: Personal communication, Toronto ON, 2016. Technical report, Alberta Energy Regulator, 2016.
124. COSIA. COSIA Mining and Extraction Reference Facility – Energy and Material Balance – PFT. Technical report, Canadian Oil Sands Innovation Alliance, 2015.
125. COSIA. COSIA Mining and Extraction Reference Facility – Energy and Material Balance – NFT. Technical report, Canadian Oil Sands Innovation Alliance, 2015.
126. AEMERA. Fugitive GHG Emissions for SGER Oil Sands Facilities: 2011-2014. Technical report, Alberta Environmental Monitoring, Evaluation, and Reporting Agency, Lower Athabasca, 2015.
127. Johnson, M.; Crosland, B.; McEwen, J.; Hager, D.; Armitage, J.; Karimi-Golpayegani, M.; Picard, D. Estimating fugitive methane emissions from oil sands mining using extractive core samples. *Atmospheric Environment* **2016**, *144*, 111–123.
128. (S&T)². GHGenius, model version 4.03. Technical report, (S&T)² consultants, for Natural Resources Canada, 2013.
129. Consultancy, J.E. A greenhouse gas reduction roadmap for oil sands. Technical report, CCEMC, 2012.
130. Abdel-Aal, H., F.M.; Aggour, M. *Petroleum & Gas Field Processing*; CRC, 2003.
131. EPA, U. CLIMATE LEADERS GREENHOUSE GAS INVENTORY PROTOCOL OFF-SET PROJECT METHODOLOGY. Project Type: Industrial Boiler Efficiency. Technical report, U.S. Environmental Protection Agency, 2008.
132. Pacheco, D.; MacLean, H.L. Oil Sands Technology Upgrading Model (OSTUM) model documentation. Technical report, University of Toronto, 2016.
133. Dillon, J. Treatment technology review and assessment for petroleum process waters. PhD thesis, Imperial College, 2003.
134. COSIA. COSIA In situ reference facility - SAGD. Technical report, Canadian Oil Sands Innovation Alliance, 2014.
135. Moritis, G. CO₂ miscible, steam dominate enhanced oil recovery processes: EOR survey. *Oil & Gas Journal* **2010**, *108*, 36+.
136. Baibakov, N.; Garushev, A. *Thermal methods of petroleum production*; Developments in Petroleum Science 25, Elsevier, 1989.
137. Donaldson, E.C.; Chilingarian, G.V. *Enhanced oil recovery, processes and operations*; Vol. 17B, *Developments in Petroleum Science*, Elsevier: Amsterdam, 1989.
138. Knovel. Knovel Steam Tables. Technical report, Available from www.knovel.com, 2006, Accessed 2012.
139. Tackett, H.H.; Cripe, J.A.; Dyson, G. Positive displacement reciprocating pump fundamentals - Power and direct acting types. Proceedings of the twenty-fourth international pump users symposium, 2008.
140. Ganapathy, V. *Industrial boilers and heat recovery steam generators: Design, applications and calculations*; Marcel Dekker: New York, 2003.

141. Cengel, Y.A.; Boles, M. *Thermodynamics: An engineering approach*, 5th ed.; McGraw-Hill: New York, 2006.
142. Buchanan, I.; Westphalen, D.; Davies, S.; Chawla, N.; Gieseman, J. SAGD Energy Efficiency Study. Technical report, Jacobs Consultancy, Prepared for Alberta Energy Research Institute, 2009.
143. Speight, J.G. *The chemistry and technology of petroleum*; Chemical Industries, Marcel Dekker: New York, 1994.
144. Swafford, P. Understanding the quality of Canadian bitumen and synthetic crudes. Technical report, Spiral Software, 2009.
145. Cantera: An object-oriented software toolkit for chemical kinetics, thermodynamics, and transport processes. Technical report, <http://code.google.com/p/cantera/>, 2012.
146. Siemens. Industrial gas turbines: The comprehensive product range from 5 to 50 megawatts. Technical report, Siemens AG, 2012.
147. Badeer, G. GE Aeroderivative Gas Turbines - Design and Operating Features. Technical report, GE Power Systems, 2012.
148. Gas Turbine World: 2010 GTW Handbook. Technical report, Fairfield, CT, 2010.
149. Kim, T. Comparative analysis on the part load performance of combined cycle plants considering design performance and power control strategy. *Energy* **2004**, *29*, 71–85.
150. Ganapathy, V. Heat-recovery steam generators: Understand the basics. *Chemical Engineering Progress* **1996**.
151. Wang, J.; O'Donnell, J.; Brandt, A.R. Potential solar energy use in the global petroleum sector. *Energy* **2016**.
152. Sandler, J.; Fowler, G.; Cheng, K.; Kovsek, A.R. Solar-generated steam for oil recovery: Reservoir simulation, economic analysis, and life cycle assessment. *Energy Conversion and Management* **2014**, *77*, 721–732.
153. Palmer, D.; O'Donnell, J.; Walter, B. Solar enhanced oil recovery application to Kuwait's heavy oil fields. *SPE Kuwait oil and gas show and conference* **2015**.
154. company authors, V. In situ progress reports to Alberta Energy Regulator. Technical report, Alberta Energy Regulator, Various.
155. The Engineering Toolbox. Technical report, www.engineeringtoolbox.com, 2012.
156. NOAA. Global Gas Flaring Estimates. Technical report, National Geophysical Data Center, 2010.
157. EIA. International Energy Statistics - Petroleum. Technical report, U.S. Energy Information Administration, 2010.
158. Johnson, M.R.; Kostiuk, L. A parametric model for the efficiency of a flare in cross-wind. *Proceedings of the Combustion Institute* **2002**, *29*, 1943–1950.
159. Gogolek, P. Methane emissions factors for biogas flares. *Industrial combustion* **2012**, p. 17.
160. EPA. EPA Flaring Regulation. Technical Report 60.18 40CFR Ch.1, US Environmental Protection Agency, 2010.

161. da Rossa, A. *Fundamentals of Renewable Energy Processes*; Vol. Version 3, Elsevier Inc., 2012.
162. Johnson, M.; Kistiuk, L. Efficiencies of low-momentum jet diffusion flames in cross-winds. *Combustion and Flame* **2000**, *123*, 189–200.
163. Solomon, S.; Qin, D.; Manning, M.; Chen, Z.; Marquis, M.; Averyt, K.B.; Tignor, M.; Miller, H.L., Eds. *Contribution of Working Group I to the Fourth Assessment Report of the Intergovernmental Panel on Climate Change 2007*; Cambridge University Press, 2007.
164. Inc., M. MATLAB 2016B.
165. Nawaz, M.; Jobson, M. Synthesis and optimization of demethanizer flowsheets for low temperature separation processes. *Distillation Absorption* **2010**, pp. 79–84.
166. U.S. Department of Energy, N.E.T.L. NETL Life Cycle Inventory Data - Unit Process: Gas Stream Chilling, 2012.
167. U.S. Department of Energy, N.E.T.L. NETL Life Cycle Inventory Data - Unit Process: Ryan Holmes Gas Separation, 2012.
168. Kidney, A.J.; Parrish, W.R.; McCartney, D. *Fundamentals of Natural Gas Processing*; CRC Press: Boca Raton, FL, 2011.
169. Parro, D. Membrane CO₂ Separation Proves Out At Sacroc Tertiary Recovery Project. *Oil & Gas Journal* **1984**, pp. 85–88.
170. Parro, D. Membrane Technology Matters. *Oil & Gas Journal* **2002**, pp. 43–47.
171. Khan, M.; Manning, W. Practical Designs for Amine Plants. Technical report, Petroenergy Workshop, Houston, TX, 1985.
172. Jones, V.; Perry, C. Fundamentals of gas treating. Gas Conditioning Conference, 1973.
173. Mondor, C.; Dymont, J. *Jump Start Guide: Sulsim™ Sulfur Recovery in Aspen HYSYS® V9*. Aspen Technology Inc., 2018.
174. Masnadi, M.S.; El-Houjeiri, H.M.; Schunack, D.; Li, Y.; Englander, J.G.; Badahdah, A.; Monfort, J.C.; Anderson, J.E.; Wallington, T.J.; Bergerson, J.A.; others. Global carbon intensity of crude oil production. *Science* **2018**, *361*, 851–853.
175. Roy, P.S.; Amin, M.R. Aspen-HYSYS simulation of natural gas processing plant. *Journal of Chemical Engineering* **2011**, *26*, 62–65.
176. Luyben, W.L. NGL demethanizer control. *Industrial & Engineering Chemistry Research* **2013**, *52*, 11626–11638.
177. Nawaz, M.; Jobson, M. Synthesis and optimization of demethanizer flowsheets for low temperature separation processes. *Distillation Absorption* **2010**, pp. 79–84.
178. Milligan, E. Evaluation of Permit Application No. 2005-100-TVR, Whiting Oil and Gas Corporation, Dry Trail Gas Plant (SIC 1321), NE/4 of Section 14, T5N, R13E, Texas County, 2007.
179. UNEP. Electrical Energy Equipment: Compressors and Compressed Air Systems. Technical report, United Nations Environment Programme, 2006.
180. Bocker, N.; Grahl, M.; Tota, A.; Haussinger, P.; Leitgeb, P.; Schmucker, B., Ullmann's Encyclopeda of Industrial Chemistry; Wiley, 2013; chapter Nitrogen.

181. Oxy Denver Unit CO₂ Subpart RR Monitoring, Reporting and Verification (MRV) Plan. Report submitted by Occidental Petroleum to U.S. Environmental Protection Agency, available online at https://www.epa.gov/sites/production/files/2015-12/documents/denver_unit_mrv_plan.pdf, 2015. Accessed April 2016.
182. Oxy CO₂ EOR Project. Presentation submitted by Occidental Petroleum to California Energy Commission, available online at http://www.energy.ca.gov/sitingcases/hydrogen_energy/documents/others/2012-06-20_OEHI_Project_Overview_workshop_presentation.pdf, 2012. Accessed April 2016.
183. Benson, S.; Cook, P., IPCC Special Report on Carbon Dioxide Capture and Storage; IPCC, 2005; chapter Chapter 5: Underground Geologic Storage.
184. Caterpillar. Oil & Gas Production Power Spec Sheets. Technical report, Caterpillar Oil & Gas Resource Center, 2012.
185. GE. GE Motors Catalog 1.3. Technical report, General Electric, 2011.
186. U.S. Department of Energy, N.E.T.L. NETL Life Cycle Inventory Data - Unit Process: Membrane Separation of CO₂ and Hydrocarbons, 2012.
187. Turbines, S. Gas Turbine Generator Sets. Technical report, Solar Turbines, 2012.
188. Caterpillar. 3512C Offshore Drilling Module. Technical report, Caterpillar Oil & Gas Resource Center, 2012.
189. ISO. ISO 14040: Environmental management - Life cycle assessment - Principles and framework, 2006.
190. ISO. ISO 14044: Environmental management - Life cycle assessment - Requirements and guidelines, 2006.
191. Centre, E. EcoInvent v.3.0 Dataset. Technical report, Swiss Centre for Life Cycle Inventories, 2014.
192. Wang, M. GREET Model 2_2012. Computer program, Argonne National Laboratory, <http://greet.es.anl.gov/>, 2012.
193. Nguyen, J. *Drilling: Oil and Gas Field Development Techniques*; Editions Technip, 1996.
194. Vetco Gray. Specialty Connectors & Pipe: For land, platform, jackup, floater and deepwater applications. Technical report, Vetco Gray: a GE oil & gas business, http://site.ge-energy.com/businesses/ge_oilandgas/en/literature/en/downloads/specialty_connectors_p 2008, accessed April 2014.
195. API. API Tubing Table. Technical report, American Petroleum Institute, <http://www.oilproduction.net/files/005-apitubing.pdf>, Accessed April 2014.
196. Inc., A.D. Oilfield Data Handbook. Technical report, Apex Distribution Inc., <http://www.monarchapex.com/pdf/Oilfield>
197. Corporation, S.E. Two & Three Phase Vertical & Horizontal Separators & Gas Scrubbers. Technical report, Surface Equipment Corporation, <http://www.surfaceequip.com/two-three-phase-vertical-horizontal-separators-gas-scrubbers.html>, 2014.
198. Exterran. Production Solutions: Glycol Dehydration Unit. Technical report, Exterran Holdings Inc., <http://www.terran.com/Content/Docs/Products/Glycol-Dehydration-Unit-English-Letter.pdf>, 2012.

199. API. Specification for shop welded tanks for storage of production liquids. Technical Report API Specification 12F, American Petroleum Institute, 1994.
200. CIA. The World Factbook. Technical report, Central Intelligence Agency, <https://www.cia.gov/library/publications/the-world-factbook/>, 2013.
201. Management, N.R. Methane Emissions from the NG Industry. Technical report, Environmental Protection Agency, 1996.
202. Brantley, H.L.; Thoma, E.D.; Squier, W.C.; Guven, B.B.; Lyon, D. Assessment of methane emissions from oil and gas production pads using mobile measurements. *Environmental science & technology* **2014**, *48*, 14508–14515.
203. Goetz, J.D.; Avery, A.; Werden, B.; Floerchinger, C.; Fortner, E.C.; Wormhoudt, J.; Massoli, P.; Herndon, S.C.; Kolb, C.E.; Knighton, W.B.; others. Analysis of local-scale background concentrations of methane and other gas-phase species in the Marcellus Shale. *Elem Sci Anth* **2017**, *5*.
204. Lan, X.; Talbot, R.; Laine, P.; Torres, A. Characterizing Fugitive Methane Emissions in the Barnett Shale Area Using a Mobile Laboratory. *Environmental Science & Technology* **2015**, *49*, 8139–8146.
205. Omara, M.; Sullivan, M.R.; Li, X.; Subramanian, R.; Robinson, A.L.; Presto, A.A. Methane emissions from conventional and unconventional natural gas production sites in the Marcellus Shale Basin. *Environmental science & technology* **2016**, *50*, 2099–2107.
206. Yacovitch, T.I.; Herndon, S.C.; Pétron, G.; Kofler, J.; Lyon, D.; Zahniser, M.S.; Kolb, C.E. Mobile laboratory observations of methane emissions in the Barnett Shale region. *Environmental science & technology* **2015**, *49*, 7889–7895.
207. Rella, C.W.; Tsai, T.R.; Botkin, C.G.; Crosson, E.R.; Steele, D. Measuring emissions from oil and natural gas well pads using the mobile flux plane technique. *Environmental science & technology* **2015**, *49*, 4742–4748.
208. Robertson, A.M.; Edie, R.; Snare, D.; Soltis, J.; Field, R.A.; Burkhardt, M.D.; Bell, C.S.; Zimmerle, D.; Murphy, S.M. Variation in methane emission rates from well pads in four oil and gas basins with contrasting production volumes and compositions. *Environmental Science & Technology* **2017**, *51*, 8832–8840.
209. Bell, C.S.; Vaughn, T.L.; Zimmerle, D.; Herndon, S.C.; Yacovitch, T.I.; Heath, G.A.; Pétron, G.; Edie, R.; Field, R.A.; Murphy, S.M.; others. Comparison of methane emission estimates from multiple measurement techniques at natural gas production pads. *Elementa* **2017**, *5*.
210. Conley, S.; Franco, G.; Faloona, I.; Blake, D.R.; Peischl, J.; Ryerson, T. Methane emissions from the 2015 Aliso Canyon blowout in Los Angeles, CA. *Science* **2016**, p. aaf2348.
211. Schwietzke, S.; Pétron, G.; Conley, S.; Pickering, C.; Mielke-Maday, I.; Dlugokencky, E.J.; Tans, P.P.; Vaughn, T.; Bell, C.; Zimmerle, D.; others. Improved mechanistic understanding of natural gas methane emissions from spatially resolved aircraft measurements. *Environmental Science & Technology* **2017**, *51*, 7286–7294.
212. Englander, J.G.; Brandt, A.R.; Conley, S.; Lyon, D.R.; Jackson, R.B. Aerial Interyear Comparison and Quantification of Methane Emissions Persistence in the Bakken Formation of North Dakota, USA. *Environmental science & technology* **2018**, *52*, 8947–8953.

213. Lavoie, T.N.; Shepson, P.B.; Cambaliza, M.O.; Stirm, B.H.; Karion, A.; Sweeney, C.; Yacovitch, T.I.; Herndon, S.C.; Lan, X.; Lyon, D. Aircraft-based measurements of point source methane emissions in the Barnett Shale basin. *Environmental science & technology* **2015**, *49*, 7904–7913.
214. Lavoie, T.N.; Shepson, P.B.; Cambaliza, M.O.; Stirm, B.H.; Conley, S.; Mehrotra, S.; Faloona, I.C.; Lyon, D. Spatiotemporal variability of methane emissions at oil and natural gas operations in the Eagle Ford Basin. *Environmental science & technology* **2017**, *51*, 8001–8009.
215. Lavoie, T.N.; Shepson, P.B.; Gore, C.A.; Stirm, B.H.; Kaeser, R.; Wulle, B.; Lyon, D.; Rudek, J. Assessing the methane emissions from natural gas-fired power plants and oil refineries. *Environmental science & technology* **2017**, *51*, 3373–3381.
216. Mehrotra, S.; Faloona, I.; Suard, M.; Conley, S.; Fischer, M.L. Airborne Methane Emission Measurements for Selected Oil and Gas Facilities Across California. *Environmental science & technology* **2017**, *51*, 12981–12987.
217. Frankenberg, C.; Thorpe, A.K.; Thompson, D.R.; Hulley, G.; Kort, E.A.; Vance, N.; Borchardt, J.; Krings, T.; Gerilowski, K.; Sweeney, C.; others. Airborne methane remote measurements reveal heavy-tail flux distribution in Four Corners region. *Proceedings of the National Academy of Sciences* **2016**, *113*, 9734–9739.
218. Nathan, B.J.; Golston, L.M.; O'Brien, A.S.; Ross, K.; Harrison, W.A.; Tao, L.; Lary, D.J.; Johnson, D.R.; Covington, A.N.; Clark, N.N.; others. Near-field characterization of methane emission variability from a compressor station using a model aircraft. *Environmental science & technology* **2015**, *49*, 7896–7903.
219. Omara, M.; Zimmerman, N.; Sullivan, M.R.; Li, X.; Ellis, A.; Cesa, R.; Subramanian, R.; Presto, A.A.; Robinson, A.L. Methane emissions from natural gas production sites in the United States: Data synthesis and national estimate. *Environmental science & technology* **2018**.
220. Mitchell, A.L.; Tkacik, D.S.; Roscioli, J.R.; Herndon, S.C.; Yacovitch, T.I.; Martinez, D.M.; Vaughn, T.L.; Williams, L.L.; Sullivan, M.R.; Floerchinger, C.; others. Measurements of methane emissions from natural gas gathering facilities and processing plants: Measurement results. *Environmental science & technology* **2015**, *49*, 3219–3227.
221. Brandt, A.R.; Heath, G.A.; Cooley, D. Methane leaks from natural gas systems follow extreme distributions. *Environmental science & technology* **2016**, *50*, 12512–12520.
222. Brandt, A.R.; Heath, G.; Kort, E.; O'sullivan, F.; Pétron, G.; Jordaan, S.; Tans, P.; Wilcox, J.; Gopstein, A.; Arent, D.; others. Methane leaks from North American natural gas systems. *Science* **2014**, *343*, 733–735.
223. Allen, D.T.; Torres, V.M.; Thomas, J.; Sullivan, D.W.; Harrison, M.; Hendler, A.; Herndon, S.C.; Kolb, C.E.; Fraser, M.P.; Hill, A.D.; others. Measurements of methane emissions at natural gas production sites in the United States. *Proceedings of the National Academy of Sciences* **2013**, *110*, 17768–17773.
224. Allen, D.T.; Sullivan, D.W.; Zavala-Araiza, D.; Pacsi, A.P.; Harrison, M.; Keen, K.; Fraser, M.P.; Daniel Hill, A.; Lamb, B.K.; Sawyer, R.F.; others. Methane emissions from process equipment at natural gas production sites in the United States: Liquid unloading. *Environmental science & technology* **2014**, *49*, 641–648.
225. Shires, T.; Loughran, C.; Jones, S.; Hopkins, E. Compendium of greenhouse gas emissions methodologies for the oil and natural gas industry. Technical report, Prepared by URS Corporation for the American Petroleum Institute, Washington DC., 2009.

226. Alvarez, R.; Zavala-Araiza, D.; Lyon, D.; Allen, D.; Barkley, Z.; Brandt, A.; Davis, K.; Herndon, S.; Jacob, D.; Karion, A.; others. Assessment of methane emissions from the US oil and gas supply chain, *Science*, eaar7204, 2018.
227. Balcombe, P.; Brandon, N.; Hawkes, A. Characterising the distribution of methane and carbon dioxide emissions from the natural gas supply chain. *Journal of Cleaner Production* **2018**, *172*, 2019–2032.
228. Boothroyd, I.; Almond, S.; Qassim, S.; Worrall, F.; Davies, R. Fugitive emissions of methane from abandoned, decommissioned oil and gas wells. *Science of the Total Environment* **2016**, *547*, 461–469.
229. Boothroyd, I.M.; Almond, S.; Worrall, F.; Davies, R.K.; Davies, R.J. Assessing fugitive emissions of CH₄ from high-pressure gas pipelines in the UK. *Science of the Total Environment* **2018**, *631*, 1638–1648.
230. CAPP. Update of fugitive equipment leak emission factors. Technical Report 2014-0023, Canadian Association of Petroleum Producers, 2014.
231. Ltd., C.E. Identification and evaluation of opportunities to reduce methane losses at four gas processing plants. Technical report, Gas Technology Institute, 2002.
232. Ltd., C.E. Potential cost-effective flare and vent gas reduction opportunities at selected production facilities in Mexico. Technical report, Petroleum Technology Alliance Canada, 2015.
233. Day, S.; Dell'Amico, M.; Fry, R.; Tousi, H. Field measurements of fugitive emissions from equipment and well casings in austalian coal seam gas production facilities. Technical report, CSIRO Energy Technology, 2014.
234. Corporation, E.I. Upstream Oil and Gas Tank Emission Measurements TCEQ Project 2010 – 39. Technical Report 06-17477X, Texas Commission on Environmental Quality, 2010.
235. EPA, U. Protocol for equipment leak emission estimates. Technical Report EPA-453/R-93-026, U.S. Environmental Protection Agency, 1993.
236. EPA, U. Protocol for equipment leak emission estimates. Technical Report EPA-453/R-95-017, U.S. Environmental Protection Agency, 1995.
237. Eastern Research Group, I.; Sage Environmental Consulting, L. City of Fort Worth Natural Gas Air Quality Study. Technical report, City of Fort Worth, 2011.
238. Eastern Research Group, I. Condensate Tank Oil and Gas Activities. Technical report, Texas Commission on Environmental Quality, 2012.
239. Gidney, B. Upstream oil and gas storage tank project flash emissions models evaluation. Technical report, Texas Commission on Environmental Quality and Eastern Research Group, 2009.
240. Ltd., G.E. Historical Canadian Fugitive Emissions Management Program Assessment. Technical report, Petroleum Technology Alliance Canada, 2017.
241. Handler, A.; Nunn, J.; Lundein, J. VOC Emissions from Oil and Condensate Storage Tanks. Technical report, Texas Environmental Research Consortium, 2009.
242. Harrison, M.R.; Galloway, K.E.; Al, H. Natural gas industry methane emission factor improvement study. Technical report, U.S. Environmental Protection Agency, 2011.

243. Hendrick, M.F.; Ackley, R.; Sanaie-Movahed, B.; Tang, X.; Phillips, N.G. Fugitive methane emissions from leak-prone natural gas distribution infrastructure in urban environments. *Environmental pollution* **2016**, *213*, 710–716.
244. Johnson, D.R.; Covington, A.N.; Clark, N.N. Methane emissions from leak and loss audits of natural gas compressor stations and storage facilities. *Environmental science & technology* **2015**, *49*, 8132–8138.
245. Kang, M.; Kanno, C.M.; Reid, M.C.; Zhang, X.; Mauzerall, D.L.; Celia, M.A.; Chen, Y.; Onstott, T.C. Direct measurements of methane emissions from abandoned oil and gas wells in Pennsylvania. *Proceedings of the National Academy of Sciences* **2014**, *111*, 18173–18177.
246. Kuo, J. Estimation of methane emissions from the California natural gas system. Technical Report CEC-500-2014-072, California Energy Commission, 2012.
247. Inc., J.T. Uinta Basin well pad pneumatic controller emissions research study. Technical Report QAPP-1J16-019.R1, Environmental Protection Agency, 2016.
248. Lamb, B.K.; Edburg, S.L.; Ferrara, T.W.; Howard, T.; Harrison, M.R.; Kolb, C.E.; Townsend-Small, A.; Dyck, W.; Possolo, A.; Whetstone, J.R. Direct measurements show decreasing methane emissions from natural gas local distribution systems in the United States. *Environmental Science & Technology* **2015**, *49*, 5161–5169.
249. Lyman, S.N.; Watkins, C.; Jones, C.P.; Mansfield, M.L.; McKinley, M.; Kenney, D.; Evans, J. Hydrocarbon and carbon dioxide fluxes from natural gas well pad soils and surrounding soils in Eastern Utah. *Environmental science & technology* **2017**, *51*, 11625–11633.
250. Laboratory, N.G.M.; Ltd., C.E.; Ltd., I.E.S. Cost-effective direct inspection and maintenance control opportunities at five gas processing plants and upstream gathering compressor stations and well sites. Technical report, Environmental Protection Agency, 2006.
251. Picard, D.; Panek, J. Directed inspection and maintenance leak survey at a gas fractionation plant using traditional methods and optical gas imaging. *Proceedings of the Air and Waste Management Association* **2006**.
252. Subramanian, R.; Williams, L.L.; Vaughn, T.L.; Zimmerle, D.; Roscioli, J.R.; Herndon, S.C.; Yacovitch, T.I.; Floerchinger, C.; Tkacik, D.S.; Mitchell, A.L.; others. Methane emissions from natural gas compressor stations in the transmission and storage sector: Measurements and comparisons with the EPA greenhouse gas reporting program protocol. *Environmental science & technology* **2015**, *49*, 3252–3261.
253. Thoma, E.D.; Deshmukh, P.; Logan, R.; Stovern, M.; Dresser, C.; Brantley, H.L. Assessment of Uinta Basin Oil and Natural Gas Well Pad Pneumatic Controller Emissions. *Journal of Environmental Protection* **2017**, *8*, 394.
254. Townsend-Small, A.; Ferrara, T.W.; Lyon, D.R.; Fries, A.; Lamb, B.K. Emissions of coalbed and natural gas methane from abandoned oil and gas wells in the United States. *Geophysical Research Letters* **2016**, *43*, 2283–2290.
255. Vaughn, T.L.; Bell, C.S.; Yacovitch, T.I.; Roscioli, J.R.; Herndon, S.C.; Conley, S.; Schwietzke, S.; Heath, G.A.; Pétron, G.; Zimmerle, D. Comparing facility-level methane emission rate estimates at natural gas gathering and boosting stations. *Elementa Science of the Anthropocene* **2017**, *5*.

256. von Fischer, J.C.; Cooley, D.; Chamberlain, S.; Gaylord, A.; Griebenow, C.J.; Hamburg, S.P.; Salo, J.; Schumacher, R.; Theobald, D.; Ham, J. Rapid, vehicle-based identification of location and magnitude of urban natural gas pipeline leaks. *Environmental Science & Technology* **2017**, *51*, 4091–4099.
257. Zimmerle, D.J.; Williams, L.L.; Vaughn, T.L.; Quinn, C.; Subramanian, R.; Duggan, G.P.; Willson, B.; Opsomer, J.D.; Marchese, A.J.; Martinez, D.M.; others. Methane emissions from the natural gas transmission and storage system in the United States. *Environmental science & technology* **2015**, *49*, 9374–9383.
258. Zimmerle, D.J.; Pickering, C.K.; Bell, C.S.; Heath, G.A.; Nummedal, D.; Pétron, G.; Vaughn, T.L. Gathering pipeline methane emissions in Fayetteville shale pipelines and scoping guidelines for future pipeline measurement campaigns. *Elem Sci Anth* **2017**, *5*.
259. Kutz, M., Ed. *Mechanical Engineer's Handbook*, 3rd ed.; Vol. 4, John Wiley & Sons, 2006.
260. Elvidge, C.D. Satellite Data Estimation of Gas Flaring Volumes. Technical report, NOAA, 2012.